

# **THE POTENTIAL OF THE PRODUCTION OF FUELS AND CHEMICALS FROM MARINE BIOMASS**

By

Konstantinos Anastasakis

Supervised by Prof. Jenny M. Jones and Dr. Andrew B. Ross

Submitted in accordance with the requirements for the degree of  
PhD

The University of Leeds  
Energy Resources and Research Institute

May, 2011

The candidate confirms that the work submitted is his own and appropriate credit has been given where reference has been made to the work of others.

This copy has been supplied on the understanding that it is copyright material and that no quotation from the thesis may be published without proper acknowledgement.

## Acknowledgements

First of all I would like to acknowledge and express my sincere thanks to my supervisors Dr. Andrew Ross and Prof. Jenny Jones for their constant and precious assistance and advice. Thank you Andy for introducing me into your idea of using algae for energy, for your invaluable support and encouragement during both experimental work and writing up. Thank you for your expertise advice and practical assistance. Thank you also for being a friend and for your solidarity during the difficult periods of the PhD which were quite a few. Thank you Jenny for your guidance advice and words of wisdom that made problems seem much easier. Your immeasurable wisdom helped overcoming issues both personal and work related very quickly. Thank you both of being such great supervisors. I couldn't have imagined having any better people as supervisors.

I would also like to thank Mr. Simon Lloyd for his invaluable help and advice during experimental work and for being a great person to talk and work with.

I would like to express my gratitude to my fantastic colleagues Robert Johnson, Abha Saddawi, Patrick Biller for being such good friends and for their encouragement during difficult periods. I would also like to thank the previous group members who are all doctors now, Dr. Michal Kubacki, Dr. Toby Bridgeman and Dr. Emma Fitzpatrick for their help during my first steps of PhD and for being good friends as well.

I would also like to thank the SUPERGEN members for the collaborations and the exchange of ideas. Individual thanks to Dr. Jessica Adams from Aberystwyth University, Dr. Maeve Kelly and Mr. Lars Brunner from the Scottish Association of Marine Science for our collaborations.

I would also like to thank EPSRC for the financial support during this study without which it wouldn't come through.

Last but not least I would like to thank my family and all of my friends in Leeds, in Greece and everywhere else for their love and support. I dedicate this

thesis to my father Tasos, to my mother Anna, and to my sister Irini who have been always loving me, supporting me and believing in me.

To conclude I would like to say farewell to all the people I have met here. I've met fantastic people during my 5 years in UK and I hope that with some of them will meet again at some part of the world in the future. Until we meet again then my friends!

*'A good decision is based on knowledge and not on numbers'*

Plato

## **Abstract**

The need for sustainability, energy security and reduction of global warming has brought many alternative energy sources into the foreground. Already there are well established technologies that can produce renewable energy but when it comes to the production of renewable liquid fuels and chemicals, biomass is the primary feedstock. Biomass is a renewable source of energy that can provide heat, electricity and transport fuels. However, utilisation of biomass poses some limitations such as land availability and competition of energy crops with food crops. In order to overcome these problems “third generation” biofuels from alternative feedstock such as macro-algae have recently come into the foreground. Oceans and seas cover over 70% of the earth’s surface, most of which is under exploited, resulting in additional potential for biomass production.

This thesis concentrates on the potential for production of bio-energy and chemicals from macro-algae through thermochemical processes such as pyrolysis, combustion and hydrothermal liquefaction. Utilisation of aquatic biomass for production of bioenergy is a very recent concept and there is a lack of information on their thermochemical behaviour. This investigation contributes to a wider study and forms part of the Supergen II bionergy programme investigating the potential for utilisation of macroalgae in the UK. This investigation includes a detailed characterisation of the fuel properties and thermal behaviour of a range of wild seaweeds around the UK provided by the Scottish Association of Marine Sciences. In addition, a range of model biochemical components have been investigated, in particular, the model carbohydrates present in macro-algae.

Alginic acid, mannitol, laminarin, fucoidan and cellulose are the main carbohydrates present in brown macro-algae. The rest of the plant material comprises of protein and ash. Freshly harvested macro-algae contain 80-90wt% moisture. Their ash content is high, reflecting their high inorganic content. Potassium is the most abundant metal present in macro-algae although other metals are also present including sodium, calcium, magnesium, Their carbohydrate, protein

and ash content undergo a seasonal variation during their growth cycle. This variation was found to affect their properties as fuel.

Carbon content reaches its maximum during summer – early autumn. During the same period, the inorganic (and thus ash) content is at its minimum suggesting summer – early autumn as the optimum period for harvesting macro-algae for bio-energy. The high carbon and low inorganic content during this period is reflected in its higher heating value but it is still relatively low (13-14 MJ/kg) when compared with terrestrial biomass. The nature of the inhabitant location was found to significantly influence macro-algae fuel properties with samples grown in the open ocean having better fuel properties (higher HHV and lower inorganic content) than samples growing in canals and estuaries.

Investigation of the pyrolysis behaviour was performed using thermal analysis such as TGA and Py-GC/MS. The volatile matter evolved during pyrolysis was higher for samples collected during summer and early spring due to their higher carbon content. The main volatiles evolved during decomposition were found to originate either from their carbohydrates or from their protein content. Specific marker compounds were identified for the carbohydrates such as dianhydromannitol, 1-(2-furanyl)-ethanone, 2-hydroxy-3-methyl-2-cyclopenten-1-one and furfural for manitol, laminarin and alginic acid respectively. Proteins are found to produce a range of indoles and pyrroles. Some of the compounds identified may have industrial applications indicating the possibility of producing chemicals through pyrolysis of macro-algae. The high moisture content of seaweed necessitates that significant amounts of water must be removed before this feedstock can be converted by pyrolysis.

The high moisture content is similar an issue for combustion which has been assessed by a combination of TGA and characterisation of the biomass. Macro-algae have a low HHV, high halogen content and high ash content and are predicted to have high slagging and fouling behaviour in conventional combustion chambers. This fouling behaviour is predicted through empirical indexes such as the alkali index and is shown to be higher than terrestrial biomass even during summer – early autumn when their inorganic content is at minimum. Typical ash contents vary from 18 to 45wt% and contain mainly oxides of  $K_2O$ ,  $Na_2O$ ,  $CaO$  and  $MgO$ .

Pre-treatment prior to combustion can significantly reduce the ash content leading to improved combustion properties, but this also leads to removal of some biochemical components. Using an acid pre-treatment, some of the seaweed's biopolymers, such as mannitol or fucoidan, can be removed presenting the possibility for acquiring valuable chemicals from seaweed before combustion of the residue.

An alternative processing route, capable of processing wet feedstocks called hydrothermal liquefaction (HTL) involves the processing of the macro-algae in subcritical water. HTL converts the starting material into four product streams including a bio-crude, a char, an aqueous stream consisting primarily of process water and a gaseous stream. A parametric study of HTL has been investigated using high pressure batch reactors with or without the presence of catalysts. The bio-crude produced from the liquefaction of macroalgae was found to have a high heating value and resembling chemical composition to crude-oil. It can be used directly as a fuel however it still contains significantly high nitrogen levels and will require suitable upgrading (e.g. denitrogenation). The bio-char was found to also have a high heating value. Both bio-crude and bio-char produced from HTL are virtually free of alkali metals suggesting they are suitable for combustion. Reaction conditions such as temperature and the ratio of biomass to water have the greatest influence on product yields and properties. Typical bio-crude yields were in the range of 10 to 19wt% on a daf basis with their HHVs ranging from 32 to 38 MJ/kg. The yields of bio-chars were in similar range (10wt% to 19wt% on a db) with HHVs between 10 and 26 MJ/kg. An energy balance was calculated in order to investigate the energy required to heat the mixture of macro-algae and water. The energy recovery in the bio-crude and bio-char was relatively low, between 50 and 65%, indicating that a significant portion of the energy content of macro-algae is passing in to the other product streams.

The aqueous phase (process water) was found to be rich in metals, especially alkali metals, and sugars, and its composition suggests it may be possible to utilize it as a fertilizer. A fraction of the sugars present in macro-algae (mannitol and laminarin) pass in to the aqueous stream, suggesting there is also potential for

fermentation to bioethanol. The gaseous stream is composed mainly of CO<sub>2</sub>, N<sub>2</sub>, CO and lower concentrations of H<sub>2</sub> and CH<sub>4</sub>.

The most suitable thermochemical processing route for macro-algae is proposed to be hydrothermal liquefaction and has potential for utilization of all the product streams producing fuels and chemicals using a bio-refinery concept.

## Table of contents

<b>Acknowledgements .....</b>	<b>ii</b>
<b>Abstract.....</b>	<b>iv</b>
<b>Table of contents .....</b>	<b>viii</b>
<b>List of figures.....</b>	<b>xii</b>
<b>List of tables.....</b>	<b>xix</b>
<b>Abbreviations &amp; nomenclature.....</b>	<b>xxiv</b>
<b>CHAPTER 1 - Introduction.....</b>	<b>27</b>
1.1 Energy needs, Climate change and policies.....	27
1.2 The role of biomass.....	29
1.3 Marine biomass.....	32
1.4 Species of interest .....	37
1.4.1 Structure.....	37
1.4.2 Physiology.....	42
1.4.3 Characteristics and chemical composition.....	43
1.4.3.1 <i>Laminaria digitata</i> .....	43
1.4.3.2 <i>Laminaria Saccharina</i> .....	46
1.4.3.3 <i>Laminaria hyperborea</i> .....	47
1.4.3.4 <i>Alaria esculenta</i> .....	49
1.4.4 Seasonal variations in composition.....	50
<b>CHAPTER 2 - Biomass conversion technologies .....</b>	<b>56</b>
2.1 Introduction.....	56
2.2 Biochemical Processes.....	56
2.2.1 Anaerobic digestion .....	56
2.2.2 Fermentation .....	57
2.3 Thermo-chemical processes.....	58
2.3.1 Pyrolysis.....	59
2.3.2 Combustion.....	62



2.3.3 Liquefaction .....	64
2.4 Aims and Outline the Thesis .....	72
<b>CHAPTER 3 - Experimental .....</b>	<b>75</b>
3.1 Introduction .....	75
3.2 Species selection .....	76
3.3 Sample preparation .....	77
3.4 Model carbohydrates .....	78
3.5 Ultimate analysis .....	78
3.6 Metal analysis .....	78
3.7 Proximate analysis .....	78
3.8 High heating value (HHV) determination .....	79
3.9 Pre-treatment of seaweed .....	79
3.10 Slagging and fouling .....	80
3.11 Thermogravimetric analysis .....	80
3.12 Kinetics .....	81
3.13 Analytical pyrolysis (py-GC/MS) .....	83
3.14 Hydrothermal liquefaction .....	83
3.14.1 Hydrothermal liquefaction setup .....	83
3.14.2 Separation of liquefaction products .....	84
3.13.3 Product yields .....	85
3.14.4 Energy balance .....	86
3.15 GC-MS .....	88
3.16 Carbon and nitrogen determination of the aqueous phase .....	89
3.17 Biomass fuel properties .....	89
<b>CHAPTER 4 – Thermal behaviour of model carbohydrates .....</b>	<b>91</b>
4.1 Introduction .....	91
4.2 Pyrolysis behaviour of model carbohydrates .....	91
4.2.1 Characterisation of model carbohydrates .....	91
4.2.2 Thermogravimetric analysis (TGA) of model carbohydrates .....	92
4.2.3 Thermogravimetric analysis (TGA) of alginate salts in nitrogen .....	99

4.2.4 Prediction of seaweed degradation based on their biochemical content.....	102
4.2.5 Pyrolysis kinetics of model carbohydrates.....	104
4.2.6 Flash pyrolysis of model carbohydrates by py-GC/MS .....	107
4.3 Combustion behaviour of model carbohydrates .....	119
4.3.1 Thermogravimetric analysis (TGA) of model carbohydrates in air .....	119
4.3.2 Thermogravimetric analysis (TGA) of alginate salts in air.....	122
4.4 Conclusions.....	124
<b>CHAPTER 5 - Characterization of brown macro-algae .....</b>	<b>125</b>
5.1 Introduction.....	125
5.2 Sample preparation .....	126
5.3 Ash determination.....	127
5.4 Typical composition of brown macro-algae and differences between blades and stipes .....	129
5.5 Seasonal variations and effect of harvesting site .....	137
5.6 Effect of drying method .....	154
5.7 Conclusions.....	157
<b>CHAPTER 6 - Pyrolysis of brown macro-algae.....</b>	<b>158</b>
6.1 Introduction.....	158
6.2 Typical pyrolysis behaviour of brown macro-algae and differences between blades and stipes .....	158
6.3 Effect of harvest season .....	175
6.4 Effect of pre-treatment .....	181
6.5 Conclusions.....	187
<b>CHAPTER 7 - Combustion of brown macro-algae .....</b>	<b>189</b>
7.1 Introduction.....	189
7.2 Classification of seaweed as fuel .....	189
7.3 Slagging and fouling .....	192
7.4 Thermogravimetry of seaweed in air .....	205
7.5 Demineralization.....	209
7.6 Conclusions.....	213

<b>CHAPTER 8 - Hydrothermal liquefaction of brown macro-algae .....</b>	<b>214</b>
8.1 Introduction.....	214
8.2 Effect of reaction conditions.....	214
8.2.1 Product yields.....	215
8.2.2 Analysis and classification of the bio-crude .....	220
8.2.3 Analysis of the residue .....	229
8.2.4 Analysis of aqueous phase .....	232
8.2.5 Elemental balance in product streams.....	233
8.2.6 Energy balance .....	237
8.3 Optimization of reaction conditions for positive energy balance .....	240
8.4 Effect of sample composition .....	249
8.5 Hydrothermal liquefaction of seaweed biomass compared with biological processing.....	258
8.6 Conclusions.....	261
<b>CHAPTER 9 - Summary of conclusions and future research .....</b>	<b>262</b>
9.1 Introduction.....	262
9.2 Conclusions.....	262
9.2.1 Variations in seaweed fuel properties .....	262
9.2.2 Pyrolysis of brown macro-algae.....	264
9.2.3 Combustion and demineralization of brown macro-algae .....	265
9.2.4 Hydrothermal liquefaction of brown macro-algae .....	266
9.3 Future research.....	268
<b>Bibliography .....</b>	<b>270</b>
<b>APPENDIX A - PY-GC/MS chromatograms of model compounds and     identified compounds.....</b>	<b>286</b>
<b>APPENDIX B - Proximate and ultimate analysis of freeze dried, oven     dried and air dried seaweed samples. ....</b>	<b>310</b>
<b>APPENDIX C - Metal analysis of freeze dried, oven dried and air dried     seaweed samples. ....</b>	<b>322</b>

## List of figures

<b>Figure 1.1 Global anthropogenic greenhouse gas emissions in 2004 (IPCC, 2007).</b> .....	28
<b>Figure 1.2 World marketed energy consumption (data from EIA, 2010).</b> .....	28
<b>Figure 1.3 Energy consumption in EU-27 for the years 1990-2007 (data from EEA, 2010).</b> .....	30
<b>Figure 1.4 World primary energy demand in the reference scenario (figure from IEA, 2008).</b> .....	31
<b>Figure 1.5 Simplified diagram for offshore cultivation of seaweeds.</b> .....	36
<b>Figure 1.6 Offshore wind farm with proposed integrated seaweed cultivation (Buck et al., 2006).</b> .....	37
<b>Figure 1.7 The structure of the two types of laminarin with mannitol attached to the end (M-chains) or glucose attached to the end (G-chains) (Davis et al., 2003).</b> .....	38
<b>Figure 1.8 The structure of a) D-mannose and b) mannitol.</b> .....	39
<b>Figure 1.9 Algal cellulose.</b> .....	39
<b>Figure 1.10 The structure of cell wall in brown algae (Davis et al., 2003).</b> .....	40
<b>Figure 1.11 The structure of alginic acid (c) and its monomers (a) L-Guluronic acid (GG block) and (b) D-Mannuronic acid (MM block).</b> .....	41
<b>Figure 1.12 Proposed main structural unit of fucoidan (Berteau and Mulloy, 2003).</b> .....	41
<b>Figure 1.13 Parts of a seaweed plant.</b> .....	43
<b>Figure 1.14 Photograph of <i>Laminaria digitata</i> (Guiry, 2007a).</b> .....	44
<b>Figure 1.15 Photograph of <i>Laminaria saccharina</i> (Guiry, 2007b).</b> .....	46
<b>Figure 1.16 Photograph of <i>Laminaria hyperborea</i> (Guiry, 2003).</b> .....	48
<b>Figure 1.18 Photograph of <i>Alaria esculenta</i> (Guiry, 2006).</b> .....	50
<b>Figure 1.19 Diagram for the production of sodium alginate (McHaug, 2003).</b> .....	54
<b>Figure 2.1 Uses of pyrolysis products (Bridgwater, 2004; Goyal et al., 2008).</b> .....	59
<b>Figure 2.2 Simplified scheme for the liquefaction process.</b> .....	66
<b>Figure 3.1 Sampling sites on the west coast of Scotland (©2011 Google).</b> .....	77

<b>Figure 3.2 Example of pyrolysis temperature characteristics on a DTG curve.</b> .....	<b>81</b>
<b>Figure 3.3 Simplified schematic of the liquefaction reactor.</b> .....	<b>84</b>
<b>Figure 3.4 Separation procedure of liquefaction products.</b> .....	<b>85</b>
<b>Figure 3.5 Van Krevelen diagram for a variety of solid fuels (Jenkins et al., 1998)</b> .....	<b>90</b>
<b>Figure 4.1 TGA and DTG profile of alginic acid in nitrogen at 25°C/min.</b> .....	<b>96</b>
<b>Figure 4.2 TGA and DTG profile of mannitol in nitrogen at 25°C/min.</b> .....	<b>96</b>
<b>Figure 4.3 TGA and DTG profile of laminarin in nitrogen at 25°C/min.</b> .....	<b>97</b>
<b>Figure 4.4 TGA and DTG profile of fucoïdan in nitrogen at 25°C/min.</b> .....	<b>98</b>
<b>Figure 4.5 (a) TGA and (DTG) profiles in nitrogen at 25°C/min of alginic acid, Ca alginate and Na alginate.</b> .....	<b>100</b>
<b>Figure 4.6 (a) TGA and (b) DTG profiles of a mixture of the four carbohydrates compared with sample of <i>L. digitata</i>.</b> .....	<b>103</b>
<b>Figure 4.7 Validation of kinetic models for alginic acid. (a) Senum and Yang approximation and (b) reaction rate constant method.</b> .....	<b>107</b>
<b>Figure 4.8 Effect of temperature in the main volatiles evolved during py-GC/MS of alginic acid.</b> .....	<b>109</b>
<b>Figure 4.9 Effect of temperature in the main volatiles evolved during py-GC/MS of fucoïdan.</b> .....	<b>110</b>
<b>Figure 4.10 Effect of temperature in the main volatiles evolved during py-GC/MS of mannitol.</b> .....	<b>111</b>
<b>Figure 4.11 Effect of temperature in the main volatiles evolved during py-GC/MS of laminarin.</b> .....	<b>112</b>
<b>Figure 4.12 Pyrolysis-GC-MS of Ca alginate at 500°C. The main peaks are assigned from mass spectral detection as follows: (1) 2-methyl-2-propanamine; (2) 2-methyl-furan, (3) N-butyl-1-butanamine, (4) acetic acid, (5) N-nitrosodimethylamine, (6) furfural, (7) n-butylethylenediamine, (8) 4-cyclopentene-1,3-dione, (9) 1,2-cyclopentanedione, (10) 2(5H)-furanone, (11) 2-hydroxy-3-methyl-2-cyclopenten-1-one, (12) Phenol, (13) 2(3H)- 5-acetyldihydro-furanone.</b> .....	<b>113</b>

<b>Figure 4.13 Pyrolysis-GC-MS of Na alginate at 500°C. The main peaks are assigned from mass spectral detection as follows: (1) 2-methyl-2-propanamine, (2) 2-amino-4-methyl-pentanamide, (3) N-nitrosodimethylamine, (4) Cyclopentanone, (5) 2-methyl-cyclopentanone, (6) 3-methyl-cyclopentanone, (7) Furfural, (8) 2-methyl-2-cyclopenten-1-one, (9) 1,2-cyclopentanedione, (10) 2,3-dimethyl-2-cyclopenten-1-one, (11) 3-methyl-2-cyclopenten-1-one, (12) 3,4-dimethyl-2-cyclopenten-1-one, (13) 2,3-dimethyl-2-cyclopenten-1-one, (14) 2-hydroxy-3-methyl-2-cyclopenten-1-one, (15) 3-ethyl-2-hydroxy-2-cyclopenten-1-one, (16) phenol, (17) 3-ethyl-2-cyclopenten-1-one, (18) 3-ethyl-2-hydroxy-2-cyclopenten-1-one, (19) 4-isopropylcyclohexanone, (20) 2-ethyl-2-methyl-1,3-cyclopentanedione, (21) 3-methyl-phenol, (22) 5-acetyldihydro-2(3H)-furanone, (23) 2-methyl-1,4-benzenediol. ....</b>	<b>114</b>
<b>Figure 4.14 TGA profiles of alginic acid, mannitol, laminarin and fucoidan in air at 25°C/min. ....</b>	<b>119</b>
<b>Figure 4.15 DTG profiles of alginic acid, mannitol, laminarin and fucoidan in air at 25°C/min. ....</b>	<b>120</b>
<b>Figure 4.16 (a) TGA and (b) DTG profiles in air at 25°C/min of alginic acid, Ca alginate and Na alginate. ....</b>	<b>123</b>
<b>Figure 5.1 Seasonal variation in composition of brown-algae (data from Black, 1950, a, b; Gevaert, et al., 2001; Lewis and Smith, 1966). ....</b>	<b>126</b>
<b>Figure 5.2 Pyrolysis-GC-MS of extracted material during <i>L. saccharina</i> drying at 500°C. The main peaks are assigned from mass spectral detection as follows: (1) furan, (2) 2-methyl-3-buten-1-ol, (3) methyl-pyrazine, (4) pyrrole, (5) 2-methyl[1,3,4]oxadiazole, (6) furfural, (7) 2-propyl-furan, (8) 2-furanmethanol, (9) 1-(2-furanyl)-ethanone, (10) 5-methyl-2-furancarboxaldehyde, (11) resorcinol, (12) 3-methyl-1,2-cyclopentanedione, (13) dianhydromannitol, (14) isosorbide, (15) n-hexadecanoic acid, (16) oleic acid. ....</b>	<b>127</b>
<b>Figure 5.3 Influence of time on ash and carbon content of <i>Laminaria digitata</i> (winter harvest). ....</b>	<b>128</b>
<b>Figure 5.4. Influence of temperature on ash and carbon content of <i>Laminaria hyperborea</i> (winter harest). ....</b>	<b>129</b>
<b>Figure 5.5 Ash variation between blades and stipes of oven dried seaweed samples harvested during winter of 2009 from (a) sampling site Clachan sound and (b) sampling site Easdale. ....</b>	<b>130</b>
<b>Figure 5.6 Influence of ash content in elemental composition of oven dried, winter harvested seaweed samples. ....</b>	<b>131</b>
<b>Figure 5.7 Influence of K and Na concentration in ash content of seaweed samples. ....</b>	<b>137</b>

Figure 5.8 Seasonal variation in ash content on dry basis of freeze dried samples of (a) <i>L. digitata</i> , (b) <i>L. hyperborea</i> , (c) <i>L. saccharina</i> and (d) <i>A. esculenta</i> collected from different harvest sites. ....	139
Figure 5.9 Seasonal variation in ash content on dry basis for samples of <i>L. digitata</i> harvested from Aberystwyth beach, Wales.....	140
Figure 5.10 Seasonal variation in total metal content (ppm) on dry basis of freeze dried samples of (a) <i>L. digitata</i> , (b) <i>L. hyperborea</i> , (c) <i>L. saccharina</i> and (d) <i>A. esculenta</i> collected from different harvest sites....	143
Figure 5.11 Seasonal variation in total metals, potassium and sodium concentration of <i>L. digitata</i> on a monthly basis.....	144
Figure 5.12 Seasonal variation in potassium and sodium of freeze dried samples of (a) <i>L. digitata</i> , (b) <i>L. hyperborea</i> , (c) <i>L. saccharina</i> and (d) <i>A. esculenta</i> collected from different harvest sites, (CS=Clachan sound, Eas=Easdale, Brn=Barancarry). ....	146
Figure 5.13 Seasonal variation in calcium and magnesium of freeze dried samples of (a) <i>L. digitata</i> , (b) <i>L. hyperborea</i> , (c) <i>L. saccharina</i> and (d) <i>A. esculenta</i> collected from different harvest sites, (CS=Clachan sound, Eas=Easdale, Brn=Barancarry). ....	147
Figure 5.14 Seasonal variation in carbon content on dry basis of freeze dried samples of (a) <i>L. digitata</i> , (b) <i>L. hyperborea</i> , (c) <i>L. saccharina</i> and (d) <i>A. esculenta</i> collected from different harvest sites.....	152
Figure 5.15 Seasonal variation in carbon content on dry basis of freeze dried samples of (a) <i>L. digitata</i> , (b) <i>L. hyperborea</i> , (c) <i>L. saccharina</i> and (d) <i>A. esculenta</i> collected from different harvest sites.....	153
Figure 5.16 Seasonal variation on ash content of <i>Laminaria digitata</i> harvested from Clachan sound by using different drying methods (♦) freeze-dried (FD) (■)oven -dried (OD) and (▲)air-dried (AD).....	155
Figure 5.17 Seasonal variation on carbon content of <i>Laminaria digitata</i> harvested from Clachan sound by using different drying methods (♦) freeze-dried (FD) (■)oven -dried (OD) and (▲)air-dried (AD).....	156
Figure 6.1 (a) TGA and (b) DTG profiles in nitrogen at 25°C/min of winter harvested macro-algae samples' blades.....	159
Figure 6.2 (a) TGA and (b) DTG profiles in nitrogen at 25°C/min of winter harvested macro-algae samples' stipes. ....	162
Figure 6.3 Validation of kinetic model for <i>L. digitata</i> blades.....	165
Figure 6.4 Pyrolysis-GC/MS chromatograms of macro-algae samples blades pyrolysed at 500°C, (a) <i>L. digitata</i> , (b) <i>L. hyperborea</i> and (c) <i>L. saccharina</i> . ....	166
Figure 6.5 Pyrolysis-GC/MS chromatograms of macro-algae samples stipes pyrolysed at 500°C, (a) <i>L. digitata</i> , (b) <i>L. hyperborea</i> and (c) <i>L. saccharina</i> . ....	167

Figure 6.6 (a) TGA and (b) DTG profiles in nitrogen at 25°C/min of summer harvested macro-algae samples as a function of temperature. ....	176
Figure 6.7 1-(2-furanyl)-ethanone and 2-hydroxy-3-methyl-2-cyclopenten-1-one peak areas per mg <i>L. digitata</i> sample variation throughout the year. ....	178
Figure 6.8 5-methyl-2-furancarboxaldehyde and 2-methoxy-5-methyl-thiophene peak areas per mg <i>L. digitata</i> sample variation throughout the year. ....	179
Figure 6.9 Pyrrole and phytol peak areas per mg <i>L. digitata</i> sample variation throughout the year. ....	180
Figure 6.10 (a) TGA and (b) DTG profiles in nitrogen at 25°C/min of giant kelp (GK) as received, water washed and acid washed. ....	182
Figure 6.11 Pyrograms at 500°C for (a) <i>M. pyrifera</i> as received, (b) <i>M. pyrifera</i> pre-treated in water and (c) <i>M. pyrifera</i> pre-treated in acid. ....	185
Figure 7.1 Van Krevelen diagram of blades and stipes of oven dried seaweed harvested during winter and comparison with other fuels. ....	190
Figure 7.2 Van Krevelen diagram of freeze dried seaweed harvested throughout the year. ....	191
Figure 7.3 Inorganic composition of ash for samples of <i>L. digitata</i> harvested from Clachan sound during (a) autumn, (b) winter, (c) spring, and (d) summer and for samples harvested from Easdale during (e) autumn, (f) winter, (g) spring and (h) summer. ....	195
Figure 7.4 Inorganic composition of ash for samples of <i>L. hyperborea</i> harvested from Clachan sound during (a) autumn, (b) winter, (c) spring, and (d) summer and for samples harvested from Easdale during (e) autumn, (f) winter, (g) spring and (h) summer. ....	196
Figure 7.5 Inorganic composition of ash for samples of <i>L. saccharina</i> harvested from Clachan sound during (a) autumn, (b) winter, (c) spring, and (d) summer and for samples harvested from Barnaccary during (e) autumn, (f) winter, (g) spring and (h) summer. ....	197
Figure 7.6 Inorganic composition of ash for samples of <i>A. esculenta</i> harvested from Easdale (a) autumn, (b) winter, (c) spring, and (d) summer. ....	198
Figure 7.7 Seasonal variation in alkali index (AI) for samples of (♦) <i>L. digitata</i> harvested from Clachan sound, (■) <i>L. digitata</i> harvested from Easdale, (▲) <i>L. hyperborea</i> harvested from Clachan sound, (x) <i>L. hyperborea</i> harvested from Easdale, (*) <i>L. saccharina</i> harvested from Clachan sound, (◊) <i>L. saccharina</i> harvested from Barancarry and (+) <i>A. esculenta</i> harvested from Easdale. ....	199



<b>Figure 7.8 Inorganic composition of ash for air dried samples of <i>L. digitata</i> harvested from Easdale (a) winter, (b) spring, (c) summer, and (d) autumn.</b>	<b>201</b>
<b>Figure 7.9 Inorganic composition of ash for air dried samples of <i>L. hyperborea</i> harvested from Easdale (a) winter, (b) spring, (c) summer, and (d) autumn.</b>	<b>202</b>
<b>Figure 7.10 Inorganic composition of ash for air dried samples of <i>L. saccharina</i> harvested from Easdale (a) winter, (b) spring, (c) summer, and (d) autumn.</b>	<b>203</b>
<b>Figure 7.11 Inorganic composition of ash for air dried samples of <i>A. esculenta</i> harvested from Easdale (a) winter, (b) spring, (c) summer, and (d) autumn.</b>	<b>204</b>
<b>Figure 7.12 (a) TGA and (b) DTG profiles in air at 25°C/min of summer harvested freeze dried samples.</b>	<b>206</b>
<b>Figure 7.13 Removal of alkali and alkaline earth metals from seaweed samples by pre-treatment in (a) water and (b) acid.</b>	<b>211</b>
<b>Figure 7.14 Alkali index of seaweed samples before and after pre-treatment.</b>	<b>212</b>
<b>Figure 8.1 Effect of reactor loading on yields of liquefaction products, ♦ bio-crude yield, ■ residue yield, ▲ water yield, ○ gas yield, x conversion.</b>	<b>216</b>
<b>Figure 8.2 Effect of residence time on yields of liquefaction products, ♦ bio-crude yield, ■ residue yield, ▲ water yield, ○ gas yield, x conversion.</b>	<b>217</b>
<b>Figure 8.3 Effect of temperature on yields of liquefaction products, ♦ bio-crude yield, ■ residue yield, ▲ water yield, ○ gas yield, x conversion.</b>	<b>218</b>
<b>Figure 8.4 Effect of catalyst (KOH) loading on yields of liquefaction products, ♦ bio-crude yield, ■ residue yield, ▲ water yield, ○ gas yield, x conversion.</b>	<b>219</b>
<b>Figure 8.5 Van Krevelen diagram of seaweed bio-crude compared with different fuel oils.</b>	<b>222</b>
<b>Figure 8.6 Chromatogram of bio-crude obtained from hydrothermal liquefaction of 3g of seaweed biomass in 30ml of water at 350°C for 15min residence time.</b>	<b>222</b>
<b>Figure 8.7 Effect of reactor loading in the main constituents of bio-crude.</b>	<b>224</b>
<b>Figure 8.8 Effect of temperature in the main constituents of bio-crude.</b>	<b>225</b>
<b>Figure 8.9 Effect of catalyst (KOH) loading in the main constituents of bio-crude.</b>	<b>225</b>
<b>Figure 8.10 Effect of liquefaction temperature on the main volatiles evolved during py-GC/MS of the dried aqueous extracts.</b>	<b>233</b>

<b>Figure 8.11 Carbon and nitrogen partitioning in the product streams during hydrothermal liquefaction of 3g seaweed biomass in 30ml of water for 15min residence time at (a) 250°C and (b) 350°C. ....</b>	<b>234</b>
<b>Figure 8.12 Alkali and alkaline earth metals partitioning in the product streams during hydrothermal liquefaction of 3g seaweed biomass in 30ml of water for 15min residence time at (a) 250°C and (b) 350°C.....</b>	<b>236</b>
<b>Figure 8.13 Energy Conversion Ratio (ECR) and Energy Recovery Ratio (ERR) as a function of (a) water loading, (b) biomass loading and (c) temperature. ....</b>	<b>239</b>
<b>Figure 8.14 Products distribution from hydrothermal liquefaction of 8g of <i>L. saccharina</i> in 30ml of water at 350°C with 15min RT. ....</b>	<b>241</b>
<b>Figure 8.15 Boiling point distribution of bio-crude obtained from hydrothermal liquefaction of 8g of <i>L. saccharina</i> in 30ml of water at 350°C with 15min RT compared to the bio-crude obtained from hydrothermal liquefaction of 3g of <i>L. saccharina</i> under the same conditions. ....</b>	<b>241</b>
<b>Figure 8.16 –TGA and –DTG profiles in air (25ml/min) of char produced from hydrothermal liquefaction of 8g of <i>L. saccharina</i> in 30ml of water at 350°C for 15min. ....</b>	<b>244</b>
<b>Figure 8.17 Alkali and alkaline earth metals partitioning in the product streams during hydrothermal liquefaction of 8g seaweed biomass in 30ml of water for 15min residence time 350°C. ....</b>	<b>246</b>
<b>Figure 8.18 Py-GC/MS chromatogram of dried aqueous extract obtained from hydrothermal liquefaction of 8g of <i>L. saccharina</i> in 30ml of water at 350°C for 15 min. ....</b>	<b>247</b>
<b>Figure 8.19 Hydrothermal liquefaction product yields of freeze dried summer harvested seaweed samples.....</b>	<b>251</b>
<b>Figure 8.20 Alkali and alkaline earth metals partitioning in the product streams during hydrothermal liquefaction of summer harvested seaweed samples. ....</b>	<b>257</b>
<b>Figure A.1 Py-GC/MS profile for alginic acid at (a) 200°C, (b) 300°C, (c) 400°C, (d) 500°C and (e) 800°C. ....</b>	<b>287</b>
<b>Figure A.2 Py-GC/MS profile for fucoidan at (a) 200°C, (b) 300°C, (c) 400°C, (d) 500°C and (e) 800°C. ....</b>	<b>289</b>
<b>Figure A.3 Py-GC/MS profile for laminarin at (a) 200°C, (b) 300°C, (c) 400°C, (d) 500°C and (e) 800°C. ....</b>	<b>291</b>
<b>Figure A.4 Py-GC/MS profile for mannitol at (a) 200°C, (b) 300°C, (c) 400°C, (d) 500°C and (e) 800°C. ....</b>	<b>293</b>

## List of tables

<b>Table 1.1 Significant characteristics of the most common algal divisions (Bold and Wynne, 1978).</b> .....	<b>34</b>
<b>Table 1.2 Chemical composition of <i>Laminaria digitata</i>.</b> .....	<b>45</b>
<b>Table 1.3 Chemical composition of <i>Laminaria saccharina</i>.</b> .....	<b>47</b>
<b>Table 1.4 Chemical composition of <i>Laminaria hyperborea</i></b> .....	<b>49</b>
<b>Table 2.1 Characteristics and product distribution of different types of woody biomass pyrolysis (Bridgwater, 2004; Goyal et al., 2008).</b> .....	<b>60</b>
<b>Table 2.2 Yields and HHVs of oils obtained by hydrothermal liquefaction of lignocellulosic biomass.</b> .....	<b>69</b>
<b>Table 2.3 Yields and HHVs of oils obtained by hydrothermal liquefaction of microalgae.</b> .....	<b>71</b>
<b>Table 4.1 Proximate and ultimate analysis of the four carbohydrates of brown algae</b> .....	<b>94</b>
<b>Table 4.2 Metal concentration (ppm) of the carbohydrates of brown seaweed determined by ICP-OES</b> .....	<b>95</b>
<b>Table 4.3 Pyrolysis temperature characteristics of alginic acid, mannitol, laminarin and fucoidan.</b> .....	<b>98</b>
<b>Table 4.4 Pyrolysis temperature characteristics of alginates</b> .....	<b>101</b>
<b>Table 4.5 The pyrolysis kinetic parameters of the model carbohydrates determined by the Senum and Yang approximation and the reaction constant method.</b> .....	<b>106</b>
<b>Table 4.6 Volatiles yields (wt %) at different pyrolysis temperatures for alginic acid, mannitol, laminarin and fucoidan.</b> .....	<b>108</b>
<b>Table 4.7 Structures and origin of the main volatiles evolved during py-GC/MS of the main carbohydrates of brown macro-algae.</b> .....	<b>115</b>
<b>Table 4.8 Combustion temperature characteristics of the carbohydrates of brown macro-algae (where, VMIT, volatile matter ignition temperature, VMPT, volatile matter peak temperature, FCIT, fixed carbon ignition temperature, FCPT, fixed carbon peak temperature, BT, burnout temperature)</b> .....	<b>121</b>
<b>Table 5.1 Proximate and ultimate analysis of blades and stipes of winter harvested oven dried seaweed samples.</b> .....	<b>132</b>
<b>Table 5.2 Metal analysis of blades and stipes of winter harvested oven dried seaweed samples (Eas = Easdale, CS = Clachan sound, Brn = Barancarry).</b> .....	<b>134</b>

<b>Table 5.3 Variation in ash content on dry basis of freeze dried seaweed samples harvested from different locations through their annual growth cycle.....</b>	<b>142</b>
<b>Table 5.4 Variation in main metals of freeze dried seaweed samples harvested from different locations through their annual growth cycle. ....</b>	<b>148</b>
<b>Table 5.5 Variation in carbon content on dry basis of freeze dried seaweed samples harvested from different locations through their annual growth cycle. ....</b>	<b>150</b>
<b>Table 5.6 Variation in nitrogen content of freeze dried seaweed samples harvested from different locations through their annual growth cycle. ....</b>	<b>154</b>
<b>Table 6.1 Temperature characteristics, moisture, volatile matter and char yields of macro-algae samples' blades harvested during winter as determined by thermogravimetric analysis in nitrogen (25 °C/min). ....</b>	<b>160</b>
<b>Table 6.2 Temperature characteristics, moisture, volatile matter and char yields of macro-algae samples' stipes harvested during winter as determined by thermogravimetric analysis in nitrogen (25 °C/min). ....</b>	<b>163</b>
<b>Table 6.3 Initial devolatilisation kinetics for different parts of macro-algae harvested during winter as determined by the Senum and Yang approximation .....</b>	<b>164</b>
<b>Table 6.4 the main identified peaks from py-GC-MS chromatograms for oils obtained from pyrolysis of blades and stipes of <i>Laminaria Digitata</i>, <i>Laminaria hyperborea</i> and <i>Laminaria saccharina</i>.....</b>	<b>168</b>
<b>Table 6.5 Temperature characteristics, moisture, volatile matter and char yields of macro-algae samples harvested during summer as determined by thermogravimetric analysis in nitrogen (25 °C/min). ....</b>	<b>177</b>
<b>Table 6.6 Initial devolatilisation kinetics for macro-algae harvested during summer as determined by the Senum and Yang approximation. ....</b>	<b>177</b>
<b>Table 6.7 Temperature characteristics, moisture, volatile matter and char yields of different washes of <i>Macrocystis pyrifera</i> as determined by thermogravimetric analysis in nitrogen (25 °C/min). ....</b>	<b>183</b>
<b>Table 6.8 Initial devolatilisation kinetics for different treatments of <i>M. pyrifera</i> as determined by the Senum and Yang approximation. ....</b>	<b>183</b>
<b>Table 6.9 Main compounds identified in pyrograms from py-GC/MS of different treatments of <i>M. pyrifera</i>. ....</b>	<b>186</b>
<b>Table 7.1 Variation in high heating value (HHV) of freeze dried seaweed samples harvested from different locations through their annual growth cycle. ....</b>	<b>192</b>

<b>Table 7.2 Combustibility temperature characteristics of summer harvested freeze dried samples as determined by thermogravimetric analysis in air (25 °C/min).....</b>	<b>207</b>
<b>Table 7.3 Weight loss of summer harvested freeze dried samples during the different combustion stages as determined by thermogravimetric analysis in air (25 °C/min).....</b>	<b>208</b>
<b>Table 7.4 Proximate and ultimate analysis of brown macro-algae before and after treatment in water and acid .....</b>	<b>210</b>
<b>Table 8.1 Ultimate analysis and HHV of the bio-crudes from different experimental conditions.....</b>	<b>221</b>
<b>Table 8.2 Identification of compounds in bio-crude obtained from hydrothermal liquefaction of 3g of seaweed biomass in 30ml of water at 350°C for 15min residence time by GC-MS analysis.....</b>	<b>223</b>
<b>Table 8.3 Boiling point distribution of bio-crudes obtained at different experimental conditions.....</b>	<b>228</b>
<b>Table 8.4 Ultimate, proximate analysis and HHV of the solid residues obtained at different experimental conditions .....</b>	<b>230</b>
<b>Table 8.5 Yields, proximate, ultimate analysis and energy balance of bio-crudes and bio-chars obtained from hydrothermal liquefaction of 3g and 8g of seaweed biomass in 30 ml of water at 350°C for 15min.....</b>	<b>243</b>
<b>Table 8.6 Identification of compounds in dried aqueous extract obtained from hydrothermal liquefaction of 8g of <i>L. saccharina</i> in 30ml of water at 350°C for 15 min by py-GC/MS. ....</b>	<b>247</b>
<b>Table 8.7 Proximate, ultimate and metal analysis of summer harvested freeze dried samples used for hydrothermal liquefaction experiments.....</b>	<b>250</b>
<b>Table 8.8 Ultimate analysis, HHVs and yields of the bio-crudes produced from hydrothermal liquefaction of summer harvested seaweed samples. ....</b>	<b>252</b>
<b>Table 8.9 Boiling point distribution of bio-crudes obtained from hydrothermal liquefaction of summer harvested seaweed samples. ....</b>	<b>253</b>
<b>Table 8.10 Proximate and ultimate analysis, HHVs and yields of the bio-chars produced from hydrothermal liquefaction of summer harvested seaweed samples. ....</b>	<b>254</b>
<b>Table 8.11 Energy balance for hydrothermal liquefaction products of summer harvested seaweed samples.....</b>	<b>255</b>
<b>Table A.1 The main peaks identified in pyrograms of alginic acid at different temperatures by mass spectral detection. ....</b>	<b>294</b>
<b>Table A.2 The main peaks identified in pyrograms of fucoidan at different temperatures by mass spectral detection. ....</b>	<b>297</b>

<b>Table A.3 the main peaks identified in pyrograms of laminarin at different temperatures by mass spectral detection .....</b>	<b>300</b>
<b>Table A.4 The main peaks identified in pyrograms of mannitol at different temperatures by mass spectral detection. ....</b>	<b>306</b>
<b>Table B.1 Proximate and ultimate analysis of freeze dried samples of <i>L. digitata</i> (wt%) .....</b>	<b>310</b>
<b>Table B.2 Proximate and ultimate analysis of freeze dried samples of <i>L. hyperborea</i> (wt%) .....</b>	<b>311</b>
<b>Table B.3 Proximate and ultimate analysis of freeze dried samples of <i>L. saccharina</i> (wt%) .....</b>	<b>312</b>
<b>Table B.4 Proximate and ultimate analysis of freeze dried samples of <i>A. esculenta</i> (wt%) .....</b>	<b>313</b>
<b>Table B.5 Proximate and ultimate analysis of oven dried samples of <i>L. digitata</i> (wt%) .....</b>	<b>314</b>
<b>Table B.6 Proximate and ultimate analysis of oven dried samples of <i>L. hyperborea</i> (wt%) .....</b>	<b>315</b>
<b>Table B.7 Proximate and ultimate analysis of oven dried samples of <i>L. saccharina</i> (wt%) .....</b>	<b>316</b>
<b>Table B.8 Proximate and ultimate analysis of oven dried samples of <i>A. esculenta</i> (wt%) .....</b>	<b>317</b>
<b>Table B.9 Proximate and ultimate analysis of air dried samples of <i>L. digitata</i> (wt%) .....</b>	<b>318</b>
<b>Table B.10 Proximate and ultimate analysis of air dried samples of <i>L. hyperborea</i> (wt%) .....</b>	<b>319</b>
<b>Table B.11 Proximate and ultimate analysis of air dried samples of <i>L. saccharina</i> (wt%) .....</b>	<b>320</b>
<b>Table B.12 Proximate and ultimate analysis of air dried samples of <i>A. Esculenta</i>(wt%) .....</b>	<b>321</b>
<b>Table C.1 Metal analysis of freeze dried samples of <i>L. digitata</i> (wt%) .....</b>	<b>322</b>
<b>Table C.2 Metal analysis of freeze dried samples of <i>L. hyperborea</i> (wt%) .....</b>	<b>325</b>
<b>Table C.3 Metal analysis of freeze dried samples of <i>L. saccharina</i> (wt%) .....</b>	<b>328</b>
<b>Table C.4 Metal analysis of freeze dried samples of <i>A. esculenta</i> (wt%) .....</b>	<b>331</b>
<b>Table C.5 Metal analysis of oven dried samples of <i>L. digitata</i> (wt%) .....</b>	<b>334</b>
<b>Table C.6 Metal analysis of oven dried samples of <i>L. hyperborea</i> (wt%) .....</b>	<b>337</b>
<b>Table C.7 Metal analysis of oven dried samples of <i>L. saccharina</i> (wt%) .....</b>	<b>340</b>
<b>Table C.8 Metal analysis of oven dried samples of <i>A. esculenta</i> (wt%) .....</b>	<b>343</b>
<b>Table C.9 Metal analysis of air dried samples of <i>L. digitata</i> (wt%) .....</b>	<b>346</b>

**Table C.10 Metal analysis of air dried samples of *L. hyperborea* (wt%) ..... 349**  
**Table C.11 Metal analysis of air dried samples of *L. saccharina* (wt%) ..... 352**  
**Table C.12 Metal analysis of air dried samples of *A. esculenta* (wt%)..... 355**

## **Abbreviations & nomenclature**

### **Abbreviations**

AAS	Atomic Absorption Spectroscopy
AD	Air Dried
AI	Alkali Index
ar	As received
CV	Calorific Value
DAE	Dissolved Aqueous Extract
daf	Dry ash free
db	Dry basis
DCM	Dichloromethane
DTG	Differential Thermal Gravimetric
ECR	Energy Consumption Ratio
ERR	Energy Recovery Ratio
FC	Fixed Carbon
FD	Freeze Dried
GC/MS	Gas Chromatography / Mass Spectrometry
HHV	High Heating Value
HTL	Hydrothermal Liquefaction
ICP-OES	Inductively Coupled Plasma - Optical Emission Spectrometry
OD	Oven Dried
Py-GC/MS	Pyrolysis Gas Chromatography – Mass Spectrometry
TGA	Thermo-Gravimetric Analysis
TN	Total Nitrogen
TOC	Total Organic Carbon
VM	Volatile Matter



## Nomenclature

		units
A	Pre-exponential factor	L/mol*s
$a_i$	Reaction progress variable at a given time (i) ( $a_i=1-m_i/m_0$ )	
B	Predetermined heating rate (dT/dt)	
BT	Burnout temperature	°C
$C_p$	Specific heat capacity	J/kg*K
E	Activation energy	KJ/mol
$E_l$	Energy required for liquefaction	MJ
$E_p$	Energy of the products (bio-crude and bio-char)	MJ
FCIT	Fixed carbon ignition temperature	°C
FCPT	Fixed carbon peak temperature	°C
$k_i$	Reaction coefficient at a given time (i)	
$m_0$	Initial mass	g
$m_i$	Mass at a given time (i)	g
Q	Heat energy	KJ
R	Universal gas constant	8.314 J/mol*K
T	Temperature	K
$T_e$	Temperature of ease of main devolatilisation	°C
$T_i$	Temperature of initial devolatilisation	°C
$T_p$	Temperature at maximum conversion rate	°C
VMIT	Volatile matter ignition temperature	°C
VMPT	Volatile matter peak temperature	°C
$W_{\text{bio-char}}$	Mass of bio-char	g
$W_{\text{bio-crude}}$	Mass of bio-crude	g
$W_{\text{DAE}}$	Mass of the dried aqueous extract	g
$W_{\text{KOH}}$	Mass of catalyst fed in the reactor	g

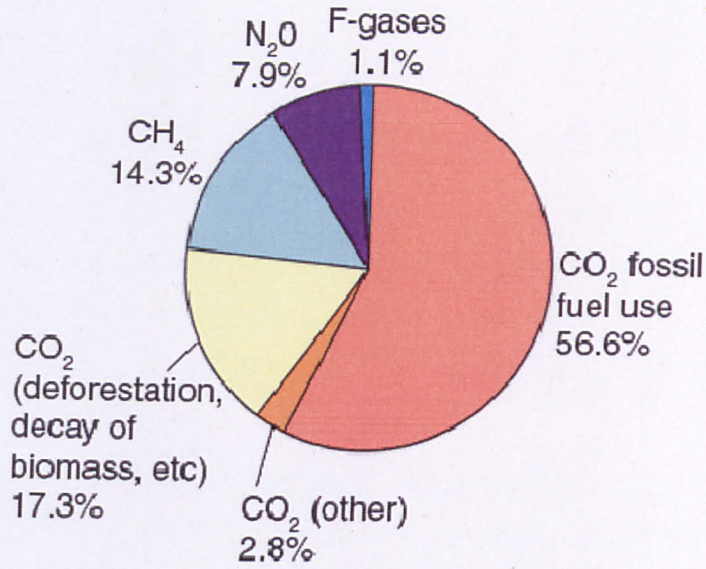
$W_{\text{seaweed}}$	Mass of seaweed biomass fed in the reactor	g
$W_{\text{solids}}$	Mass of solids fed in the reactor	g
$W_{\text{water}}$	Mass of water fed in the reactor	g

## CHAPTER 1 - Introduction

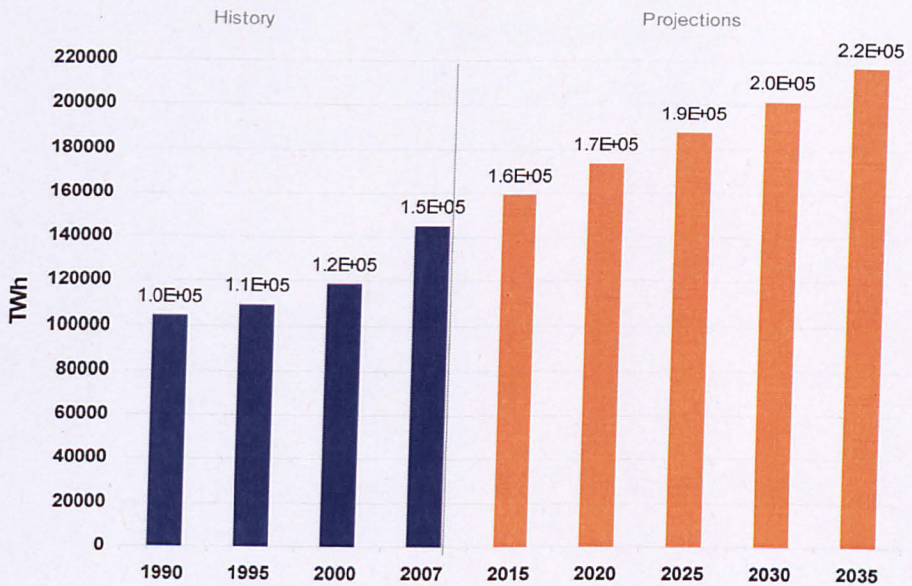
### 1.1 Energy needs, Climate change and policies

Energy is the driving force for our civilization. Most of modern every-day activities are interwoven directly or indirectly with the consumption of energy. The continuous modernization of societies is constantly increasing the need for energy, and thus energy consumption. This energy has been historically provided mainly by burning fossil fuels such as crude oil, coal and natural gas. However utilization of these fossil fuels causes the emissions of gases such as carbon dioxide (CO<sub>2</sub>), methane (CH<sub>4</sub>) and nitrogen oxides (NO<sub>x</sub>) which are contributing to global warming as they increase their natural occurring atmospheric concentration. These greenhouse gases, as their concentration dramatically increases, have a catastrophic impact on the earth's climate and life (e.g. melting of the ice caps due to a much warmer climate, switching off the North Atlantic circulation which will lead to a drop in temperatures across northern Europe etc.). As public awareness heightens, the need to tackle climate change is being increasingly stressed. **Figure 1.1** presents the global anthropogenic greenhouse gas emissions where the burning of fossil fuels is liable for more than half of these emissions.

Furthermore, fossil fuels are an exhaustible source of energy, so at some point in the future will be depleted. This depletion is accelerated with the continuous population growth and economic development and therefore continuous increase in energy consumption of large developing countries such as China, India and Africa. This increase in energy demand is clear in **Figure 1.2** where projections of the world energy consumption until the year 2035 are presented (**EIA, 2010**). Additionally, their existence is limited in certain areas of the world which will leave most of the world depending on a few countries for fossil fuel supply. The unstable political situation that many of these countries have as well as the increase in demand gives large increases and fluctuations in fossil fuel prices, which has a direct impact on the economies of the importing countries.



**Figure 1.1** Global anthropogenic greenhouse gas emissions in 2004 (IPCC, 2007).



**Figure 1.2** World marketed energy consumption (data from EIA, 2010).

In order to tackle climate change, increase energy security and meet the future increase in energy demand, the European Union has come into a European agreement towards these goals. The strategy of this agreement is explained in detail in the Energy White Paper and consists of three main tasks in order to achieve low carbon economy (DTI, 2007):

- Save energy,
- Develop cleaner supplies, and
- Secure reliable energy supplies at prices set in competitive markets.

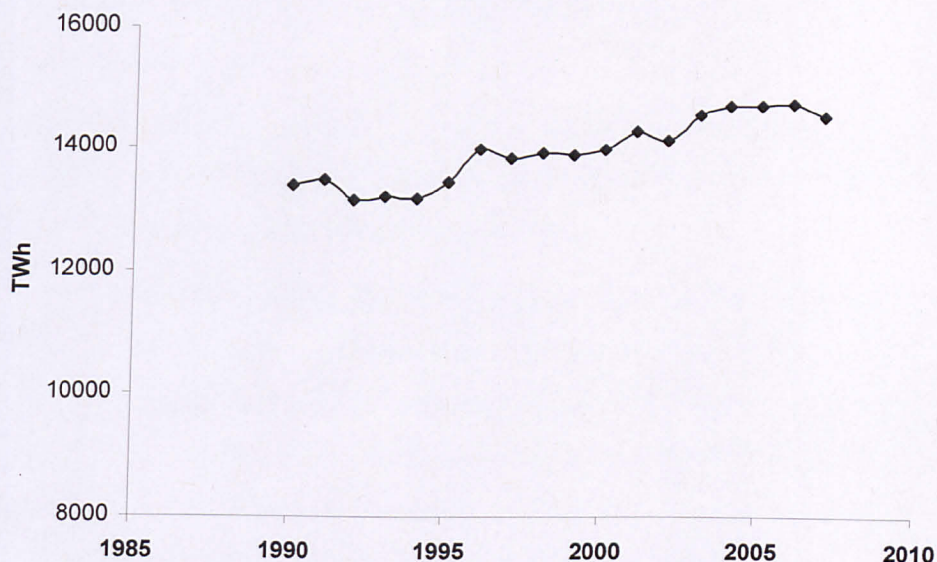
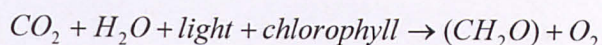
Utilization and improvement of renewable sources of energy can help towards accomplishing these two last tasks. Renewable energy sources generate power with zero (or near zero) emissions, while at the same time increase the energy security of each state as there is less need for imports of fossil fuels, leading to the development of sustainable societies.

Nowadays, renewable sources of energy are being rapidly developed in order to improve their design and efficiency so they can contribute significantly in power generation. All of them can contribute to electricity generation (solar energy, wind energy, hydroelectricity, tidal energy, wave energy, geothermal energy, and bio-energy), a few can contribute to heating (solar energy, geothermal energy, and bio-energy), but only one can contribute in the production of liquid fuels and chemicals: biomass. Biomass can contribute in all sectors of power generation so it has to be used carefully according to the needs of each sector.

### 1.2 The role of biomass

Biomass is any source of living or recently lived organism. Biomass for power generation falls into two main categories: utilization of wastes and utilization of energy crops. Wastes include wood residues, other crop residues, animal wastes, municipal solid waste, landfill gas and industrial wastes. However, the amount of wastes is fixed, so their contribution to power generation is limited. **Figure 1.3** presents the energy consumption in EU-27 for the years 1990 to 2007. According to data from **CEWEP (2009)** the generation of both electricity and heat from wastes across Europe for the year 2006 was just below 40 TWh, while for the same year the energy consumption across Europe was just below 15,000 TWh (**Figure 1.3**), making waste contribution to total energy consumption less than 0.27 %. Optimistic projections for 2020 are about 75 TWh of electricity and heat being produced from wastes (**CEWEP, 2009**). Thus, in order for biomass to have a significant contribution to power generation energy crops have to be cultivated.

Energy crops include fast growing woody and agricultural crops dedicated for power generation. During their growth, they utilize carbon dioxide from the atmosphere through photosynthesis to create organic compounds necessary for their growth according to the equation (Klass, 1998):



**Figure 1.3** Energy consumption in EU-27 for the years 1990-2007 (data from EEA, 2010).

In that way each plant contributes to the carbon cycle during its growth as it transforms the atmospheric carbon dioxide into organic compounds. The carbon dioxide that is emitted during the combustion of biomass fuels or during their conversion, is being captured by the energy crops that are being grown towards that reason, so the overall carbon cycle is in theory zero. In order for biomass to be considered as a renewable source of energy, sustainable cultivation has to be established. This means the continuous plantation of crops replacing the ones that have been used for fuels.

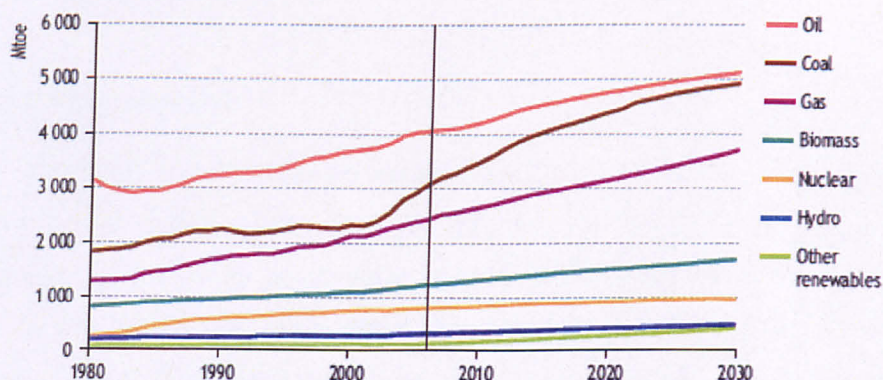
Biomass has gained a lot of interest because it posses several advantages when compared with other renewable sources or with fossil fuels. According to **Sims and Bassam (2004)** these advantages are:

- Biomass is carbon neutral when produced sustainably,

- has a relatively even geographic distribution,
- can be grown close to where it is used,
- has the potential to produce clean modern carriers
- can largely contribute to rural development, and
- can be economic when compared with imported fossil fuels in many countries.

It also offers the ability to produce liquid fuels or chemicals that are traditionally derived from petrochemicals, as well as biomaterials, apart from the traditional uses for electricity generation and heating.

According to **Sims and Bassam (2004)** biomass is potentially the largest sustainable source of fuels and chemicals. This can be seen in **Figure 1.4** where biomass has a bigger contribution in the energy sector than hydroelectric plants and all the other renewables. Also according to the reference scenario of the International Energy Agency this contribution is going to increase in the future as the use of biomass for power generation grows at 5.4 % per year (**IEA, 2008**).



**Figure 1.4** World primary energy demand in the reference scenario (figure from **IEA, 2008**).

Feedstocks such as corn, sugarcane, wheat, soybean, rapeseed and sunflower were firstly used for the production of the 1<sup>st</sup> generation biofuels. However, they caused international discussion on the effect they have on food prices (**Ajanovic, 2011; Rathmann et al., 2010**). The majority agrees that they are pushing up the price of food to some extent (**Ajanovic, 2011**). Additionally, the large arable areas

required for their cultivation along with the large quantities of water needed for their growth and the resultant emissions to the environment from the use of fertilizers and pesticides, raised the need for the development of other biomass feedstocks.

This need resulted in the development of 2<sup>nd</sup> generation biofuels from woody and perennial plants known as lignocellulosic biomass. Typical lignocellulosic crops include willow, Miscanthus and switchgrass (**Reijnders, 2010**). These feedstocks do not compete with food, have higher energy yield with less agrochemicals being used leading to higher greenhouse gas reduction potential (**Ajanovic, 2011**) and have significantly less water requirements (**Stone et al., 2010**). However, these crops do not solve the problem of competition with food crops, as despite their ability to be cultivated in abandoned or marginal agricultural soils, the profitability is diverting them into being cultivated on good agricultural soils (**Reijnders, 2010**).

In order to overcome this problem 3<sup>rd</sup> generation biofuels have recently come into the foreground. These derive from feedstocks that are being cultivated in aquatic environment and include unicellular (microalgae) or multicellular (macro-algae) species grown in freshwater and in marine systems. Macro-algae or seaweed are part of this investigation.

### 1.3 Marine biomass

Macro-algae or seaweeds are aquatic plant-like organisms that can be grown in freshwater, sea or ocean. They belong to the common plant group of Algae and are sometimes referred to as macro-algae in order to be distinguished them from the single celled micro-algae (**Tett, 2003**). The structure of algae differs from that of terrestrial plants. They don't contain the strong lignocellulosic material in their cell walls but contain other polysaccharides that are insoluble in sea water (**BeMiller, 2001**).

Classification of algae is based on the nature of phototropic pigment (eg chlorophylls), the cell wall chemistry, the storage products and presence or absence of flagellation (**Davis et al., 2003**). However, due to different classification methods, there is a variety in classification of algae by different researchers. **Bold and Wynne, 1978** have given the wider classification of algae, where 9 divisions of



algae, Cyanochloronta, Chlorophycophyta, Charophyta, Euglenophycophyta, Phaeophycophyta, Chrysophycophyta, Pyrrophytocyta, Cryptophycophyta and Rhodophycophyta have been recognised. Among these, three are the divisions that are recognised by all researchers, Chlorophycophyta, Phaeophycophyta and Rhodophycophyta. **Table 1.1** shows the most important characteristics of the three algal divisions. There are significant differences in pigments, stored food, cell wall composition and flagellar between the green, brown and red algae.

Seaweeds can be cultivated in the sea in a similar way that energy crops are cultivated on land. Oceans and seas cover over 70% of the earth's surface, most of which is not being exploited, making the marine environment ideal, in terms of area availability for biomass production. Also seaweeds are not being used extensively for human food (only some countries such as China and Japan are consuming seaweeds for food) adding the advantage of that no future fluctuations in the demand is likely due to overpopulation. An apparent positive effect to the aqueous environment caused by the artificial cultivation of seaweed, will be the increase in seaweed and therefore in fish populations (**Chynoweth, 2002**).

Furthermore, marine biomass has much higher photosynthetic activity (6-8%) than the terrestrial one (1.8-2.2%) leading to much more CO<sub>2</sub> absorption by the aquatic plants (**Aresta et al., 2005**) and therefore to higher greenhouse gas reduction potential. Also, marine biomass is not limited by water or temperature but by the availability of nutrients which can be artificially supplied leading to large biomass yields (**Chynoweth, 2002**). There is also no need for fertilizer or pesticides.

Seaweeds have the ability to bind CO<sub>2</sub> and HCO<sub>3</sub> during their photosynthesis and convert the inorganic carbon they take in into organic molecules (**Gevaert et al., 2001**). They also take up nitrogen contained in the nutrients (NO<sub>3</sub> and NH<sub>4</sub>) contributing in that way to the nitrogen cycle (**Gevaert et al., 2001**).

The growth of seaweed require the presence of certain nutrients in the water such as nitrogen, phosphorus and trace metals such as iron and manganese with the minimum levels of nitrogen and phosphorus being 1-3 µg/L and 0.2-0.6 µg/L respectively (**Beavis and Charlier, 1987**).

**Table 1.1** Significant characteristics of the most common algal divisions (**Bold and Wynne, 1978**).

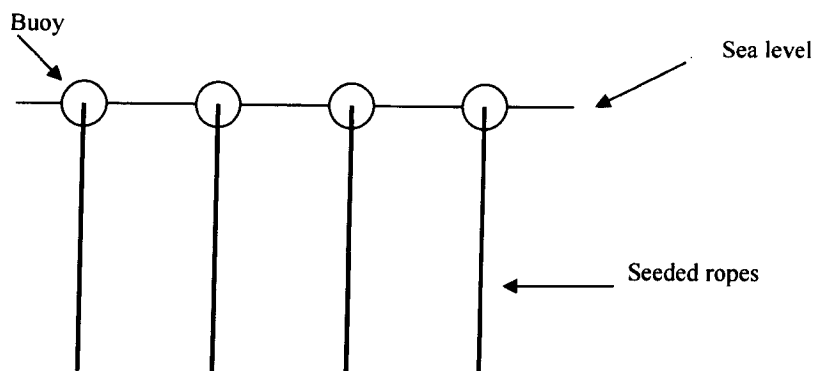
Division	Common Name	Pigments	Food Reserve	Cell Wall	Flagellar
Chlorophycophyta	Green algae	Chlorophyll a, b; a-, b-, and $\gamma$ -carotenes and several xanthophylls; 2-5 thylacoids/stack	Starch (amylase and amylopectin) (oil in some)	Cellulose in many ( $\beta$ -1, 4-glycopyranoside), hydroxyproline glycosides; xylans and mannans; or wall absent; calcified in some	1, 2-8, many, equal, apical
Phaeophycophyta	Brown algae	Chlorophyll a, c; $\beta$ -carotene and fucoxanthin and several other xanthophylls; 2-6 thylacoids/stack	Laminarin ( $\beta$ -1, 3-glucopyranoside, predominantly); mannitol	Cellulose, alginic acid and sulphated mucopolysaccharides (fucoidan)	2, unequal lateral
Rhodophycophyta	Red algae	Chlorophyll a, (d in some Florideophycidae); R- and C-phycoerythrin; allophycocyanin; R- and B-phycoerythrin; a- and b-carotene and several xanthophylls; thylakoids single, not associated	Floridean starch (glycogen like)	Cellulose, xylans, several sulphated polysaccharides (galactans) calcification in some	absent

The artificial farming of seaweeds has recently commenced, mainly in Asia, where the demand for seaweeds has overcome the natural production because of the extra use of seaweeds as a human food in this region (**Kain & Dawes 1987**). This type of cultivation offers the following advantages according to **Kain and Dawes (1987)** when compared with the natural occurrence of seaweeds:

- 1) Harvesting is easier as it avoids open seas which are prone to bad weather and storms.
- 2) Harvesting of the specific species (monocultures) only without co-harvesting unnecessary material as the cultivation conditions are being controlled.
- 3) Harvesting seaweeds with the same quality as the cultivation is controlled and seaweeds of the same age can be planted.
- 4) Possibility of improving stocks by genetic strain collection.

However, when cultivating specific seaweed species outdoors where there is limited control of the environmental conditions, the site has to be carefully chosen to have the physical requirements (wave exposure, suitable seabed, rocky or sandy environment etc.) necessary for the growing of the selected seaweed (**Lipkin, 1985**).

The cultivation of seaweeds can be achieved quite simply by using the same techniques that are being used for mussel farming (**Figure 1.5**). A horizontal rope which holds together a number of buoys floating on the sea level. From each buoy, a vertical seeded rope (with the appropriate seaweed seeds) is immersed into the sea and the seaweed eventually grows on the rope. By using this technique, collection of the cultivated seaweeds becomes simple as each rope is dragged out of the water and the seaweed is collected manually.



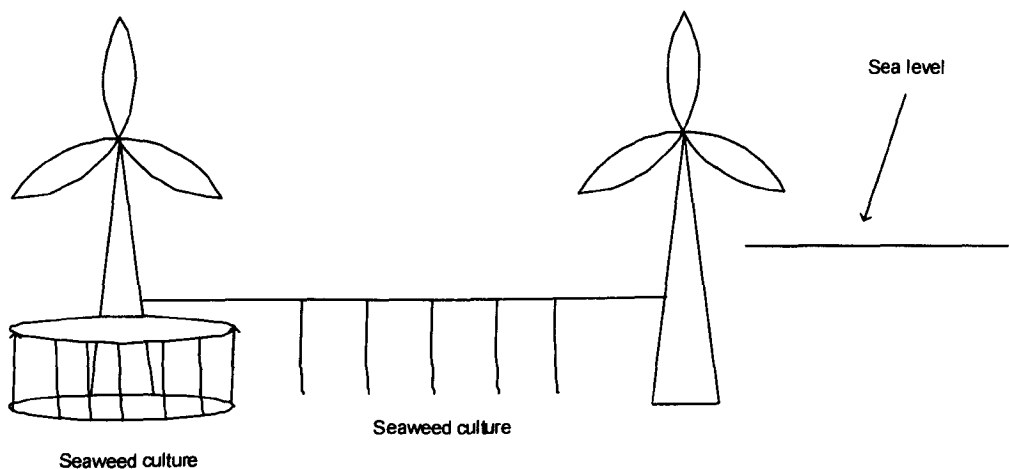
**Figure 1.5** Simplified diagram for offshore cultivation of seaweeds.

Apart from the offshore cultivation, seaweeds can be cultivated onshore also in ponds or tanks in land. **Kain and Dawes (1987)** cultivated seaweeds by combining both onshore and offshore cultivation: firstly seaweeds were cultivated in a closed-circuit system of tanks where nutrient enriched seawater was continuously circulating through vertical placed frames and secondly, after a period of 20 days these frames were placed vertically on a horizontal surface rope, in an arrangement similar with the one shown on the previous figure. Other cultivation technique includes the integrated cultivation of seaweed with offshore wind farms as proposed by **Buck and co-workers (2006)** and is shown in **Figure 1.6**. There seaweeds are cultivated on rings or horizontal ropes that are being placed between the poles of the wind turbines underneath the sea level.

Cultivation of seaweed can give high potential yields. Initial studies of cultivation of the brown macro-alga *Alaria Esculenta* in the Scottish Association of Marine Sciences in a cultivation system similar to the one shown in **Figure 1.5**, gave yield of 45 kg per meter of cultivating rope on a wet basis (usually freshly harvested seaweed contain about 90% moisture) (**Kelly et al., 2008**). **Jupp and Drew (1974)** found mean biomass yields of 2.1 kg/m<sup>2</sup>/yr dry weight during the cultivation of *Laminaria hyperborea* at 3m depth, leading to a potential biomass yield from cultivation of *Laminaria hyperborea* of 21.3 t/ha/yr in dry weight. Other aquatic biomass yield from seaweed cultivation range between 25 and 60 dry t/ha/yr for *Laminaria japonica*, 12 dry t/ha/yr for *Alaria*, 15 dry t/ha/yr for *Laminaria saccharina* and 22.5 dry t/ha/yr for *Saccorhiza polyschides* (**Bruton et al., 2009**).

Cultivation of aquatic biomass can lead to even higher yields than those reported if it is cultivated in three-dimensions, where the depth of the sea is also utilised in addition to length and breadth that is utilised by terrestrial biomass (**Gunaseelan, 1997**).

In this way, cultivation of seaweed for biomass feedstock offer a potential of overcoming some of the main problems related to biomass supply such as land availability, food demand and crop yields (**Ajanovic, 2011**). Furthermore, no water or agrochemicals are needed for their growth, reducing thereby main environmental considerations associated with cultivation of terrestrial biomass.



**Figure 1.6** Offshore wind farm with proposed integrated seaweed cultivation (**Buck et al., 2006**).

## 1.4 Species of interest

In this particular research the brown algae (Phaeophycophyta) are the algae of interest. More specifically brown kelps that can be commonly found around the British coasts and dominate the flora in temperate seas.

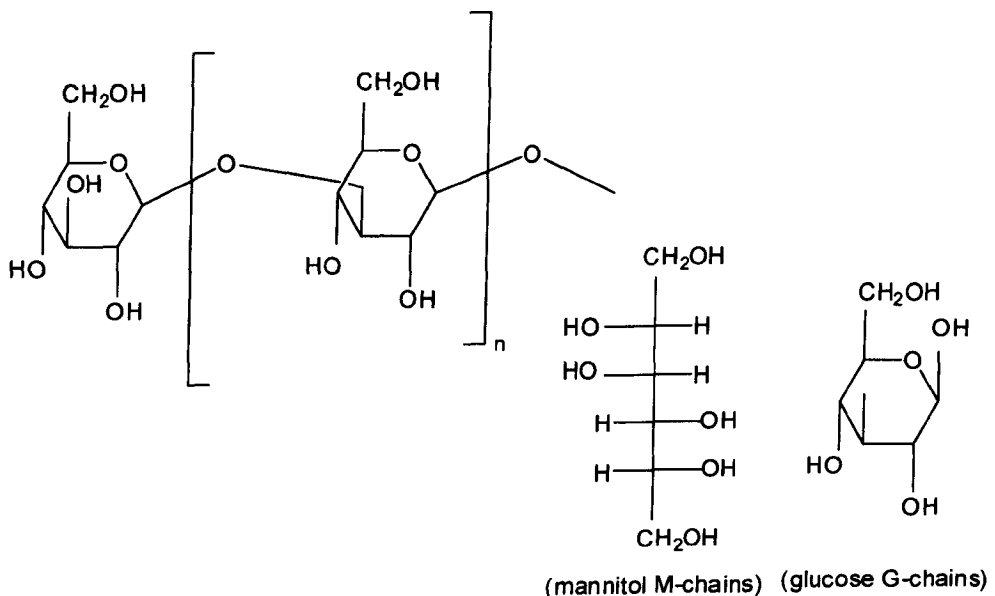
### 1.4.1 Structure

The division of brown algae can be further divided into 9 orders, 250 genera and over 1500 species which are mostly of marine occurrence (only 5 species occur in freshwater) and have a large diversity in their growing environment ranging from

temperate to cold ocean waters (**Bold and Wynne, 1978**). They are multi-cellular, photoautotrophic organisms with their main characteristics being described previously in **Table 1.1**.

Their photosynthetic pigments are chlorophyll a and c,  $\beta$ -carotene, fucoxanthin (which is responsible for the brown colour of this division of algae) and several other xanthophylls while their food reserve is primarily laminarin and mannitol, with sucrose and glycerol being present in some genera (**Sharma, 1986**).

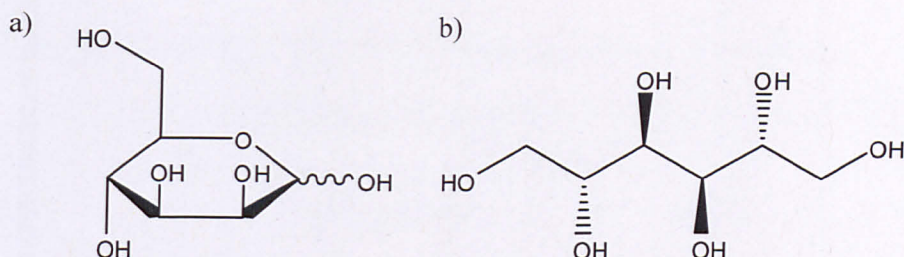
These two main food reserves are the major carbon storage compounds in monomeric (mannitol) or polymeric (laminarin) (**Davis et al., 2003**). Laminarin is composed of  $\beta$ -glucan with the main component being  $\beta$ , 1-3-linked glucans, containing large amounts of sugars and a low fraction of uronic acids (**Rioux et al., 2007**). There are two types of laminarin depending on the type of their polymer chain: in the first type glucose is attached to the end (G-chains) while in the second type mannitol is attached to the end (M-chains) (**Figure 1.7**) (**Chizhov et al., 1998**).



**Figure 1.7** The structure of the two types of laminarin with mannitol attached to the end (M-chains) or glucose attached to the end (G-chains) (**Davis et al., 2003**).

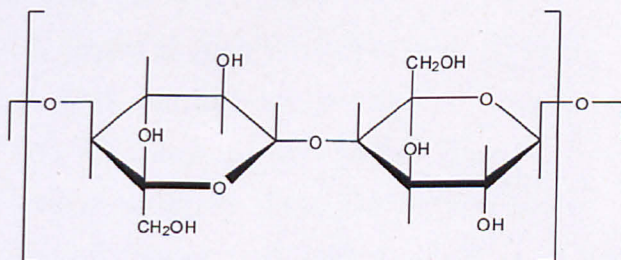
The proportion of laminarin in brown algae ranges between 2 and 34% of the algal dry weight (**Bold and Wynne, 1978**), while mannitol exists in 2% of laminarin in M-chains (**Lewis & Smith, 1967**).

Mannitol can be found also on its own, out of the M-chains, in a range of 5-25% of dry weight (**Lewis & Smith, 1967**). It is a sugar alcohol (polyol) derived from the 6 carbon sugar D-mannose (**Figure 1.8**) (**Davis et al., 2003**) and appears to be the primary product of photosynthesis (**Black, 1950b**).



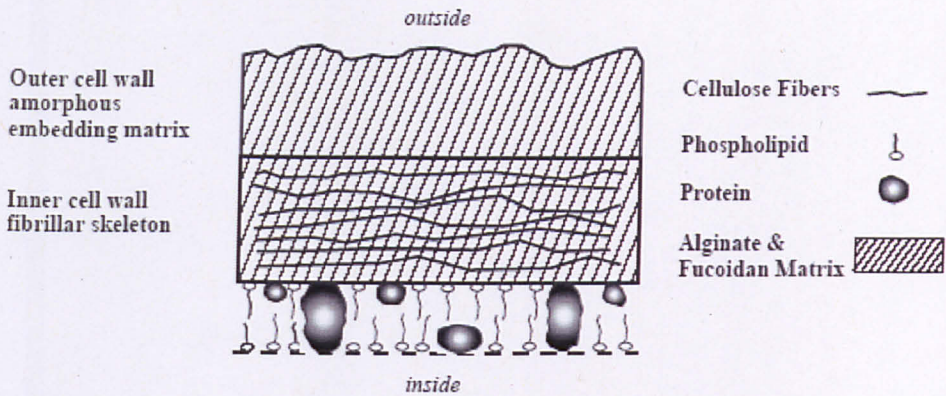
**Figure 1.8** The structure of a) D-mannose and b) mannitol.

The structure of the cell wall in almost all the brown algae is the same (**Sharma, 1986**). It is composed of cellulose, alginic acid and fucoidan (also known as fucan) as it was described in **Table 1.1**. The presence of cellulose (**Figure 1.9**) is believed to help reinforce the structure of the seaweed in order to be more resistant in wave action (**Black, 1950b**).



**Figure 1.9** Algal cellulose.

Cell walls are composed of an inner fiber skeleton and of an outer amorphous embedding matrix as shown in **Figure 1.10** (**Davis et al., 2003**). Alginic acids and sulphated fucans are the acid polysaccharides present in both sides of that wall (**Andrade et al., 2004**).

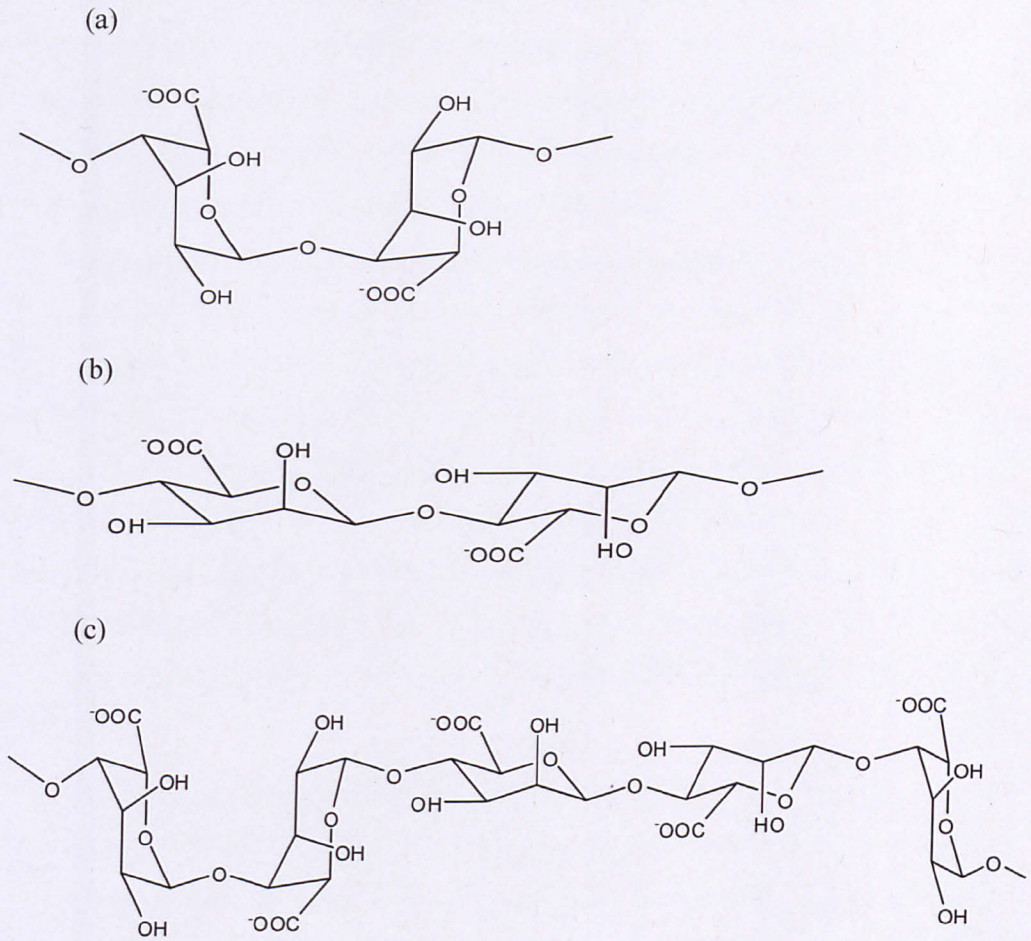


**Figure 1.10** The structure of cell wall in brown algae (Davis et al., 2003).

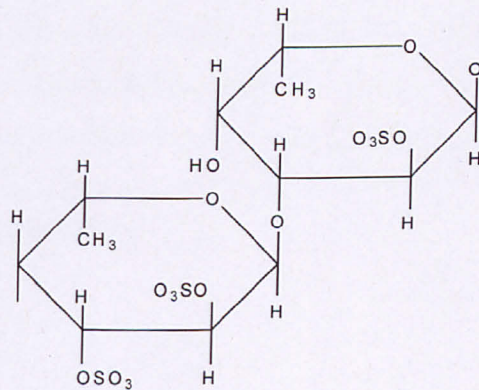
Alginic acid is the major polysaccharide in brown algae (Percival, 1979). It is a polymer of 5-carbon acids, D-mannuronic (M-block) and L-guluronic acid (G-block) with the formula  $(C_6H_8O_6)_n$  (Figure 1.11) and its salts, the alginates, have both structural and ion-exchanger roles (Bold and Wynne, 1978). The average length of these blocks is about 20 units with a different mixture of the two acids (Percival, 1979). The proportion of alginic acid in algae can be between 10 and 40% of the alga dry weight (Davis et al., 2003). Different parts of the algal thallus contain different proportions of the two uronic acids and therefore different proportion of alginic acid (Khotimchenko et al., 2001).

Fucans or fucoidan are the sulphated polysaccharides present in brown algae. They are composed mainly by L-fucose (a six carbon sugar) with small proportions of other sugars, such as mannose, galactose, xylose and glucuronic acid (Andrade et al., 2004; Percival, 1979). Fucoidan has an extremely complex structure and is shown on Figure 1.12. Its presence in the cell wall of brown algae protects them from desiccation (Percival, 1979). The proportion of fucans is 5 to 20% of alga dry weight (Davis et al., 2003). Mabeau and Kloareg (1987) suggested that there is a relation between the content of sulphated fucans and the species zonation, with the higher the species being in the intertidal region, the higher their fucan content.





**Figure 1.11** The structure of alginic acid (c) and its monomers (a) L-Guluronic acid (GG block) and (b) D-Mannuronic acid (MM block).

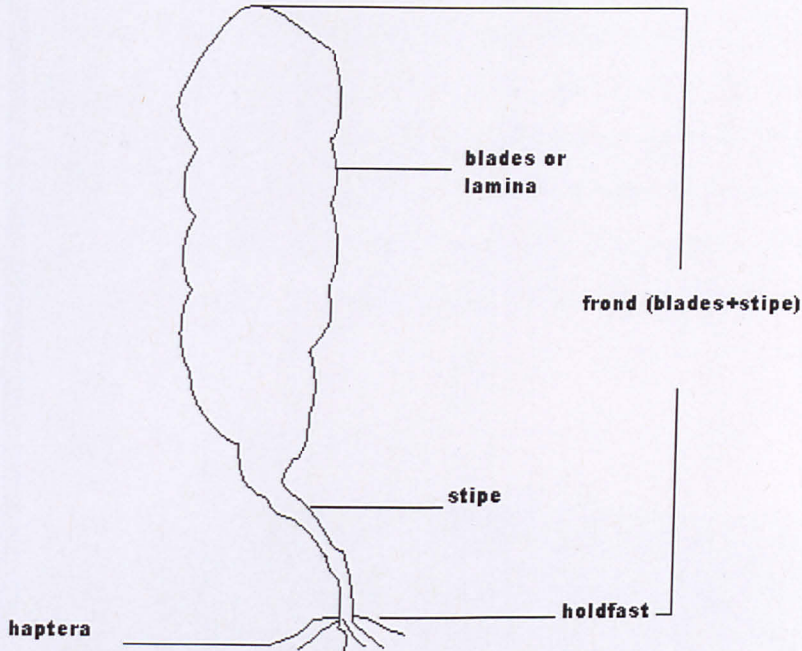


**Figure 1.12** Proposed main structural unit of fucoidan (Berteau and Mulloy, 2003).

### 1.4.2 Physiology

Seaweeds have similar physiology with terrestrial plants, but the naming of each part is different in aquatic and terrestrial species. There are three main parts, the holdfast, the stipe and the blades. A general diagram of a typical seaweed showing its different parts is shown in **Figure 1.13**. Starting from the bottom, there is the holdfast which consists of several haptera. The holdfast is similar with the roots of terrestrial plants but instead of obtaining nutrients like the roots, its main use is to help seaweed attach to rocky surfaces. Just above the holdfast there is the stipe, respective to the bole of a tree, which is very flexible in order to handle the pressure from the waves and avoiding seaweed from braking. The stipe connects the upper part with the blades (or often called laminas) which are similar to the leaves of a terrestrial plant and is the medium for producing energy from sunlight via photosynthesis. Sometimes between the blades and the stipe there is the float (or air bladders) which help the stipe and the blades float near the surface. The whole algal body is called the thallus while sometimes the stipe with the blades is referred to as the frond.

Each part of the seaweed contains different amounts of its constituents (e.g. laminaran, mannitol, alginic acid, ash etc.). Black, 1954 found that there are differences even in the same parts of seaweed. He divided the blade of *Laminaria saccharina* into five parts and showed that the part of the blade nearest the stipe has a high mannitol and ash content whilst the crude protein content is low and laminarin is almost absent. Total ash from the highest content near the stipe, showed a decrease in the middle parts of the blade followed by re-increase in the upper parts. The levels of mannitol and iodine showed a remarkable decrease when moving to the upper parts of the blade. On the contrary, contents of laminarin, crude proteins and alginic acid showed the opposite trend, increasing in upper parts, except the final one where a slight decrease was observed, while levels of cellulose were found to be steady in all parts of the blade.



**Figure 1.13** Parts of a seaweed plant.


### 1.4.3 Characteristics and chemical composition

In this study four different species of brown algae have been chosen for investigation, *Laminaria digitata*, *Laminaria saccharina*, *Laminaria hyperborea* and *Alaria esculenta*. The first three species belong to the Laminariales order, which is the largest and most structurally complex order of all algae and consists of perennial plants (**Bold and Wynne, 1978**). *Alaria esculenta* belongs to the family of *Alariaceae* which is very closely related to Laminariales, with their only difference being the presence of a midrib and special reproductive leaflets on the uppermost part of the stipe of *Alariaceae* (**Dickinson, 1963**).

#### 1.4.3.1 *Laminaria digitata*

*Laminaria digitata* (**Figure 1.14**) grows in rocky environments in the upper sub-littoral zone (until the depth of about 27.5m) just above that of *Laminaria hyperborea* (**Dickinson, 1963**). It is widely distributed in the Northern Hemisphere and is found in abundance in the British Isles coasts along with the European seaboard from Norway to Spain (**Drew, 1910**). It is a large brown seaweed, often referred to as 'kelp' or as 'tangle', with a thick cylindrical stipe, large 'leaves' or

fronds and masses of haptera which consists the holdfast, were the stipe is attached and which helps the plant get attached to rocks (Vincent and Gravel, 1986). The stipe is narrow at the top and expands into a flat and smooth lamina which consists of a number of lobes at the bottom (Drew, 1910). During the development of the plant lamina is increasing in length and width, until maturity, reaching over 60cm across the middle (Dickinson, 1963). Every early spring new lamina is forming, slowly replacing the old one (Dickinson, 1963). Its chemical composition is summarized in Table 1.2.

 algaeBASE



**Figure 1.14** Photograph of *Laminaria digitata* (Guiry, 2007a)

**Table 1.2** Chemical composition of *Laminaria digitata*.

<b>Parameter</b>	<b>%</b>	<b>References</b>
Ash	19-44 (blades)	Black, 1950b; Black, 1950a; Beavis and Charlier, 1987.
	29-42 (stipe)	
	22-43 (whole plant)	
Carbon	42-62	Darwin oceanics, 2008
Alginate	14-25.7 (blades)	Black, 1950b; Black, 1950a
	26.5-33.5 (stipe)	
	15-26.5 (whole plant)	
Cellulose	3-5 (blades)	Black, 1950b; Black, 1950a
	6-7.8 (stipe)	
	4-6 (whole plant)	
Laminaran	0.5-28 (blades)	Black, 1950b; Black, 1950a; Darwin oceanics, 2008
	0.5-24.5 (whole plant)	
Mannitol	3-29 (blades)	Black, 1950b; Black, 1950a
	4-14 (stipe)	
	4-20 (whole plant)	
Fucoidan	1.6-5.5	Marbeu and Kloareg, 1987; Darwin oceanics, 2008
Protein	4.5-14 (blades)	Black, 1950b; Black, 1950a; Marbeu and Kloareg, 1987; Darwin oceanics, 2008
	5.5-10 (stipe)	
	6.5-13 (whole plant)	

### 1.4.3.2 *Laminaria Saccharina*

*Laminaria saccharina* (Figure 1.15), being quite widespread in British coasts, grows in sheltered and rocky environments, quite similar to those of *Laminaria digitata*, from a little above the low tide mark until the depth of approximately nine to eighteen meters (Drew, 1910). Like *Laminaria digitata* it consists of a holdfast, a cylindrical stipe and fronds. The stipe is smaller, about 30cm, and the lamina consists of a single long tapering lobe (Drew, 1910). Fronds of *Laminaria saccharina* have a yellowish-brown colour distinguishing it from the other *Laminaria* species (Dickinson, 1963). It has been found to be the ideal seaweed species for winter temperature, with water temperature below 18°C (Beavis and Charlier, 1987). *Laminaria saccharina* is currently referred as *Saccharina latissima* and its chemical composition is summarized in Table 1.3.



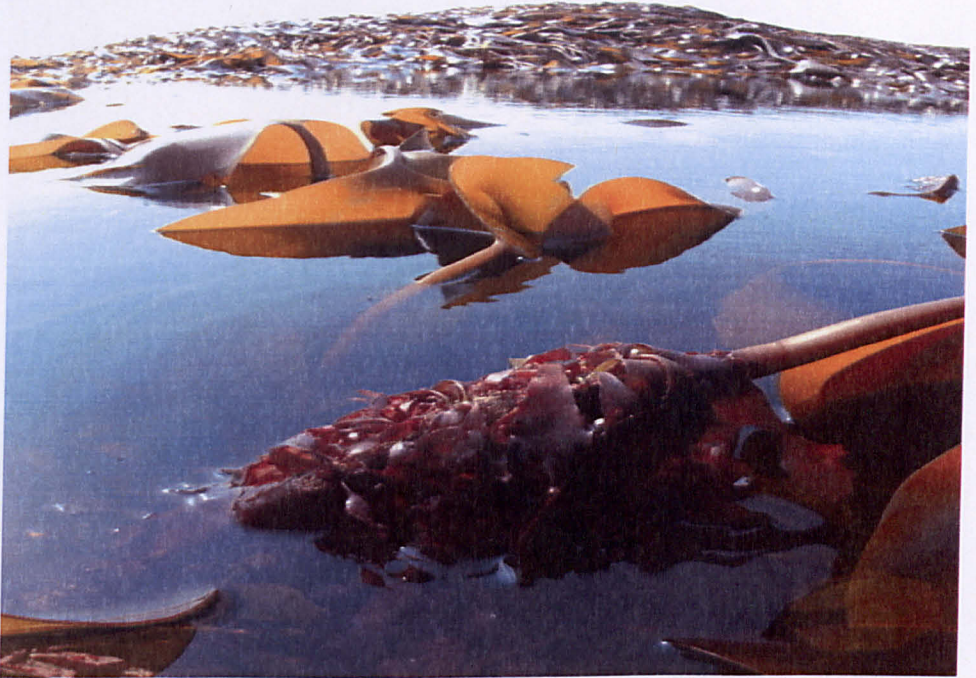
Figure 1.15 Photograph of *Laminaria saccharina* (Guiry, 2007b)

**Table 1.3** Chemical composition of *Laminaria saccharina*.

Parameter	%	References
Ash	24.12-34.18	Black, 1954; Obluchinskaya, 2008
Carbon	28 (DW, mean) 27.1 (DW, stipe) 27.5 (DW, blade)	Gevaert et al., 2001
Alginate	33.52-35.52	Obluchinskaya, 2008
Cellulose	4-5 (blades) 6.9-8 (stipe) 5-5.8 (thallus)	Black, 1950b; Black, 1950a
Laminaran	9-14.28	Black, 1954; Obluchinskaya, 2008
Mannitol	13-17.82	Black, 1954; Obluchinskaya, 2008
Fucoidan	7.9-9.7	Obluchinskaya, 2008
Protein	18.1% (blade)	Black, 1954
Fat	1.2-1.36	Obluchinskaya, 2008

### 1.4.3.3 *Laminaria hyperborea*

*Laminaria hyperborea* (Figure 1.16) grows on bedrocks from 8m depth till 30m depth and is rarely exposed in tides (Dickinson, 1963). It can be found in the north-eastern Atlantic, from Iceland to Norway and to Portugal (Sjotun et al., 1993). The length of the plant can reach up to 3.5m (Marlin, 2011a). The stipe can be between 0.3m and 1.2m in length, is hard, thick at the base (about 0.3m diameter) and is tapering as it get close to the blades (Dickinson, 1963). The blade is about the same length as the stipe, is divided into segments (up to 24) and has a shiny, golden brown to black brown colour (Dickinson, 1963; Marlin, 2011a). The holdfast is large, conical and is consisted of a number of haptera (Marlin, 2011a). The stipes of this specific specie is used as a raw material for the alginate industry (Dickinson, 1963). Its chemical composition is summarized in Table 1.4.



**Figure 1.16** Photograph of *Laminaria hyperborea* (Guiry, 2003)



**Table 1.4** Chemical composition of *Laminaria hyperborea*

Parameter	%	References
Ash	32.5-36.5 (stipe) 16-37 (blades)	Horn, 2000
Carbon	63.68	Chapman, 1970
Alginate	18.5-38 (stipe) 8.5-33 (frond)	Beavis and Charlier, 1987; Lunde (1937, 1938); Kirby, 1950
Cellulose	9.8-11.2 (stipe)	Horn, 2000
Laminaran	1.5-32.4	Black, 1950a
Mannitol	6.1-25.7	Levring et al., 1969
Fucoidan	2-4 (stipe)	Horn, 2000
Protein	5.86	Hoagland, 1915
Fat	0.77-1.67	Chapman, 1970

#### 1.4.3.4 *Alaria esculenta*

*Alaria esculenta* (Figure 1.18) grows in the northern hemisphere along rocky shores with strong wave exposure (Kraan et al., 2001). It is an olive to yellowish-brown plant with a distinct midrib and sporangia on the blades. The stipe is relatively small when compared with the other species as it reaches the length of 15cm while the blades can reach the length of 4m (Dickinson, 1963). The characteristic of this specie is the presence of midrib and the presence of sporangia on the blades. A research in the available literature for *Alaria esculenta* didn't find any information about the chemical composition of this seaweed.



**Figure 1.18 Photograph of *Alaria esculenta* (Guiry, 2006).**

#### **1.4.4 Seasonal variations in composition**

**Gevaert et al., 2001** studied the fluctuation of carbon and nitrogen content of *laminaria saccharina* during the year and found that carbon content increases during spring and summer with the highest values being at the end of the summer (31.4% DW) and the lowest being during winter (23.9% DW), while nitrogen content showed the opposite trend with the lowest values being in late spring (2.23% DW) and the highest being in late winter (3.42% DW).

The high summer values of carbon content can be explained by the fact that during summertime the photosynthetic activity is much higher; leading to accumulation of carbon as the carbon that assimilating is higher than the carbon consumed (**Gevaert et al., 2001**). Accordingly during spring and winter where the photosynthetic activity is lower, the accumulated carbon is being used for the production of new tissues in seaweed leading to lower carbon content.

The cellulose content of the plants varies throughout the year. On a dry basis the cellulose content from the maximum value around March begins to decrease

from April till June-July mainly because of the increase in mannitol levels (**Black, 1950b**). Then, after a slow increase till September, the cellulose content starts decreasing again, mainly because of the increase in laminarin content (**Black, 1950b**). Concluding, two maximum values (March/April and September/October) and one minimum value (June/July) of cellulose content are obtained throughout a year.

Mannitol levels vary throughout the year also. In most brown algae there is a minimum mannitol level during winter or early spring after which levels begin increasing reaching the maximum levels during October (**Black, 1950a**). This seasonal variation in mannitol content is often proportional to laminarin variation (**Lewis & Smith, 1966**), where maximum values are occurring between October and December (**Black, 1950a**).

Ash levels show exactly the opposite trend with mannitol and laminarin. During October when the mannitol and laminarin levels are in maximum the ash level is minimum while maximum values of ash are occurring during January (**Black, 1950a**).

Alginic acid content in brown seaweeds reaches its maximum value during winter and early spring (January-April) followed by a constant decrease until August when the minimum value is occurring (**Black, 1950a**).

Protein levels show a similar trend with alginic acid. Maximum levels of proteins are occurring during winter and early spring (January-March) followed by a constant decrease till August when the minimum value is occurring (**Black, 1950a**).

### **1.5 Current uses of species of interest**

Macro-algae throughout history until present have been used as human or animal food, fertilizer and manure. *Laminaria* and *Alaria* species among others are extensively consumed as food, because of their conciseness in minerals, vitamins and fatty acids, mostly in Asian countries such as China, Japan and Korea (**Hallmann, 2007**). The largest producer is China with a production of 5 million wet tones per year (**McHaug, 2003**). The use of seaweed in animal foods aims in enriching the nutrient content of animal feed and the main seaweed species used in order to accomplish that are *Ulva*, *Porphyra*, *Palmaria palmata*, *Gracilaria* and

*Alaria esculenta* (Hallman, 2007). Their application to soils (as composts) increases the water holding capacity and the plant growth, acting both as an organic fertilizer and as a solution to environmental problems (McHaug, 2003). Especially brown seaweeds, which contain large amounts of insoluble carbohydrates and trace metals, can act as good soil conditioners (by improving soil aeration and soil structure) and have good moisture retention properties (McHaug, 2003).

Apart from the traditional uses, seaweeds are also used for the production of valuable chemicals (McLean et al., 2002). Agars, carrageenans and alginates (derivatives of alginic acid), often referred to as 'industrial gums', are hydrocolloids located either in the cell walls or within the cells and can be extracted from the seaweed and used in a variety of food and industrial products (Carlsson et al., 2007). These polysaccharides are not found in terrestrial plants and they possess unique properties such as solubility in warm water and formation of gels when cooling (Carlsson et al., 2007). They are water soluble carbohydrates used as stabilizers in some products, as thickening agents in aqueous solutions in order to increase their viscosity, as gels or used to form water soluble films (McHugh, 2003).

Currently, the utilization of seaweeds offers annually the production of 40.000 t of Nori (food) out of 400.000 wet tonnes harvested, 7.630 t of agar out of 55.650 t of algae harvested, 33.000 t of carrageenan out of 168.400 t of algae harvested and 30.000 t of alginate out of 126.500 t of algae harvested (McHugh, 2003). Agar and carrageenan are extracted from different species of rhodophycophyta (red algae) while alginates are extracted from species of phaeophycophyta (brown algae), which are the species under investigation in this study.

The extraction of alginates is currently the main application of brown macro-algae harvested. Alginates and their salts, often referred as 'algins', are extracted mainly from the species of *Laminaria*, *Macrocystis* and *Ascophyllum* (Carlsson et al., 2007), as alginic acid is the major component of their cell wall. They are polymers of D-mannuronic and L-guluronic acids monomers and are found usually as a mixture of sodium, potassium, magnesium and calcium salts (McCormick, 2001). The alginate content varies in seaweeds and depends on the conditions, in which they grow, with turbulent growth conditions giving higher alginate content

(**McHugh, 2003**). Although alginates formed from brown seaweeds have a variety of applications, none of the brown algae species (apart from *Laminaria japonica* which is cultivated for food and sometimes the production is shifting to alginate production) is cultivated because the costs of cultivation are much higher than the costs of harvesting and transporting wild seaweeds (**McHaug, 2003**).

The usage of alginates lies on their main ability to form viscous solutions when dissolved in cold water and are used for thickening, forming gels, retaining water and providing suspending properties in solutions containing them (**Radmer, 1996**). The viscosity of the alginate when dissolved in cold water as well as the strength of the gel produced depends on the M/G (mannuronic acid /guluronic acid) ratio and on the way these units are arranged in the chain (**McHaug, 2003**). Alginates are commonly used as stabilizers for emulsions and suspensions in the food and pharmaceutical industry (**Carlsson et al., 2007**), as thickeners in the textile industry (**McHaug, 2003**), for cell immobilization and encapsulation (**Hallman, 2007**), for reducing fluffing in paper industry, as well as the calcium alginate is used in a variety of pharmaceutical and medical products (**McHaug, 2003**).

The main alginate product is sodium alginate but smaller quantities of calcium, ammonium and potassium salts as well as propylene glycol alginate are also being produced (**McHaug, 2003**). The production of sodium alginate can be achieved by two ways and has been described by **McHaug** and is shown in **Figure 1.19**. In both ways the goal is to convert all alginate salts (calcium, magnesium and potassium) into sodium alginate.

Calcium and magnesium salts are insoluble so they have to be converted to sodium salts. The procedure as described schematically in **Figure 1.19** is as follows. Firstly a solution of alkali (sodium carbonate) is added in order for the alginate to dissolve and give thick slurry. In this slurry there are parts of seaweed that do not dissolve such as cellulose and these parts are removed. The remaining solution is very viscous and has to be diluted in water before being filtered. Then precipitation of the alginate solution either by the calcium alginate or the alginic acid process is made. In the calcium alginate process, a calcium salt is added which causes calcium alginate to form a fibrous texture which cannot be dissolved in water, so calcium alginate can be separated. Then acid is added in order to convert the calcium alginate

fibres into alginic acid fibres which with the addition of alkali salts (such as sodium carbonate) and alcohol can be converted into sodium alginate. In the alginic acid process, acid is added in the sodium alginate solution and alginic acid gel is produced which can be separated from water as it does not dissolve. After dewatering of the gel, alcohol along with an alkali salt (sodium carbonate) is added to the alginic acid which converts it into sodium alginate.

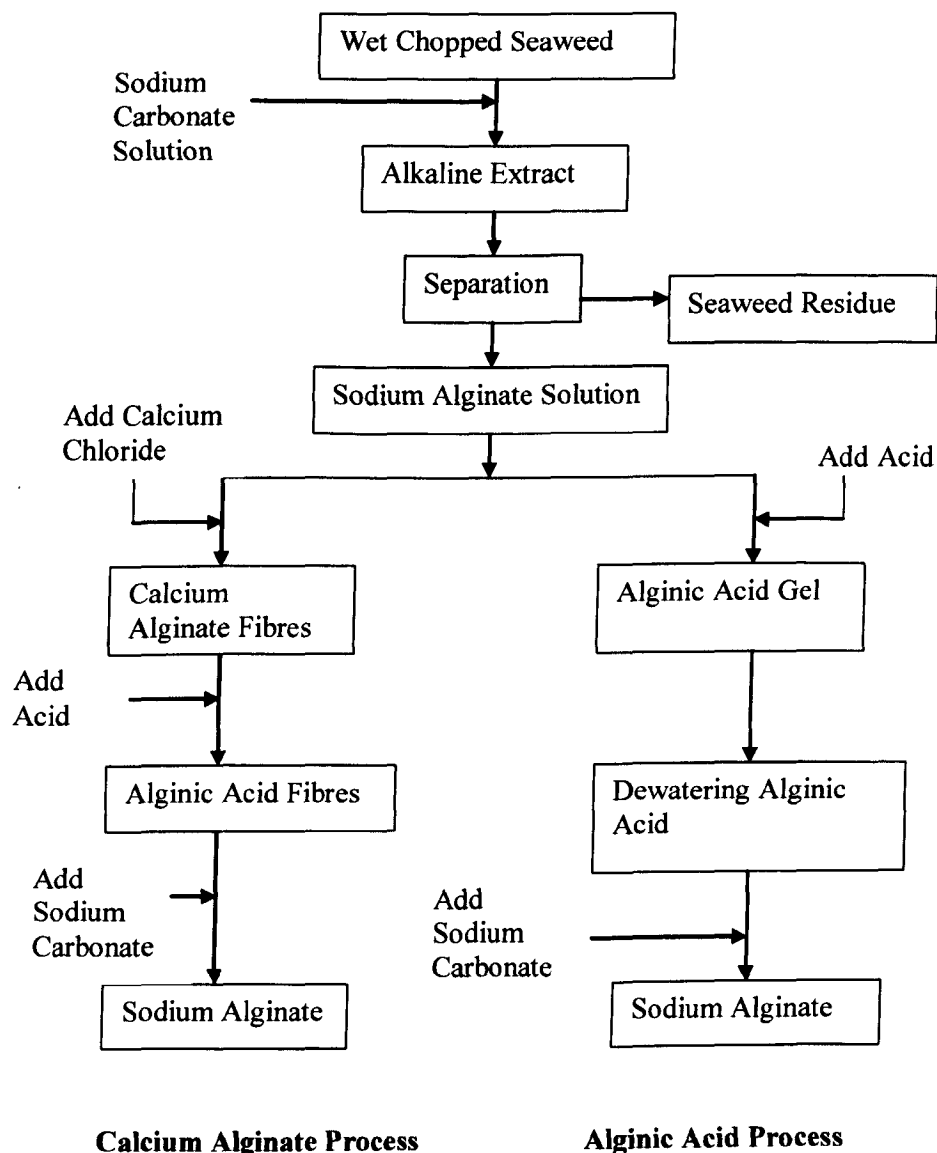


Figure 1.19 Diagram for the production of sodium alginate (McHaug, 2003).

Sodium alginate is the main alginate product from seaweeds, but is not the only one. In different stages of the precipitation processes calcium alginate and alginic acid are produced which can be removed, washed, dried and milled to certain particle size (**McHaug, 2003**). Also ammonium, calcium and potassium salts can be produced by neutralization of alginic acid by using certain alkali (such as ammonium hydroxide or potassium carbonate) among with water or alcohol (**McHaug, 2003**).

As well as the alginates, the rest of the carbohydrates of brown macro-algae have a variety of applications. Mannitol which is a sugar alcohol has extensive applications in the food, pharmaceutical, medical and chemical industries as a sweetening and texturing agent, in chewable tablets and granulated tablets, because of it is a powerful osmotic diuretic and finally because of its chemical inertia (**Saha and Racine, 2011**). Fucoidan, the sulphated polysaccharide present in brown algae, is receiving extended research for its medical and pharmaceutical applications due to its antiviral, anticoagulant, antitumour and antioxidant activity (**Barahona et al., 2011; Collic et al., 1991; Ponce et al., 2003; Synytsya et al., 2010**), while it is also used in a variety of cosmetics (**Fitton, 2007**).

## **CHAPTER 2 - Biomass conversion technologies**

### **2.1 Introduction**

Since the depletion of fossil fuels became apparent, a lot of technologies for converting biomass into fuels have been developing. These technologies are still in the development stage for terrestrial biomass and recently a lot of interest for utilising these for marine biomass conversion has been initiated. These technologies include biochemical methods such as fermentation, anaerobic digestion and transesterification and thermochemical methods which include combustion, gasification, pyrolysis and liquefaction. However, macro-algae have not received much attention since the focus so far has been constrained into utilising micro-algae. This chapter is going to present a short overview on the theory behind the biochemical and the thermochemical processes of biomass, as well as the available literature of the application of these processes with seaweed. Macro-algae have low lipid content so transesterification for the production of biodiesel is not under investigation. Also from the thermochemical processes gasification was not part of this research and will not be examined.

### **2.2 Biochemical Processes**

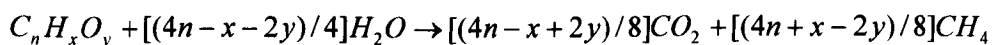
Biochemical processes utilize microbes, enzymes and bacteria to break down biomass components and convert them to other forms. They offer a significant advantage compared to most of the thermochemical processes, that they utilize wet feedstock. Macro-algae have high moisture content, so a wet conversion process would be ideal. Brown macro-algae (kelps) have been investigated through anaerobic digestion and fermentation for the production of biogas and ethanol respectively.

#### **2.2.1 Anaerobic digestion**

Organic matter can be converted into a gaseous fuel, called biogas, with the aid of anaerobic microbes through anaerobic digestion. Biogas is mainly composed of



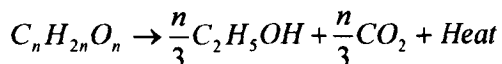
methane and carbon dioxide, with trace amounts of other gases such as carbon monoxide and hydrogen (Lim and Sims, 2004). During anaerobic digestion, energy is released by the break down of the substances without consuming any oxygen (Beavis and Charlier, 1987). There are three phases during anaerobic digestion (Jones, 2006): In the first phase fermentative bacteria hydrolyse the complex polysaccharides, proteins and lipids to lower molecular weight fragments, acetate, CO<sub>2</sub> and H<sub>2</sub>. Then, another group of bacteria break down the longer chain organic acid to alcohols and other degradation products to additional acetate, CO<sub>2</sub> and H<sub>2</sub>. Finally, methanogenic bacteria convert intermediate acetate to methane and carbon dioxide by decarboxylation. In general, the overall anaerobic digestion process can be summarized in the following equation (Lim and Sims, 2004):



Anaerobic digestion has been demonstrated for a variety of biomass feedstock, such as, weeds, woods, grasses, leaves, fruit and vegetable solid wastes, municipal solid wastes, freshwater and marine biomass (Gunaseelan, 1997). Brown algae such as *Laminaria hyperborea* (Hanssen et al., 1987), *Laminaria saccharina* (Hanssen et al., 1987; Toiano et al., 1976), *Ascophyllum nodosum* (Hanssen et al., 1987), *Macrocystis pyrifera* (Fernandez et al., 2008), *Durvillea antarctica* (Fernandez et al., 2008) and *Sargassum tenerrimum* (Tarwadi and Chauhan, 1987) have been successfully demonstrated for anaerobic digestion, with evolved methane yields ranging between 0.11 and 0.28 l/gVS. According to Gunaseelan (1997) the carbohydrates of brown algae contributing the most in biogas generation during anaerobic digestion are mannitol and the alginates, while protein and cellulose have the least contribution and laminarin and fucoidan have minimal influence.

### 2.2.2 Fermentation

Bioethanol can be produced by fermentation of the simple sugars present in biomass according to the following equation (Harun et al., 2011):



During fermentation a variety of microbial strains can be used in order to ferment the sugars contained in the seaweed to ethanol. Often the feedstock used has to be broken down (hydrolyzed) into hexoses and pentoses which then can be fermented (**Klass, 1998**). A variety of different feedstock has been investigated in fermentation like sugar cane, sugar beets, corn, maize and wheat crops, waste straw, willow and poplar trees, sawdust, reed canary grass, cord grasses, Jerusalem artichoke, miscanthus, sorghum plants (**Drewette et al., 2003**) and microalgae (**Harun et al., 2011**).

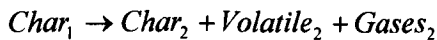
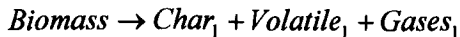
The utilization of seaweeds to produce ethanol is a relatively new concept currently receiving a lot of research. Brown macro-algae contain significant sugar content in the form of mannitol and laminarin. **Horn et al (2000a)** demonstrated the fermentation of mannitol, where an ethanol yield of 0.38 g of ethanol/g of mannitol was obtained, by fermenting a synthetic mannitol mixture. Similarly **Adams et al (2009)** successfully fermented samples of *Laminaria saccharina* yielding to a maximum 0.45 % v/v ethanol yield. In this study only the laminarin component of the alga was used. **Horn et al (2000b)** managed to ferment seaweed extract from *Laminaria hyperborea* containing both laminarin and mannitol yielding to a maximum 0.43 g of ethanol/g of extract yield. They found that mannitol is the preferred sugar in batch fermentations while in continuous fermentations laminarin was the preferred substrate.

### 2.3 Thermo-chemical processes

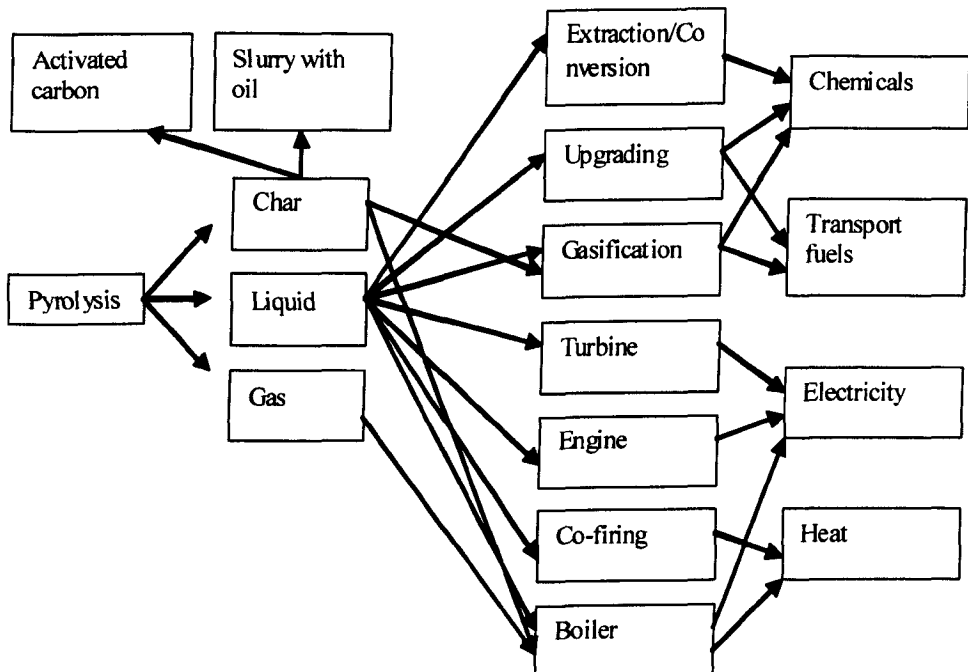
Thermochemical processes use heat in order to break down biomass components and convert them to other forms. Most of them require a relatively dry feedstock, (combustion, pyrolysis) so an additional drying stage is added in the total process before the feedstock is utilized for power. However, hydrothermal liquefaction involves the heating of the fuel with water, making the drying stage unnecessary. This advantage makes hydrothermal liquefaction ideal for the conversion of a wet feedstock such as seaweed.

### 2.3.1 Pyrolysis

Pyrolysis is the thermal decomposition of organic material occurring in the absence of oxygen/air. Generally it involves the heating of the organic material (biomass) at a range of 350-700°C under atmospheric pressure. This leads to the formation of three products, bio-oil which is the liquid part, char which is the solid part and gas. These products have a range of applications as shown in **Figure 2.1**. **Demirbas (2004)** proposed that biomass is converted under pyrolysis through the following two step mechanism:



where biomass is decomposed into volatiles, char and gases and then the formed volatile and gases can react with the char produced to form additional volatiles.



**Figure 2.1** Uses of pyrolysis products (Bridgwater, 2004; Goyal et al., 2008).

The yield distribution along with the properties of these products is affected by the specific conditions used such as the chemical composition of the biomass used, the heating rate, the temperature and the residence time (**Peng et al., 2001**). Slow

pyrolysis (low heating rate) favours the formation of solids (char) while fast or flash pyrolysis (high heating rate) favours the formation of liquids (bio-oil) or gases. There are several different types of pyrolysis, distinguished according to the residence time, the heating rate and the temperature used. The main types along with the conditions needed and the product distribution are shown in **Table 2.1**. From these types, flash pyrolysis for maximizing the liquid yield is of greater interest currently (**Bridgwater, 2004**).

**Table 2.1** Characteristics and product distribution of different types of woody biomass pyrolysis (**Bridgwater, 2004; Goyal et al., 2008**).

Pyrolysis type	Residence time	Heating rate	Temperature (°C)	Liquid	Char	Gas
Carbonisation	Hrs-days	5-7°C /min	400	30%	35%	35%
Flash (liquid)	<1s	300°C /min	<600	75%	12%	13%
Flash (gas)	<1s	300°C /min	>700	5%	10%	85%

The bio-oil is a high viscosity, highly oxygenated dark brown liquid with high water content and high acidity (**Klass, 1998**). It contains several organic and inorganic species (**Goyal et al., 2008**). The main organic groups present in the bio-oil obtained by pyrolysis of terrestrial biomass are acids, esters, alcohols, ketones, aldehydes, phenols, alkenes, nitrogen compounds, furans, guaiacols, syringols and sugars while the main inorganics present include Ca, Si, K, Fe, Al, Na, S, P, Mg, Ni, Cr, Zn, Li, Ti, Mn, Ln, Ba, V, Cl (**Goyal et al., 2008**). A typical wood derived bio-oil from flash pyrolysis has high conversion yield (up to 75%), but with high oxygen (45-50wt. %) and water (15-35%) content which leads to a low energy density (~18 MJ/Kg HHV), about half of that of petroleum (**Bridgwater, 2004**). However its density is higher (1.2kg/l) than that of a light fuel oil (0.85kg/l) so it has about 42% of the energy content of fuel oil on a weight basis but 61% on volumetric basis (**Bridgwater, 2004**).

The possible uses of pyrolysis oil were described in **Figure 2.1** but because of its high viscosity, thermal instability and corrosiveness it can not be used as a substitution to fossil fuels without further upgrading to reduce the oxygen content

(**Qi et al., 2007**). The technologies available for upgrading the bio-oil include hydrodeoxygenation, catalytic cracking of pyrolysis vapors, emulsification and steam reforming (**Qi et al., 2007**). However, a variety of chemicals can be extracted from bio-oil without further upgrading. Chemicals for food flavourings, pharmaceuticals and synthons, fertilizers, environmental chemicals and resins can be extracted from bio-oil (**Bridgwater and Peacocke, 2000**).

The char contains carbon and hydrogen along with various inorganic species while the gaseous fraction is composed mainly of CO, CO<sub>2</sub>, H<sub>2</sub>, CH<sub>4</sub>, C<sub>2s</sub> and C<sub>3s</sub> (**Goyal et al., 2008**).

Whilst the pyrolysis of terrestrial biomass has received enormous attention during the last decades, pyrolysis of marine biomass is a totally new concept. Currently most of the research has been focused on pyrolysing micro-algae rather than macro-algae. Pyrolysis of heterotrophic microalgal cells leads to higher conversion yields in bio-oil (above 50%) than that of lignocellulosic materials (**Peng et al., 2000; Miao and Wo, 2004**) with better bio-oil quality. **Miao and Wu, 2004** produced bio-oil from pyrolysis of the heterotrophic cells of *Chlorella protothecoides* with lower oxygen content (11.24 %), higher heating value (41MJ/kg), lower density (0.92kg/l) and lower viscosity (0.02 Pa s) than the oils produced from lignocellulosic biomass. Furthermore, the main pyrolysis reactions (depolymerizaion, decarboxylation, and cracking) take place at a lower temperature range (200-500°C) than those of woody materials (400-650°C) (**Peng et al., 2000; Peng et al., 2001a**) because of the different composition of micro-algae (protein, lipid and water soluble carbohydrate) and woody biomass (cellulose, lignin and hemicellulose) (**Peng et al., 2001b**).

More recently, seaweed biomass has been also investigated under pyrolysis. **Wang et al (2006)** compared the thermolysis characteristics of seaweed (brown, green and red macro-algae) and fir wood and found that seaweed devolatilise at a lower temperature than wood, due to its lower thermal stability. Similar observation was made by **Wang et al., 2007** during their study on the pyrolysis characteristics of a green macro-alga by thermogravimetric analysis. Hence the temperature needed for the pyrolysis of seaweed, in proportion to micro-algae, is lower than the one needed for terrestrial land plants.

**Ross et al (2008)** found significant differences in the composition of bio-oil produced from flash pyrolysis of brown seaweeds and terrestrial biomass. Bio-oil obtained from seaweed was found to contain much more nitrogen containing compounds (such as pyrrole and indole) and furan derivatives while significantly less phenolic compounds and no methoxyphenols which are very commonly formed in pyrolysis of woody biomass (due to the absence of lignin in seaweeds). Other compounds identified in the bio-oil included linear chain alcohols, many compounds with sterol type structure (such as iso-sorbide) and the main sugar unit was di-anhydro mannitol.

**Bae et al (2011)** found that pyrolysis of seaweed results in less bio-oil, with maximum yield occurring at lower temperature (500°C) than pyrolysis of lignocellulosics. Their study on the pyrolysis of two brown seaweed (*Undaria pinnatifida* and *Laminaria japonica*) resulted in 39.5 wt% and 37.5 wt% bio-oil yield respectively but with high water content (39 wt% and 43.6 wt% respectively). The high heating values of the bio-oils were relatively high after separation of the water phase (23.33 MJ/kg and 33.57 MJ/kg respectively). Similar results were obtained by **Choi et al (2011)** during the pyrolysis of *Laminaria japonica* in a fluidized bed reactor. Maximum bio-oil yield of 35.4 wt% was obtained at 425°C pyrolysis temperature with 70.7 wt% water content.

**Choi et al (2011)** also studied the resultant bio-char from pyrolysis of *Laminaria japonica* at 425°C. The char was found to be low in carbon content (20.7 wt %), high nitrogen content (1.63 wt %) and rich in inorganic matter (10.5 wt% K, 2.92 wt% Na and 1.01 wt% Ca). This suggests that seaweed bio-chars have low carbon sequestration potential but can provide nutrient benefits when applied to poor soils. **Bichat et al (2010)** demonstrated another possibility of utilizing brown seaweed bio-chars. They pyrolysed the brown macro-algae *Lessonia nigrescens* in a tubular furnace, at a final temperature of 700°C, and the resulting bio-char was found to have relatively high specific surface area (750-1080 m<sup>2</sup>/g) and high oxygen content (10-15 wt%) with possible application as electrodes for supercapacitors.

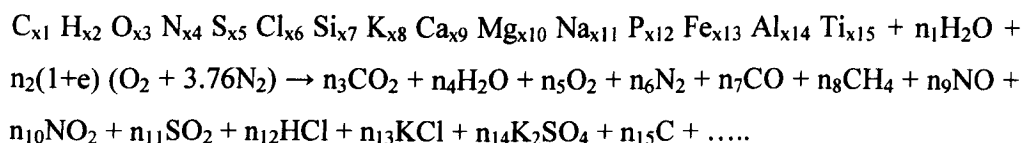
### 2.3.2 Combustion

Combustion is the burning of a fuel in the presence of air, converting the chemical energy stored in the fuel into heat and gases at temperatures above 800°C.

It usually takes place in stoves, furnaces, boilers, steam turbines, turbo generators etc. (McKendry, 2002b). Alternative to conventional fuels (e.g. coal), biomass can also be used for combustion. A variety of different biomass fuels can be combusted, but in practice only biomass fuels with less than 50% moisture can be combusted (McKendry, 2002b). The combustion process of biomass propagates in three steps (Williams et al., 2001):

1. devolatilisation to volatiles and char,
2. combustion of the volatiles and
3. combustion of char.

Because of the high moisture content of biomass fuels compared to coal a drying step is added before the beginning of the combustion process (Williams et al., 2001). Biomass combustion can be described by a global reaction proposed by Jenkins et al (1998):



As it can be seen from the previous equation combustion of biomass is a very complex reaction. Thus, in order to have an accurate prediction of the behaviour of biomass fuels upon combustion, the physical, chemical, thermal and mineral properties of the fuels have to be known (Demirbas, 2004). However, knowledge of these properties for every different biomass fuel is unrealistic, so correlations of some of these properties such as the heating values, the H/C and O/C ratios, the ash content, the inorganic composition, the nitrogen and sulphur content etc. have been proposed in order to classify the different biomass fuels (Jenkins et al., 1998; Williams et al., 2001).

Whilst terrestrial biomass has received much attention under combustion, and has been successfully demonstrated and applied in co-combustion in coal-fired plants (McKendry, 2002b), marine biomass has received little attention. A few studies have been made on the combustion characteristics of brown seaweed and was found that seaweed biomass has higher ash and moisture content while its thermal value (HHV) and oxygen content is lower than in lignocellulosic biomass

(Ross et al., 2008; Wang et al., 2008; Wang et al., 2009; Yu et al., 2008). Their ash is rich in inorganic material and especially alkali metals such as K and Na which lower the ash fusion temperature of seaweed biomass (Wang et al., 2009; Yu et al., 2008) that could possibly lead to problems related with slagging, fouling and agglomeration in conventional combustion chambers. Wang et al (2008) studied on the fusion characteristics of seaweed ash and found that at 815°C the ash is melting while at 600°C slag adhesion phenomena were observed. Seaweed biomass is easy to ignite as their mass loss starts earlier than terrestrial biomass but is harder to burn out (Wang et al., 2009; Yu et al., 2008).

### 2.3.3 Liquefaction

Petroleum that is nowadays drilled from underground, originates from biomass materials. These materials have been converted into petroleum by natural mechanisms of applying high pressure and temperature over millions of years. These natural mechanisms can be accelerated in reactors using high pressure (up to 20MPa) and temperature (up to 400°C). In this way processing time is reduced to minutes. The resulting intermediates can be converted to hydrocarbon fuels and commodity chemicals for products similar to those produced by petroleum. Therefore, liquefaction is a process of ‘simulating’ nature.

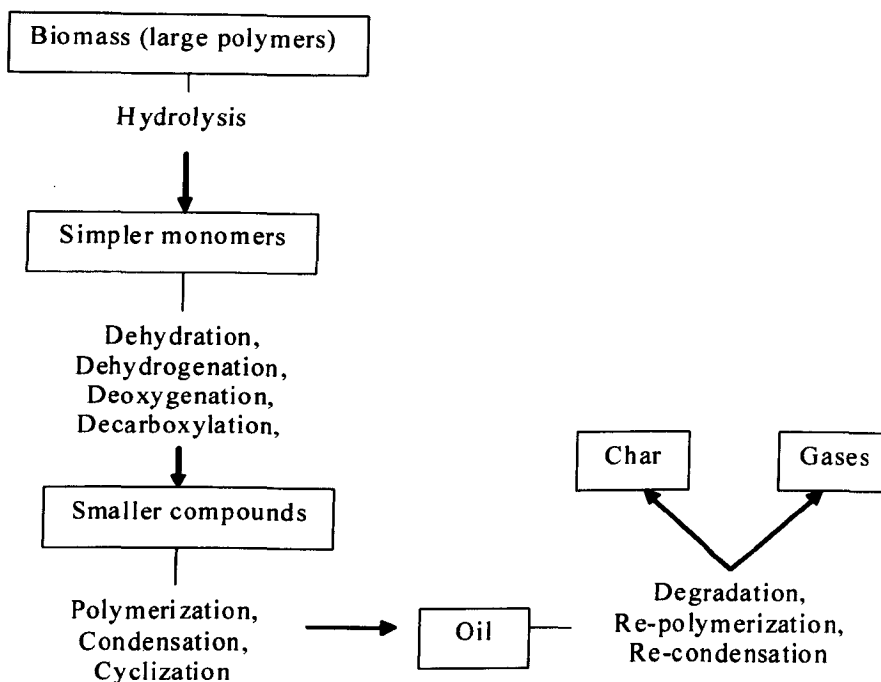
Because of the high pressures required for the liquefaction process, a high pressure resistant autoclave is required, into which the reactants including biomass feedstock, water or/and solvent and catalyst are being heated. While water is heated, it expands to create high pressure in the reactor. Under these conditions biomass is decomposed into a variety of products in the three phases (liquids, solids and gases). Control of the reaction conditions can favor any of the three phases. The liquid products include the bio-crude fraction (often referred to as bio-petroleum or bio-oil) and an aqueous phase. The bio-crude resembles crude oil but has a very high viscosity which makes it difficult to handle and is produced in lower yields than pyrolysis oil (Goyal et al., 2008). It can be upgraded into a transport fuel or as a feedstock for providing valuable chemicals. The aqueous phase consists of a large organic fraction dissolved in water (often referred to as water soluble hydrocarbons WSH). The solid product is bio-char (often referred to as residue) while the gaseous fraction consists mainly of carbon dioxide.



There are several important parameters when considering hydrothermal liquefaction. These are water, biomass composition, temperature, catalysts and solvents.

When undergoing liquefaction process, it is necessary for the presence of a medium that can act as a hydrogen donor for the reactions. Water not only acts like the hydrogen donor, but is necessary for the hydrolysis of the high molecular weight carbohydrates that are present in biomass (**Appell, 1967**). In hydrolysis, water can act both as the solvent and as the reactant (**Kruse and Dinjus, 2007**). Hydrolysis is responsible for the reduction of the oxygen content of the products, which is the main advantage of liquefaction resulting in a higher heating value. The key to production of a liquid fuel is to maintain water below its critical point (the critical point of water occurs at a temperature of 374.3°C and a pressure of 22.12MPa). Water below this critical temperature and pressure is usually referred as superheated water and organic compounds are more soluble in superheated water because of its higher temperature, lower polarity, density and dielectric constant (**Kruse and Dinjus, 2007**). Above that critical conditions water vapour cannot be liquefied no matter the pressure applied. In the presence of supercritical water, biomass is completely dissolved and favours the production of gaseous fuels (**Feng et al., 2004**).

The liquefaction process does not require pre-drying of the feedstock, unlike other thermochemical processes (pyrolysis, combustion) where biomass must be dry. Hence liquefaction seems an ideal process for the conversion of seaweeds as their water content is extremely high. This is an important benefit of liquefaction because the overall cost of the process is decreased as no drying processes are needed (**Yang et al., 2004**). Under liquefaction, biomass components are hydrolyzed and are ultimately converted into oil. A simplified reaction scheme for the liquefaction process is shown in **Figure 2.2**.

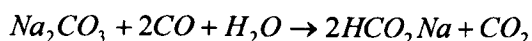


**Figure 2.2** Simplified scheme for the liquefaction process.

The presence of superheated water in the reactor hydrolyzes the biomass macromolecules and they are degraded into smaller fragments which then are further degraded into even smaller compounds by dehydrogenation, dehydration, deoxygenation and decarboxylation (Demirbas, 2004). These newly formed compounds, being unstable and reactive (Demirbas, 2001), can rearrange through condensation, cyclization and polymerization (Demirbas, 2004) to form new oily compounds. However, careful control of the experimental conditions can avoid re-polymerization or re-condensation of the newly formed products (Zhong et al., 2004). Through this mechanism biomass is transformed into oil which is the main product and into the by-products which are water soluble hydrocarbons (WSH) gases and residue. A variety of different biomass feedstocks have been investigated by liquefaction. These include wood and wood residues, grasses, algae, straws, barley, sludge from waste treatment facilities, animal waste and garbage from domestic houses and food processing industries. The obtained oil and WSH consist of numerous compounds, each of which originates from the decomposition of the main biomass components.

Raw biomass has usually a significant metal content (metals such as Al, K, Fe, Ca, Mg, Na, P, Zn etc.) which can act as a catalyst for hydrolysis. However, this content is usually not enough and catalysts are used to supplement these natural catalysts for increasing the rate of hydrolysis (**Bridgwater, 1994**). Though, little description has been made about their role in liquefaction. **Appell (1967)** proposed the following mechanism for the conversion of carbohydrates to oil by using sodium carbonate ( $\text{Na}_2\text{CO}_3$ ) as catalyst and carbon monoxide as the reducing agent:

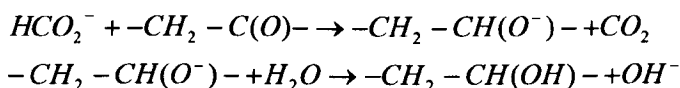
Reaction of sodium carbonate and water with carbon monoxide to yield sodium formate



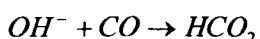
Dehydration of vicinal hydroxyl groups in a carbohydrate to an enol, followed by isomerization to a ketone



Reduction of the newly formed carbonyl group to the corresponding alcohol with formate ion and water



The hydroxyl ion reacts with additional carbon monoxide to regenerate the formate ion



The most commonly used catalysts are potassium hydroxide (KOH), sodium hydroxide (NaOH), sodium carbonate ( $\text{Na}_2\text{CO}_3$ ) and potassium carbonate ( $\text{K}_2\text{CO}_3$ ) but others can be used. Generally hydroxides, carbonates, bicarbonates and formates of the alkali metal are used as catalysts (**Appell, 1967**). They have a direct effect on the product oil yields. The addition of catalyst usually increases the conversion of raw biomass and this conversion is proportional to the ratio of catalyst to the sample (**Akdeniz and Gundogdu 2007; Demirbas et al., 2000**). However, there is an upper limit of this ratio above which the conversion is decreasing. Also for the same sample different catalysts have different effect in the conversion of biomass into oil (**Akdeniz and Gundogdu 2007; Demirbas et al., 2000**). Apparently their effect

relies on the metal content of raw biomass, but the writer is not aware of any related research (e.g. if the use of a hydroxide or carbonate of the highest content alkali metal of the feedstock will have the highest conversion or if the use of a different hydroxide or carbonate alkali metal will give the highest yield). There has to be a specific catalyst for each biomass feedstock that can give the higher conversion for that particular feedstock.

The conversion of biomass to oil has been studied in the temperature range of 250-400°C. Below 250°C the reaction appears to be slow while for temperature greater than 375°C, water becomes supercritical and this complicates the interpretation of the results (**Appell, 1967**). The increase in temperature is followed by an increase in the conversion to product oil (**Demirbas, 2005; Murakami et al., 1990; Qu et al., 2003**). However, there seems to be a threshold in temperature of each biomass sample above which further increase leads to the decrease of conversion (**Qu et al., 2003; Murakami et al., 1990**). This is due to the competition of hydrolysis and repolymerization which are the main reactions involved in liquefaction (**Qian et al., 2007**). On the contrary, the increase in temperature is always followed by an increase in HHV of the product oil (**Demirbas, 2005; Murakami et al., 1990; Qu et al., 2003**). This occurs because the increase in temperature is reducing the oxygen content of the oil produced and the HHV is higher for a product with less oxygen content. The higher the oxygen content the greater the water solubility of the oil (which decreases the energy density of the oil) and therefore less energy is released during combustion (**Akdeniz et al., 2007**). In hydrothermal liquefaction, oxygen can be removed either as water by dehydration or as carbon dioxide by decarboxylation (**Goudriaan et al., 2000; Peterson et al., 2008**). If the removal is as carbon it leads to a higher H/C ratio of the product oil and therefore a higher HHV (**Goudriaan et al., 2000; Peterson et al., 2008**). Generally, liquefaction oils have lower oxygen content (thus higher heating value) and therefore are higher quality products than pyrolysis oils (**Bridgwater, 1994**), but have lower yields than pyrolysis oils. Typically liquefaction oils have less than 15wt. % oxygen and have a heating value 25-40 MJ/Kg, while pyrolysis oils have about ~35wt.% oxygen and 20-25 MJ/kg HHV (**Bridgwater, 1994**).

**Table 2.2** Yields and HHVs of oils obtained by hydrothermal liquefaction of lignocellulosic biomass.

Lignocellulosic biomass	Catalyst	Yield (wt. %)	HHV (MJ/kg)	Reference
Wood	K <sub>2</sub> CO <sub>3</sub>	32.21	29.3	Zhong and Wei, 2004.
Wood ( <i>Cunninghamia lanceolata</i> )	-	23.78	30.2	Qu et al., 2003.
Oak	Na <sub>2</sub> CO <sub>3</sub>	56.7	25.1	Ogi et al., 1994
Sawdust	-	8.6	-	Karagoz et al., 2005.
Rice husk	-	8.3	-	Karagoz et al., 2005.
Cellulose	-	3.2	-	Karagoz et al., 2005.
Lignin	-	3.9	-	Karagoz et al., 2005.
Rice straw	-	10	42.79	Wang et al., 2007.
Legume straw	-	10.5	43.34	Wang et al., 2008
Cotton stalk	-	5.2	44.38	Wang et al., 2008
Corn stalk	-	8.1	44.41	Wang et al., 2008
Wheat straw	-	8.2	41.42	Wang et al., 2008

**Table 2.2** shows the yields and higher heating values (HHVs) of oils produced by hydrothermal liquefaction of lignocellulosic biomass. The bio-oils have high heating values comparable with the HHV of petroleum crude (42.7 MJ/kg) but the yields are low (8.3 – 32.1 wt. %). The study by **Ogi et al (1994)** gave high oil yield (56.7 wt. %) but the liquefaction medium was 2-propanol instead of water. Other liquefaction mediums apart of water have been proposed such as propanol, butanol, acetone, methyl ethyl ketone, tetralin and ethyl acetate in order to improve product yields and properties (**Demirbas, 2004; Ogi et al., 1994; Yan et al., 1999**). Other schemes that have been proposed in order to improve oil yields include using different process gases in the reactor. Yin et al (2010) found that use of CO<sub>2</sub>, H<sub>2</sub> and N<sub>2</sub> as process gases improved the oil yields from liquefaction of cattle manure with CO<sub>2</sub> having the greater influence.

Microalgae that have a different biochemical composition than lignocellulosic biomass have higher oil yields in hydrothermal liquefaction. **Table 2.3** shows the yields and higher heating values (HHVs) of oils produced by hydrothermal liquefaction of microalgae. While during liquefaction of terrestrial biomass the addition of catalyst is usually increasing the oil yields this is not the case for microalgae. Yields as high as 43 wt. % have been reported, without the addition of catalyst in the reactants, with HHV remaining at high values. This can be attributed in the different biochemical composition of microalgae such as the absence of lignin and the higher lipid content.

Whilst hydrothermal liquefaction of microalgae and other wet biomass feedstocks, such as cattle manure, sewage waste, swine manure etc., are receiving a lot of interest lately, there is only one study published on hydrothermal liquefaction of macro-algae. Recently, a study on the hydrothermal liquefaction of the green seaweed *E. prolifera* was made by Zhou et al (2010) which showed maximum yield of bio-crude of 23 wt. % with an energy density of 29.89 MJ/kg.

**Table 2.3** Yields and HHVs of oils obtained by hydrothermal liquefaction of microalgae.

Microalgae	Catalyst	Yield (wt %)	HHV (MJ/kg)	Reference
<i>Microcystis viridis</i>	Na <sub>2</sub> CO <sub>3</sub>	39.5	31	Yang et al., 2004.
<i>Spirulina</i>	Na <sub>2</sub> CO <sub>3</sub>	20	34.8	Ross et al., 2010.
<i>Spirulina</i>	KOH	15.2	33.4	Ross et al., 2010.
<i>Spirulina</i>	HCOOH	14.2	35.6	Ross et al., 2010.
<i>Spirulina</i>	CH <sub>3</sub> COOH	16.6	35.1	Ross et al., 2010.
<i>Spirulina</i>	-	29	36.8	Biller and Ross, 2011.
<i>Chlorella</i>	Na <sub>2</sub> CO <sub>3</sub>	27.3	37.1	Ross et al., 2010.
<i>Chlorella</i>	KOH	22.4	39.9	Ross et al., 2010.
<i>Chlorella</i>	HCOOH	19.1	35.1	Ross et al., 2010.
<i>Chlorella</i>	CH <sub>3</sub> COOH	20.4	33.2	Ross et al., 2010.
<i>Chlorella</i>	-	~ 36	35.1	Biller and Ross, 2011.
<i>Dunaliella tertiolecta</i>	Na <sub>2</sub> CO <sub>3</sub>	25.8	30.74	Shuping et al., 2010.
<i>Nannochloropsis</i>	-	~ 36	34.5	Biller and Ross, 2011.
<i>Nannochloropsis</i>	-	43	39	Brown et al., 2010.
<i>Porphyridium</i>	-	~ 20	35.7	Biller and Ross, 2011.

## 2.4 Aims and Outline the Thesis

During this investigation several factors were assessed in order to develop a basic understanding of the thermochemical decomposition of brown macro-algae biomass. The main aims of this investigation were to examine the variation of fuel properties of macro-algae with site, season, species and different parts of the macro-alga plant and to evaluate macro-algae for their thermochemical conversion potential. In order to achieve this the following tasks were considered:

- A detailed literature review on how macro-algae can contribute to the overall biomass potential. This included a review on published literature for the types of macro-algae, their chemical composition, their industrial uses, the possibility of cultivation and potential yields.
- Thermal studies on macro-algae carbohydrates and how they might affect the thermochemical processes.
- Chemical and thermochemical analysis (ultimate, proximate, ash, CV, py-GC/MS, TGA etc.) of macro-algae harvested from different locations around the UK and during different harvest periods (winter, spring, summer, autumn).
- Hydrothermal liquefaction trials including influence of reaction conditions on the products, mass balances, energy balances, influence of macro-algae chemical composition and analysis of the liquefaction products.

A summary of the global energy scene and its relation to climatic concerns as well as the policies applied is provided in chapter 1. It continues with a brief description of the role of biomass in the energy sector, its possibilities and limitations before focusing on marine biomass and more specifically on brown macro-algae. A description of their physiology, structure and harvesting methods is provided before focusing on their characteristics and chemical composition. Finally a brief description of the current uses of brown macro-algae is given.

Chapter 2 gives an overview of the available conversion processes of macro-algae into fuels. A brief description of the bio-chemical processes such as fermentation and anaerobic digestion is given, before describing in more detail the thermochemical processes such as pyrolysis, combustion and hydrothermal



liquefaction. The last section of this chapter summarizes the work presented in this thesis. The sources of the fuels as well as the various methods and equipment used for analysis are described in chapter 3.

Chapter 4 presents thermal analysis in both inert and oxidative atmospheres of model carbohydrates of brown macro-algae. Model seaweed carbohydrates were investigated in order to understand the thermal decomposition of seaweed biomass. Correlations between the decomposition of each carbohydrate with the decomposition of the seaweed plant material were also made. Work presented in this chapter was published in two journals, *Fuel* and *Journal of Applied and Analytical Pyrolysis* (Anastasakis et al., 2011a; Ross et al., 2011).

Chapter 5 presents a series of standard fuel analyses performed on four brown macro-algae species harvested from different locations and during different period of year. The results illustrate the differences between the samples, their differences according to their harvest location and their seasonal variation in their properties as fuels. Some work presented on this chapter was published in the journal *Bioresource Technology* (Adams et al., 2011) and in a conference journal (Anastasakis et al., 2010).

Chapter 6 presents work carried out to investigate the pyrolysis process of brown macro-algae. The different parts of seaweed plant material such as blades and stipes, as well as samples harvested during different season of the year, were examined during pyrolysis process on an analytical scale. The devolatilization of brown macro-algae was linked with the degradation of their carbohydrates. Finally the influence of two pre-treatment methods for macro-algae on the pyrolysis process was examined. Some of the results were published in the journals of *Bioresource Technology* (Adams et al., 2011) and the *Journal of Applied and Analytical Pyrolysis* (Ross et al., 2009).

Chapter 7 examines the combustion process of brown macro-algae. Their high inorganic ash content has been assessed through empirical indexes to assess the fouling probability of macro-algae during combustion and how it varies seasonally. The influence of two pre-treatment methods on the seaweed fuel properties was also

assessed. Some of the results were published in the journal *Journal of Applied and Analytical Pyrolysis* (**Ross et al., 2009**).

Chapter 8 presents work that has been carried out to convert brown macro-algae into fuels through hydrothermal liquefaction. The effect of the reaction conditions such as temperature, pressure, biomass and water loading, residence time and catalyst dosage, on product yields and properties was assessed. A subsequent energy balance for the process was performed.. After optimisation of the reaction conditions, the influence of the different sample composition during hydrothermal liquefaction was assessed. Finally a comparison of hydrothermal liquefaction with the biochemical processes for conversion of brown macro-algae into bio-energy was made. Some of the results were published in the journal of *Bioresource Technology* (**Anastasakis et al., 2011b**).

Each results chapter contains a conclusion section discussing the main findings of each chapter. The final chapter, chapter 9, presents a summary of the main findings on the different thermochemical processes for utilising brown macro-algae. Finally, the second section in this chapter provides recommendations for future research, which completes the chapter and the thesis.

## CHAPTER 3 - Experimental

### 3.1 Introduction

This investigation forms part of the Supergen II programme investigating all steps in the bioenergy chain from production of biomass to delivery of a useful and valuable energy product, such as heat, power, and transport fuels. This programme investigates the production of different types of biomass and investigates their behaviour in different conversion processes, with particular emphasis on the interaction and interface between production and conversion. The resources theme includes an investigation of alternative biomass resources through a plus activity which is focused on the potential for production of bio-energy, fuels and chemicals from marine biomass. This plus activity involves an evaluation of the potential to exploit the macro-algae resource in the UK. This work is focused on the characterization and conversion of macro-algae.

The main objectives of this evaluation can be broken down into 6 main themes including:

- **TASK 1:** A selection of candidate species of marine biomass with best potential to contribute significantly to the UK biomass resource, and to compare their properties and yields to terrestrial sources.
- **TASK 2:** To perform an investigation of the potential to culture the selected candidates for farming.
- **TASK 3:** Characterisation and evaluation of the selected biomass for their suitability to different conversion routes
- **TASK 4:** To perform an evaluation of the total biomass availability around the UK available for harvesting.
- **TASK 5:** An examination of the sustainability and environmental issues associated with increased use of seaweeds, public acceptability and life cycle analysis.
- **TASK 6:** And finally to perform a techno-economic assessment of the preferred processes.

This work contributes to TASK 3 and is mainly focussed on the characterisation and conversion of macro-algae by thermochemical processing

### 3.2 Species selection

Species selection and cultivation trials have been led by The Scottish Association of Marine Sciences (SAMS) in Oban with the assistance from the seaweed centre in Galway. The selection process has chosen four seaweeds for culture including:

*Laminaria digitata*,

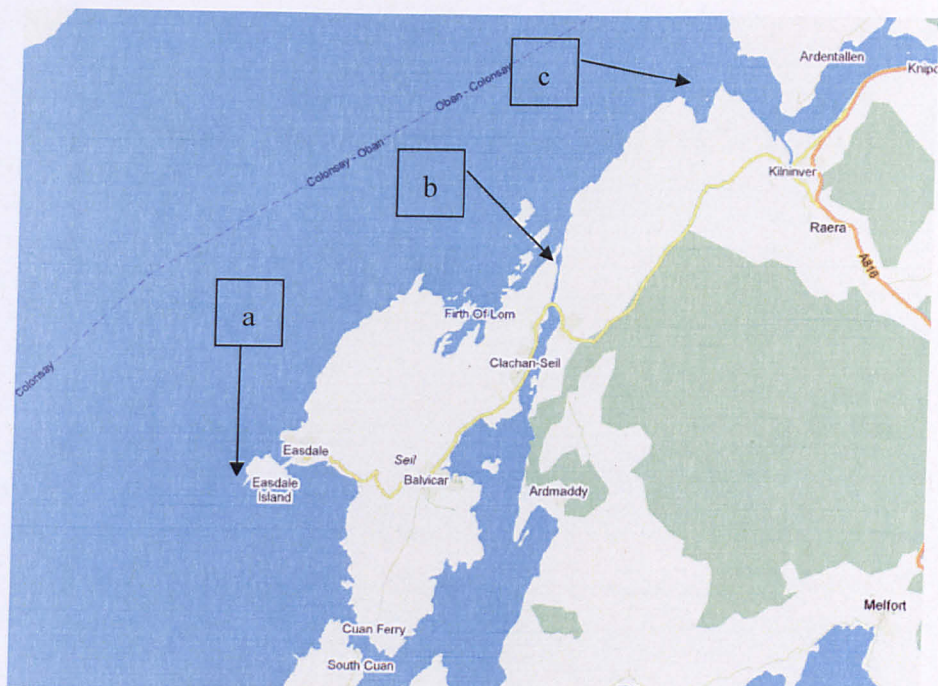
*Laminaria saccharina*,

*Laminaria hyperborea*, and

*Alaria esculenta*.

The species have been selected based upon proven trials of seeding and on-growth, high growth rates, lower polyphenol content which is advantageous for fermentation and ready availability of feedstock. Three main sampling sites were identified on the west coast of Scotland near Oban for wild kelp harvest. Sampling was made at regular intervals throughout the growth cycle to assess seasonal variations and samples were collected quarterly during winter, spring, summer and autumn. The sampling sites which are noted on the map in **Figure 3.1** include Easdale (a) which is open to the sea, Clachan Sound (b) which is a strait and Barnacarry Bay (c) which is a bay connected to the sea.

In addition to the main supply of samples from Scotland, samples of *L. digitata* harvested monthly from wild stock at Aberystwyth beach, Wales and samples of *Macrocystis pyrifera* supplied by the Irish Seaweed Centre were also used for analysis. In addition to samples of *M. pyrifera*, seaweed litter (recently deposited thus subject to minimal decomposition) of *L. digitata* and *Fucus vesiculosus* were used for the pre-treatment / demineralization experiments.



**Figure 3.1** Sampling sites on the west coast of Scotland (©2011 Google).

### 3.3 Sample preparation

Three different drying methods were employed for wild samples harvested from the west coasts of Scotland. After collection, samples were weighed and frozen in order to avoid changes to their chemical composition. No washing was applied to the macro-algae as this might affect their composition. One annual set of samples was sent frozen to Leeds where the samples were air-dried at room temperature. These samples are referred to as air dried (AD) samples. Another annual set of samples were dried in an oven at the SAMS following collection and sent to Leeds. The final drying method employed was freeze drying where again an annual set of samples were freeze dried at SAMS and sent to Leeds. Samples of *L. digitata* collected from Wales were air dried, while the sample of *M. pyrifera* was provided freeze dried by the Irish Seaweed Centre. This sample was collected of the coast of North America from an undisclosed location.

All dried samples were ground by a Retsch PM100 ball mill and sieved to a particle size  $<90\mu\text{m}$  before analysis.

### **3.4 Model carbohydrates**

Model carbohydrates of brown macro-algae such as alginic acid, mannitol, laminarin, fucoidan, Ca-alginate and Na-alginate were purchased from Sigma Aldrich.

### **3.5 Ultimate analysis**

The C, H, N and S content of all samples (dried seaweed, liquefaction oils and chars, ash) were measured using a CE Instruments Flash EA 1112 Series elemental analyzer. Most measurements were repeated in duplicate and a mean value is reported. The oxygen content was calculated by difference. The values of hydrogen and oxygen were corrected according to the moisture content of the samples.

### **3.6 Metal analysis**

Samples of dried seaweed, chars and oils from liquefaction were digested in  $\text{HNO}_3$  on a hot plate at  $200^\circ\text{C}$ . The solutions were analysed for metals by inductively coupled plasma (ICP) optical emission spectroscopy (OES) on a Perkin Elmer optima 5300DV and by atomic absorption spectroscopy (AAS) on a AA240FS Varian fast sequential atomic absorption spectrometer. All digestions were repeated in duplicate and a mean value is reported. Silica and phosphorus analysis was performed by colorimetry. Aqueous phases from hydrothermal liquefaction after filtration were made to 1 liter with de-ionized water and subsequent aliquots of sample were analyzed by ICP-OES and AAS for their metal content.

### **3.7 Proximate analysis**

Determination of moisture content was performed in accordance with standard CEN/TS 14774-3:2004, by drying the samples in a Gallenkamp hotbox oven for 2hrs. The ash content was obtained after slow combustion of the samples in a

Gallenkamp hotbox oven for 12hrs at 550°C. The volatile matter was calculated by difference according to the equation:

$$VM(\text{wt}\%)=100-\text{Ash}(\text{wt}\%)-\text{Moisture}(\text{wt}\%)$$

### 3.8 High heating value (HHV) determination

The high heating value (HHV) of seaweed samples, ashes, liquefaction chars and oils was determined by the equation proposed by **Channiwala and Parikh (2002)** based on their elemental and ash content:

$$HHV = 0.3491 \times C + 1.1783 \times H + 0.1005 \times S - 0.1034 \times O - 0.0151 \times N - 0.0211 \times A$$

where C, H, S, O, N and A are the carbon, hydrogen, sulfur, oxygen, nitrogen and ash mass percentages of the material on a dry basis.

This equation was chosen to be representative for seaweed samples as it incorporates the sulfur and ash content which are significant in seaweed biomass. This equation is validated for  $0\text{wt}\% < C < 92.25\text{wt}\%$ ,  $0.43\text{wt}\% < H < 25.15\text{wt}\%$ ,  $0\text{wt}\% < O < 50\text{wt}\%$ ,  $0\text{wt}\% < N < 5.6\text{wt}\%$ ,  $0\text{wt}\% < S < 94.08\text{wt}\%$ ,  $0\text{wt}\% < A < 71.4\text{wt}\%$  and  $4.745\text{MJ/kg} < HHV < 55.345\text{MJ/kg}$ .

### 3.9 Pre-treatment of seaweed

Pre-treatment in water was performed by heating 10g of sample in 200 ml of water under reflux for 6 hours. The sample was then filtered, and washed with deionised water. The sample was then oven dried at 60°C to constant weight. Pre-treatment in acid was performed by heating of 10 g of sample in 50 cm<sup>3</sup> of 2.0 M HCl for 6 hours at 60°C. The sample was filtered, then washed using de-ionised water until the filtrate was Cl<sup>-</sup> free (checked by 0.1 M silver nitrate solution). The sample was then oven dried at 60°C to constant weight.

### 3.10 Slagging and fouling

The combustion behaviour and ash deposition tendencies of seaweed and liquefaction products (bio-crudes and bio-chars) were assessed by using the alkali index (AI):

$$AI = \frac{kg(K_2O + Na_2O)}{GJ}$$

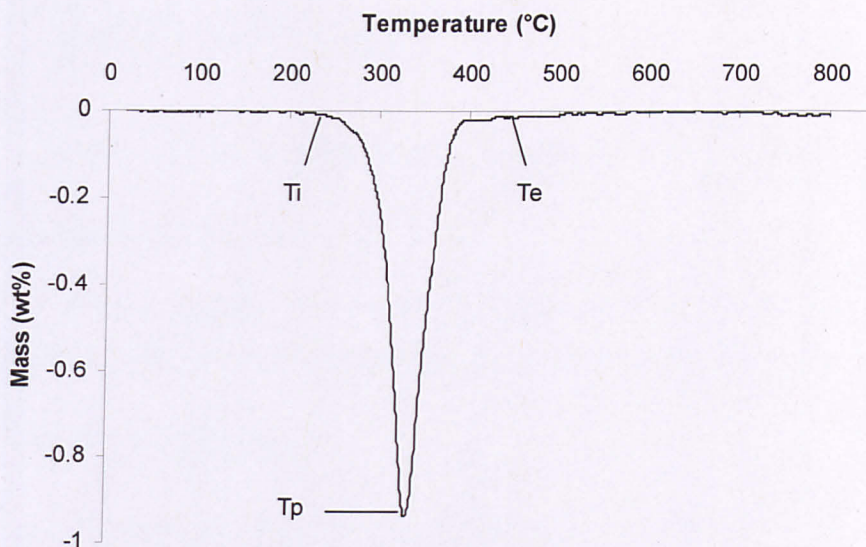
The alkali index was first developed by the coal industry, expressing the amount of alkali in fuel per fuel unit energy (Miles et al., 1995; Jenkins et al., 1998; Vamvuka and Zografos, 2004). Indexes' values above 0.34 kg/GJ show that the fuel is certainly going to slag or foul.

### 3.11 Thermogravimetric analysis

Thermal gravimetric analysis (TGA) and differential thermal gravimetric (DTG) were performed in either nitrogen or air using a Stanton Redcroft STA in a total flow rate of 50ml/min. 5 to 10 mg of samples were heated from 40°C to 900°C. Seaweed samples were heated both in an inert (nitrogen) and oxidative (air) environment at a ramp rate of 25°C/min. Liquefaction oils were also heated in both environments at a ramp rate of 10°C/min to estimate the boiling point distribution of the oils, while liquefaction chars were heated in an oxidative environment at a ramp rate of 25°C/min to assess the combustion behaviour.

TGA and DTG profiles can provide useful information for the fuel under investigation. Heating in nitrogen provides the moisture content (which is the mass loss till 110°C), the char content (fixed carbon + ash) which is the remaining mass at the final temperature (900°C) and the volatile matter content which is the difference between the moisture and char content from the starting mass. The DTG profile in nitrogen can provide the temperature of initiation of devolatilisation ( $T_i$ ), the temperature where the main devolatilization ends ( $T_e$ ) and the temperature where maximum conversion rate is occurring ( $T_p$ ).  $T_i$  was taken at temperature higher than 110°C where the rate of weigh loss was more than 1%/min while  $T_e$  was taken when the rate of weight loss was less than 1%/min. **Figure 3.2** illustrates these temperature characteristics on a DTG curve.





**Figure 3.2** Example of pyrolysis temperature characteristics on a DTG curve.

During combustion of a fuel, there is an additional step after the main devolatilisation attributed to burnout of the char. When heating a sample in an oxidative environment (air), the final remaining mass corresponds to the ash content of the sample. Similarly, the DTG profile in air can provide information about the combustion characteristics of the fuel such as ignition, burnout and reactivity. The temperature corresponding to the onset of volatile matter release was noted as the volatile matter ignition temperature (VMIT), while the temperature of maximum conversion rate was noted as the volatile matter peak temperature (VMPT). The higher the VMPT, the less reactive the fuel. Similarly, the temperature corresponding to the onset of char burning was noted as the fixed carbon ignition temperature (FCIT) and the maximum char conversion rate was noted as the fixed carbon peak temperature (FCPT). Finally the temperature where combustion eases was noted as the burnout temperature (BT). The lower the BT, the more extensive the burnout of the fuel.

### 3.12 Kinetics

The rate of devolatilisation during the pyrolysis process is described by a first order reaction using the following equation:

$$\frac{da}{dt} = \sum_{i=1}^n \frac{da_i}{dt} = -\sum_{i=1}^n k_i (1 - a_i)$$

Where,  $a_i$  is the reaction progress variable ( $a_i = 1 - \frac{m_i}{m_0}$ ) and  $k_i$  is the rate coefficient at a given time.

By assuming that the activation energy remains constant at a certain temperature range, then the reaction follows the Arrhenius equation:

$$k = A \exp\left(-\frac{E}{RT}\right), \text{ where}$$

A is the frequency or pre-exponential factor (L/mol\*s), E is the activation energy (KJ/mol), R is the universal gas constant (=8.314 J/mole\*K) and T is the temperature in Kelvin.

By combining the above equations we get:

$$\frac{da}{dt} = A(1 - a) \exp\left(-\frac{E}{RT}\right)$$

Many different approaches to determine the kinetic parameters (E and A) using the above equation have been made. In this paper, by taking into account the work of **Weber, 2008 and Saddawi et al., 2010** where the most widely used methods for extracting kinetic parameters in biomass have been compared; the temperature integral approximation by Senum and Yang was used. In this approximation a predetermined heating rate  $B = dT/dt$  which remains constant is employed. The derivative  $da/dt$ , after integrating is now expressed as:

$$-\ln(1 - a) = \frac{AE}{BR} p(x)$$

Where a new variable  $x = E/RT$  is introduced and according to Senum and Yang polynomial approximation:

$$p(x) \cong \frac{\exp(-x)}{x^2} \frac{x^4 + 18x^3 + 86x^2 + 96x}{x^4 + 20x^3 + 120x^2 + 240x + 120}$$

A non linear regression is used to calculate activation energy (E) and pre-exponential factor (A).

For validation purposes, the calculated 1-a based on the prediction of E and A from the model applied versus the observed 1-a from the thermogravimetric data was plotted.

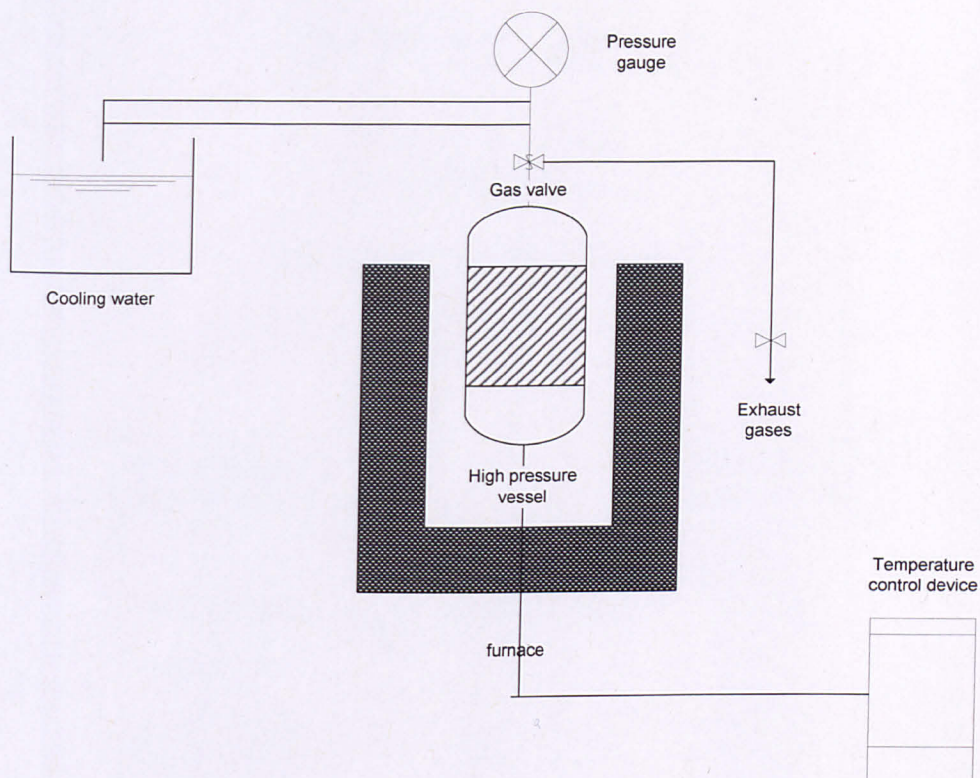
### **3.13 Analytical pyrolysis (py-GC/MS)**

Pyrolysis-gc-ms analysis was performed on a CDS 5200 series pyrolyser connected to a Shimadzu 2010 GC-MS. Samples of approximately 2 mg were pyrolysed at the desired temperature at a ramp rate of 20 °C /mS with a hold time of 20 seconds. The products were separated on an Rtx 1701 60m capillary column, 0.25 id, 0.25 µm film thickness, using a temperature program of 40°C, hold time 2 minutes, ramped to 250°C, hold time 30 minutes, column head pressure at 40°C of 30 psi. Assignments of the main peaks were made from mass spectral detection by a combination of a NIST05a MS library and retention data for standard components. Only the peaks with a high degree of certainty are reported.

### **3.14 Hydrothermal liquefaction**

#### **3.14.1 Hydrothermal liquefaction setup**

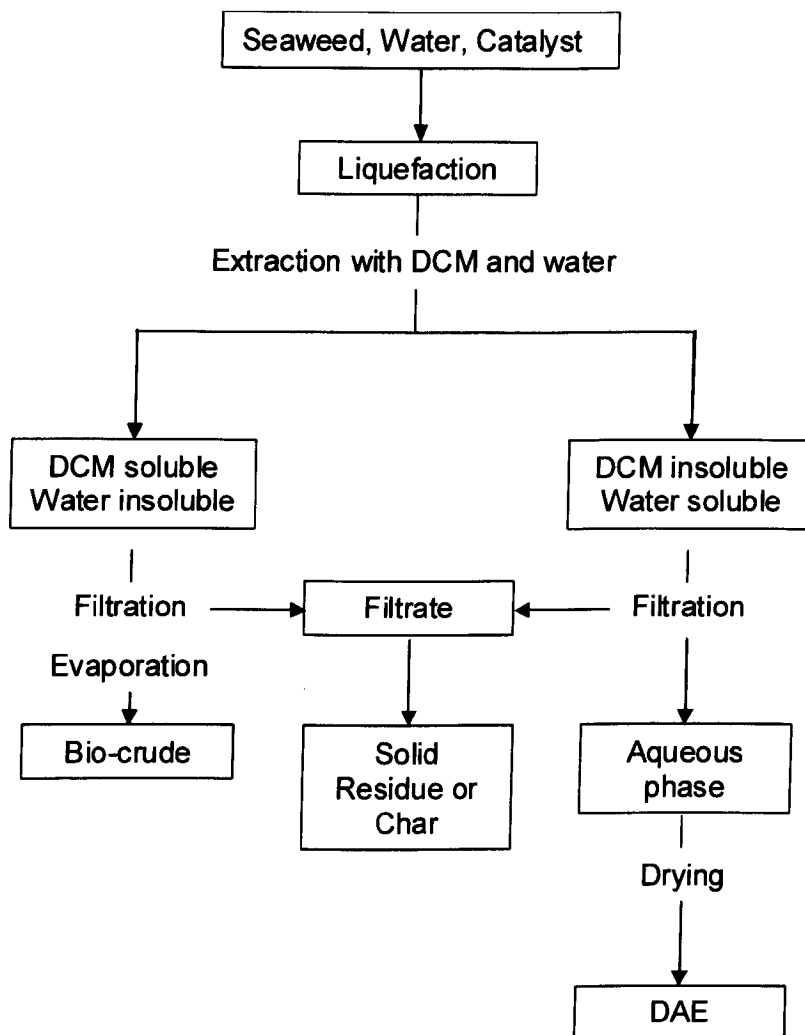
Hydrothermal liquefaction experiments were performed in a batch bomb type stainless steel reactor (75ml, Parr, USA) with a heating rate of 25°C/min. A simplified diagram of the experimental setup is shown in **Figure 3.2**. It consists of a high pressure sealed vessel seated in an electrically heated furnace connected with a temperature control device. Cooling water is used to cool the pressure transducer. In a typical run, the appropriate amounts of seaweed biomass, deionised water and catalyst were fed in to the reactor, and the reactor was sealed. Once sealed the reactor was heated to the desired final temperature and was held there for the desired residence time. After the reaction was complete, the reactor was cooled down by compressed air blowing at its walls.



**Figure 3.3** Simplified schematic of the liquefaction reactor

### 3.14.2 Separation of liquefaction products

Once the reactor was cooled, the gas valve was opened and the gases were vented. The rest of the products were separated according to the procedure shown in **Figure 3.3**. Dichloromethane (DCM) and demonized water were used to extract the products out of the bomb which appear as a two phase mixture. The bio-crude fraction is defined as the dichloromethane soluble fraction and was measured following filtration and evaporation of the DCM. The aqueous fraction was filtered to determine the solid residue fraction. The water fraction was dried at 60°C in a Gallenkamp Hotbox oven and after water evaporation, the resulting products formed the dissolved aqueous extract (DAE).



**Figure 3.4** Separation procedure of liquefaction products.

### 3.13.3 Product yields

The yields of the products were calculated on a dry basis based on the mass of seaweed and catalyst feed and the mass of the resultant products by the following equations:

$$bio-crude(wt\%) = \frac{W_{bio-crude}}{W_{seaweed} \times (100 - H_2O)} \times 100 \quad (1)$$

$$residue(wt\%) = \frac{W_{residue}}{W_{seaweed} \times (100 - H_2O) + W_{KOH}} \times 100 \quad (2)$$

$$DAE = \frac{W_{DAE}}{W_{seaweed} \times (100 - H_2O) + W_{KOH}} \times 100 \quad (3)$$

where  $W_{bio-crude}$  is the mass of bio-crude(g),  $W_{seaweed}$  is the mass of seaweed biomass fed into the reactor (g),  $W_{DAE}$  is the mass of the dissolved organics in water (g), and  $W_{KOH}$  refers to the mass of catalyst fed (g).

The bio-crude yield was also expressed on a dry ash free basis (daf) by the following equation:

$$bio - crude(wt\%) = \frac{W_{bio-crude}}{W_{seaweed} \times (100 - H_2O - Ash)} \times 100 \quad (4)$$

The gas yield was calculated from the ideal gas law using the residual pressure (after cooling down the reactor) and the average molecular weight of the gases (30.2). A typical gas composition was analyzed in a VARIAN CP-3800 gas chromatograph and was found to consist of 46% CO<sub>2</sub>, 25% N, 15% CO, and 2.8% H<sub>2</sub>.

The final conversion was calculated by adding up the dry yields of all product streams.

#### 3.14.4 Energy balance

In order to investigate the energy of the resultant products compared to the energy input of the material, the energy recovery ratio (ERR) was used as proposed by **Minowa et al., 1998** and **Yokoyama et al., 1987**. The energy recovery of starting material to oil and residue was calculated according to the following equation:

$$ERR (\%) = \frac{Energy(bio - crude + char) \times 100}{Energy(startingmaterial)} = \frac{((Yield_{bio-crude}(wt\%d.b.) \times HHV_{bio-crude}(MJ / kg) \times W_{feed}(kg, d.b.)) + (Yield_{char}(wt\%, d.b.) \times HHV_{char}(MJ / kg) \times W_{feed}(kg, d.b.))) \times 100}{W_{feed}(kg, d.b.) \times HHV_{feed}(MJ / kg)} \quad (5)$$

where  $W_{feed}$  is the weight in kg of the starting material on a dry basis. All product yields were taken on a dry basis.

This relationship only describes the conversion of energy from the starting material to bio-crude and char and does not take into account the energy required for the liquefaction process. Hydrothermal liquefaction is an energy intensive process as it involves heating of water which has a high specific heat capacity ( $C_p$ ). In order to compare the energy content of the resultant products (bio-crude and char) with the energy required to bring the slurry of seaweed and water to the desired temperature, the energy consumption ratio (ECR) was introduced. ECR is defined as:

$ECR = \frac{E_l}{E_p}$  (6), where  $E_l$  is the energy required for liquefaction (MJ) and  $E_p$  is the energy of the products (bio-crude and char) (MJ).

When  $ECR < 1$ , then the reaction is energy favourable as the products have higher energy content than that required for the reaction. When  $ECR > 1$ , more energy is required for the reaction to occur than the energy content of the products.

The energy of the products ( $E_p$ ) was calculated based on their HHV and yields (on a dry basis) as follows:

$$E_p = (Yield_{bio-crude} (wt\%d.b.) \times HHV_{bio-crude} (MJ / kg) \times W_{feed} (kg, d.b.)) + (Yield_{char} (wt\%, d.b.) \times HHV_{char} (MJ / kg) \times W_{feed} (kg, d.b.)) \quad (7)$$

The energy required to heat up the slurry of seaweed and water was calculated according to the following procedure:

The amount of heat energy ( $Q$ ) gained or lost by a substance is equal to the mass of the substance ( $m$ ) multiplied by its specific heat capacity ( $c_p$ ) multiplied by the change in temperature ( $T$ ):

$$Q (kJ) = c_p (kJ/kgK) \times m (kg) \times dT (K) \quad (8)$$

The specific heat capacity of a solution is given by the following equation:

$$C_p (\text{solution}) = C_p (\text{solids}) \times wt_{\text{solids}}\% + C_p (\text{water}) \times wt_{\text{water}}\% \quad (9)$$

$C_p$  of water is known and is 4.1813 J/gK at 25°C. However, this  $c_p$  changes dramatically with temperature and becomes 4.51 J/gK at 200°C, 4.87 J/gK at 250°C, 5.2 J/gK at 275°C, 5.65 J/gK at 300°C, 6.86 J/gK at 325°C and 10.1 J/gK at 350°C.

The  $c_p$  of solids is unknown but can be calculated by applying Kopp's rule based on their elemental composition and the heat capacities of each element.

Seaweed's C, H, N, S, O, K, Na, Ca and Mg content makes up over 90wt% of seaweed's mass making it a very good representation of the  $c_p$  of the biomass material. The heat capacities of these elements at 25°C are: 0.709 J/gK for C, 14.304 J/gK for H<sub>2</sub>, 1.04 J/gK for N<sub>2</sub>, 0.71 J/gK for S, 0.918 J/gK for O<sub>2</sub>, 0.757 J/gK for K, 1.228 J/gK for Na, 0.647 J/gK for Ca and 1.023 J/gK for Mg. These values increase with increasing temperature but this increase is not as significant as that for water so any increase in these values with temperature was not taken into account. According to Kopp's rule, the specific heat capacity of any seaweed used can be calculated according to the following equation:

$$C_p \text{ (solids)} = 0.709x + \frac{14.304}{2}y + \frac{1.04}{2}z + 0.71w + \frac{0.918}{2}a + 0.757b, 1.228d + 0.647e + 1.023f \text{ (J/gK) or (kJ/kgK) (10)}$$

where x, y, z, w, a, b, d, e and f are the weight percentages of C, H, N, S, O, K, Na, Ca and Mg of the biomass material.

By substituting eq. (9) and (10) to eq. (8) we get:

$$Q = (((0.709x + \frac{14.304}{2}y + \frac{1.04}{2}z + 0.71w + \frac{0.918}{2}a + 0.757b, 1.228d + 0.647e + 1.023f) \times \text{wt}_{\text{solids}}\%) + (C_p \text{ (water)} \times \text{wt}_{\text{water}}\%)) \times m \times dT \text{ (11)}$$

From this equation, the heat required for the liquefaction of any mixture of water and biomass and subsequently the ECR can be calculated. Because of the significant increase in water's  $c_p$  with temperature, several temperature intervals were taken in order to solve the above equation. These intervals were: 0-200°C, 200-250°C, 250-275°C, 275-300°C, 300-325°C, 325-350°C and 350-370°C.

### 3.15 GC-MS

Bio-crudes obtained by hydrothermal liquefaction were diluted in DCM and subsequently analyzed by gas chromatograph equipped with a mass selective detector (GC-MS) (Agilent Technologies GC-MS equipment was used with a 6890N Gas Chromatograph coupled with a 5975B Inert XL Mass Selective Detector). Separation was achieved on a Restek 60m stabilwax capillary column, 0.32 i.d., 0.25 μm film thickness using a temperature program of 40°C, hold time 2 min; ramped to



150°C with a heating rate of 6°C /min; and then ramped to 250°C with a heating rate of 3°C /min, hold time 10 min, column head pressure of 30 psi. Assignments of the main peaks were made from mass spectral detection by a combination of a NIST05a MS library and retention data for standard components.

### 3.16 Carbon and nitrogen determination of the aqueous phase

The aqueous phase after filtration was made to 1 liter with de-ionized water and then analyzed for its total organic carbon content by a TOC analyzer (HACH IL 550 TOC-TN) and for its ammonium concentration by colorimetry using a Hach Lange Lasa 100 mobile spectrometer.

### 3.17 Biomass fuel properties

**Moisture:** Freshly harvested seaweed can contain up to 90% moisture. After drying, seaweed still contains a relatively large amount of moisture that can be up to 10%. When using biomass for energy conversion, moisture is a significant parameter. High moisture content feedstock can cause problems during thermochemical conversion technologies and generally require dry sample for combustion, gasification or pyrolysis. For high moisture content feedstock such as seaweeds, energy conversion technologies that can utilise wet biomass such as fermentation and liquefaction are preferred.

**Ash content:** The amount of inorganic matter (not moisture) is determined by the ash content of a material. The majority of inorganic material is metals and silica. The ash content reduces the available energy in a fuel, the higher the ash content the smaller the energy containing fraction of the sample and hence the lower the heating value. Samples with high ash content can cause severe problems in high temperature thermochemical conversion technologies.

**Calorific value:** The energy content of a fuel is expressed by the calorific value (CV) which is the energy or heat released from the fuel when burnt in air. It is measured in MJ/kg for solid fuels, in MJ/m<sup>3</sup> for liquids and in MJ/Nm<sup>3</sup> for gases. It can be expressed in two forms, the gross CV (GCV), or higher heating value (HHV)

and the net CV (NCV), or lower heating value (LHV). HHV is the total energy released from the fuel when burnt in air while LHV is the energy without the latent heat of the water vapour (McKendry, 2002a).

**Proximate analysis:** Proximate analysis includes the determination of ash content, moisture content, volatile matter (VM) and fixed carbon (FC) in a given sample. It is a standard analysis used for solid fuels such as coal and biomass. VM and FC provide a measure of the ignition of the biomass (McKendry, 2002a).

**Ultimate analysis:** Ultimate analysis involves the determination of the elemental composition of solid fuels and more specifically the concentration of the five basic elements present, carbon, hydrogen, nitrogen, oxygen and sulphur. When considering solid fuels, the elemental composition is expressed in O:C and H:C ratios which are illustrated by using a Van Krevelen diagram (Figure 3.4). The higher the proportion of oxygen and hydrogen, compared with carbon, the less the energy value of a fuel, due to the lower energy contained in carbon–oxygen and carbon–hydrogen bonds, than in carbon–carbon bonds (McKendry, 2002a).

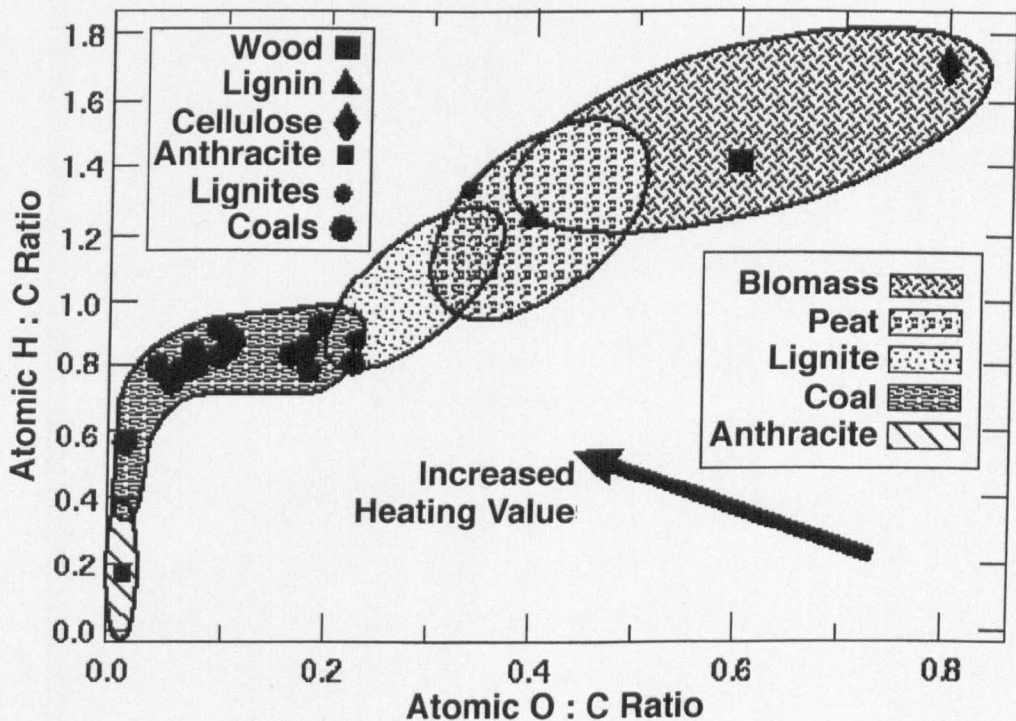


Figure 3.5 Van Krevelen diagram for a variety of solid fuels (Jenkins et al., 1998)

## **CHAPTER 4 – Thermal behaviour of model carbohydrates**

### **4.1 Introduction**

The first step in evaluating the potential of using brown macro-algae as fuel through thermo-chemical processing routes is to have a basic understanding of the behaviour of its constituents in these processes. As was mentioned earlier, the major fraction of brown macro-algae in terms of mass is the carbohydrate fraction. Apart from cellulose which is common to both marine and terrestrial biomass, little is known of the behaviour of the other carbohydrates (alginic acid, mannitol, laminarin and fucoidan) during thermo-chemical processing. The thermal decomposition properties of these four carbohydrates, under inert and oxidative atmospheres, have been explored in detail in this chapter. Thermogravimetric analysis (TGA) was used in order to study the different decomposition pathway as well as the temperature range of decomposition of each of the carbohydrates. The influence of the cation ( $\text{Na}^{++}$  and  $\text{Ca}^{+}$ ) bound on alginic acid was also examined. Initial pyrolysis kinetic parameters of these model compounds have been calculated. These provide useful information for the design of reactors for thermochemical conversion. Pyrolysis gas chromatography – mass spectroscopy (py-GC/MS) was used in order to study the evolution of volatiles at different temperatures from the flash pyrolysis of the model compounds. Also, py-GC/MS provided an indication of the char and volatile yields during flash pyrolysis and how they compare with the slow heating rate pyrolysis (TGA).

### **4.2 Pyrolysis behaviour of model carbohydrates**

#### **4.2.1 Characterisation of model carbohydrates**

Ultimate analysis of the carbohydrates revealed their C, H, N and S content and is shown in **Table 4.1**. The food polysaccharides (mannitol and laminarin) were found to have the highest carbon and hydrogen content. Fucoidan was found to have significantly lower carbon content (about 25%) compared to the other carbohydrates (over 40%) while it contains a significant amount of sulfur (about 8%). Metal

analysis (**Table 4.2**) revealed their metal concentration. The highest concentration of metals in all the carbohydrates was found to be the alkali and alkaline earth metals (Ca, K and Na). Fucoïdan was found to have significantly higher metal concentration than the other carbohydrates.

#### 4.2.2 Thermogravimetric analysis (TGA) of model carbohydrates

The TGA and DTG curves of the four carbohydrates are shown in **Figures 4.1-4.4**. The graphs reveal 2 degradation steps common to all the four carbohydrates after the small initial weight loss due to dehydration which accounts for the moisture content and covers a temperature range between 25°C and 110°C. The first stage represents the main devolatilization reactions, where most of the sample weight is lost as volatile matter. The temperature where devolatilization begins is noted as  $T_i$  and the max peak temperature is noted as  $T_p$ . Following the main peak, devolatilization continues slowly over a wide temperature range terminating at a temperature noted as  $T_e$  (end of main devolatilization). From  $T_e$  to the final programmed temperature of 800°C, a slow weight loss is observed. This is attributed to the continuous decomposition of the residue. The mass remaining at 800°C corresponds to the char content of the sample. The second stage begins with the introduction of air, at 800°C, when an instant major weight-loss is observed due to the burning of the residual carbon present in the residue. The mass remaining after this stage corresponds to the ash content of the samples.

The thermal degradation of laminarin and fucoïdan is characterized by an additional weight-loss peak which occurs toward the end of the first stage mentioned previously. The devolatilization of these two carbohydrates occurs over two distinct steps. Therefore there are two main peaks where the maximum peak temperature is noted ( $T_{p1}$  and  $T_{p2}$ ).

The pyrolysis temperature characteristics of the four carbohydrates are shown in **Table 4.3**. Alginic acid, like all the other carbohydrates (apart from mannitol), shows a rapid weight loss from the initial temperature until the temperature reaches about 110°C due to the moisture, followed by a steady weight loss until a temperature of about 160°C when the pyrolysis reactions begin. These reactions end at about 545°C with most of the volatile matter evolving between 200 and 350°C. The maximum rate of weight loss was found to occur at 220°C. The thermal

## Chapter 4 – Thermal behaviour of model carbohydrates

degradation after 545°C until the time that air was introduced at 800°C was not of a great significance.

**Table 4.1** Proximate and ultimate analysis of the four carbohydrates of brown algae.

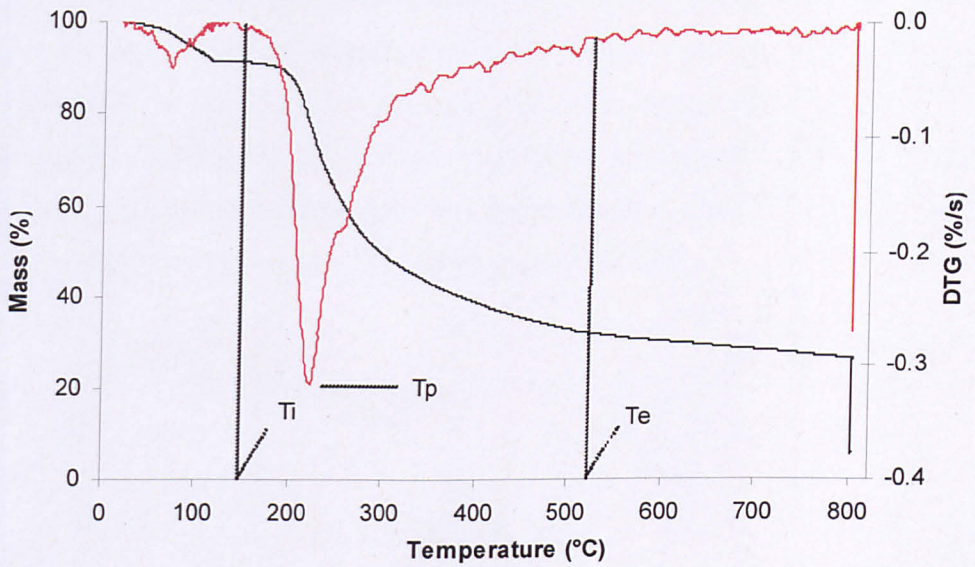
Carbohydrate	Moisture* (%)	VM* (%)	Total Residue* (%)	Char* (%)	Ash* (%)	C (%)	H (%)	N (%)	S (%)
						(a.r)	(a.r)	(a.r)	(a.r)
<b>Alginate acid</b>	8.5	66	25.5	20	5	36.3	4.8	<0.2	<0.2
<b>Mannitol</b>	1.3	95.3	3.4	1.7	1.7	39.7	7.8	<0.2	<0.2
<b>Laminarin</b>	9.4	88.3	2.3	0.6	1.7	39.2	6.4	<0.2	0.3
<b>Fucoxanthin</b>	12.5	61.7	31	-**	31	24.3	4.2	<0.2	8.2

\* Calculated from TGA

\*\*Char cannot be estimated because of the increase in fucoidans weight with introduction of air

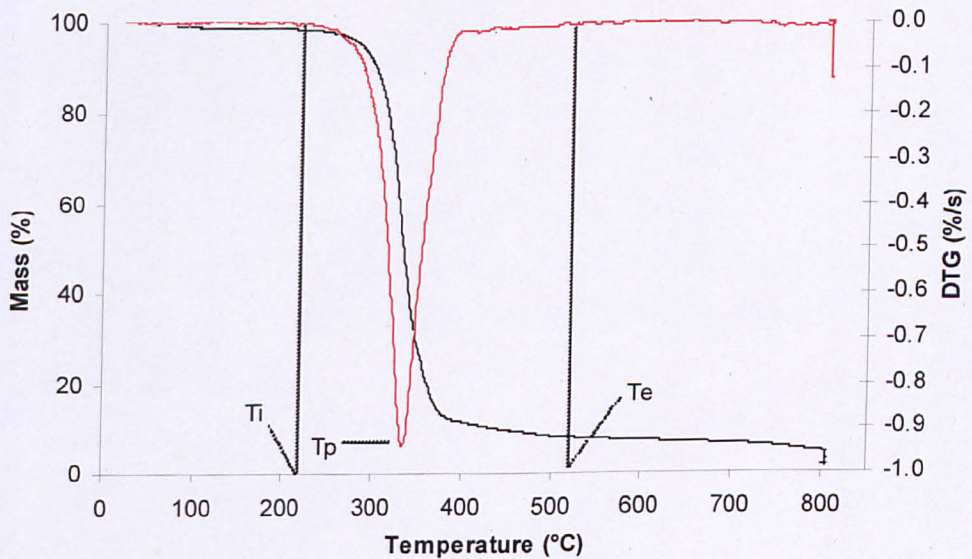
**Table 4.2** Metal concentration (ppm) of the carbohydrates of brown seaweed determined by ICP-OES

Carbohydrate	Al	Ba	Ca	Cr	Cu	Fe	K	Mg	Mn	Na	Ni	Sr	Zn	SUM
Mannitol	0	0.0	260	0	1.7	0	286	5.5	0	92	0	0.0	30	675
Alginate	0	10	3481	40	2.1	198	537	12	4	12955	23	192	4.3	17457
Laminarin	0	0.7	345	0.7	1.2	4.7	140	5.6	0	6542	0.3	0.0	14	7054
Fucoidan	20	42	2518	1	3.6	514	41239	212	103	64450	6	240	117	109465



**Figure 4.1** TGA and DTG profile of alginic acid in nitrogen at 25°C/min.

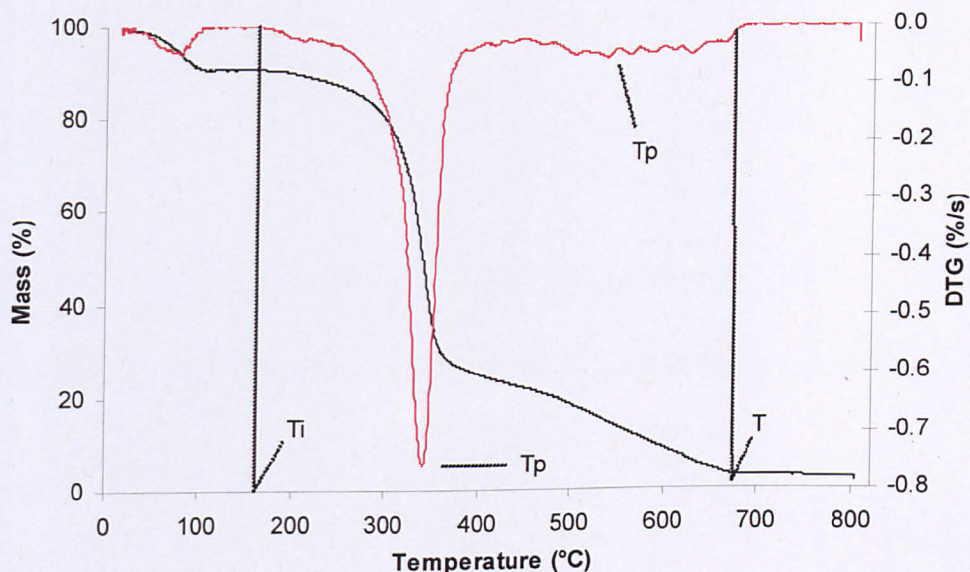
Mannitol has lower moisture content and does not start to lose weight until 230°C. Most of the volatile matter was evolved between 250°C and 400°C, while the pyrolysis reactions appeared to end at 520°C. The maximum rate of weight loss was observed at 335°C.



**Figure 4.2** TGA and DTG profile of mannitol in nitrogen at 25°C/min.

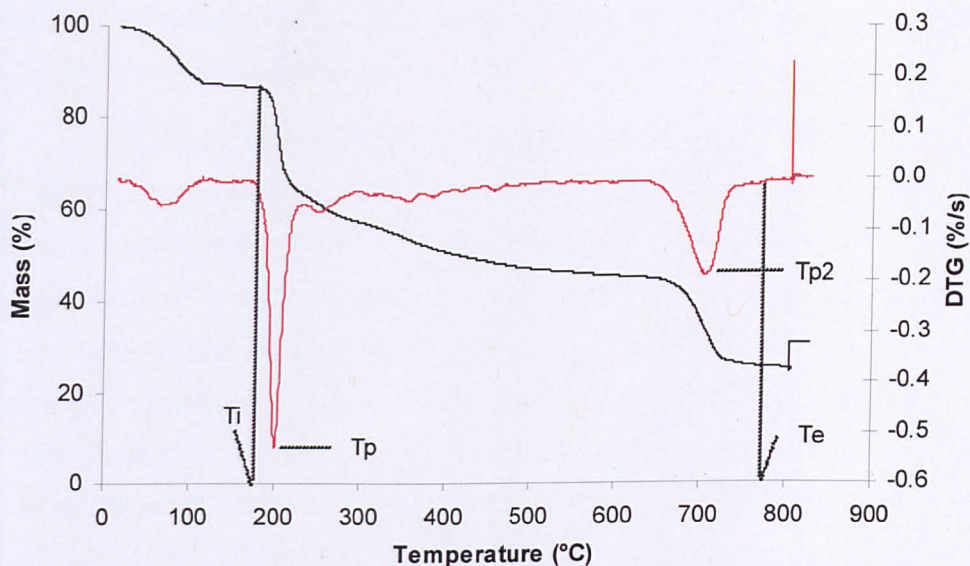


The pyrolysis reactions for laminarin begin at about 175°C ending at a relatively high temperature of about 685°C. The decomposition was found to occur in two distinct steps as revealed by the two DTG peaks. The first step was from the temperature of the onset of pyrolysis ( $T_i$ ) until about 420°C where a rapid decomposition occurred, followed by a less rapid decomposition from 420°C until the end of the pyrolysis reactions. The maximum rate of weight loss was found to happen during the first stage of the decomposition at 340°C.



**Figure 4.3** TGA and DTG profile of laminarin in nitrogen at 25°C/min.

The main decomposition of fucoidan was found to occur, like laminarin in two steps. The pyrolysis reactions, like laminarin started at 175°C but ended at a higher temperature (775°C). The first stage of the evolution of the volatile matter happened between 175°C and 500°C with the maximum weight loss occurring at 200°C, while the second step occurred between 645°C and 775°C with the maximum weight loss occurring at 710°C.



**Figure 4.4** TGA and DTG profile of fucoidan in nitrogen at 25°C/min.

**Table 4.3** Pyrolysis temperature characteristics of alginic acid, mannitol, laminarin and fucoidan.

Carbohydrate	$T_i$ (°C)	$T_p$ (°C)	$T_{p2}$ (°C)	$T_e$ (°C)
Alginic acid	160	220	-	545
Mannitol	230	335	-	520
Laminarin	175	340	540	685
Fucoidan	175	200	710	775

Fucoidan exhibits a unique characteristic when air is introduced which differs with the other carbohydrates. For alginic acid, laminarin and mannitol the residual carbon in the residue is rapidly oxidized upon addition of air. However, when air is introduced to the residual matter of fucoidan, its mass increases by 5.5 wt%. Because of this unusual characteristic, the degradation of fucoidan was examined in both inert and oxidative atmospheres. The TGA and DTG profiles in both atmospheres agreed with the final mass showing that the increase in fucoidan's mass with the transition from inert to oxidative atmosphere is real. Metal analysis (**Table 4.2**) revealed the presence of a much higher concentration of metals in fucoidan than in the other carbohydrates. The increase in fucoidan's mass is attributed to the

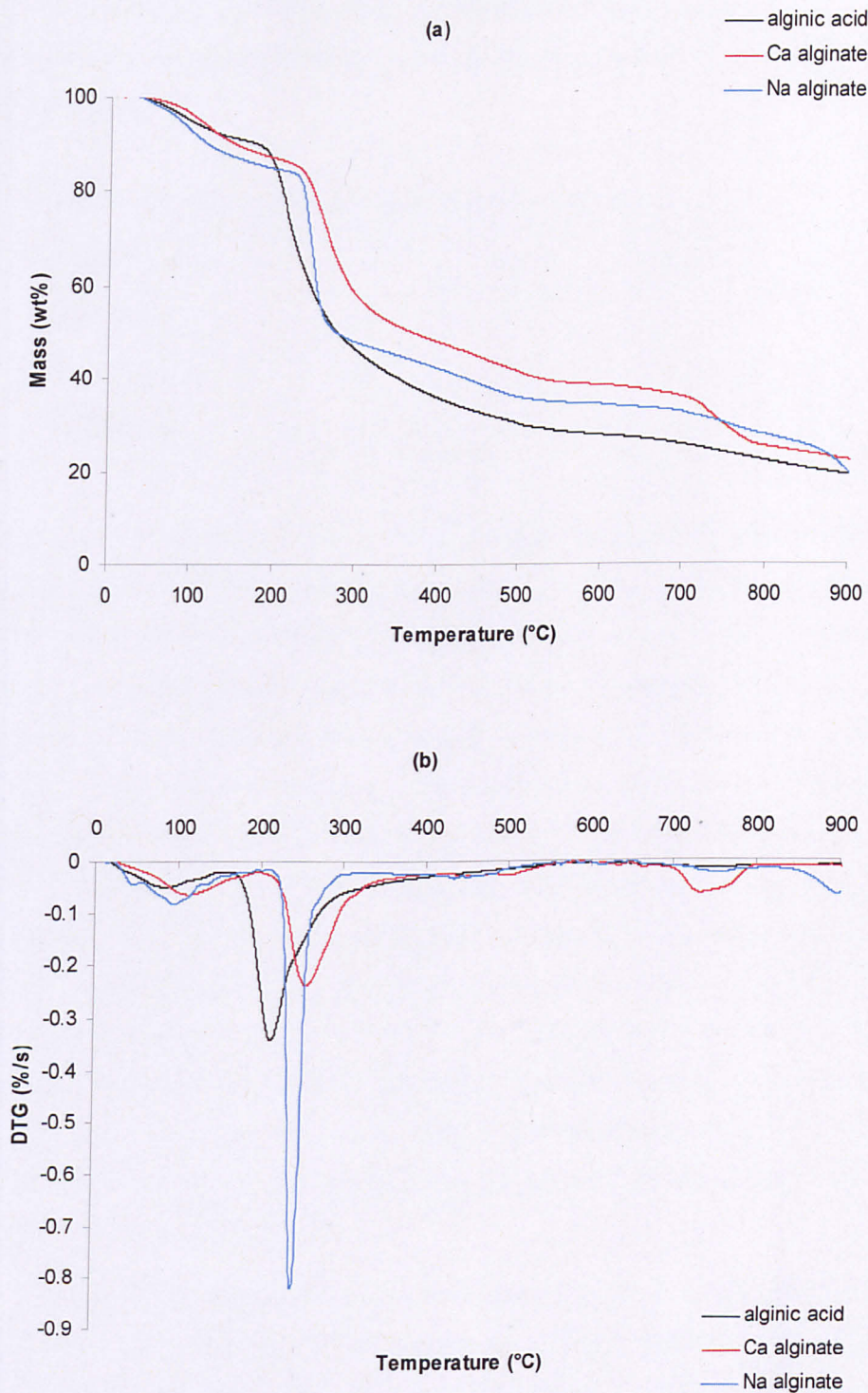
metals forming more stable metal oxides and possibly sulphates, phosphates and carbonates when air is introduced.

The proximate analysis for the carbohydrates as revealed by the different steps of thermo gravimetric analysis is listed in **Table 4.1**. The moisture yields range between 1.3wt% and 12.5wt%. Fucoidan was found to have the highest moisture content (12.5wt%) while mannitol has the least (1.3wt%). The volatile matter content was found to be between 61.7wt% and 95.3wt% with mannitol and laminarin indicating the highest (95.3wt% and 88.3wt% respectively). The total residue (char and ash) content was found to range between 2.3wt% and 31wt%. From the total residue most of it was found to be ash rather than char. The alginic acid exhibits the highest char levels in the residue (20wt%) and is significantly higher than the other carbohydrates, this agrees with other work which indicates that the alginates favor high char levels. Mannitol and laminarin show the highest volatile matter content and indicate significantly less residue content than alginic acid and fucoidan.

### 4.2.3 Thermogravimetric analysis (TGA) of alginate salts in nitrogen

The onset of pyrolysis reactions ( $T_i$ ) for alginic acid was found lower than the other carbohydrates. However, the devolatilization propagated for a wide temperature range unlike the other carbohydrates where fast and sharp DTG peaks were recorded during their main devolatilization stages. This more complicated devolatilization stage for alginic acid might be attributed to metals such as Na and Ca chelated to alginic acid to form alginates which are simply the salts of alginic acid. In order to have a better understanding of the influence of the cation bound to alginic acid on its thermal decomposition, two of the most common alginates, Na alginate and Ca alginate were examined in more detail by TGA.

The thermal decomposition of alginic acid and the alginate salts have been found to behave differently upon heating in an inert environment. **Figure 4.5a-b** shows the TGA and DTG profiles for the pyrolysis of the three alginates in nitrogen respectively, while **Table 4.4** lists their pyrolysis temperature characteristics. The temperature where devolatilisation begins is noted as  $T_i$  and the maximum peak temperature is noted as  $T_p$ .



**Figure 4.5** (a) TGA and (DTG) profiles in nitrogen at 25°C/min of alginic acid, Ca alginate and Na alginate.

. Following the main peak, devolatilisation continues slowly over a wide temperature range terminating at a temperature noted as  $T_e$  (end of main devolatilisation).

**Table 4.4** Pyrolysis temperature characteristics of alginates

Carbohydrate	$T_i$ (°C)	$T_p$ (°C)	$T_{p2}$ (°C)	$T_e$ (°C)
<b>Alginic acid</b>	160	215	-	545
<b>Ca alginate</b>	200	255	730	545
<b>Na alginate</b>	210	245	-	520

The onset of pyrolysis ( $T_i$ ) is lower for alginic acid (160°C) than for both the alginate salts (~200°C). Both alginate salts have a two step decomposition path within the temperature range of main devolatilisation (i.e.  $T_i$ - $T_e$ ). The first step occurs over a temperature range 210-270°C for the Na alginate, whereas for the Ca alginate this step occurs over a wider temperature range of 200-300°C. This first step is more rapid for the Na alginate as illustrated by the DTG curve in **Figure 4.5b**, indicating that Na might be catalysing the reaction. The max peak temperature ( $T_p$ ) for this step is lower for the Na alginate (245°C) than for the Ca alginate (255°C). The overall mass loss occurring after step 1 is higher (approximately 10wt% higher) for the Na alginate than the Ca alginate, similarly this is also observed after the second decomposition stage at 545°C ( $T_e$ ). Alginic acid exhibits less defined stepwise behaviour. By a closer observation of the DTG curves of alginic acid and its alginates, it seems that while alginic acid is decomposing first its main devolatilisation peak is broadened by its Ca and Na content to end where the decomposition Ca alginate ends.

The thermal degradation of the Ca alginate by TGA is characterised by an additional weight-loss peak which occurs at a higher temperature (700-800°C). There are therefore two main peaks where the maximum temperature peak is noted ( $T_p$  and  $T_{p2}$ ). This second step ( $T_{p2}$ ) corresponds to the region where  $\text{CaCO}_3$  decomposes and so it is thought that CaO which is first formed during decomposition of the alginate salt rapidly reacts with  $\text{CO}_2$  to form the carbonate. At

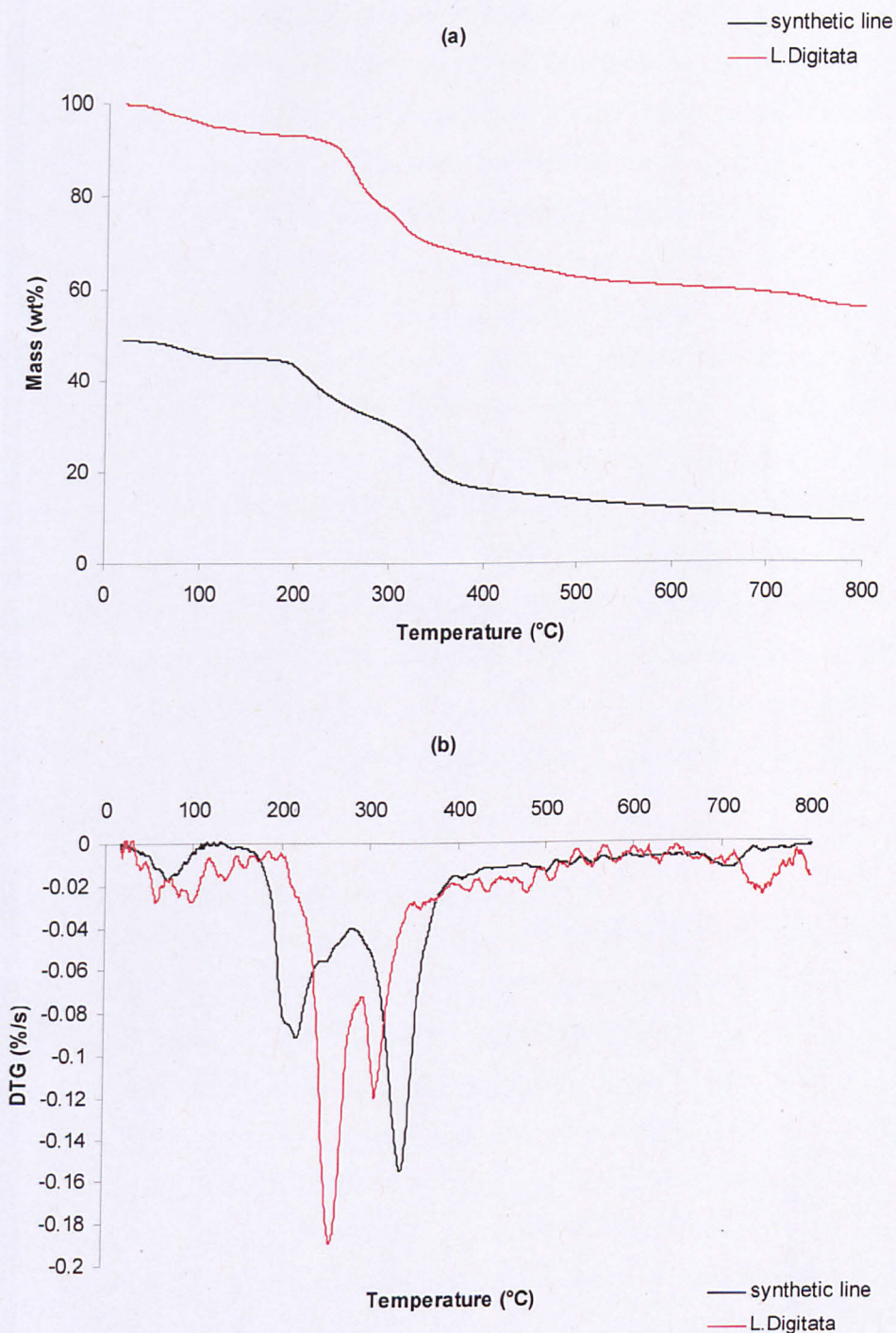
higher temperature (cir 900°C), the Ca alginate char is stable whereas the Na alginate char begins to decompose further.

#### **4.2.4 Prediction of seaweed degradation based on their biochemical content**

The previous discussion described the different temperature ranges in which each carbohydrate is decomposed. It was of interest to compare the behavior of a real brown seaweed to a synthetic mixture of the model carbohydrates by combining all the carbohydrates under investigation in an appropriate ratio. Only alginic acid and not its alginates was considered as it is hard to know how much of the Ca and Na content is bound to alginic acid. In this manner a synthesized decomposition curve can be compared to a brown seaweed to confirm the interpretation of decomposition stages. .

The biochemical composition of brown algae varies significantly with the species, the season and the location that have been collected. Variation on specific species can be quite high depending on the time of year it is collected. For example *Laminaria digitata*'s alginate content can be 15-26.5%, mannitol content 4-20%, laminarin content 0.5-24.5% and fucoidan content 1.6-5.5% (**Black, 1950b**). Apart from these carbohydrates, seaweeds also contain significant amount of cellulose and protein which can together be up to 20%, but these two were not part of this present study. Cellulose has received extensive investigation as a terrestrial biomass component.

The synthetic line was created by assuming a sample of *Laminaria digitata* collected during winter. It's exact biochemical composition was unknown but according to the work of Black (**1950b**) it is known that alginic acid content reach their maximum during winter and early spring while laminarin and mannitol content reach their minimum during winter. So by making an assumption that this sample had 26.5% content of alginic acid, 7% content of mannitol, 10% content of laminarin and 5.5% content of fucoidan, a synthetic line was created. The TGA and DTG synthetic line in comparison with a sample of *Laminaria digitata* collected during December are shown in **Figure 4.6**. Although this present representation makes up only 50% of the total mass of the seaweed samples the similarities of the actual sample decomposition and the mixture of the carbohydrates are obvious.



**Figure 4.6** (a) TGA and (b) DTG profiles of a mixture of the four carbohydrates compared with sample of *L. digitata*.

Between 200-300°C alginic acid and fucoidan are thermally decomposed. The bigger peak of *L. digitata* suggests either that the alginic acid and fucoidan content when making the synthetic curve were underestimated or due to the decomposition of alginates at the same temperature region. The next decomposition step is happening between 300-400°C where laminarin and mannitol are thermally decomposed. The larger peak of the synthetic curve suggests overestimation of laminarin and mannitol content. The final decomposition step is occurring at 700-800°C where fucoidan and Ca alginate are thermally decomposed. The larger peak in *L. digitata* curve is because the degradation of Ca alginate was not taken into account. It is also known from studies of terrestrial biomass that cellulose is decomposing in the temperature region of 175-400°C (Nowakowski et al., 2008). The maximum peak is occurring at 369°C (Nowakowski et al., 2008) so decomposition of cellulose is happening at the same temperature region with the decomposition of laminarin and mannitol. Studies on algal cellulose in order to evaluate any potential differences with the terrestrial one and on a representative protein sample can give a complete representation of the thermal degradation of a brown macro-algae sample.

### 4.2.5 Pyrolysis kinetics of model carbohydrates

The pyrolysis kinetic parameters of the carbohydrates were calculated from the data generated from their thermal degradation by using the Senum and Yang approximation and the reaction constant method. The reaction rate constant method provides a linear solution for the kinetic parameters which strongly depends on the quality of data set used (i.e. how well they fit linearly), while the nonlinear regression of Senum and Yang approximation is not dependant on the linear fit of the data set. The reason for using the two methods is not only for validation purposes, but also due to the fact that the Senum and Yang approximation did not report feasible kinetic parameters for compounds in which devolatilization occurs in two steps. As it was shown before, laminarin and fucoidan devolatilize in two steps. The Senum and Yang approximation for these stages therefore results in mathematically sound but physically improbable kinetic parameters. Many methods for calculating kinetic parameters from TGA use a predetermined pre-exponential factor, solving for activation energy (E) based on that assumption. In Senum and

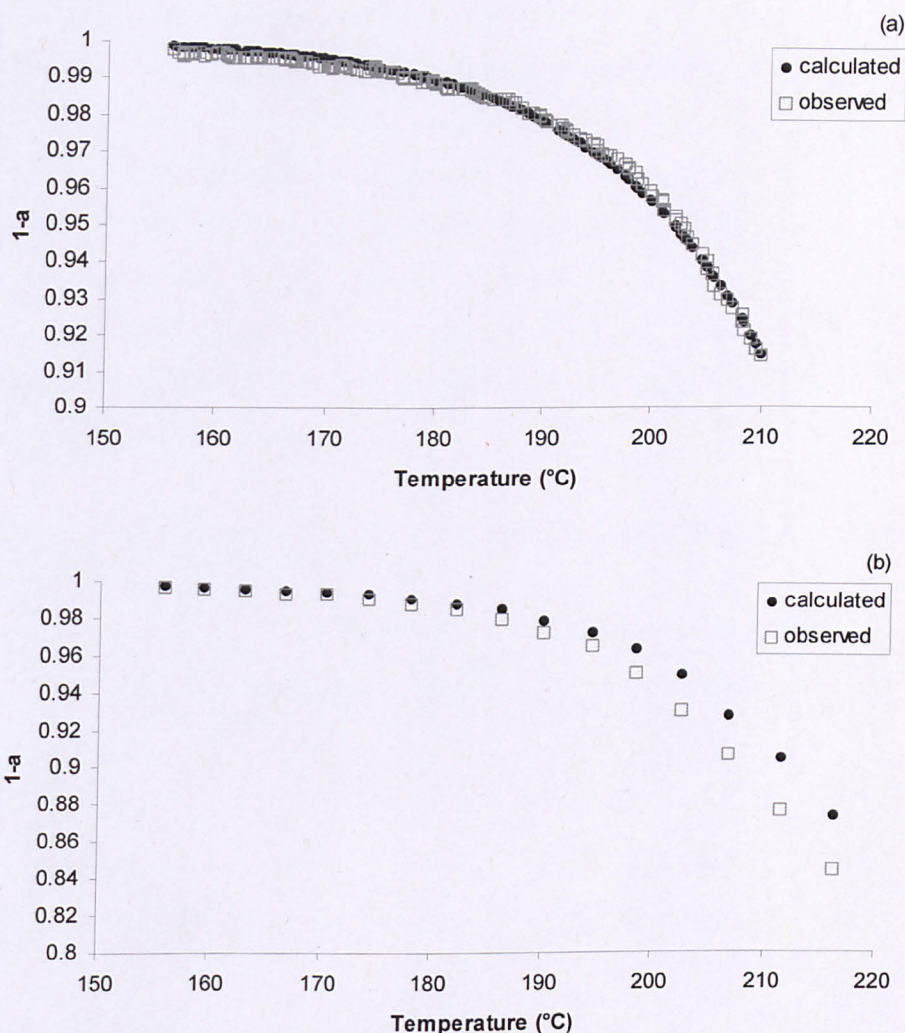


Yang approximation a solution is provided by solving for both A and E. Because of the mathematical solution of this approximation, lower activation energies are consistent with lower pre-exponential factors and are consistent with the literature (Saddawi, et al., 2010).

The initial kinetic parameters of the model compounds are listed in **Table 4.5**. The two methods employed showed similar results. The variation in the results of the two methods depends on how linear the data set used for the reaction rate constant method fit. Laminarin and alginic acid were found to have the lowest activation energies (107 and 120 KJ/mol) followed by mannitol (161 KJ/mol). Previous study on the thermal decomposition of mannitol found lower activation energy (120.61 KJ/mol) by using Kissinger, Friedman and Flynn-Wall-Ozawa methods (Tong, et al., 2010). However, all these methods provide kinetic parameters by a graphical solution which depends on how well the data set used fit linearly. The 2<sup>nd</sup> decomposition step of laminarin was found to have even lower activation energy (53 KJ/mol) by using the reaction rate constant method. Fucoidan was found to have a relatively high activation energy of 247 KJ/mol indicated by both methods used. Typically biomass samples have activation energies between 30 and 200 KJ/mol (Weber, 2008). The unusual high value of E for fucoidan was validated by plotting the weight loss versus temperature curve based on the calculated E and A and comparing it with the actual weight loss curve. The calculated weight loss curve was found to fit very well with the experimental one. Similar validations were done for all the carbohydrates under investigation. An example of the fit of the methods used, with the experimental data is shown in **Figure 4.7**. It can be seen that the Senum and Yang approximation uses a larger set of data and also the variance of the results is lower. Thus, Senum and Yang approximation gives more accurate values than the reaction constant method. The second decomposition step of fucoidan was found to have an E of 521 KJ/mol by using the reaction rate constant method. It is possible that the reaction order (n) was not 1 for this case.

**Table 4.5** The pyrolysis kinetic parameters of the model carbohydrates determined by the Senum and Yang approximation and the reaction constant method.

	Activation Energy (E, KJ/mol)	Pre-exponential factor (lnA)	Variance
<b>Alginic acid</b>			
Senum and Yang approximation	120.4	23.9	$3.2 \times 10^{-4}$
Reaction rate constant	111.5	21.6	$1.2 \times 10^{-2}$
<b>Mannitol</b>			
Senum and Yang approximation	161.7	27.9	$3.4 \times 10^{-3}$
Reaction rate constant	138.9	23.3	$2.7 \times 10^{-2}$
<b>Laminarin</b>			
Senum and Yang approximation	107.2	16.4	$8.9 \times 10^{-3}$
Reaction rate constant	102.1	15.5	$2.5 \times 10^{-2}$
2 <sup>nd</sup> step			
Reaction rate constant	53.2	2.1	$1.3 \times 10^{-2}$
<b>Fucoidan</b>			
Senum and Yang approximation	247.2	55.5	$2.3 \times 10^{-3}$
Reaction rate constant	247.1	55.5	$1.3 \times 10^{-1}$
2 <sup>nd</sup> step			
Reaction rate constant	521.8	56.9	$2.2 \times 10^{-1}$



**Figure 4.7** Validation of kinetic models for alginic acid. (a) Senum and Yang approximation and (b) reaction rate constant method.

#### 4.2.6 Flash pyrolysis of model carbohydrates by py-GC/MS

Py-GC/MS was introduced in order to assess the pyrolysis behaviour of the model carbohydrates at high heating rates. During py-GC/MS small amount of sample is being pyrolysed in very high heating rate (simulation of flash pyrolysis) and the resultant volatiles are being separated in the GC and identified by the MS. Five different temperatures (200  $^{\circ}\text{C}$ , 300  $^{\circ}\text{C}$ , 400  $^{\circ}\text{C}$ , 500  $^{\circ}\text{C}$  and 800  $^{\circ}\text{C}$ ) of pyrolysis were chosen in order to study the evolution of volatiles with temperature. The py-GC/MS chromatograms together with analytical tables of the identified compounds are shown in **Appendix A**.

**Table 4.6** shows the yields of these volatiles. The carbohydrates found to decompose first (alginic acid and fucoidan) from slow heating rate pyrolysis (TGA), were found to have significant volatile evolution at lower temperature (300 °C), while significant evolution of volatiles from the sugars (mannitol and laminarin) occurred at 500 °C. It can be seen that at 800 °C the volatile matter of all the carbohydrates apart from alginic acid is lower than that found from thermogravimetric analysis. This suggests that slow heating rates favour the decomposition of mannitol, laminarin and fucoidan while fast heating rates favour the decomposition of alginic acid.

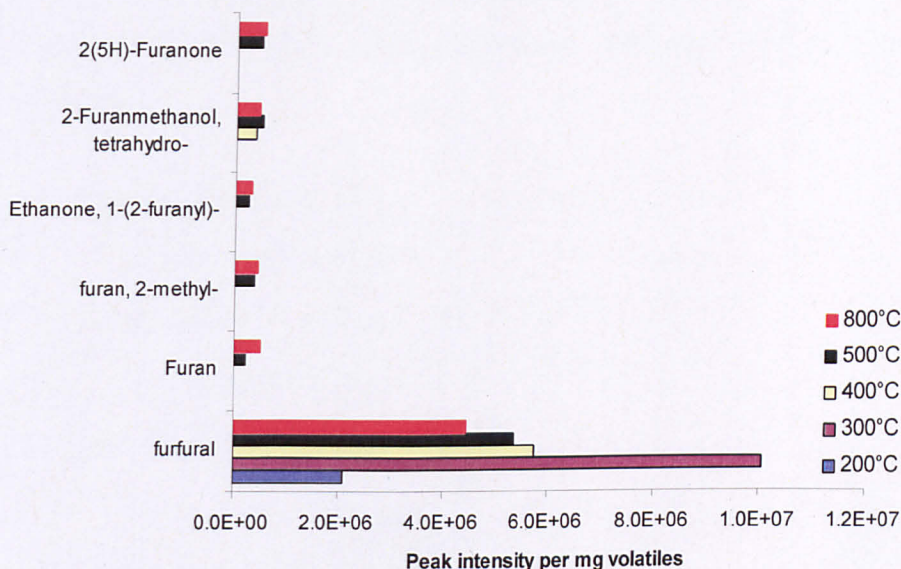
**Table 4.6** Volatiles yields (wt %) at different pyrolysis temperatures for alginic acid, mannitol, laminarin and fucoidan.

Carbohydrate	Volatiles (wt%) evolved at different temperature				
	200 (°C)	300 (°C)	400 (°C)	500 (°C)	800 (°C)
Alginic acid	10.5	23.5	49.5	56.5	77.5
Mannitol	9.5	10.5	12.5	46.5	73.5
Laminarin	4.5	8.5	12.5	59.5	70.5
Fucoidan	3.5	15.5	22.5	41.5	54.5

The volatiles evolved were identified from mass spectral detection and the peak intensities in the chromatograms were normalised per mg of volatile products in order to compare the peak intensities for the same carbohydrate at different temperatures. The peak intensities of the main volatiles evolved at each pyrolysis temperature are shown graphically in **Figures 4.8-4.11**.

The main decomposition product of alginic acid was found to be furfural and this is evident over the range of different temperatures. **Figure 4.8** shows the evolution of the main volatiles with temperature. At lower temperatures (ca200°C) alginic acid is decomposed to furfural. By increasing the pyrolysis temperature to 300°C formation of furfural reaches a maximum and other compounds begin to be observed including ketones and alcohols. At a temperature greater than 300°C, the concentration of furfural decreases further to form furfural derivatives such as tetrahydro 2-furanmethanol., furans, 1-(2-furanyl) ethanone, 2(5H)-furanone. These

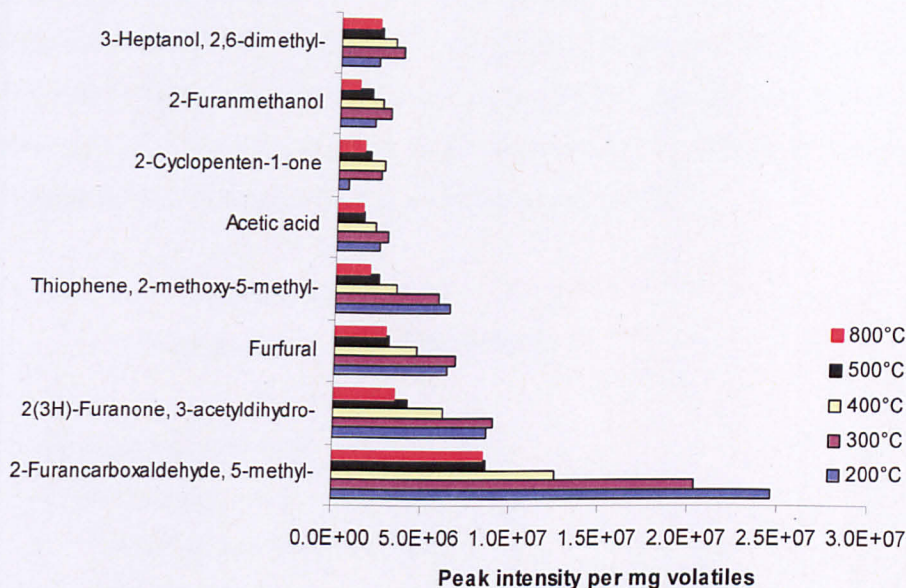
are thought to be formed via oxidation and decarboxylation reactions of furfural. At high temperature (800°C) phenolic compounds are formed, along with some straight chain alcohols such as 3-buten-1-ol and 2-methyl 2-butenol. Other compounds identified include acetic acid and toluene.



**Figure 4.8** Effect of temperature in the main volatiles evolved during py-GC/MS of alginic acid.

The main decomposition product of pyrolysis of fucoidan was observed to be 5-methyl-2-furancarboxaldehyde, Along with it, three more secondary decomposition products are formed including 3-acetyldihydro 2(3H)-furanone, furfural and 2-methoxy-5-methyl thiophene. **Figure 4.9** shows the evolution of the main volatiles from pyrolysis of fucoidan with temperature. All of the main decomposition products are evident at 200°C although the volatiles evolved at this temperature were low (3.5 wt %). Three of them are furanic originated while the fourth (thiophene) is a sulphur containing heterocycle. Furfural is a common decomposition product from alginic acid and fucoidan but formed in lower amounts from fucoidan. At 300°C the concentration of furfural and 3-acetyldihydro 2(3H)-furanone remain the same while there is a decrease in the concentrations of 5-methyl-2-furancarboxaldehyde and 2-methoxy-5-methyl thiophene. This decrease is followed by an increase in other furanic compounds such as 2-methyl-furan, 5-(1-methylethyl)-2(5H)-furanone, 2-furanmethanol along with 2-cyclopenten-1-one and

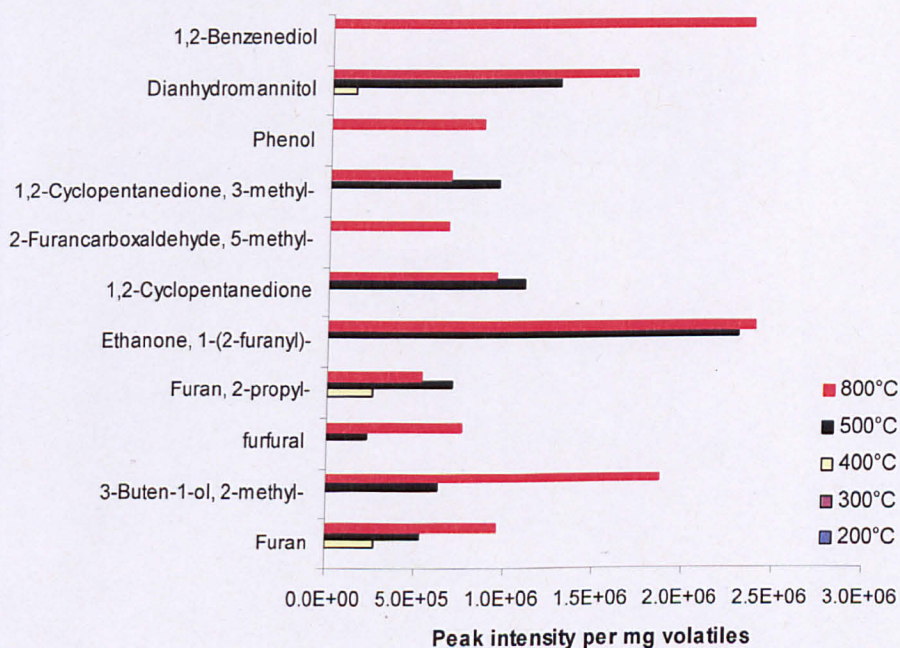
2, 6-dimethyl-3-heptanol. At temperature of 400°C the concentration of all the main decomposition products decrease as two new products are formed (4-methyl-3-heptanone, and 5-[(5-methyl-2-furanyl) methyl]-2-furancarboxaldehyde,). At 500°C the main decomposition products stabilize as there is no further decrease at 800°C. The only newly formed compound at high temperature (800°C) is phenol just as in the case of alginic acid. Other compounds identified include butanal and pantolactone.



**Figure 4.9** Effect of temperature in the main volatiles evolved during py-GC/MS of fucoidan.

The generation of volatile compounds from the pyrolysis of mannitol begins at 400°C. During pyrolysis at the lower temperatures of 200°C and 300°C there was no devolatilization observed. Initial devolatilization products included furan, 2-propyl-furan and dianhydromannitol. Pyrograms indicated the presence of many different compounds and do not exhibit an obvious stepwise reaction scheme like those of alginic acid and fucoidan. **Figure 4.10** illustrates the influence of pyrolysis temperature in the evolution of volatiles from mannitol. The initial devolatilization products include dianhydromannitol, 2-propyl furan and furan. The dianhydromannitol increases with temperature although there maybe some reduction in the transfer of this component through the analytical system. Dianhydromannitol is known to condense in the pyrolysis unit at lower temperatures and so the results

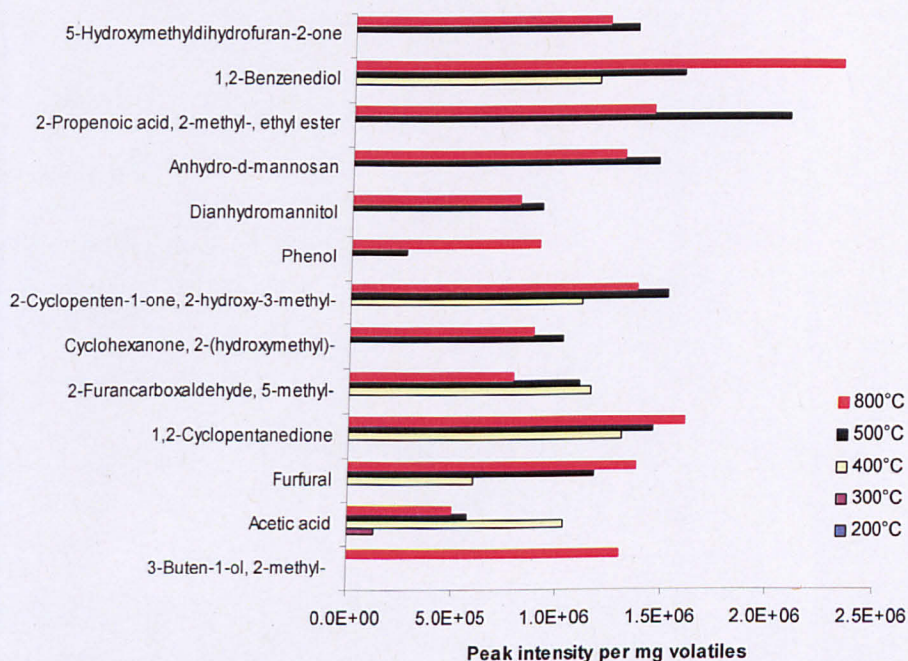
maybe misleading. The TGA indicates that devolatilization occurs at a lower temperature and so the lack of dianhydromannitol at lower temperatures supports the assumption that condensation is occurring. At 500°C other volatiles such as 1-(2-furanyl) ethanone, 2-methyl-3-buten-1-ol, furfural, 1,2-cyclopentanedione, and 3-methyl-1,2-cyclopentanedione are formed. Increasing the temperature to 800°C, there is an increase in the intensities of 1-(2-furanyl) ethanone, 2-methyl-3-buten-1-ol and furfural while the intensities of the cyclopentanediones is decreasing. Once again, at temperatures above 800°C there is evidence for the formation of phenols, with the addition of another new compound formed at this temperature, 1,2-benzenediol. Other secondary compounds identified include isosorbide and 1,3-butadiene. The main decomposition products from the pyrolysis of mannitol were found to be 1-(2-furanyl) ethanone and dianhydromannitol.



**Figure 4.10** Effect of temperature in the main volatiles evolved during py-GC/MS of mannitol.

Laminarin was found to produce a series of characteristic compounds during pyrolysis. The influence of temperature on the main volatiles is illustrated in **Figure 4.11**. These are 1,2-cyclopentanedione, 2-hydroxy-3-methyl-2-cyclopenten-1-one, anhydro-d-mannosan, 2-methyl-, ethyl ester 2-propenoic acid, 1,2-benzenediol and

5-hydroxymethyl-dihydrofuran-2-one. However, none of these characteristic compounds were formed at the lower temperatures (200°C and 300°C). At 200°C 2-methyl-propanal, 2-butenol, 1-(2-furanyl) ethanone and 5-hydroxy-2-methyl-4H-pyran-4-one were formed while at 300°C 2-methyl-furan, along with acetic acid started forming as well. 1,2-cyclopentanedione and 1,2-benzenediol were formed among others at 400°C and their peak intensities showed increase with the increase of temperature while 2-hydroxy-3-methyl-2-cyclopenten-1-one, showed a decrease at temperature greater than 500°C. At 500°C all the major and characteristic compounds (apart of 2-methyl-3-buten-1-ol) were formed followed by a decrease in their intensities at 800°C apart from 1,2-cyclopentanedione and 1,2-benzenediol as was mentioned before. Phenol started producing at 500°C followed by a significant increase in its peak intensity at 800°C. Other compounds identified include levoglucosenone and pantolactone.



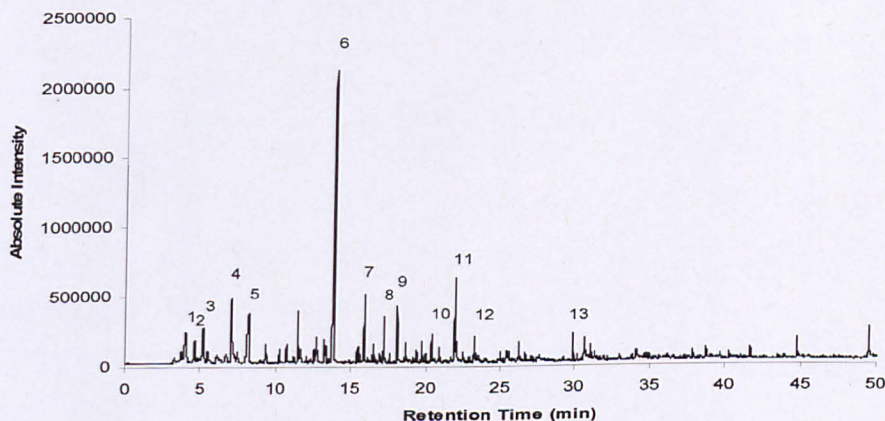
**Figure 4.11** Effect of temperature in the main volatiles evolved during py-GC/MS of laminarin.

The influence of the cation ( $\text{Ca}^+$  or  $\text{Na}^+$ ) bound to alginic acid was also investigated by py-GC/MS. The volatile fragments evolved during pyrolysis of Na alginate differ than those evolved from alginic acid and Ca alginate as illustrated in

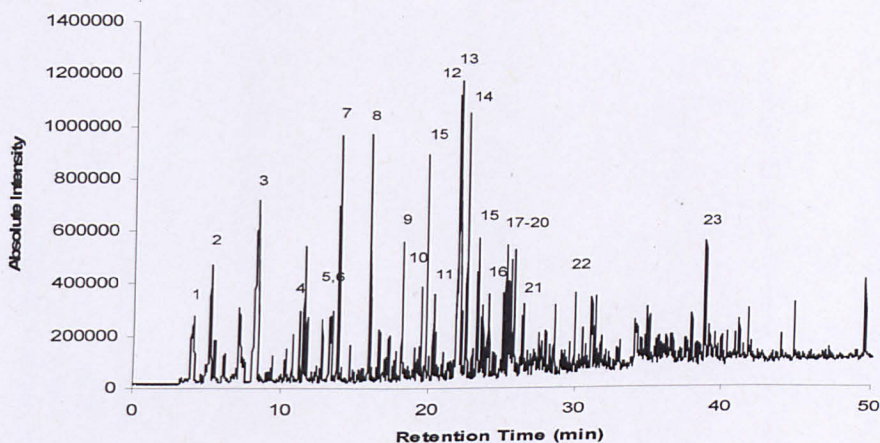


**Figures 4.12 and 4.13.** The Ca alginate produces predominantly furfural and is similar to that observed for alginic acid. For the Na alginate, furfural is no longer the major volatile and a large range of substituted cyclopentenones are formed. The exact mechanism for this difference in behavior is unclear although  $\text{Na}^+$  maybe catalyzing the decomposition as was also noticed during thermogravimetric analysis.

The carbohydrates of brown seaweeds investigated in this study were found to produce a series of characteristic volatile compounds during pyrolysis. Some of these compounds are common to two or more of the carbohydrates. For example furfural is formed when pyrolysing all of the carbohydrates. Also mannitol and laminarin have common volatile products such as 1-(2-furanyl) ethanone, 1,2-benzendiol, dianhydromannitol etc. This was expected since mannitol can be attached to the chain end of laminarin. **Table 4.7** shows the structures, retention times and origin of these volatiles.



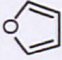
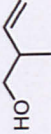
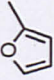
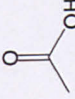
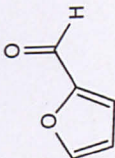
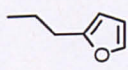
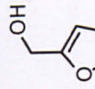
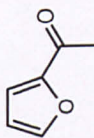
**Figure 4.12** Pyrolysis-GC-MS of Ca alginate at 500°C. The main peaks are assigned from mass spectral detection as follows: (1) 2-methyl-2-propanamine; (2) 2-methyl-furan, (3) N-butyl-1-butanamine, (4) acetic acid, (5) N-nitrosodimethylamine, (6) furfural, (7) n-butylethylenediamine, (8) 4-cyclopentene-1,3-dione, (9) 1,2-cyclopentanedione, (10) 2(5H)-furanone, (11) 2-hydroxy-3-methyl-2-cyclopenten-1-one, (12) Phenol, (13) 2(3H)- 5-acetyldihydro-furanone.

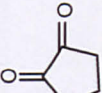
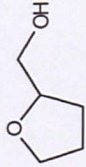
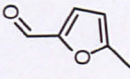
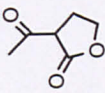
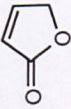
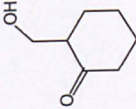
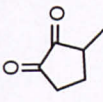


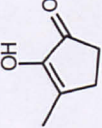
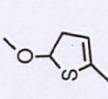
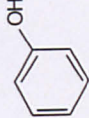
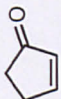
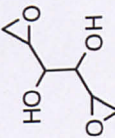
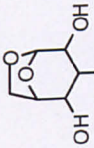
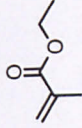
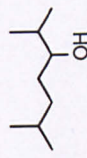
**Figure 4.13** Pyrolysis-GC-MS of Na alginate at 500°C. The main peaks are assigned from mass spectral detection as follows: (1) 2-methyl-2-propanamine, (2) 2-amino-4-methyl-pentanamide, (3) N-nitrosodimethylamine, (4) Cyclopentanone, (5) 2-methyl-cyclopentanone, (6) 3-methyl-cyclopentanone, (7) Furfural, (8) 2-methyl-2-cyclopenten-1-one, (9) 1,2-cyclopentanedione, (10) 2,3-dimethyl-2-cyclopenten-1-one, (11) 3-methyl-2-cyclopenten-1-one, (12) 3,4-dimethyl-2-cyclopenten-1-one, (13) 2,3-dimethyl-2-cyclopenten-1-one, (14) 2-hydroxy-3-methyl-2-cyclopenten-1-one, (15) 3-ethyl-2-hydroxy-2-cyclopenten-1-one, (16) phenol, (17) 3-ethyl-2-cyclopenten-1-one, (18) 3-ethyl-2-hydroxy-2-cyclopenten-1-one, (19) 4-isopropylcyclohexanone, (20) 2-ethyl-2-methyl-1,3-cyclopentanedione, (21) 3-methyl-phenol, (22) 5-acetyldihydro-2(3H)-furanone, (23) 2-methyl-1,4-benzenediol.

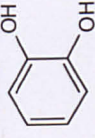
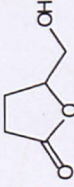
However, the relative intensities of the common volatiles differ. For example upon pyrolysis, mannitol produces dianhydromannitol in significantly higher intensity than pyrolysis of laminarin in all temperatures studied. The same was observed for 5-methyl-2-furancarboxaldehyde which is produced at higher intensity when pyrolysing fucoidan. Thus, there is a set of compounds that can verify the presence or absence of a certain carbohydrate when analysed by py-GC/MS. For alginic acid such a compound is furfural, for fucoidan these compounds are 5-methyl-2-furancarboxaldehyde and 2-methoxy-5-methyl-thriophene, for mannitol they are 1-(2-furanyl)-ethanone and dianhydromannitol and finally for laminarin 1,2-cyclopentanedione, 2-hydroxy-3-methyl-2-cyclopenten-1-one and acetic acid.

**Table 4.7** Structures and origin of the main volatiles evolved during py-GC/MS of the main carbohydrates of brown macro-algae.

Main Volatiles	RT	Formula	Structure	MW	Origin
Furan	3.655	C <sub>4</sub> H <sub>4</sub> O		68	Alginic acid, mannitol
2-methyl-3-buten-1-ol	3.846	C <sub>5</sub> H <sub>10</sub> O		86	Mannitol, laminarin
2-methylfuran	4.51	C <sub>5</sub> H <sub>6</sub> O		82	Alginic acid
Acetic acid	6.998	C <sub>2</sub> H <sub>4</sub> O <sub>2</sub>		60	Fucoxanthin, laminarin
Furfural	13.972	C <sub>5</sub> H <sub>4</sub> O <sub>2</sub>		96	Alginic acid, fucoxanthin, mannitol, laminarin
2-propyl-furan	14.416	C <sub>7</sub> H <sub>10</sub> O		110	Mannitol
2-furanmethanol	15.612	C <sub>5</sub> H <sub>6</sub> O <sub>2</sub>		98	Fucoxanthin
1-(2-furyl) ethanone	16.58	C <sub>6</sub> H <sub>6</sub> O <sub>2</sub>		110	Alginic acid, mannitol

1,2-cyclopentanedione	18.189	$C_5H_6O_2$		98	Mannitol, laminarin
2-furanmethanol, tetrahydro-	18.83	$C_5H_{10}O_2$		102	Alginate acid
5-methyl-2-furancarboxaldehyde	19.496	$C_6H_8O_2$		110	Fucoidan, mannitol, laminarin
3-acetyldihydro-2(3H)-furanone	20.197	$C_6H_8O_3$		128	Fucoidan
2(5H)-furanone	20.448	$C_4H_4O_2$		84	Alginate acid
2-(hydroxymethyl)-cyclohexanone	21.018	$C_7H_{12}O_2$		128	Laminarin
3-methyl-1,2-cyclopentanedione	21.997	$C_6H_8O_2$		112	Mannitol

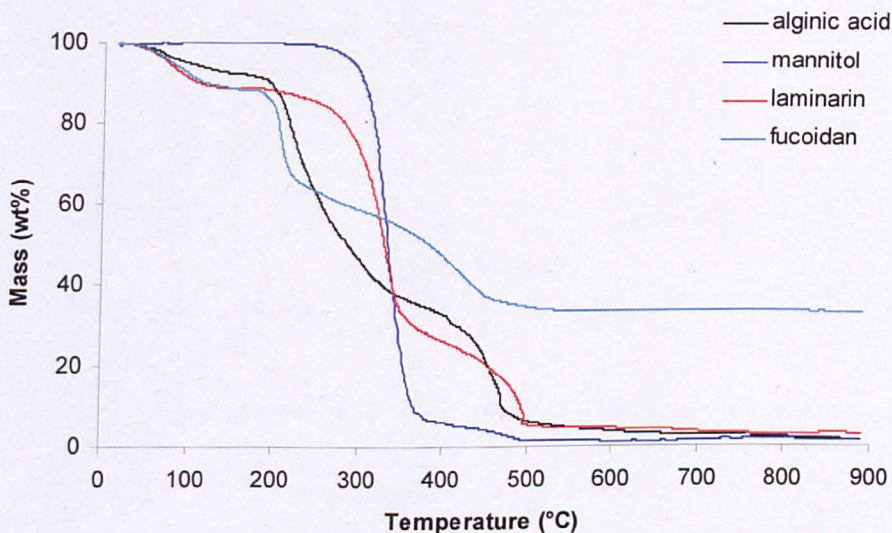
2-hydroxy-3-methyl-2-cyclopenten-1-one	22.032	$C_6H_8O_2$		112	Laminarin
2-methoxy-5-methyl-thiophene -	22.511	$C_6H_8OS$		128	Fucoidan
Phenol	23.279	$C_6H_6O$		94	Mannitol, laminarin
2-cyclopenten-1-one	24.364	$C_5H_6O$		82	Fucoidan
Dianhydromannitol	30.361	$C_6H_{14}O_4$		146	Mannitol, laminarin
Anhydro-d-mannosan	31.02	$C_6H_{10}O_5$		162	Laminarin
2-Methyl-2-propenoic acid, ethyl ester	31.555	$C_6H_{10}O_2$		114	Laminarin
2,6-dimethyl-3-heptanol	33.342	$C_9H_{20}O$		144	Fucoidan

1,2-benzenediol	34.005	$C_6H_6O_2$		110	Mannitol, laminarin
5-hydroxymethyl-dihydrofuran-2-one	34.526	$C_5H_8O_3$		116	Laminarin

### 4.3 Combustion behaviour of model carbohydrates

#### 4.3.1 Thermogravimetric analysis (TGA) of model carbohydrates in air

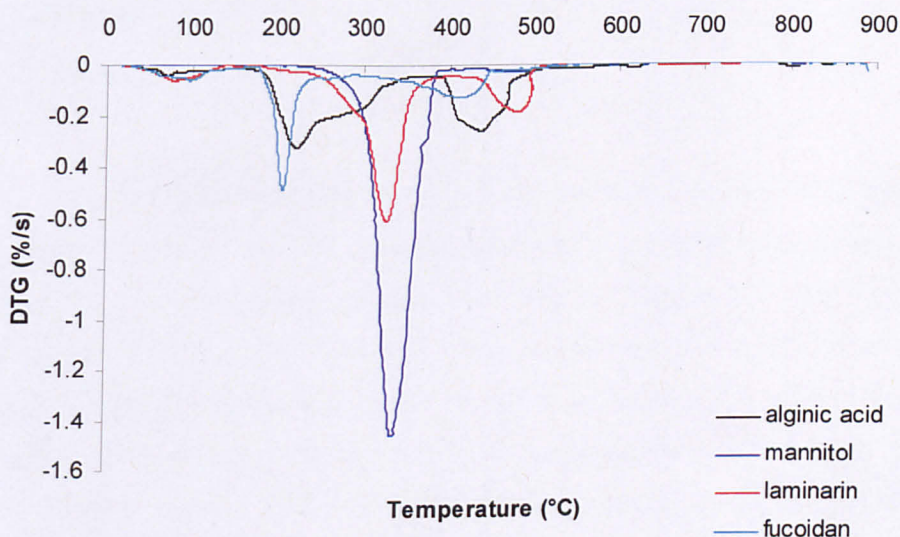
The model carbohydrates were also examined for their combustion behaviour under oxidizing atmosphere using thermogravimetric analysis. The TGA curves, where the percentage weight loss, based on the initial weight, is plotted against temperature are shown in **Figure 4.14**. Three steps of weight loss were observed for all the samples. The first is due to moisture evaporation, while the second and third are due to the combustion process. The extent of weight loss and the temperature range of this weight loss differed between the carbohydrates. In general fucoidan was found to have the highest ash content while the other three carbohydrates had similar ash content. Also, mannitol was found to have relatively no moisture content, while the rest of the carbohydrates had similar moisture content.



**Figure 4.14** TGA profiles of alginic acid, mannitol, laminarin and fucoidan in air at 25°C/min.

The DTG curves, often referred as burning profiles, where the differentiation of weight loss percentage is plotted against temperature are shown in **Figure 4.15**. In these curves the two combustion steps can be seen more clearly. During the combustion of lower rank coals there are usually two major peaks in the DTG curve which was the case for the model compounds. The first peak indicates the release,

ignition and combustion of volatile matter (devolatilization), while the second indicates the ignition and combustion of the fixed carbon (char combustion). The peaks of the model carbohydrates were found to differ in position and height and useful information about the ignition of combustion, the reactivity and the ease of combustion for each of the carbohydrates could be deduced. These combustion characteristics are shown in **Table 4.8**. The first combustion step is attributed to pyrolysis so it is the same as previously during thermogravimetry in nitrogen. Thus the initiation of combustion as well as the peak temperature of the first step is very similar to the initiation of pyrolysis and the peak pyrolysis temperature.



**Figure 4.15** DTG profiles of alginic acid, mannitol, laminarin and fucoidan in air at 25°C/min.

Combustion of mannitol started later (230°C) than that of the other carbohydrates (160-175°C). Initiation of combustion for alginic acid and fucoidan was followed by a rapid weight loss giving a low volatile matter peak temperature (220 and 205°C respectively). However, fucoidan's peak was sharper and higher indicating the higher removal rate and reactivity of fucoidan. Alginic acid's peak was wider covering larger area under the peak, indicating the removal of more material which is evident in the TGA curve. Although combustion of laminarin starts at low temperature it progresses slowly until it reaches a rapid weight loss, giving a volatile matter peak temperature of 330°C, similar to that of mannitol (340°C) that its combustion starts at later temperature. Mannitol was found to have



the highest peak, indicating that is removed with the faster rate out of all the carbohydrates.

**Table 4.8** Combustion temperature characteristics of the carbohydrates of brown macro-algae (where, VMIT, volatile matter ignition temperature, VMPT, volatile matter peak temperature, FCIT, fixed carbon ignition temperature, FCPT, fixed carbon peak temperature, BT, burnout temperature).

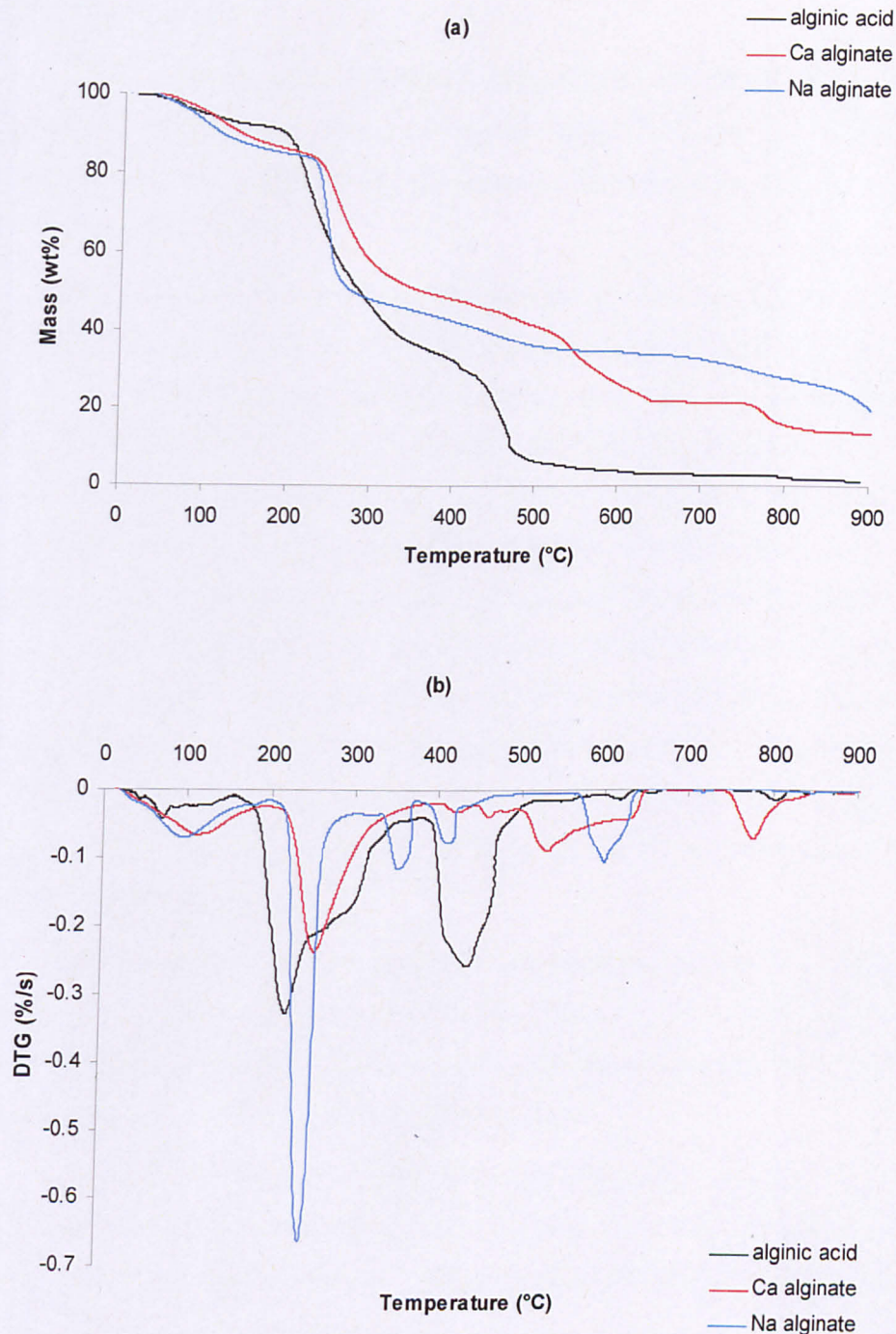
Carbohydrate	VMIT(°C)	VMPT(°C)	FCIT(°C)	FCPT(°C)	BT(°C)
<b>Alginic acid</b>	160	220	385	440	635
<b>Mannitol</b>	230	340	430	475	530
<b>Laminarin</b>	175	330	420	485	590
<b>Fucoidan</b>	175	205	305	415	555

Char burning (oxidation) starts first for fucoidan followed by alginic acid, laminarin and mannitol. Char burning peaks were shorter than the devolatilisation peaks for all carbohydrates. Alginic acid had the largest area under the peak indicating its higher char content as was shown before (**Table 4.1**). Most of mannitol's weight loss was due to volatile matter as low char burning was observed. Laminarin was shown previously during thermogravimetric analysis in nitrogen to have low char content. However, during thermogravimetry in air a significant char burning peak was observed. Mannitol had the lowest burnout temperature followed by fucoidan, laminarin and alginic acid.

Alginic acid had the lowest volatile matter ignition temperature (VMIT) but complete burnout of char (BT) occurred at higher temperature than the other carbohydrates. It was found to have the most complicated burning profile just as in case of thermogravimetry in nitrogen, possibly due to the synergetic effect of its salts (Ca and Na alginate). This synergetic decomposition in an oxidative atmosphere is studied in the next subchapter. Mannitol showed the fastest removal rate explaining the lower burnout temperature out of all the carbohydrates despite the later initiation of combustion. Combustion was found to start at the same temperature for laminarin and fucoidan, with fucoidan combustion finishing at lower temperature than that of laminarin.

#### 4.3.2 Thermogravimetric analysis (TGA) of alginate salts in air

Figure 4.16a-b shows the TGA and DTG profiles for oxidation of alginic acid and its salts (Ca and Na alginate) in air. Under an oxidative environment, the onset of combustion follows the order alginic acid > Na alginate > Ca alginate. The main decomposition step is observed over a similar temperature range to pyrolysis. Just as in thermogravimetry in nitrogen, alginic acid shows a wider main decomposition DTG peak than its alginates, which ends when the main decomposition of Ca alginate ends. However, significant differences exist between the char burnout for the alginates. For the Na alginate, the onset of char burnout begins at significantly lower temperature than the Ca alginate. For the Ca alginate char, complete burnout occurs at a temperature some 200°C higher. This suggests the Na<sup>+</sup> is promoting oxidation and is a better catalyst than Ca for char oxidation.



**Figure 4.16** (a) TGA and (b) DTG profiles in air at 25°C/min of alginic acid, Ca alginate and Na alginate.

## 4.4 Conclusions

The pyrolysis and combustion characteristics of alginic acid, mannitol, laminarin and fucoidan were investigated using TGA and py-GC/MS. Large differences in the pyrolysis and combustion behaviour were observed from the different carbohydrates.

Thermogravimetric analysis in nitrogen has revealed the different degradation pathways of the carbohydrates. Decomposition of alginic acid and mannitol was found to produce one major weight loss region, while laminarin and fucoidan were found to produce two major weight loss regions. Their decomposition was found to start at lower temperatures than terrestrial biomass constituents (cellulose, hemicellulose and lignin), revealing that seaweed constituents are easier to break. Based on the studies conducted in this work on individual carbohydrates and their specific weight-loss regions it is possible to apply these findings to accurately map the decomposition profiles of actual seaweed. TGA has been demonstrated as a good semi-quantitative method of comparing biochemical content of different samples. Studies on the thermal behaviour of protein and algal cellulose (which might differ slightly from terrestrial cellulose) will aid in gaining a more complete representation of the actual seaweed sample.

Thermogravimetry in air revealed that char combustion starts first for fucoidan followed by alginic acid and laminarin. Mannitol had no char combustion peak. Initiation of combustion reactions started first for alginic acid but it was found the carbohydrate to have the highest burnout temperature.

During alginic acid decomposition in both inert and oxidative environments there is a synergetic decomposition between alginic acid and its salts (Ca alginate and Na alginate). It appears that  $\text{Na}^+$  catalyses both devolatilisation and oxidation.

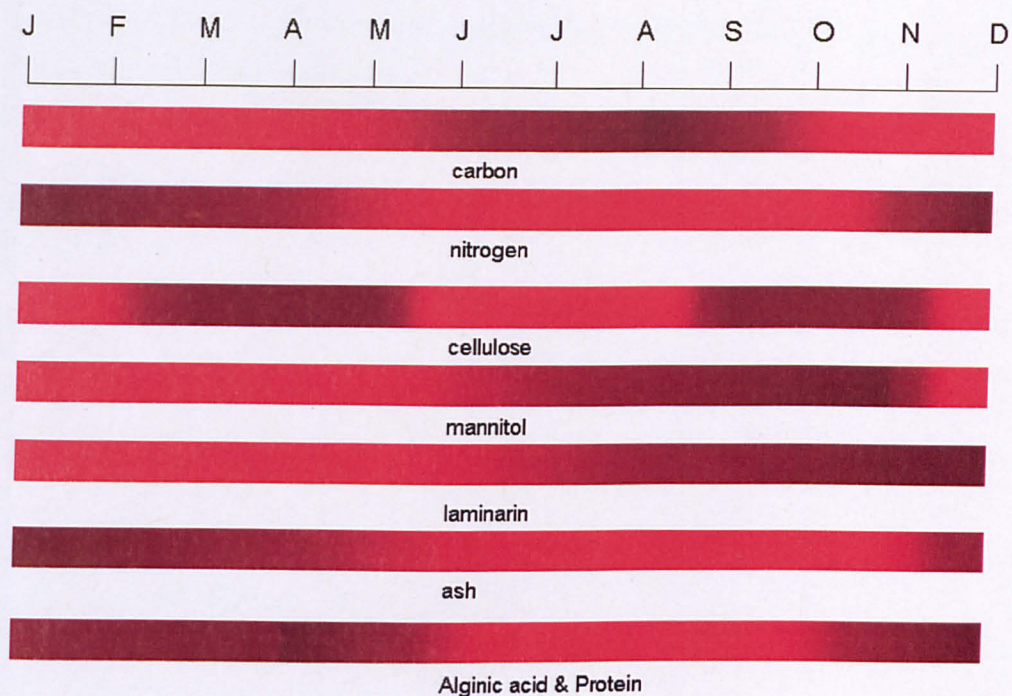
The detection of 'fingerprint' compounds by py-GC/MS can be used to determine the presence of certain carbohydrates in the seaweeds. These compounds are for alginic acid just furfural, for fucoidan 5-methyl-2-furancarboxaldehyde, 3-acetyldihydro-2(3H)-furanone, and 2-methoxy-5-methyl-triophene, for mannitol 1-(2-furanyl)-ethanone, and dianhydromannitol and finally for laminarin 1, 2-cyclopentanedione, 2-hydroxy-3-methyl-2-cyclopenten-1-one and acetic acid.

## CHAPTER 5 - Characterization of brown macro-algae

### 5.1 Introduction

Macro-algae exhibit significant changes in their biochemical composition during their growth cycle. It was discussed previously in the introduction chapter how this variation progresses throughout the year. **Figure 5.1** summarizes these variations for some brown seaweed according to data from **Black (1950, a, b); Gevaert, et al., 2001; Lewis and Smith, 1966**. Carbon content increases during spring and summer reaching its maximum value towards the end of summer and its minimum during winter, while nitrogen has the opposite trend. Cellulose content has two maximum values, the first occurring during March and April, followed by a decrease to a minimum value during June/July; cellulose then rises again to a second maximum occurring during September/October followed by another decrease. Mannitol levels reach their maximum during October, followed by a decrease leading to minimum levels during winter and early spring. Laminarin levels follow the same trend reaching maximum levels between October and December. Ash content reaches its maximum during January and its minimum during October, following the opposite trend than that of mannitol and laminarin content. Finally, alginic acid and protein levels reach their maximum between January and March with their minimum levels occurring in August.

In this chapter, the seasonal variations of the important parameters for thermochemical conversion are under investigation. More specifically, the variations in carbon, nitrogen, ash and mineral matter content. The differences between the different samples as well as the different parts of the algae (blades, stipes) are assessed. Additionally the impact of the drying method chosen (air drying, oven drying and freeze drying) and of the harvesting site on the composition of the algae is examined.

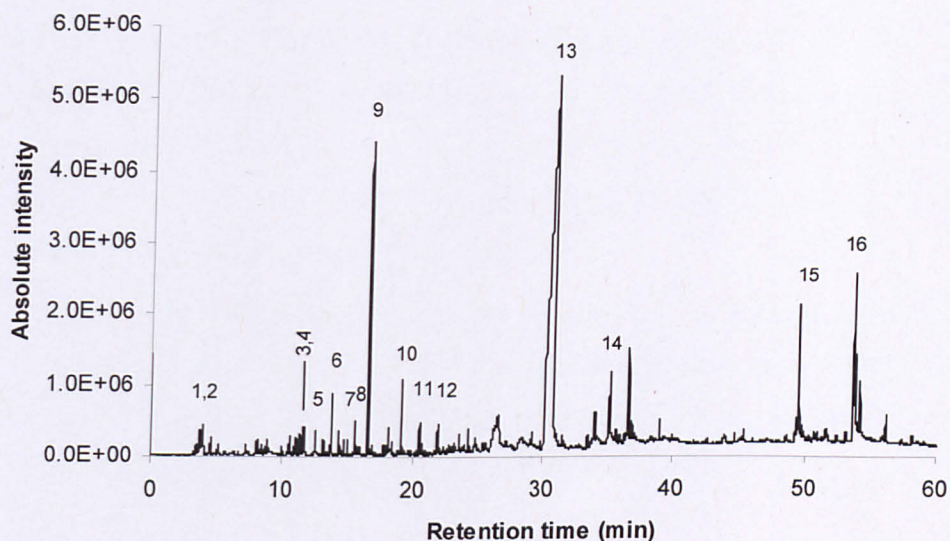


**Figure 5.1** Seasonal variation in composition of brown-algae (data from Black, 1950, a, b; Gevaert, et al., 2001; Lewis and Smith, 1966).

## 5.2 Sample preparation

Samples under investigation were weighed upon collection (wet weight) and subsequently weighed after freeze drying (dry weight) by SAMS. The resultant dry weight of the freshly harvested samples found to range between 11 and 20wt%. Unfortunately a whole seasonal set of dry weight was not provided in order to assess the seasonal variation in dry weight. According to **Black (1950a)** maximum dry weight for *L. digitata* occurs during summer and autumn with minimum dry weight content during winter and spring. He also found the seasonal variation in dry weight to be between 11 and 22.5wt%. During all the different drying methods, a brown to yellowish material was extracted by the soaking of seaweed by its water content. This material was collected, dried and analysed by py-GC/MS to determine its nature. The py-GC/MS chromatogram at 500°C of this material extracted from *L. saccharina*, along with the main identified peaks is shown in **Figure 5.2**. The main peaks identified include dianhydromannitol and 1-(2-furanyl)-ethanone suggesting that this material is mostly sugars, and contains mainly mannitol. The presence of n-

hexadecanoic acid and oleic acid suggests that a fraction of the lipid content of seaweed might be extracted also.



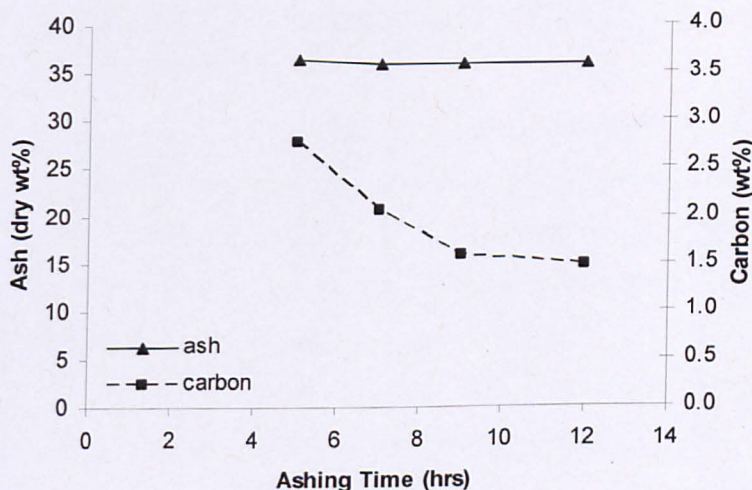
**Figure 5.2** Pyrolysis-GC-MS of extracted material during *L. saccharina* drying at 500°C. The main peaks are assigned from mass spectral detection as follows: (1) furan, (2) 2-methyl-3-buten-1-ol, (3) methyl-pyrazine, (4) pyrrole, (5) 2-methyl[1,3,4]oxadiazole, (6) furfural, (7) 2-propyl-furan, (8) 2-furanmethanol, (9) 1-(2-furanyl)-ethanone, (10) 5-methyl-2-furancarboxaldehyde, (11) resorcinol, (12) 3-methyl-1,2-cyclopentanedione, (13) dianhydromannitol, (14) isosorbide, (15) n-hexadecanoic acid, (16) oleic acid.

### 5.3 Ash determination

Seaweed fuel ashes were initially prepared according to the standard ashing procedure for terrestrial biomass which involves the heating of the fuel at 550 °C for 5 hrs. The ashes prepared in such way had a very dark greyish colour, revealing that carbon was remaining in the ash. This suggested that prolonged ashing periods were needed in order for all the carbon in the ash to burnout. Ashing periods of 5 to 12 hrs were performed and the carbon content of the ashes was measured (**Figure 5.3**). As the ashing time increased, the carbon content of the ash decreased. After 12hrs the carbon content of the ash was 1.5wt%, a reduction of half of the carbon content at 5hrs (about 3wt%). In addition, the ash content of the fuel showed only a slight decrease (about 1%) from 5 to 12 hours.

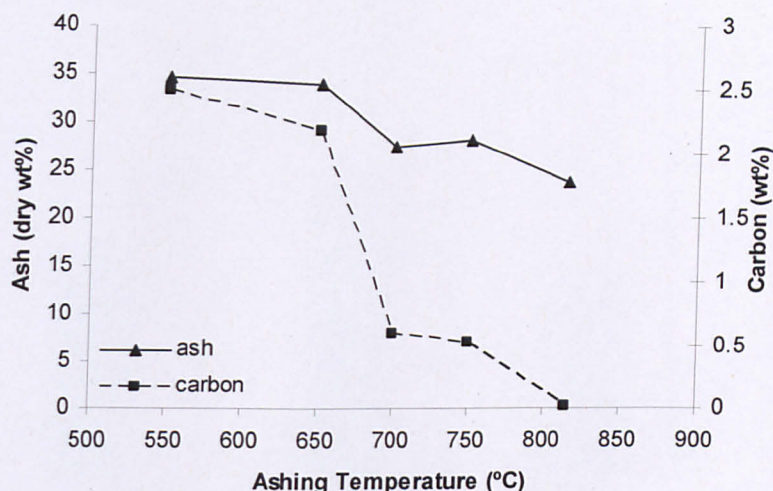
In order to study the influence of temperature on the ashing of seaweeds, samples were placed in the furnace for 5hrs at a temperature range of 550-815 °C (**Figure 5.4**). As the temperature increases the ash and carbon content is decreasing. The carbon content of the ash was depleted only at very high temperature of 815 °C. At this temperature there is a significant decrease in the ash content of the fuel (10% lower than the ash produced at 550 °C). This is due to the loss of the volatile inorganic compounds (e.g. K, Na etc.), further oxidation of the inorganic compounds and the decomposition of carbonates forming CO<sub>2</sub>.

The results indicate that low temperature ashing is the most suitable for seaweeds but a longer residence time is needed than for the standard method used for terrestrial biomass (state method) . The method that was chosen for subsequent analysis and ashing of seaweeds was 12hrs at 550 °C.



**Figure 5.3** Influence of time on ash and carbon content of *Laminaria digitata* (winter harvest).



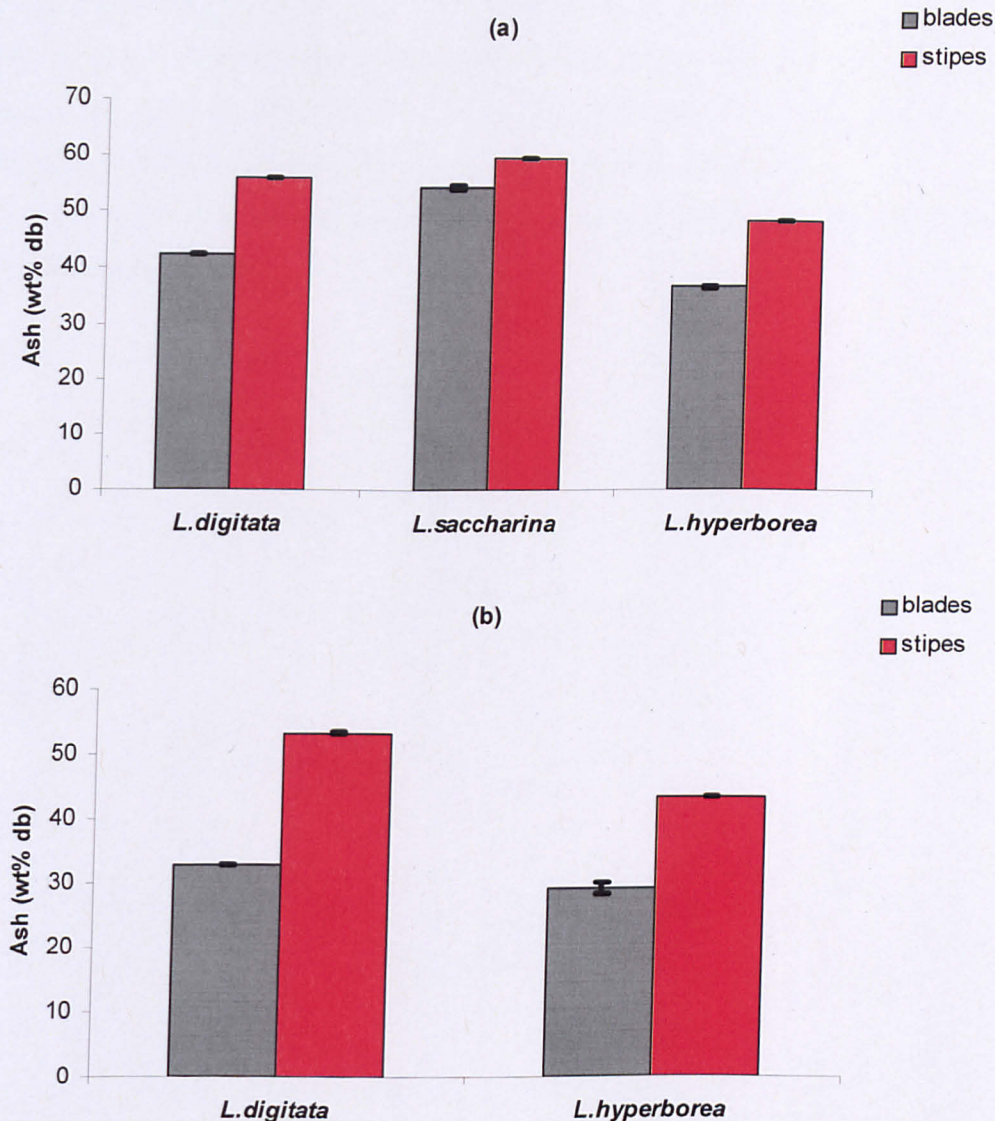


**Figure 5.4.** Influence of temperature on ash and carbon content of *Laminaria hyperborea* (winter harvest).

#### 5.4 Typical composition of brown macro-algae and differences between blades and stipes

The result of energy intake of seaweed through photosynthesis is the synthesis of different components such as carbohydrates, proteins, lipids and ash in the plant material. However, the different parts of the seaweed are expected to contain different proportions of these components resulting in different elemental and inorganic content in different parts of the plant. In order to study these differences, oven dried seaweed samples were separated into blades and stipes and were subsequently analyzed for their ultimate, proximate and inorganic content.

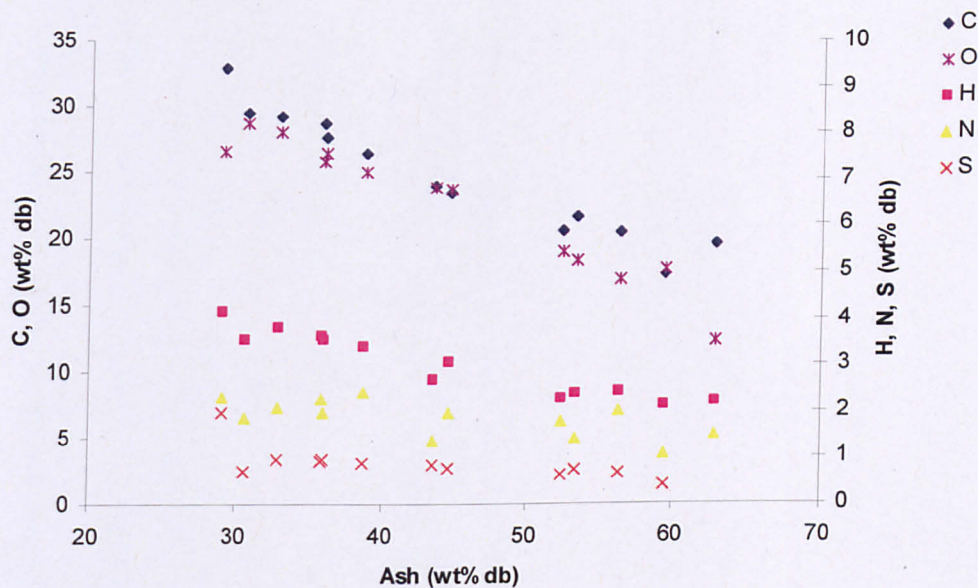
Ash levels are higher in stipes in all samples examined as shown in **Figure 5.5a-b**. The results are consistent with all the different seaweed samples and all the different harvesting sites, with ash levels being consistently 5-20wt% higher in the stipes than the blades. Ash content of the blades of the samples examined ranged between 27.9 and 54.4wt%, while for the stipes, the ash ranged between 40.6 and 59.7wt%. The seaweed *L. saccharina* contains the highest ash content in both cases. Moisture content was also found to be higher in the stipes (**Table 5.1**); the moisture content for the blades ranges between 3.3 and 5.1wt% and for the stipes ranges between 5.0 to 7.4wt%.



**Figure 5.5** Ash variation between blades and stipes of oven dried seaweed samples harvested during winter of 2009 from (a) sampling site Clachan sound and (b) sampling site Easdale.

The higher ash and moisture content in the stipes of the samples examined results in a lower elemental content (carbon, hydrogen, nitrogen, sulphur and oxygen) in the stipes of the seaweed (**Table 5.1**). Carbon content varies from 20.4 to 32.9wt% for the blades and 17.3 to 24wt% for the stipes; hydrogen content varies from 2.4 to 4.2wt% for the blades and 2.1 to 2.7wt% for the stipes; nitrogen content varies from 1.4 to 2.4wt% for the blades and 1.1 to 1.8wt% for the stipes; sulphur content varies from 0.7 to 1.9wt% for the blades and 0.4 to 0.8wt% for the stipes,

while oxygen content varies from 16.8 to 28wt% for the blades and 11.1 to 23.7wt% for the stipes. The influence of ash on the carbon, oxygen and hydrogen content of the samples is clear from **Figure 5.6** showing decreased C, H, and O content in samples with increased ash content while its influence in N and S is not so clear. Detailed tables with ultimate and proximate analysis of oven dried samples can be found in **Appendix B**.



**Figure 5.6** Influence of ash content in elemental composition of oven dried, winter harvested seaweed samples.

**Table 5.1** Proximate and ultimate analysis of blades and stipes of winter harvested oven dried seaweed samples.

Sample	Part of sample	Harvest site	Moisture (wt%)	Ash (wt%)	C (wt%)	H (wt% db)	N (wt%)	S (wt%)	O <sup>a</sup> (wt% db)
<i>L. digitata</i>	Blades	Clachan sound	4.6	42.5	23.5	3.0	2.0	0.8	23.6
	Stipes		5.4	56.2	17.3	2.1	1.1	0.4	17.5
	Blades	Easdale	4.6	31.3	29.3	3.8	2.1	0.9	28.0
	Stipes		5.3	50.4	21.6	2.4	1.4	0.7	18.2
<i>L. saccharina</i>	Blades	Clachan sound	3.3	54.4	20.4	2.4	2.0	0.7	16.8
	Stipes		5.0	59.7	19.5	2.7	1.5	0.5	11.1
<i>L. hyperborea</i>	Blades	Clachan sound	5.1	36.7	26.5	3.4	2.4	0.9	25.0
	Stipes		7.4	48.4	20.6	2.2	1.8	0.6	19.0
	Blades	Easdale	4.2	27.9	32.9	4.2	2.3	1.9	26.6
	Stipes		6.8	40.6	24.0	2.7	1.4	0.8	23.7

<sup>a</sup> calculated by difference

The inorganic (metal) content of the samples is in proportion to their ash content. Samples with higher total inorganic content have higher ash content. **Table 5.2** shows the metal concentration of the samples under examination. Detailed tables with metal analysis of oven dried samples can be found in **Appendix C**. Brown macro-algae contain high metal content with alkali metals such as potassium (K) and sodium (Na) being the dominant metals present, followed by the alkaline earth metals calcium (Ca) and magnesium (Mg). K, Na, Ca and Mg can be found dissolved in seawater but their concentration is many times lower than that in seaweed. Seaweeds accumulate large quantities of K, Na, Ca and Mg which are essential nutrients for their growth. These salts are mainly associated with alginic acid as they bound to it to create K, Na, Ca and Mg alginates and make up most of the mineral matter in brown kelps. Other elements found in significant concentration include iron (Fe) and Strontium (Sr). Trace elements identified include Al, As, B, Ba, Cd, Cr, Cu, Li, Mn, Ni and Zn. The total metal content is higher in the stipes just as in the case of the ash content. The metal content of the blades of the samples examined (oven dried, winter harvested) was found to range between 120000 and 200000 ppm while for the stipes ranged between 140000 and 280000 ppm. *L. saccharina* harvested from Barancarry had the lowest metal content while *L. digitata* harvested from Clachan sound had the highest.

**Table 5.2** Metal analysis of blades and stipes of winter harvested oven dried seaweed samples (Eas = Easdale, CS = Clachan sound, Brn = Barancarry).

	Metal Concentration (ppm) (db)											
	<i>L. digitata</i>				<i>L. saccharina</i>				<i>L. hyperborea</i>			
	blades Eas	blades CS	stipes CS	blades Brn	stipes Brn	blades CS	stipes CS	blades Eas	stipes CS	blades Eas	Easdale Eas	
<b>Al</b>	301	229	134	1402	183	295	458	117	204			
<b>stdev</b>	10.06	8.46	3.74	363.17	22.32	27.40	11.60	8.35	13.92			
<b>As</b>	143	156	58	86	61	132	63	109	66			
<b>stdev</b>	3.43	0.79	0.55	28.81	2.24	3.16	0.73	2.14	0.63			
<b>B</b>	124	138	156	101	205	116	198	100	156			
<b>stdev</b>	2.02	8.90	3.25	29.62	9.79	2.52	3.45	2.57	1.09			
<b>Ba</b>	51.78	5.61	4.73	16.34	10.57	9.80	6.73	5.69	6.02			
<b>stdev</b>	53.55	1.47	0.45	3.97	0.68	0.63	0.15	0.36	0.35			
<b>Ca</b>	17574	11105	8708	14189	16532	16466	11213	9738	13352			
<b>stdev</b>	614	116	95	1521	174	306	21	173	283			
<b>Cd</b>	2.90	3.26	1.28	2.01	1.58	2.65	1.60	2.38	1.50			

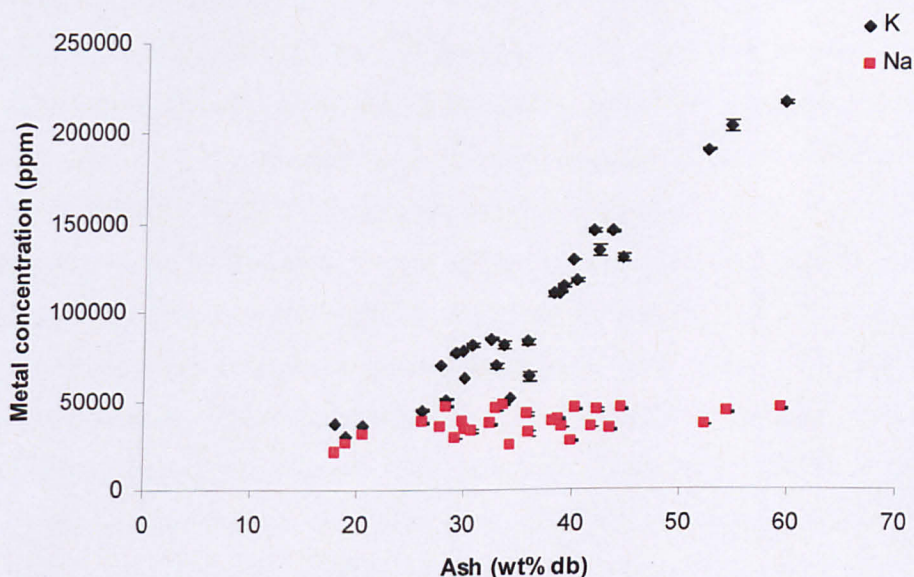
stdev	0.06	0.34	0.02	0.63	0.40	0.09	0.12	0.33	0.13
Cr	2.33	3.31	9.85	0.00	13.56	1.46	14.17	1.19	7.77
stdev	0.14	0.79	0.03	0.10	0.45	0.23	0.37	0.38	0.13
Cu	18.46	14.57	14.54	17.08	2.70	6.88	6.40	24.07	3.26
stdev	0.18	0.63	4.24	4.96	0.58	0.17	0.21	0.39	0.35
Fe	949	9444	474	2833	264	1913	1562	1057	235
stdev	4.70	94.66	0.26	452.65	6.91	55.39	19.46	19.59	0.53
K	69865	130291	217110	63872	81624	111033	190432	77116	145288
stdev	1401	2364	808	2512	1026	955	364	664	687
Li	1.63	2.05	1.79	5.18	1.09	1.59	2.97	1.06	1.50
stdev	0.10	0.45	0.03	0.98	0.39	0.07	0.12	0.33	0.13
Mg	9423	8243	6412	7110	8069	7956	6441	6865	6297
stdev	102	107	9	2232	297	142	69	81	4
Mn	13.81	34.42	4.47	47.07	18.54	19.06	94.14	7.80	18.80
stdev	0.09	0.46	0.11	15.15	0.67	0.54	1.26	0.35	0.13
Na	44976	44996	45052	31701	33253	39572	36370	29156	33668

stdev	620	655	128	1257	929	556	131	234	615
Ni	4.30	4.37	2.05	0.00	3.76	2.65	3.30	3.44	2.38
stdev	0.09	0.35	0.03	0.10	0.41	0.09	0.12	0.33	0.21
Sr	984	786	580	563	930	956	716	536	1111
stdev	11.32	19.83	0.91	187.36	28.68	15.01	1.09	4.01	3.61
Zn	100	91	29	34	33	59	33	38	24
stdev	2.05	3.20	0.24	10.93	1.66	1.30	0.50	0.66	0.22
Total	144533	205546	278752	121979	141206	178542	247614	124878	200442
stdev	1655	2460	824	3945	1427	1157	394	730	965



The higher metal content and thus the higher ash content in the stipes of seaweed is due to the fact that the stipe is perennial (while the blades are reproducing when there is an increase in the rate of photosynthesis) which helps in the accumulation of metals (**Black, 1950a**)

**Figure 5.7** shows the K and Na concentration of oven dried seaweed samples harvested during winter, spring and summer from different locations plotted against their ash content. It is clear that the potassium concentration is responsible for the increase in ash content in the samples. Increased potassium concentration leads to higher ash content in seaweeds while sodium concentration remains relatively steady with increased ash content.



**Figure 5.7** Influence of K and Na concentration in ash content of seaweed samples.

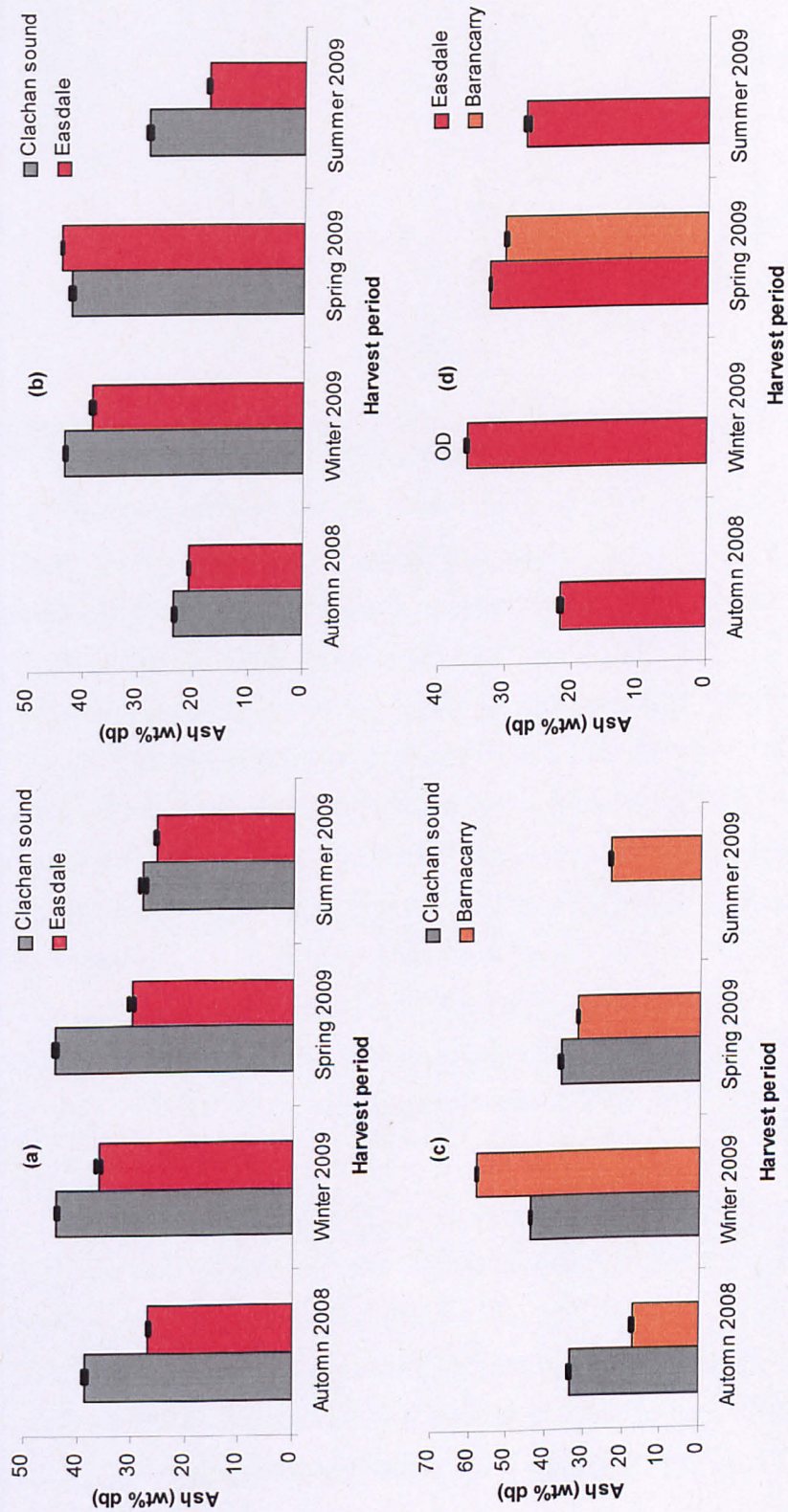
The lower elemental content and higher ash content in the stipes of the seaweed should result in less volatile matter evolved during thermochemical processes making stipes less attractive than blades for processing.

### 5.5 Seasonal variations and effect of harvesting site

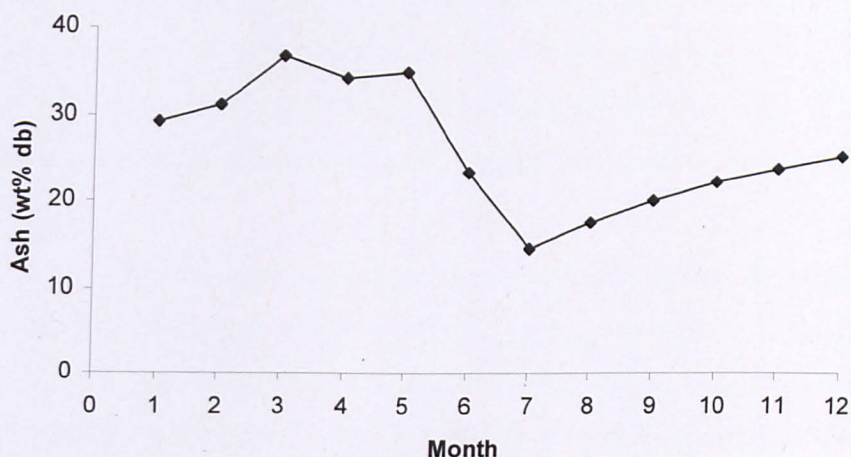
In the previous subsection (5.4) was shown the differences in seaweed properties between the different parts of the plant (blades, stipes). Significant differences were also observed in the properties of seaweed according to the season

and location of harvest and will be subsequently examined in the present subsection. For this examination, freeze dried seaweed samples (whole plant material) harvested throughout the year from different locations (Clachan sound, Barnacarry and Easdale) were examined. *L. digitata* and *L. hyperborea* were harvested from Clachan sound and Easdale while *L. saccharina* was harvested from Clachan sound and Barnacarry and *A. esculenta* was harvested from Barnacarry and Easdale. Winter harvest took place during mid January, spring harvest during mid-end April, summer harvest during mid-end July and autumn harvest during mid September.

**Figure 5.8a-d** shows the variation in ash content on a dry basis throughout the year of seaweed from different harvest sites. *L. digitata* ash (**Figure 5.8a**) reaches its minimum content during summer after which it increases during autumn, reaching its maximum content during winter. Samples harvested from Clachan sound showed the same maximum ash content during winter and spring while samples harvested from Easdale showed a decreased ash content during spring. **Black (1950a)** found maximum ash content for *L. digitata* during March, suggesting that maximum ash content occurs during late winter, early spring (March-April) when the new fronds (blades) of the plant are produced. Unfortunately the samples under investigation were harvested quarterly so no individual data for each month was measured however the results still provide a valuable trend. The difference observed in the ash levels during spring for the two sampling sites might be attributed to slight discrepancies in the harvest time. That is, the samples from Clachan sound were harvested during early April (06/04) while the samples from Easdale were harvested during the end of April (28/04). Variation in ash content was more significant for samples harvested from Clachan sound with ash levels ranging between 28 and 44wt% (db); while ash content of samples harvested from Easdale ranged between 25.5 and 36wt% (db) throughout the year. In general samples harvested from Clachan sound have higher ash content than samples harvested from Easdale during all seasons. In order to study the ash variation on a monthly basis, samples of *L. digitata* were monthly harvested from Aberystwyth beach and their ash variation throughout the year is shown in **Figure 5.9**. Ash reaches its peak maximum during March (37wt%) agreeing with the data of **Black (1950a)** while its minimum content occurs during July (14.5wt%).



**Figure 5.8** Seasonal variation in ash content on dry basis of freeze dried samples of (a) *L. digitata*, (b) *L. hyperborea*, (c) *L. saccharina* and (d) *A. esculenta* collected from different harvest sites.



**Figure 5.9** Seasonal variation in ash content on dry basis for samples of *L. digitata* harvested from Aberystwyth beach, Wales.

Seasonal variation in ash content of *L. hyperborea* (**Figure 5.8b**) shows a similar trend. Maximum ash values occur during winter and spring with samples harvested from Clachan sound having approximately the same ash content between winter and spring while samples harvested from Easdale showed an increased ash content during spring. However, minimum ash content occurred during spring for samples harvested from Clachan sound, while for samples harvested from Easdale minimum ash levels occurred during summer. Once again, samples harvested from Clachan sound were found to be higher in ash, apart from levels in the spring where the difference in ash content between the two sampling sites is very small (42wt% for Clachan sound and 44wt% for Easdale). Samples of *L. hyperborea* were found to have a bigger seasonal variation in ash content than samples of *L. digitata*. The seasonal ash variation for *L. hyperborea* was found to range from 23.5 to 43wt% for samples harvested from Clachan sound and from 17.5 to 44wt% for samples harvested from Easdale.

Variation in ash content for *L. saccharina* (**Figure 5.8c**) revealed its minimum content during autumn (17wt%) and its maximum during winter (58wt%) for samples harvested from Barancarry bay. Unfortunately no sampling was made during summer from Clachan sound so there is no complete image for the annual variation of samples harvested from this specific sampling site. Variation in the ash content between autumn and spring was in the range 34 to 44wt% with a minimum

content during autumn and maximum during winter. Ash content of samples harvested from Clachan sound were again found to be higher for two sampling seasons (autumn and summer). However during the winter harvest, the ash content of samples from Barancarry bay was significantly higher (58wt% compared to 44wt%).

*A. esculenta*'s ash content was found to vary in a similar manner to that of *L. saccharina*. During the winter harvest, the sample was oven dried (OD) instead of freeze dried and is noted on the graph (**Figure 5.8d**). Ash content reaches its minimum during autumn (22wt%) while the maximum is reached during winter (36wt%). Samples harvested from different locations showed minimum difference in their ash content (32wt% from Easdale and 30wt% from Barancarry bay during spring harvest).

Ash content in all samples examined was found to be high compared with woody and agricultural crops. However there is a significant variation in ash content throughout the year which is not as extensive in terrestrial plants. **Table 5.3** summarizes the seasonal variation in ash content throughout the annual growth cycle of a brown macro-algae. *L. hyperborea* harvested from Easdale during summer of 2009 and *L. saccharina* harvested from Barancarry bay during autumn of 2009 were found to have the lowest ash content from the samples examined (17.5wt% and 17.4wt% respectively) while *L. saccharina* harvested from Barancarry bay during winter of 2009 had the highest ash content (58wt%). In general, in all samples examined, maximum ash levels occur during winter and spring while minimum levels occur during summer and autumn reflecting the changes in their bio-chemical content. Another significant observation is that in most of the harvest periods, samples from Clachan sound were higher in ash than samples harvested from the other sites (Easdale and Barancarry bay). This is explained further later in this chapter in terms of the seasonal variation in inorganic species (metals).

**Table 5.3** Variation in ash content on dry basis of freeze dried seaweed samples harvested from different locations through their annual growth cycle.

Harvest site	Ash (wt% db)			
	<i>L. digitata</i>	<i>L. hyperborea</i>	<i>L. saccharina</i>	<i>A. esculenta</i>
Clachan sound	28.1-44.2	23.5-43.4		
Easdale	25.7-36.1	17.5-44.1		21.7-35.8
Barancarry			17.4-58	

Ash simply refers to the metal oxides present in the biomass following combustion which cannot be converted to energy. Thus, the large seasonal variation in ash content should be followed by a similar variation in the metal content of brown macro-algae. **Figure 5.10** shows the seasonal variation in metal concentration for the samples examined. As expected, the seasonal variation of metals follows the same trend as the ash variation with maximum metal content observed during winter-spring and minimum during summer-autumn. Samples harvested from Clachan sound were richer in metals which can explain the higher ash content of samples collected from this specific site. Unlike Easdale and Barancarry which are open to the sea, Clachan sound is a narrow sea path (strait) which helps in the accumulation of more metals, from natural deposits or land drainage, as the seawater is refreshed with lower rate. These metals are subsequently absorbed by the growing seaweed leading to the higher ash content of samples harvested from this site.

A more detailed investigation on metal concentration of samples of *L. digitata* collected monthly from Aberystwyth beach is shown in **Figure 5.11**. The total metal concentration follows exactly the same trend with ash (**Figure 5.9**) with maximum metal concentrations during March and minimum during July. Potassium and sodium, the dominant metals present, follow the same seasonal variation with total metals. For the months July, August and September Na exceeds K in concentration which however was not observed with any of the other samples under examination. For samples harvested from the three sampling sites in Scotland the difference between K and Na concentration is much lower during the summer but Na concentration does not exceed K concentration on any season.

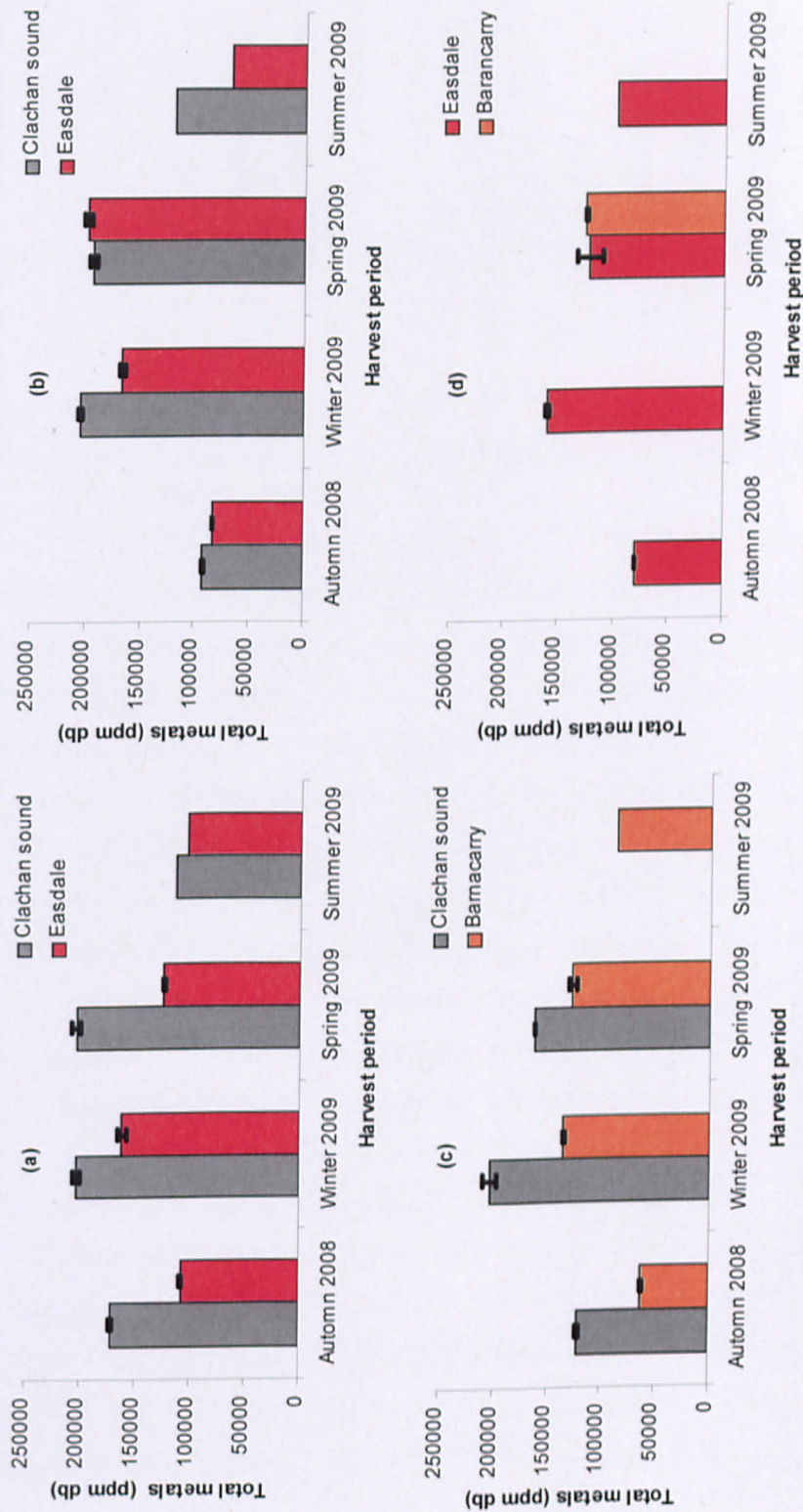
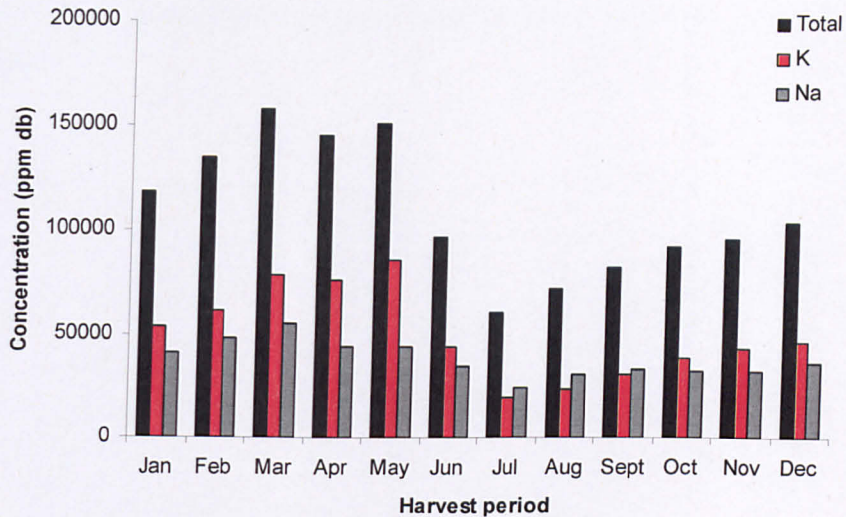


Figure 5.10 Seasonal variation in total metal content (ppm) on dry basis of freeze dried samples of (a) *L. digitata*, (b) *L. hyperborea*, (c) *L. saccharina* and (d) *A. esculenta* collected from different harvest sites.



**Figure 5.11** Seasonal variation in total metals, potassium and sodium concentration of *L. digitata* on a monthly basis

Potassium is by far the most abundant element found in seaweed followed by sodium, calcium and magnesium. These elements make up almost the total inorganic content of seaweed. **Figures 5.12a-d and 5.13a-d** shows the seasonal variation of these elements. Potassium was found to have a large seasonal variation, following the same trend as ash and total metal content with maximum values during winter and spring and minimum values during summer and autumn for all samples examined. Samples harvested during the summer of 2008 seem unusually high for the season and ash content. Sodium had less seasonal variation, with maximum levels measured during winter after which it declines to reach a minimum value during the summer and autumn for the seaweeds *L. digitata*, *L. hyperborea* and *L. saccharina*. For *A. esculenta* (**Figure 5.12d**), maximum sodium content was observed during the spring, although the large error of the measured sodium content during spring suggests that it might be lower than the winter content. Seasonal variation in calcium and magnesium (**Figure 5.13a-d**) content is clearer if we exclude the summer of 2008 harvest (as mentioned samples from this harvest have unusual high ash and metal content). Both calcium and magnesium reach their maximum content during winter for all samples examined after which their content decreases, maintaining similar levels during the rest of the seasons. **Table 5.4** summarizes the seasonal variation in the main elements of the samples examined.



## Chapter 5 – Characterisation of brown macro-algae

Detailed tables with metal analysis of freeze dried samples can be found in **Appendix C**.

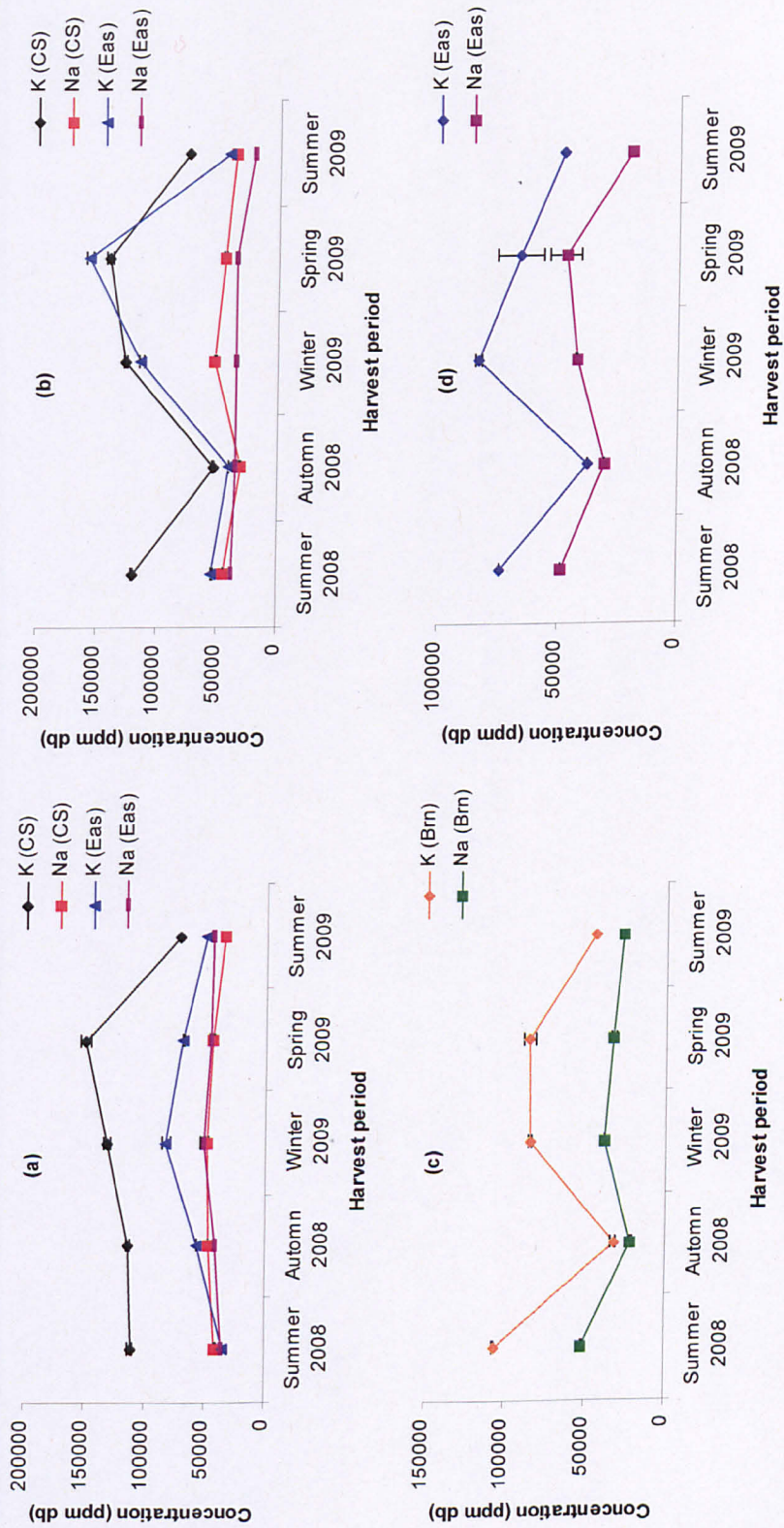
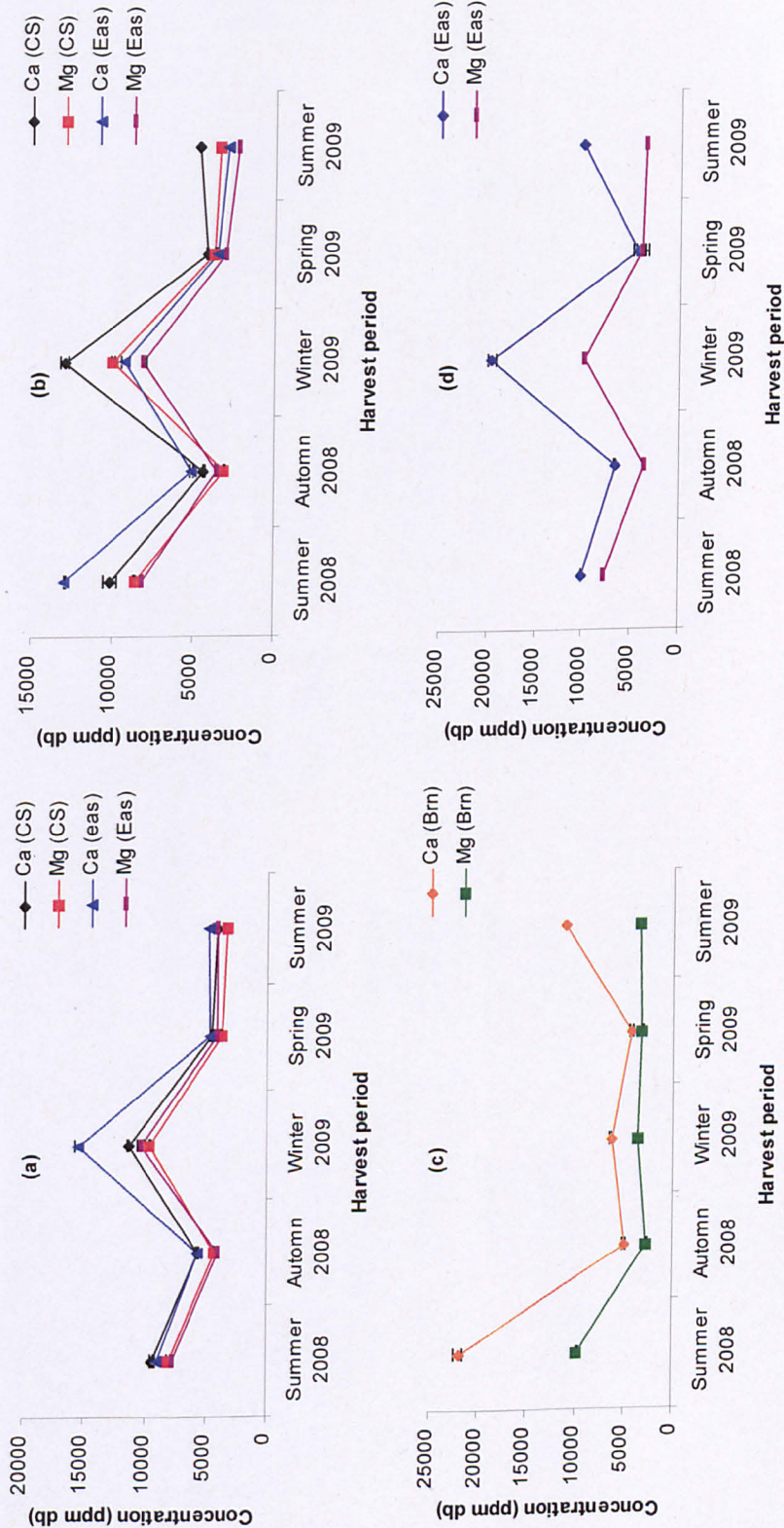


Figure 5.12 Seasonal variation in potassium and sodium of freeze dried samples of (a) *L. digitata*, (b) *L. hyperborea*, (c) *L. saccharina* and (d) *A. esculenta* collected from different harvest sites, (CS=Clachan sound, Eas=Easdale, Brn=Barancarry).



**Figure 5.13** Seasonal variation in calcium and magnesium in different harvest sites, (CS=Clachan sound, Eas=Easdale, Brn=Barancarry).

**Table 5.4** Variation in main metals of freeze dried seaweed samples harvested from different locations through their annual growth cycle.

Sample	Concentration (ppm db)							
	L. digitata		L. hyperborea		L. saccharina		A. esculenta	
Harvest site	Clachan sound	Easdale	Clachan sound	Easdale	Barancarry	Easdale	Easdale	
<b>K</b>	71825-150183	33838-82743	53016-139987	39793-157002	32497-85781	37375-83502		
<b>Na</b>	34318-48723	35458-51469	31154-52547	20150-34557	21270-38288	30497-49394		
<b>Ca</b>	4089-11369	4663-15494	4201-12936	2899-9248	4359-11185	4266-10046		
<b>Mg</b>	3280-9603	4055-10400	3110-9998	2308-8113	2686-3566	3575-9960		
<b>Fe</b>	50-300	36-166	70-629	3-326	189-720	73-487		
<b>Sr</b>	328-864	344-948	306-871	204-638	273-370	397-1744		

The carbon content of the samples undergoes a seasonal variation reflecting the seasonal change in the bio-chemical composition of seaweed. **Figure 5.14a-d** shows this variation throughout the year for different harvest locations. *L. digitata* reaches (**Figure 5.14a**) its minimum carbon content during winter and spring for both sampling locations examined (25.4wt% and 25.1%, 29.2wt% and 31.2% for Clachan sound and Easdale respectively) while its maximum carbon content occurs during summer (32.3wt% and 33.1wt% for Clachan sound and Easdale respectively). Carbon content for samples collected from Easdale remain high during autumn (32.5 wt%) while it is reduced for samples collected from Clachan sound (27.8wt%). Seasonal variation in carbon content for samples collected from Clachan sound was found to be higher than that of samples collected from Easdale (25.1wt%-32.3wt% and 29.2wt% to 33.1wt% respectively). The carbon content of *L. digitata* showed the opposite trend with its ash content with maximum carbon occurring during the summer when the ash levels are at minimum and minimum carbon content during winter when the ash levels are at a maximum.

*L. hyperborea* (**Figure 5.14b**) reaches its minimum carbon content during winter for samples harvested from Clachan sound (25.3wt%) while the samples harvested from Easdale, reaches its minimum content during spring (26wt%) corresponding to their increased ash content during these periods. Maximum carbon content occurs in summer for samples harvested from Easdale (35.8wt%) and in autumn for samples harvested from Clachan sound (33.7wt%). However in both cases carbon content is high during summer and autumn and low during winter and spring (maximum carbon content when minimum ash content and vice versa). The results suggest that maximum carbon content for *L. hyperborea* occurs during mid summer-early autumn while minimum carbon content occurs during winter-mid spring.

*L. saccharina* (**Figure 5.14c**) collected from Barancarry showed a very low carbon content (18.6wt%) during winter reflecting to its very high ash content during the same period. After that it increased significantly during spring (30.2wt%) with a continuous increase during summer (32.5wt%) to reach its maximum content during early autumn (35.6wt%). These results agree with results from **Gevaert et al (2001)** who found that carbon content in *L. saccharina* increases during spring and summer

reaching its maximum toward end of summer. Samples harvested from Clachan sound reached their maximum carbon content during spring (32.2wt%) while their minimum carbon content occurred during winter (25.9wt%).

*A. esculenta* (Figure 5.14d) showed its minimum carbon content during spring (29.3wt%) after which increases during summer (34.7wt%) to reach its maximum level during early autumn (35.2wt%).

The higher carbon content during summer and autumn can be explained by the higher photosynthetic activity of the plants during this period due to the increased light levels leading to an accumulation of carbon. Table 5.5 summarizes the seasonal variation in carbon content throughout the annual growth cycle of brown macro-algae. Samples harvested from Clachan sound had bigger seasonal variation in their carbon content than samples harvested from Easdale. *A. esculenta* was found to maintain its carbon content in relatively high values (29.2-35.2wt%) throughout the year compared with the rest seaweed.

**Table 5.5** Variation in carbon content on dry basis of freeze dried seaweed samples harvested from different locations through their annual growth cycle.

Harvest site	Carbon (wt%) (db)			
	<i>L. digitata</i>	<i>L. hyperborea</i>	<i>L. saccharina</i>	<i>A. esculenta</i>
Clachan sound	25.1-32.3	25.3-33.7		
Easdale	29.2-33.1	26-35.8		29.2-35.2
Barancarry			18.6-35.6	

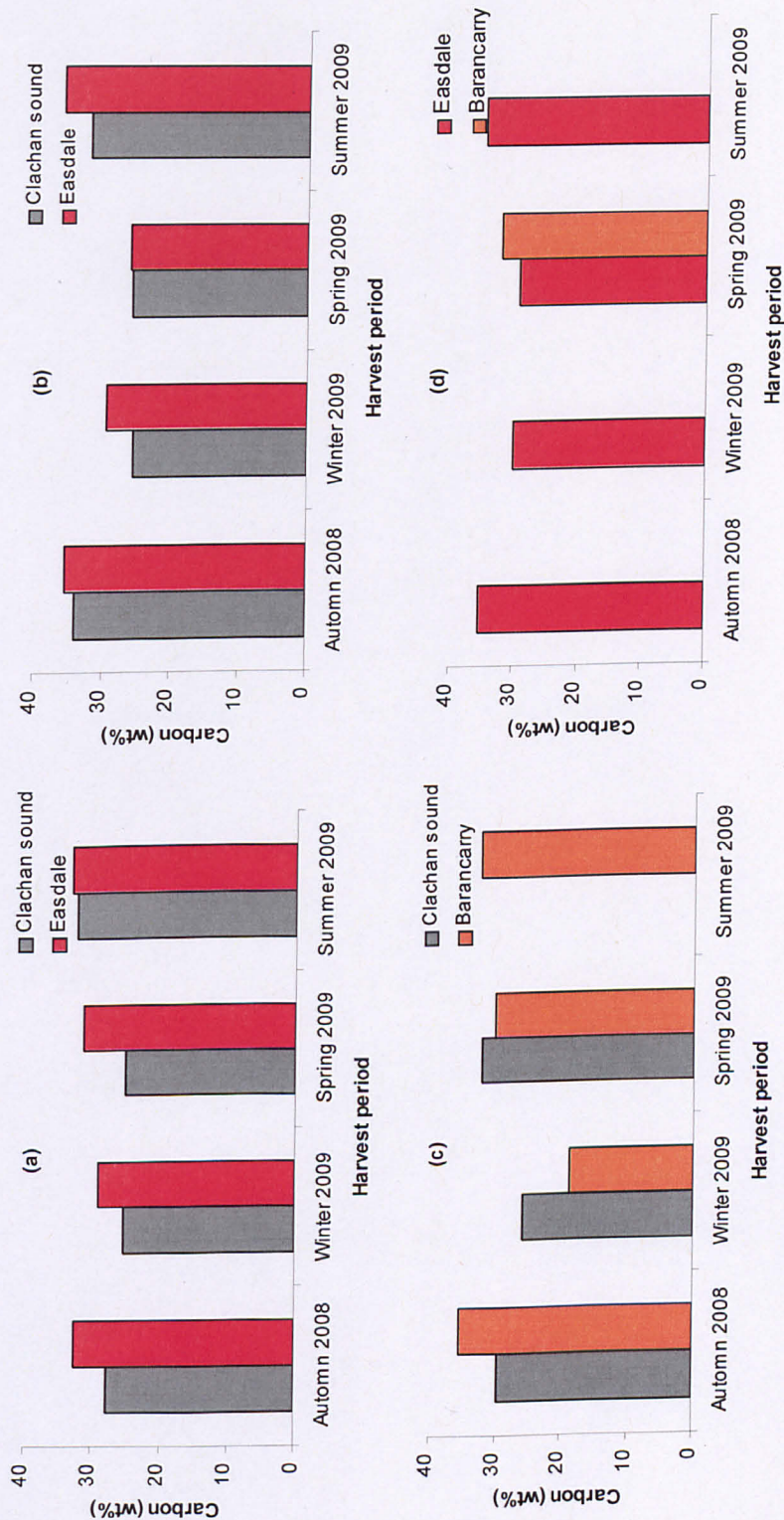
Nitrogen content in seaweed is another important parameter when considering thermochemical processes as it is directly linked with the generation of various NO<sub>x</sub> during processing. The nitrogen content in seaweed can be directly linked with their protein content and its seasonal variation throughout the year is shown in Figure 5.15. Nitrogen content for all the samples examined reaches its maximum content during winter and spring followed by a constant decrease reaching its minimum value during summer and autumn. This follows the seasonal variation of protein levels as was described by Black (1950a). On the other hand, Gevaert et al., 2001 found that maximum nitrogen content for *L. saccharina* occurs during late winter

and minimum content during late spring. The difference however between late winter and early spring where the maximum nitrogen content was observed in the study of **Gevaert et al., 2001** and this study is very small and might be due to different climatic conditions on the years of the harvests.

Nitrogen content for *L. digitata* harvested from Clachan sound and Easdale reaches its maximum content during spring (3.1wt% and 2.6wt% respectively) while minimum levels occur during summer for Clachan sound harvest (1.8wt%) and during autumn for Easdale harvest (1.5wt%). *L. hyperborea* reaches maximum nitrogen content during spring for both harvests (3.2wt% and 2.6wt% for Clachan sound and Easdale harvests respectively) while its minimum nitrogen content occurs during autumn (1.6wt% and 1.4wt% for Clachan sound and Easdale harvests respectively). Maximum nitrogen content for *L. saccharina* harvested from Barancarry occurs during spring (2.5wt%) while its minimum nitrogen content is reached during summer (1.1wt%). Finally, *A. esculenta* also reaches its minimum nitrogen content during summer (1.9wt%) while maximum nitrogen content occurs during winter (2.4wt%).

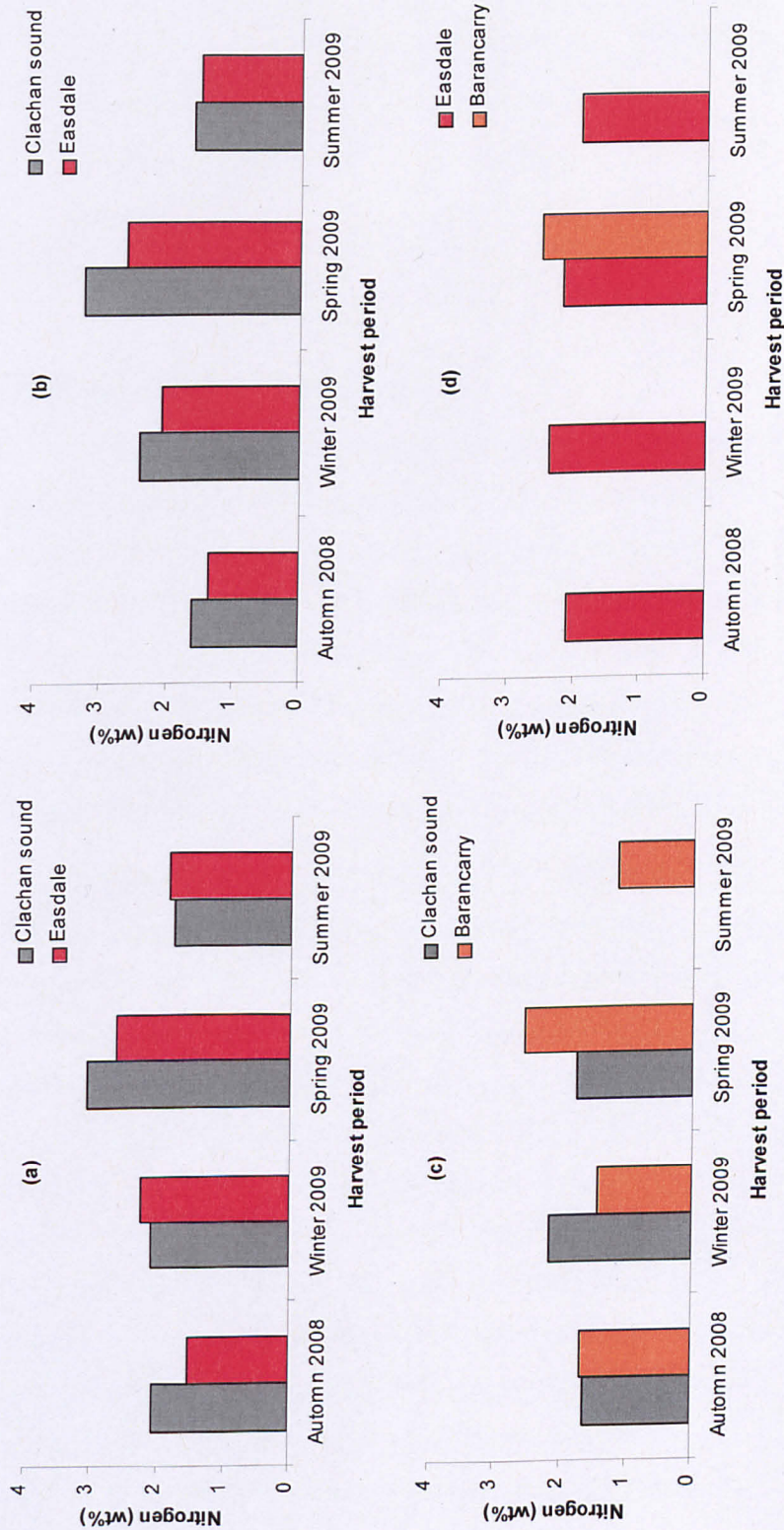
**Table 5.6** summarizes the seasonal variation in nitrogen content throughout the annual growth cycle of brown macro-algae. In general seasonal variation on nitrogen content of all seaweed examined was from about 1wt% to 3wt%. *A. esculenta* was found to have the least variation in nitrogen content throughout the year just as in case of carbon content. Samples harvested from Clachan sound were found to be higher in nitrogen content just as in case of metals and ash. This is due to the nature of this sampling site (canal) which helps accumulation of nutrients.

Detailed tables with ultimate and proximate analysis of freeze dried samples can be found in **Appendix B**.



**Figure 5.14** Seasonal variation in carbon content on dry basis of freeze dried samples of (a) *L. digitata*, (b) *L. hyperborea*, (c) *L. saccharina* and (d) *A. esculenta* collected from different harvest sites.





**Figure 5.15** Seasonal variation in carbon content on dry basis of freeze dried samples of (a) *L. digitata*, (b) *L. hyperborea*, (c) *L. saccharina* and (d) *A. esculenta* collected from different harvest sites.

**Table 5.6** Variation in nitrogen content of freeze dried seaweed samples harvested from different locations through their annual growth cycle.

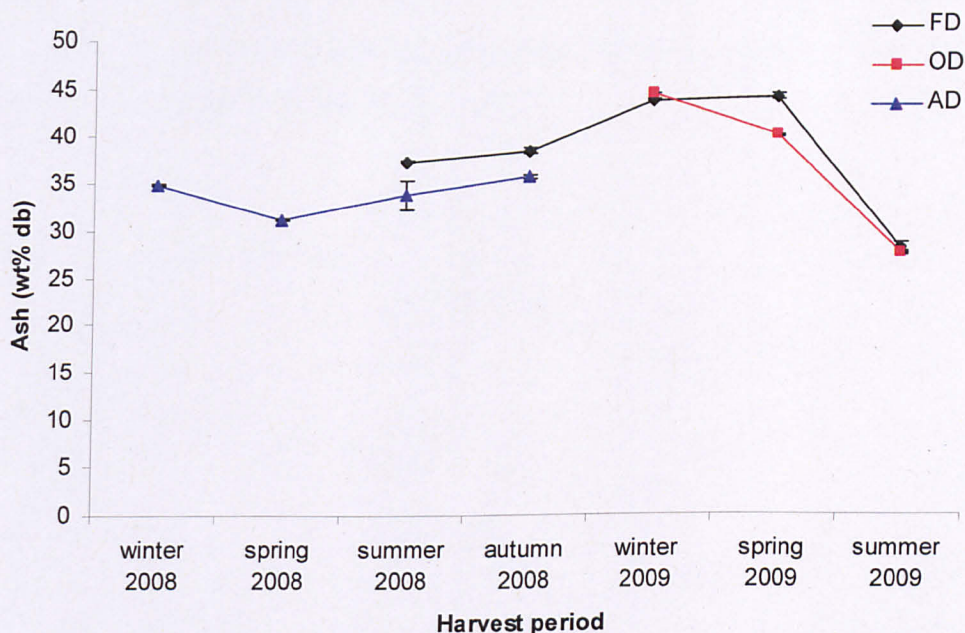
Harvest site	Nitrogen (wt%)			
	<i>L. digitata</i>	<i>L. hyperborea</i>	<i>L. saccharina</i>	<i>A. esculenta</i>
Clachan sound	1.8-3.1	1.6-3.2		
Easdale	1.5-2.6	1.4-2.6		1.9-2.4
Barancarry			1.1-2.5	

## 5.6 Effect of drying method

In the previous subsections it was shown the significant differences between different parts of seaweed plant material, the harvest period and the harvest site. It was also of interest to examine any possible differences due to the different drying methods employed. Freeze Dried (FD) and Oven Dried (OD) samples were dried in SAMS, Scotland close to their harvest site soon after collection. Air Dried (AD) samples were harvested and sent frozen to Leeds for air drying. It is possible that some degradation might have occurred to the frozen samples during the long journey to reach their destination or due to the time that were kept in the freezer.

**Figure 5.16** shows the seasonal variation in ash content of *L. digitata* harvested from Clachan sound for freeze dried; oven dried and air dried samples. Seasonal variation in ash content of freeze dried samples agrees with previous studies (**Black, 1950a**) and with what was shown in previous subsection with maximum ash levels occurring during winter-spring and minimum ash levels during summer. Oven dried samples follow the same trend. However there is a decrease in ash levels during spring while there was a slight increase in freeze dried samples during the same period. The difference however is not significant and might be attributed to the fact that for freeze dried samples the whole material was considered while for oven dried samples harvested during spring and winter the ash values for the blades and not the whole plant material were used. This was because winter and spring harvested oven dried samples were separated into blades and stipes in order to study their differences thus the whole plant material was not available. The same was done for

winter harvested air dried samples. Another important observation is the significant difference in ash levels of freeze dried samples between summer of 2008 and

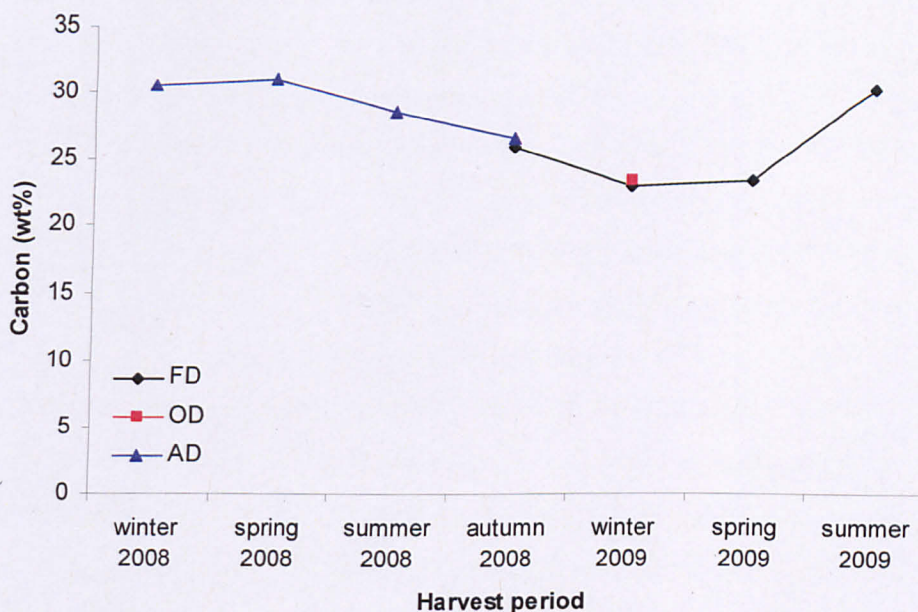


**Figure 5.16** Seasonal variation on ash content of *Laminaria digitata* harvested from Clachan sound by using different drying methods (♦) freeze-dried (FD) (■) oven-dried (OD) and (▲) air-dried (AD).

summer of 2009 (10wt%). This suggests that there are significant differences not only monthly but yearly also. This difference might be attributed to possible different climatic conditions between the two years or might be due to the different stage of development of the two harvested samples. Air dried samples showed a different seasonal variation than that shown for freeze and oven dried samples reported in literature (**Black, 1950a**) with maximum ash levels during autumn and winter and minimum ash levels during spring. The same was observed with seasonal variation in carbon content (**Figure 5.17**). Maximum carbon content for air dried samples was observed during winter and spring with minimum carbon content during summer and autumn where the opposite should be observed. Also, significantly higher variation in ash content was observed in freeze and oven dried samples (28-44 wt% dry) than in air dried samples (31-36 wt% dry). Air dried samples might have lost some organic components which are water soluble during

the time they were kept frozen or during transport. It was shown before that a fraction of mannitol content is extracted as water is removed which might be the case. The most optimum drying method for seaweed appears to be either the freeze drying or the oven drying technique.

Detailed tables with ultimate, proximate and metal analysis of air dried samples can be found in **Appendixes B and C**.



**Figure 5.17** Seasonal variation on carbon content of *Laminaria digitata* harvested from Clachan sound by using different drying methods (◆) freeze-dried (FD) (■)oven -dried (OD) and (▲)air-dried (AD).

## 5.7 Conclusions

Harvested brown macro-algae vary in dry weight between 11wt% and 20wt% depending on harvest season. During all drying methods a fraction of the sugars (mannitol and possibly some laminarin) are extracted as the water is removed. Significant differences in composition are observed between the blades and the stipes of the seaweeds. Stipes are perennial which helps in the accumulation of metals leading to higher metal content compared to the blades. This leads to higher ash content and lower carbon and hydrogen content in the stipes making them less attractive than the blades for thermochemical processes. The seasonal bio-chemical changes in seaweed were found to influence their properties as a fuel. During winter and spring the ash, metal and nitrogen content are at their peak, while minimum carbon content occurs for the same period. On the other hand during summer and autumn the opposite trend was observed. Ash, metal and nitrogen content are at their minimum while carbon reached its maximum content. This makes summer and autumn the most appropriate seasons for seaweed harvesting for thermochemical processing. The nature of the harvesting site was also found to significantly influence seaweed fuel properties. Samples harvested from Clachan sound, which is a canal where freshen of waters happens at a lower rate than open sea, were found richer in metals and thus ash content making them less attractive as a fuel for thermochemical processing. Potassium is the most abundant element present in seaweed which undergoes a big seasonal variation in proportion to the seasonal variation in ash.

## CHAPTER 6 - Pyrolysis of brown macro-algae

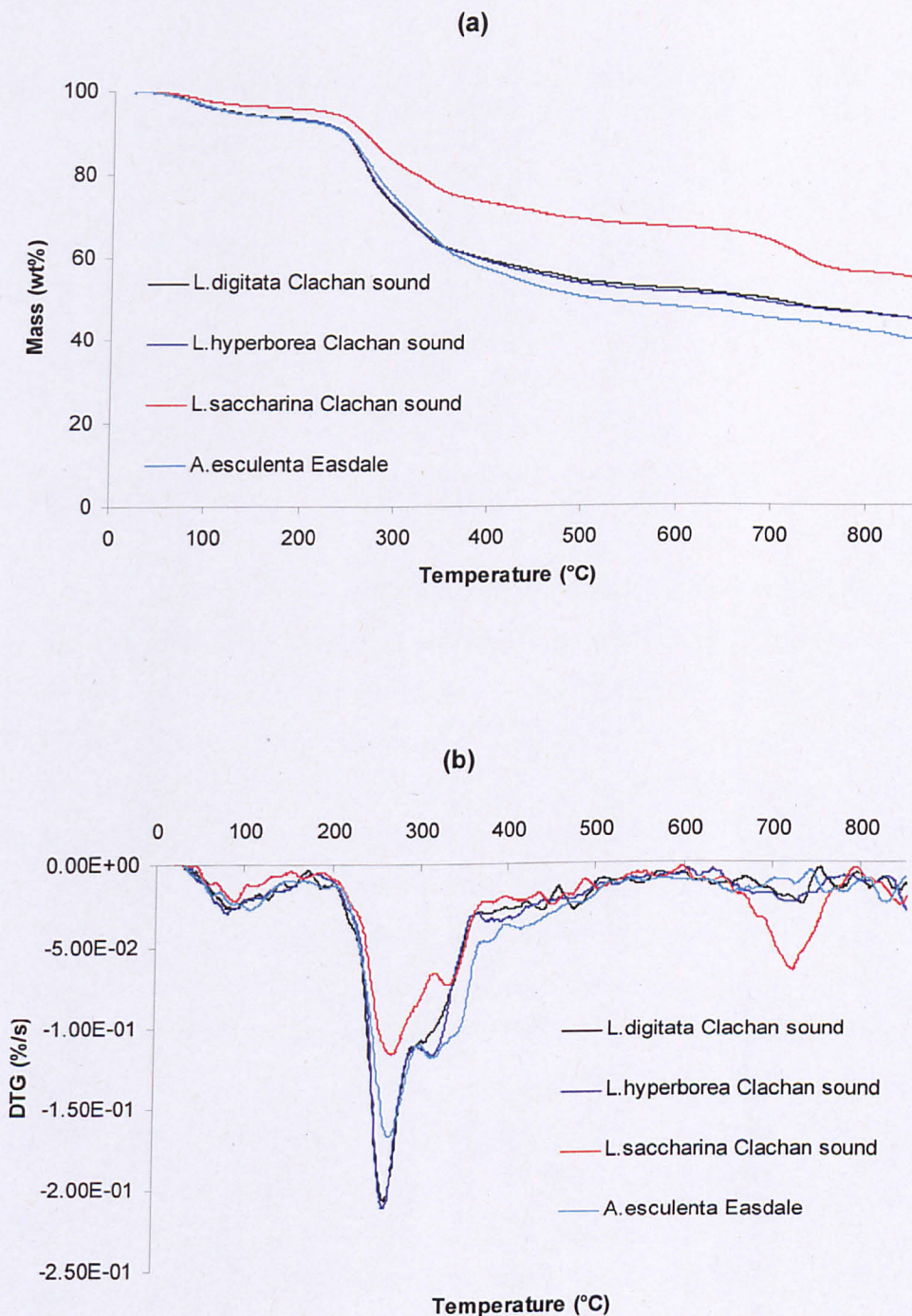
### 6.1 Introduction

This chapter examines in detail the pyrolysis behaviour of brown macro-algae. Pyrolysis studies using thermogravimetric analysis were performed on the different parts (blades, stipes) of the macro-algae samples under investigation, in order to examine the thermal degradation of the samples under a flow of nitrogen. The samples chosen for examination were oven dried samples harvested during the winter period. Summer harvest of the same set of samples was also examined in order to examine how the seasonal change in biochemical composition of brown macro-algae influences the pyrolysis process. The initial devolatilisation kinetic parameters (activation energy and pre-exponential factor) for winter and summer harvested samples were also assessed. Pyrolysis gas chromatography – mass spectrometry (py-GC/MS) was performed in order to study the behaviour of brown macro-algae at high heating rate (miniature simulation of flash pyrolysis). An attempt to link the main volatiles identified by py-GC/MS to the carbohydrates and protein present in the macro-algae as well as their seasonal variation based on peak areas of key marker compounds was made. Samples of *L. digitata* harvested monthly for 12 months were used to assess the seasonal variation by py-GC/MS. Finally, the pyrolysis behaviour of macro-algae samples after treatment in water and acid in order to reduce their inorganic content was assessed by using both thermogravimetric analyser and py-GC/MS. Samples of *M. pyrifera* were used for this purpose.

### 6.2 Typical pyrolysis behaviour of brown macro-algae and differences between blades and stipes

The thermal degradation of samples of *Laminaria digitata*, *Laminaria hyperborea*, *Laminaria saccharina* and *Alaria esculenta* was examined by TGA under a flow of nitrogen. All samples were collected during January of 2009 from the sampling site Clachan sound apart from samples of *Alaria esculenta* that was

collected from the sampling site Easdale. The TGA and DTG profiles obtained during pyrolysis of the blades of these samples are shown in **Figure 6.1a-b**.



**Figure 6.1** (a) TGA and (b) DTG profiles in nitrogen at 25°C/min of winter harvested macro-algae samples' blades.

The temperature characteristics of these samples together with the moisture, volatile matter and char yields are listed in **Table 6.1**. *Alaria esculenta* contains no stipe so the whole plant material was considered.

**Table 6.1** Temperature characteristics, moisture, volatile matter and char yields of macro-algae samples' blades harvested during winter as determined by thermogravimetric analysis in nitrogen (25 °C/min).

Sample	T <sub>i</sub> (°C)	T <sub>p1</sub> (°C)	T <sub>p2</sub> (°C)	T <sub>e</sub> (°C)	Moisture (wt%)	VM (dry) (wt%)	Char (wt%)
<i>L. digitata</i>	185	265	310	505	5.8	49.6	44.6
<i>L. hyperborea</i>	185	265	320	535	5.4	50.2	44.4
<i>L. saccharina</i>	185	270	335	530	3.9	41.7	54.4
<i>A. esculenta</i>	175	270	320	520	5.9	54.2	39.9

The degradation of the macro-algae samples was found to occur in three stages as expected (dehydration due to moisture, main devolatilisation where most of the sample matter is lost as volatile matter and a slower weight loss stage). The onset of pyrolysis reactions start between 175°C and 185°C (T<sub>i</sub>) for all the samples. *Alaria esculenta* starts to decompose first (at about 175°C) while all other samples decompose at similar temperature (185°C). The DTG profile showed two peak temperature shoulders during the main devolatilisation stage for all the samples noted as T<sub>p1</sub> and T<sub>p2</sub>. Unlike terrestrial biomass where main devolatilization occurs in a distinct step, brown macro-algae main devolatilization occur in two distinct steps due to the different temperatures in which the main carbohydrates of macro-algae decompose. As shown in **chapter 4**, in the model carbohydrates study, the first shoulder peak is attributed to the decomposition of alginic acid and fucoidan while the second shoulder peak is attributed to the decomposition of the sugar carbohydrates mannitol and laminarin. The first shoulder peak is higher than the second one because of the high alginic acid content and low mannitol and laminarin content of the samples under investigation. The samples examined were collected during winter, where alginic acid content reaches its maximum while laminarin and mannitol content reach their minimum as was discussed in **chapter 5**. Alginic acid and fucoidan are responsible for the maximum conversion rate occurring between



265°C and 270°C ( $T_{p1}$ ) for all the samples. *Laminaria digitata* and *Laminaria hyperborea* have the highest peak followed by *Alaria esculenta* and *Laminaria saccharina*, indicating the faster removal rate of the first two samples. The second temperature shoulder peak ( $T_{p2}$ ) appears between 310°C and 335°C, with *Alaria esculenta* and *Laminaria hyperborea* having the highest peak, followed by *Laminaria digitata* and *Laminaria saccharina*. The main pyrolysis reactions end between 505°C and 535°C ( $T_e$ ), with reactions easing first for *Laminaria digitata* followed by *Alaria esculenta*, *Laminaria saccharina*, and *Laminaria hyperborea*. After the end of the main pyrolysis reactions a slow weight loss is observed up to the final temperature. This is attributed to the decomposition of laminarin and fucoidan that is occurring in two temperature stages as was shown in **chapter 4**, in the model carbohydrates study. *Laminaria saccharina* shows a sharp DTG peak at 725°C (**Figure 6.1b**) due to the decomposition of fucoidan. This peak is not clear for the other samples possibly due to their low fucoidan content. All samples exhibit a small decomposition at high temperatures (above 650°C) due to the decomposition of the different alginates salts (Ca and Na) or due to the decomposition of carbonates (e.g.  $\text{CaCO}_3$ ). The release of volatile matter was found to be higher for *Alaria esculenta* followed by *Laminaria hyperborea* and *Laminaria digitata* while *Laminaria saccharina* had the lowest. This was expected, as it is in accordance with the ash content of the samples as shown in **chapter 5**. Samples with lower ash content give higher volatile matter release and vice versa.

The stipes of the samples were also examined under thermogravimetry in order to access any differences between the different parts of the macro-alga plant. The TGA and DTG profiles obtained during pyrolysis of the stipes are shown in **Figure 6.2a-b**. The temperature characteristics of the stipes together with the moisture, volatile matter and char yields are listed in **Table 6.2**.

The thermal degradation of the stipes does not show significant differences to that of the blades, as was revealed from the TGA and DTG curves (**Figure 6.2 a-b**).

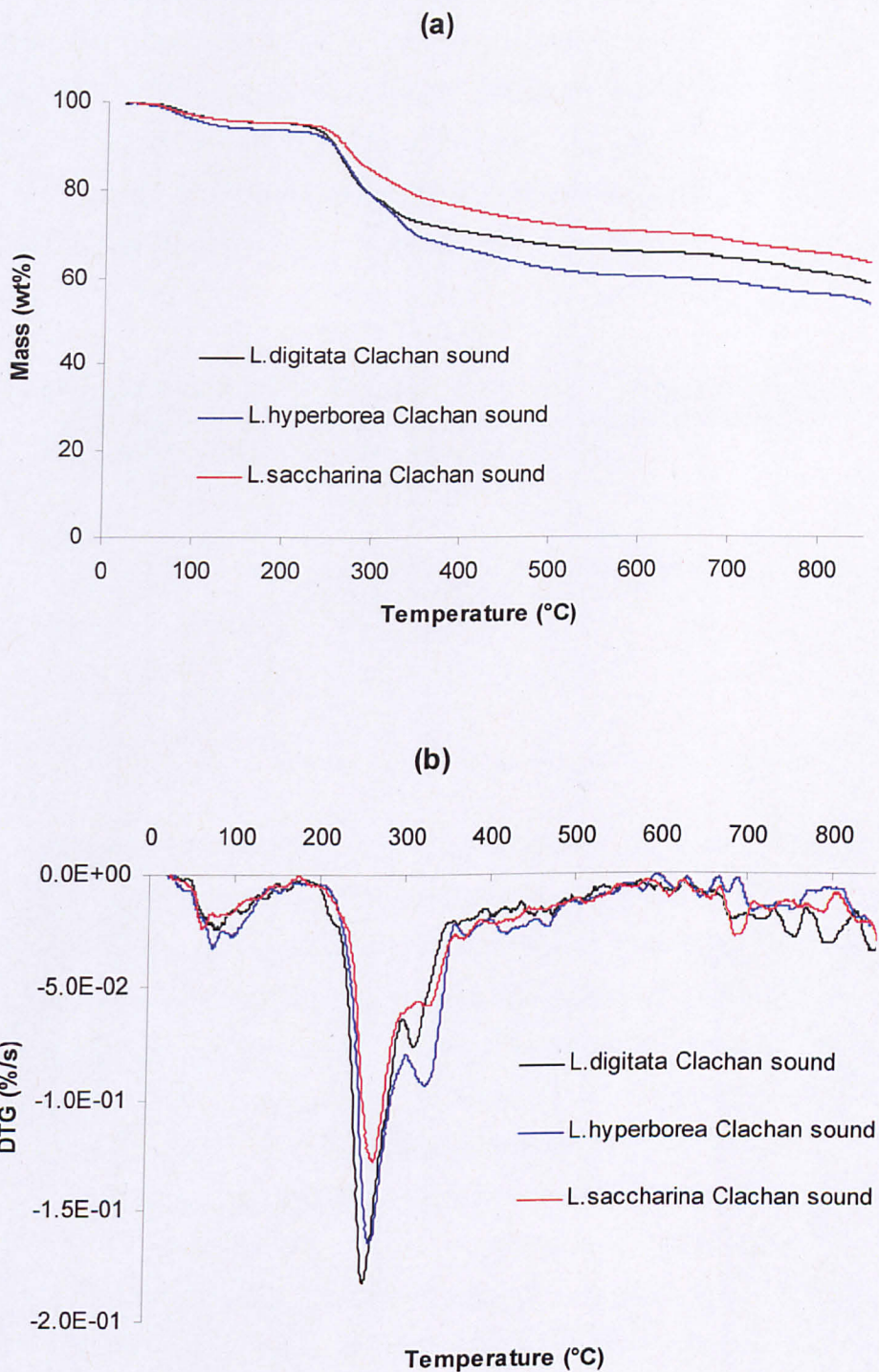


Figure 6.2 (a) TGA and (b) DTG profiles in nitrogen at 25°C/min of winter harvested macro-algae samples' stipes.

This was expected because of the similar biochemical composition between blades and stipes. Initiation of pyrolysis reactions started at slightly higher temperatures (205°C - 215°C), while maximum conversion rate and end of pyrolysis reactions occurred at almost the same temperature range (260°C - 265°C and 520°C - 535°C respectively). However, less volatile matter was released during the thermal degradation of the stipes due to their higher ash content (as it was shown in chapter 5).

**Table 6.2** Temperature characteristics, moisture, volatile matter and char yields of macro-algae samples' stipes harvested during winter as determined by thermogravimetric analysis in nitrogen (25 °C/min).

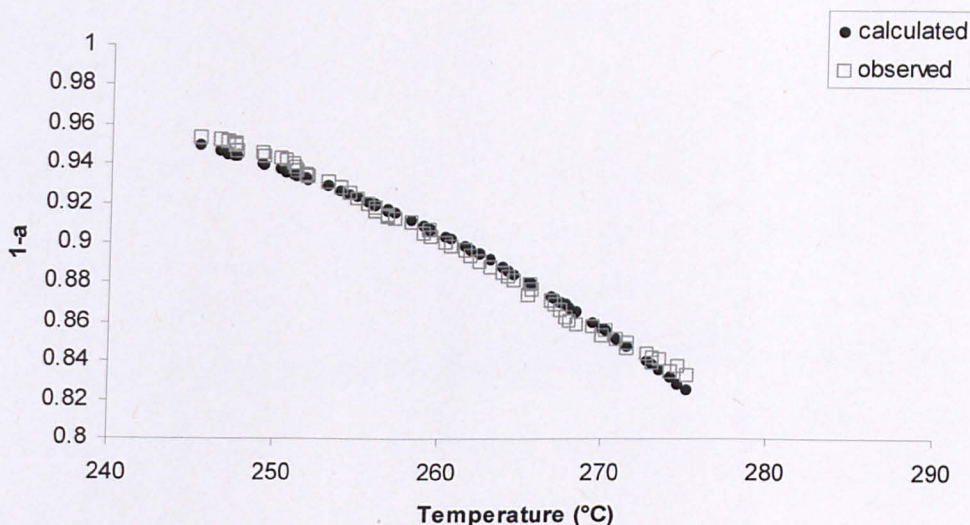
Sample	T <sub>i</sub> (°C)	T <sub>p1</sub> (°C)	T <sub>p2</sub> (°C)	T <sub>e</sub> (°C)	Moisture (Wt. %)	VM (dry) (Wt. %)	Char (Wt. %)
<i>L. digitata</i>	205	260	315	520	4.5	36.6	58.9
<i>L. hyperborea</i>	215	265	330	530	6.1	40	53.9
<i>L. saccharina</i>	212	265	330	535	4.5	32	63.5

The initial devolatilisation kinetics of the blades and stipes of macro-algae samples are listed in **Table 6.3**. The initial kinetic parameters and not the global were considered so devolatilisation of only the first temperature shoulder was considered. Activation energy ranges between 68.1 kJ/mol and 100.4 for the blades of the samples and between 89.1 kJ/mol and 113.6 kJ/mol for the stipes. The stipes have higher activation energy than the blades in the range of 10-20 kJ/mol, suggesting that more energy is required in order for the pyrolysis reactions to occur. This agrees with previous data that showed the initiation of pyrolysis reactions starting later for stipes than in the blades. *A. esculenta* was found to have the lower activation energy (68.1 kJ/mol) while the stipes of *L. digitata* were found to have a highest activation energy (113.6 kJ/mol) (i.e harder to decompose). An example of the fit of the method used with experimental data shown in **Figure 6.3** verifies the calculated kinetic parameters with experimental data. The calculated activation energies fall in the range of typical activation energies of biomass samples between 30 and 200 kJ/mol (Weber, 2008). As a comparison, the activation energy for willow determined by the same heating rate (25°C/min) and the same kinetics

method (Senum and Yang approximation) is 64.5 kJ/mol (Saddawi et al., 2010). However, activation energies for the samples under investigation were found to be significantly lower than other macro-algae samples reported in the literature. Wang and co-workers (2007) found an unusually high value for the activation energy for the green alga *Enteromorpha clathrata* between 228 and 245 kJ/mol, while Li and co-workers (2010) found an average E of 207.7 kJ/mol and 202.9 kJ/mol for the brown algae *Laminaria japonica* and *Sargassum pallidum* respectively. These differences can be attributed to the different methods employed for determination of the kinetic parameters and to differences in biochemical compositions of the samples.

**Table 6.3** Initial devolatilisation kinetics for different parts of macro-algae harvested during winter as determined by the Senum and Yang approximation

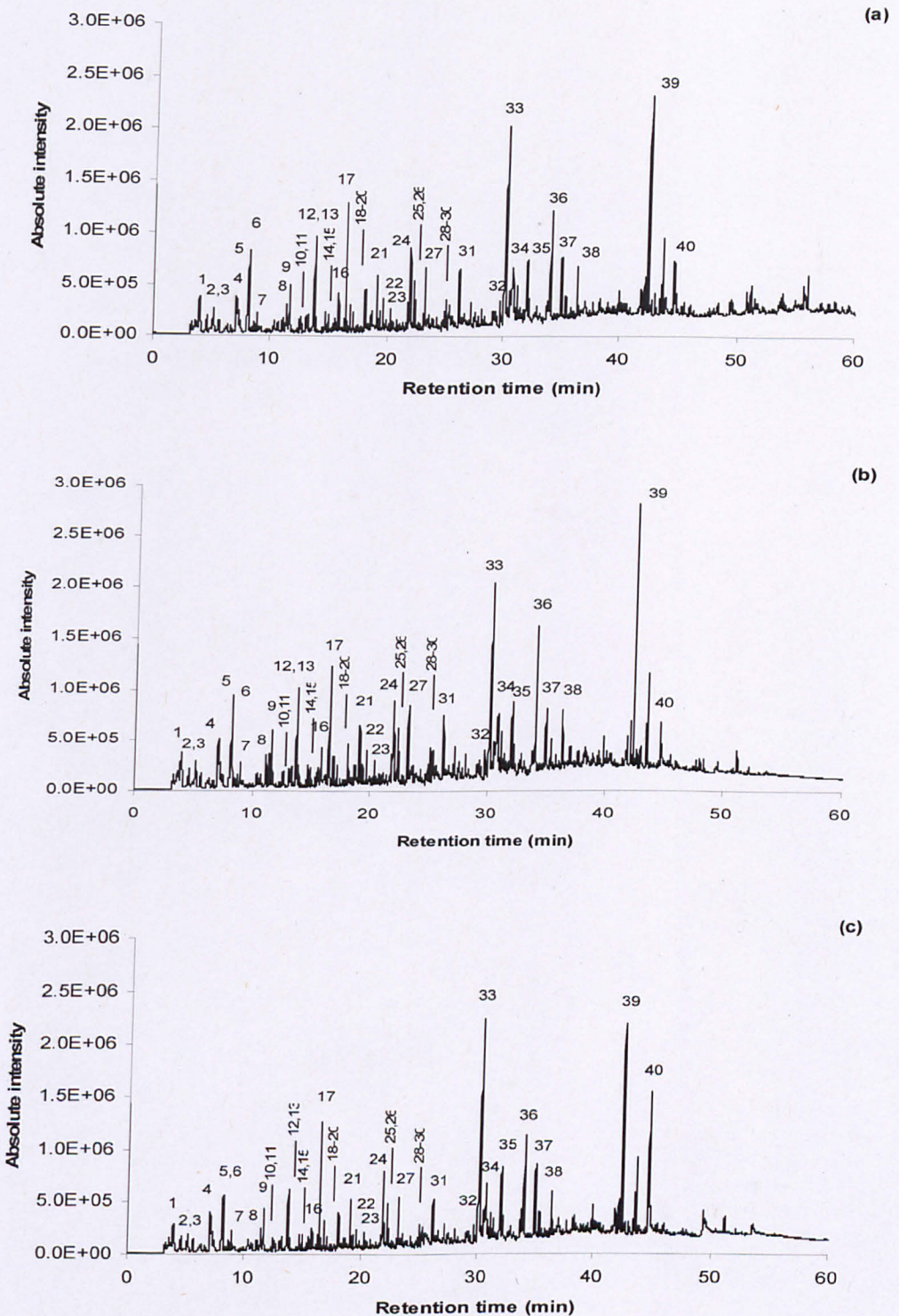
Sample	Temperature range (°C)	Activation Energy, E (kJ/mol)	Pre-exponential factor (lnA)	Variance
<i>L. digitata</i>				
Blades	245-275	94.7	15.1	$3.4 \times 10^{-3}$
Stipes	240-270	113.6	19.3	$3.2 \times 10^{-3}$
<i>L. hyperborea</i>				
Blades	245-275	100.4	16.3	$3.7 \times 10^{-3}$
Stipes	245-275	111.1	18.4	$2.9 \times 10^{-3}$
<i>L. saccharina</i>				
Blades	250-280	70.4	8.8	$1.5 \times 10^{-3}$
Stipes	250-280	89.1	13.1	$2.6 \times 10^{-3}$
<i>A. esculenta</i>	255-285	68.1	8.7	$3.1 \times 10^{-3}$



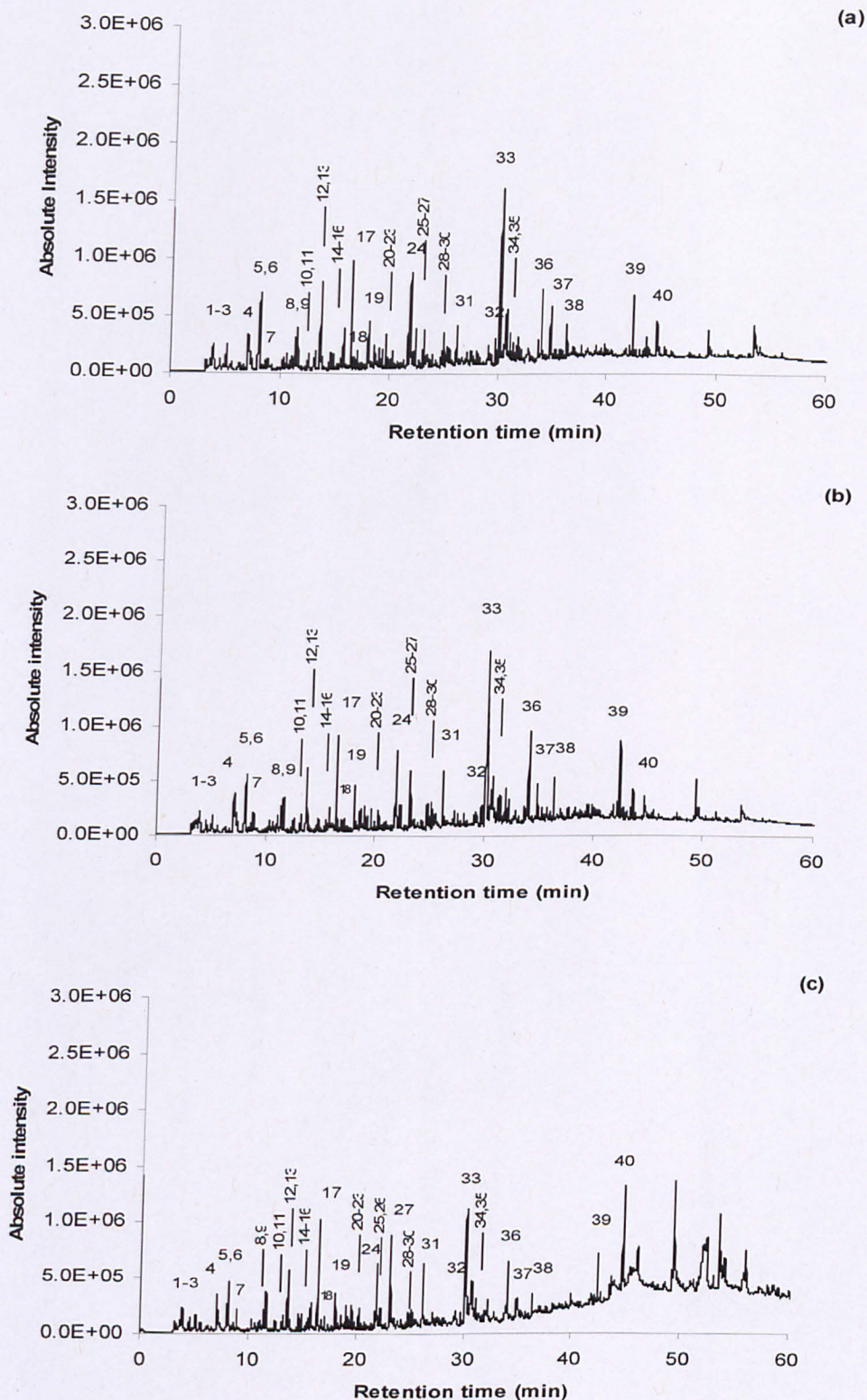
**Figure 6.3** Validation of kinetic model for *L. digitata* blades

The evolution of volatiles from these samples during pyrolysis was assessed at high heating rate conditions by pyrolysis gas chromatography mass spectrometry (py-GC/MS). Py-GC/MS is a miniature simulation of flash pyrolysis, enabling the identification of compounds present in pyrolysis oil produced from flash pyrolysis for any given sample. The pyrolysis behaviour of the samples, *Laminaria digitata*, *Laminaria hyperborea*, and *Laminaria saccharina* divided into blades and stipes was investigated at 500°C. The py-GC-MS chromatograms for the blades and stipes for the four samples are shown in **Figures 6.4 and 6.5**. The main peaks assigned have been identified from mass spectral detection and are shown in **Table 6.4** for all four macro-algae.

The pyrolysis oil resulting from flash pyrolysis of seaweed using py-GC/MS contains a large mixture of compounds. The evolved volatiles from pyrolysis of the samples and the different parts of the seaweed plant (blades and stipes) are the same. However, they appear in less abundance in stipes, mostly because of the reduction in volatile matter that was evolved during the pyrolysis of stipes. This agrees with the results from thermogravimetric analysis discussed before. The main compounds identified (compounds in higher abundance) come from the degradation of the main carbohydrates of brown macro-algae (alginic acid, mannitol, fucoidan, and laminarin) and chlorophyll.

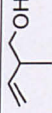
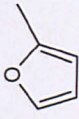
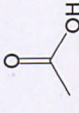
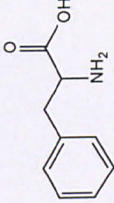

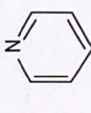
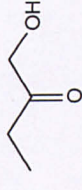


**Figure 6.4** Pyrolysis-GC/MS chromatograms of macro-algae samples blades pyrolysed at 500°C, (a) *L. digitata*, (b) *L. hyperborea* and (c) *L. saccharina*.



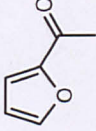
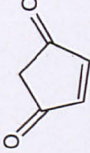
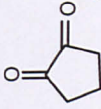
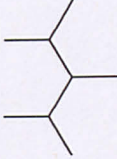
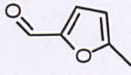
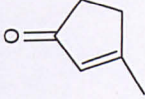
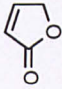
**Figure 6.5** Pyrolysis-GC/MS chromatograms of macro-algae samples stipes pyrolysed at 500°C, (a) *L. digitata*, (b) *L. hyperborea* and (c) *L. saccharina*.

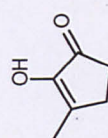
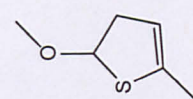
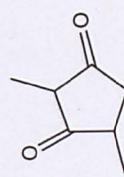
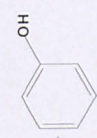
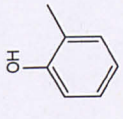
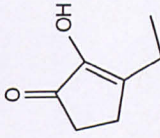
**Table 6.4** the main identified peaks from py-GC-MS chromatograms for oils obtained from pyrolysis of blades and stipes of *Laminaria Digitata*, *Laminaria hyperborea* and *Laminaria saccharina*.

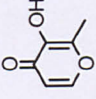
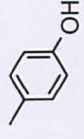
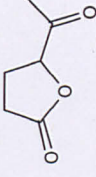
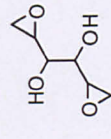
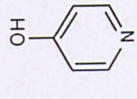
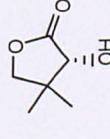
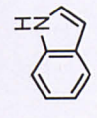
Peak No.	Compound	RT	Formula	Structure	MW
1	2-methyl-3-Buten-1-ol	3.918	C <sub>5</sub> H <sub>10</sub> O		86
2	2-methyl-Furan	4.6	C <sub>5</sub> H <sub>6</sub> O		82
3	2-amino-4-methyl-Pentanamide	5.168	C <sub>6</sub> H <sub>14</sub> N <sub>2</sub> O		130
4	Acetic acid	7.091	C <sub>2</sub> H <sub>4</sub> O <sub>2</sub>		60
5	Phenylalanine	8.165	C <sub>9</sub> H <sub>11</sub> NO <sub>2</sub>		165
6	Toluene	8.198	C <sub>7</sub> H <sub>8</sub>		92
7	Pyridine	8.927	C <sub>5</sub> H <sub>5</sub> N		79
8	1-Hydroxy-2-butanone	11.419	C <sub>4</sub> H <sub>8</sub> O <sub>2</sub>		88

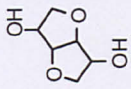
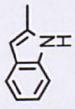
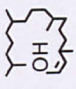



9	Pyrrole	11.65	$C_4H_5N$		67
10	1,4-dimethyl-Pyrazole	12.66	$C_3H_8N_2$		96
11	styrene	13.083	$C_8H_8$		104
12	2-Cyclopenten-1-one	13.68	$C_5H_6O$		82
13	Furfural	13.753	$C_5H_4O_2$		96
14	1H-Pyrrole, 2-methyl-	14.728	$C_5H_7N$		81
15	1H-Pyrrole, 3-methyl-	14.925	$C_5H_7N$		81
16	2-methyl-2-Cyclopenten-1-one	15.848	$C_6H_8O$		96

17	1-(2-furanyl)-Ethanone	16.476	$C_6H_6O_2$	110	
18	4-Cyclopentene-1,3-dione	17.122	$C_5H_4O_2$	96	
19	1,2-Cyclopentanedione	18.113	$C_5H_6O_2$	98	
20	2,3,4-trimethyl-1-Pentane	18.672	$C_8H_{18}$	114	
21	5-methyl-2-Furancarboxaldehyde	19.092	$C_6H_6O_2$	110	
22	3-methyl-2-Cyclopenten-1-one	19.66	$C_6H_8O$	96	
23	2(5H)-Furanone	20.31	$C_4H_4O_2$	84	

24	2-hydroxy-3-methyl-2-Cyclopenten-1-one	21.932	$C_6H_8O_2$	112	
25	2-methoxy-5-methyl-Thiophene	22.302	$C_6H_8OS$	128	
26	2,4-dimethyl-1,3-Cyclopentanedione	22.409	$C_7H_{10}O_2$	126	
27	Phenol	23.206	$C_6H_6O$	94	
28	2-methyl-Phenol	24.91	$C_7H_8O$	108	
29	3-ethyl-2-hydroxy-2-Cyclopenten-1-one	25.09	$C_7H_{10}O_2$	126	

30	Maltol	25.315	$C_6H_6O_3$	126	
31	4-methyl-Phenol	26.216	$C_7H_8O$	108	
32	5-Acetyldihydrofuran-2(3H)-one	29.782	$C_6H_8O_3$	128	
33	Dianhydromannitol	30.213	$C_6H_{10}O_4$	146	
34	4-Pyridinol	30.783	$C_5H_5NO$	95	
35	Pantolactone	31.952	$C_6H_{10}O_3$	130	
36	Indole	34.062	$C_8H_7N$	117	

37	Isosorbide	34.916	$C_6H_{10}O_4$		146
38	2-methyl-1H-Indole	36.389	$C_9H_9N$		131
39	Phytol	42.404	$C_{20}H_{40}O$		296
40	Tetradecanoic acid	44.649	$C_{14}H_{28}O_2$		228

The dominant products during pyrolysis appear to be dianhydromannitol (peak no.33), which is one of the main degradation products of mannitol and phytol (peak no.39) which derives from the chlorophyll pigment of brown macro-algae. Other main products include 1-(2-furanyl)-ethanone (peak no.17) that is also derived from mannitol, furfural (peak no.13) that is derived from alginic acid, 5-methyl-2-furancarboxaldehyde (peak no.21) and 2-methoxy-5-methyl-thiophene (peak no.25) that are derived from fucoidan and finally 2-hydroxy-3-methyl-2-cyclopenten-1-one (peak no.24), acetic acid (peak no.4) and 1, 2-cyclopentanedione (peak no.19) that are derived from laminarin. The main nitrogen compounds derived from the protein fraction of macro-algae are analogues of indole, pyrrole, pyrazole and pyridine derivatives while an amino-acid analogue phenylalanine was also identified. The phenolic fraction was low, much lower than that of terrestrial biomass pyrolysis. In general, pyrolysis of brown macro-algae produces significantly different products than that of terrestrial biomass due to their significant differences in biochemical composition.

The compounds identified from py-GC/MS in pyrolysis oil from brown macro-algae was confirmed by a recent study of **Choi et al (2011)** where the main compounds present in bio-oil produced from flash pyrolysis of the brown macroalga *Laminaria japonica* in a fluidised bed reactor were analogues of the degradation products of the seaweeds' carbohydrates such as acetic acid, dianhydromannitol, 1-(2-furanyl)-ethanone and 2-hydroxy-3-methyl-2-cyclopenten-1-one.

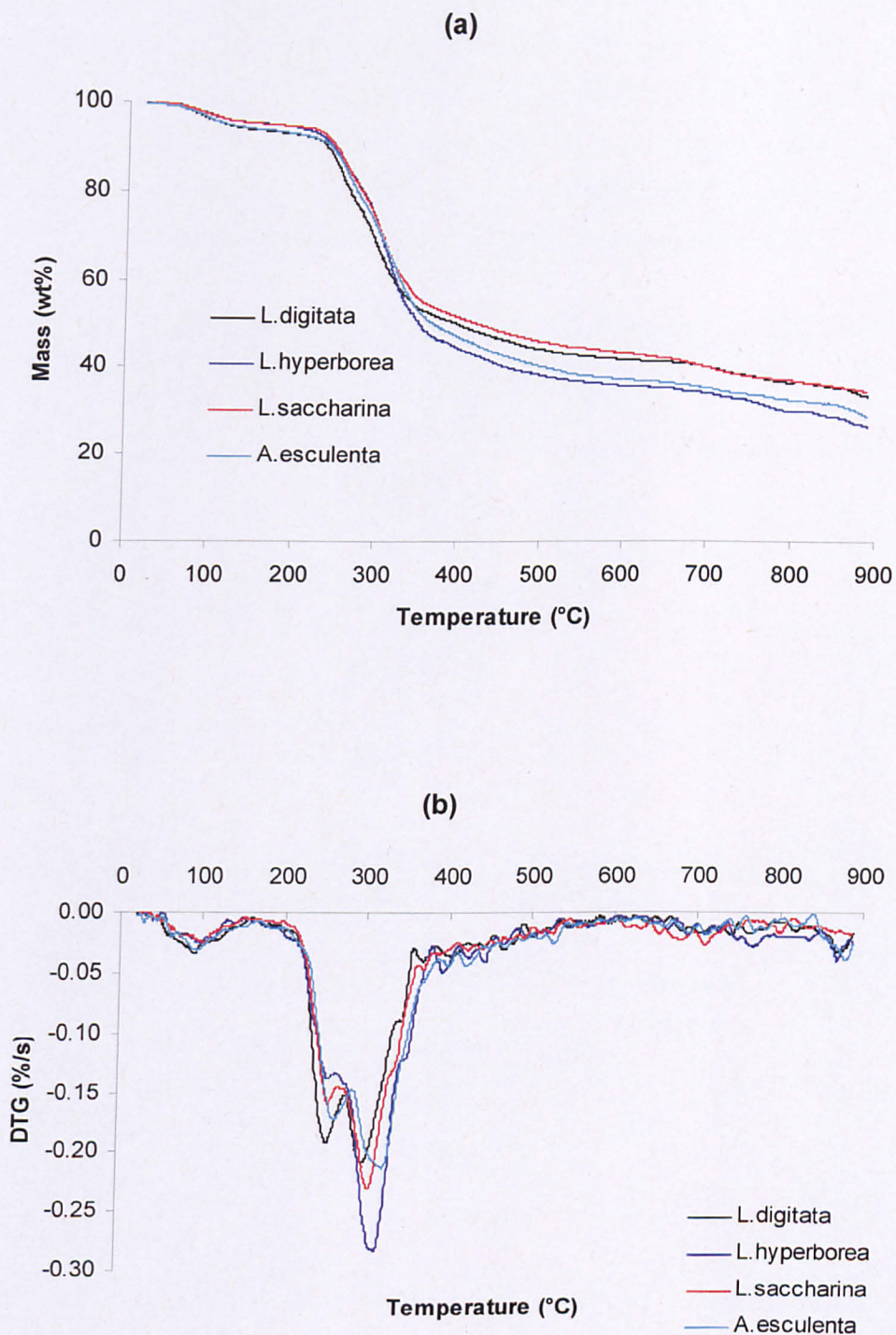
A lot of the compounds present in the pyrolysis oil have direct use as solvents or can be used as intermediates for the synthesis of pharmaceuticals, medicines, dyes, agrochemicals, perfumes etc. Thus, pyrolysis oil resulting from pyrolysis of brown macro-algae can be used as feedstock for extracting valuable compounds that are currently produced from non renewable sources such as acetic acid and toluene (mainly produced from natural gas and crude oil respectively). Other valuable compounds present include a number of furan derivatives which are used in making cements, phenolic resins, as solvents and flavorings and indole and pyrrole derivatives which are used in the synthesis of medicines, agrochemicals, dyes and perfumes. Thiophene, which is one of the main degradation products of fucoidan, is widely used in many agrochemicals and pharmaceuticals, in manufacturing dyes and

aroma compounds while it is used as monomer to make condensation copolymers. The anhydro sugars such as dianhydromannitol and isosorbide, which can exist in high concentrations in pyrolysis oil, are used for carbohydrate synthesis. Finally, phytol, which appears to be present in high concentration in the pyrolysis oil is derived from the chlorophyll content of macro-algae and can be used in manufacturing synthetic vitamins and in the production of many beauty care and household products.

### 6.3 Effect of harvest season

In previous chapter (**chapter 5**), it was shown how the chemical composition of macro-algae changes throughout the year. This difference is attributed mainly to the different carbohydrate content throughout the year. This indicates minimum levels of ash occurring during the summer period while maximum carbon content is occurring at the same period. Samples harvested during winter and summer, where the largest change in their chemical composition is observed, were investigated by thermogravimetric analysis and py-GC/MS.

The TGA and DTG profiles in nitrogen for summer harvested samples are shown in **Figures 6.6a-b**, while the temperature characteristics of these samples together with the moisture, volatile matter and char yields are listed in **Table 6.5**. The seasonal variation in biochemical content of macro-algae significantly influences their decomposition. The volatile matter evolved during pyrolysis of summer harvested samples is larger than winter harvested samples, while char content is lower following their reduction in ash content during summer period. The initiation of pyrolysis reactions ( $T_i$ ), temperatures of maximum conversion ( $T_{p1}$  and  $T_{p2}$ ) and ease of pyrolysis reactions ( $T_e$ ) fall in the same temperature range with winter harvested samples. However, the DTG profile indicates a second peak temperature shoulder ( $T_{p2}$ ) which is higher than in the winter harvested samples revealing their higher mannitol and laminarin content during summer. During summer, mannitol and laminarin are the dominant carbohydrates present in brown macro-algae and are responsible for the majority of volatile matter evolved during pyrolysis.



**Figure 6.6** (a) TGA and (b) DTG profiles in nitrogen at 25°C/min of summer harvested macro-algae samples as a function of temperature.



The initial devolatilisation kinetics of summer harvested samples are listed in **Table 6.6**. Activation energies range between 80.8 and 106.8 kJ/mol with *A. esculenta* having the lowest just as in winter harvested samples. However, activation energy for summer harvested samples is higher than that of the blades of winter harvested samples. This is attributed to the less volatile matter evolved during the first devolatilisation stage in which the kinetic parameters were considered.

**Table 6.5** Temperature characteristics, moisture, volatile matter and char yields of macro-algae samples harvested during summer as determined by thermogravimetric analysis in nitrogen (25 °C/min).

Sample	T <sub>i</sub> (°C)	T <sub>p1</sub> (°C)	T <sub>p2</sub> (°C)	T <sub>e</sub> (°C)	Moisture (Wt. %)	VM (dry) (Wt. %)	Char (Wt. %)
<i>L. digitata</i>	190	255	300	530	6.3	60.3	33.4
<i>L. hyperborea</i>	190	255	315	530	4.7	69	26.3
<i>L. saccharina</i>	200	255	305	530	4.8	60.7	34.5
<i>A. esculenta</i>	200	265	320	540	6.2	65.1	28.7

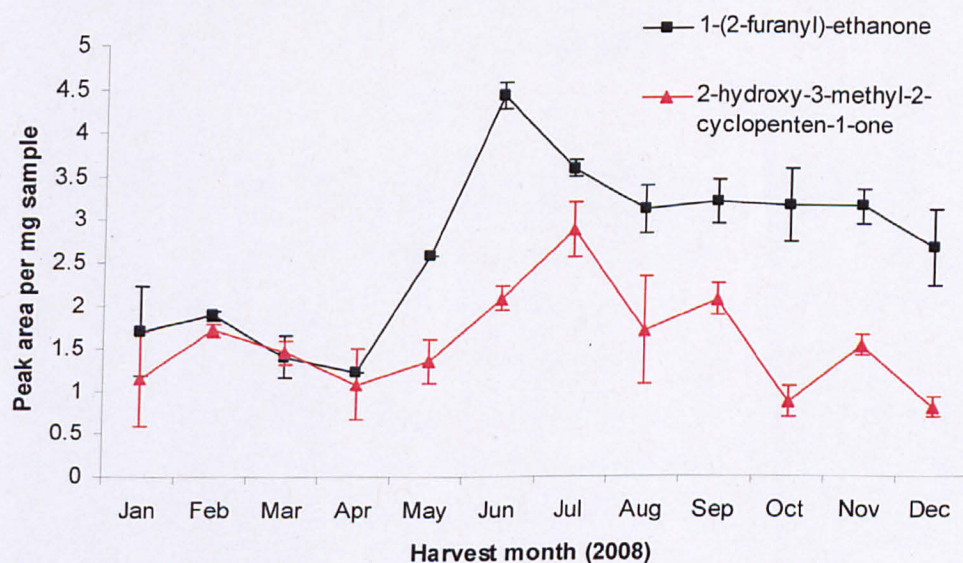
**Table 6.6** Initial devolatilisation kinetics for macro-algae harvested during summer as determined by the Senum and Yang approximation.

Sample	Temperature range (°C)	Activation Energy, E (kJ/mol)	Pre-exponential factor (lnA)	Variance
<i>L. digitata</i>	190-260	107.2	18.3	2.7 x 10 <sup>-3</sup>
<i>L. hyperborea</i>	190-260	83.5	12.5	1.3 x 10 <sup>-3</sup>
<i>L. saccharina</i>	200-260	106.6	17.9	1.6 x 10 <sup>-3</sup>
<i>A. esculenta</i>	200-270	89.2	13.7	2 x 10 <sup>-3</sup>

The seasonal variation in biochemical composition of brown macro-algae was shown to influence their devolatilisation characteristics. Py-GC/MS was used to investigate this variation. Samples of *L. digitata* harvested monthly were pyrolysed and the peak area of the identified volatiles was examined. Each sample was

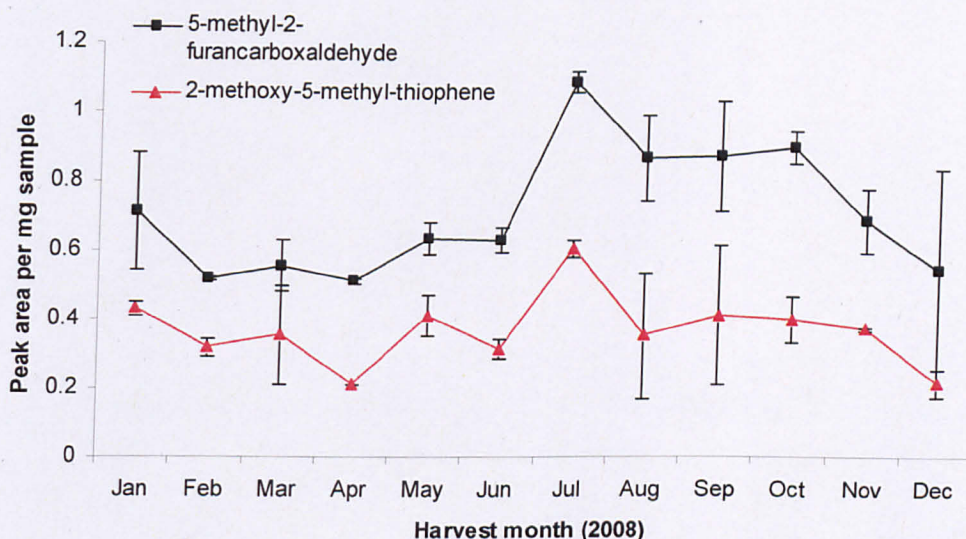
pyrolysed in duplicate and the peak areas of some key marker compounds relating to different carbohydrates and protein were plotted against the harvest month. These key marker compounds were chosen based on the main volatiles evolved during pyrolysis of each carbohydrates of brown macro-algae (**chapter 4**).

1-(2-furanyl)-ethanone was chosen as a key marker compound for mannitol content while 2-hydroxy-3-methyl-2-cyclopenten-1-one was chosen for laminarin content and their variation throughout the year is shown in **Figure 6.7**. Dianhydromannitol which is the other main volatile from the pyrolysis of mannitol was not taken into account because it appeared to stick in the GC injection port and so peaks often appeared smaller than would be expected. Peak area of 1-(2-furanyl)-ethanone starts increasing at the end of April reaching its maximum during June after which it starts to decrease reaching its minimum during winter. Peak areas of 2-hydroxy-3-methyl-2-cyclopenten-1-one show a similar trend with increase in its peak area at the end of April reaching its maximum during July after which starts decreasing reaching its minimum during winter. This data agree with the mannitol and laminarin content of the samples determined by **Adams et al (2011)** and the higher second main devolatilisation peak shown previously in DTG curves of summer harvested samples.



**Figure 6.7** 1-(2-furanyl)-ethanone and 2-hydroxy-3-methyl-2-cyclopenten-1-one peak areas per mg *L. digitata* sample variation throughout the year.

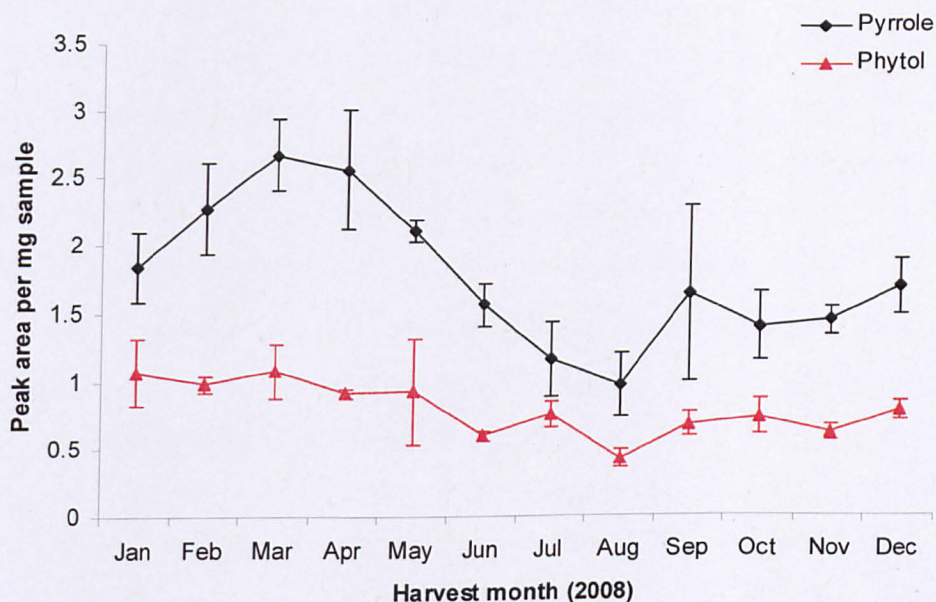
5-methyl-2-furancarboxaldehyde and 2-methoxy-5-methyl-thiophene are the main volatiles evolved from the pyrolysis of fucoidan and were taken as key marker compounds for fucoidan content. Their peak area seasonal variation is shown in **Figure 6.8**. Both of these compounds show similar trends with maximum peak occurring during July after which there is a small decrease during the end of summer and autumn. During late autumn, early winter, their peak area decreases significantly to reach their minimum during winter and spring. This suggests that fucoidan content follows the same trend throughout the year, but no data on the seasonal variation of fucoidan content was found in literature to support this argument.



**Figure 6.8** 5-methyl-2-furancarboxaldehyde and 2-methoxy-5-methyl-thiophene peak areas per mg *L. digitata* sample variation throughout the year.

Pyrrrole was taken as an indicator for the protein content of macro-algae. It was found that the main nitrogen containing volatiles resulting from pyrolysis of brown macro-algae are pyrrole and indole and their derivatives. However indole was not taken as a key marker because it appeared at very low peak areas during summer months. The variation of pyrroles' peak area along with that of phytol (another main volatile evolved) is shown in **Figure 6.9**. Peak area of pyrrole reaches its maximum during March-April after which starts decreasing to reach its minimum during August. After the end of summer, it gradually increases to reach the maximum value during spring. This agrees with data from **Black (1950, a, b)** who found that maximum protein levels reach their maximum between January and March. This

also agrees with the nitrogen content of the samples examined (**showed in chapter 5**) where samples harvested during March and April had the highest nitrogen content. Phytol is a major product of pyrolysis of brown macro-algae and can have industrial applications appears to be in higher concentration during winter and reaches its minimum during summer.



**Figure 6.9** Pyrrole and phytol peak areas per mg *L. digitata* sample variation throughout the year.

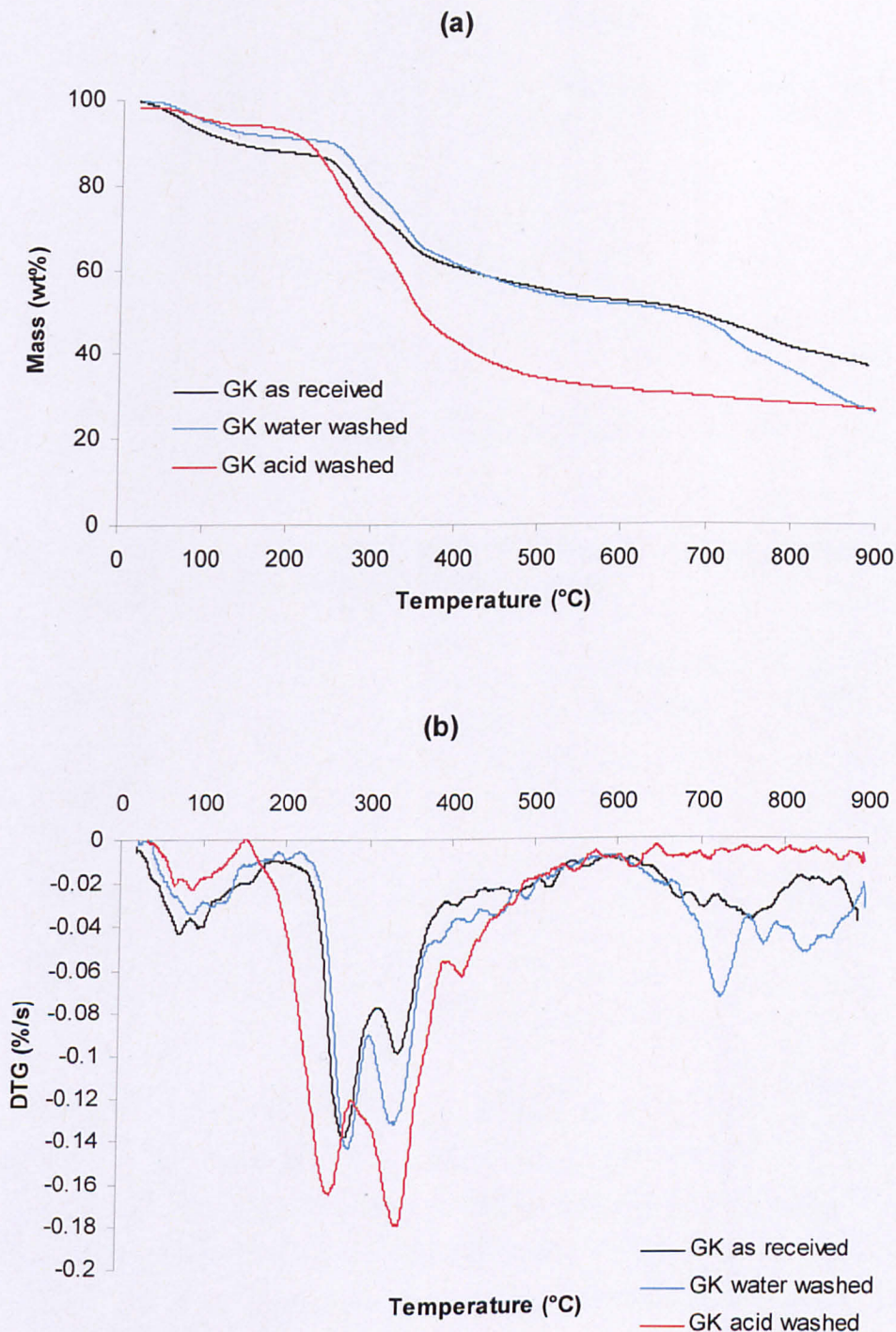
This analysis provides information on the best harvest period and can be related to the end product application. If the end product is pyrolysis oil as a renewable fuel, then harvesting during the summer period is preferred due to the higher volatile matter content of the samples and thus the higher expected pyrolysis oil yield. If the end application is extracting valuable compounds from the pyrolysis oil, then it is strongly dependent on the target chemical. A number of useful compounds appear to be in higher concentration during summer period such as furan derivatives and thiophene, while others such as pyrrole, indole and phytol appear to be in higher concentration during winter.

## 6.4 Effect of pre-treatment

The high ash and metal content of macro-algae poses many difficulties and problems during thermochemical processes (explained analytically in **chapter 7**). Therefore, an attempt to improve their properties as a fuel was attempted by trying two different pre-treatment methods, hot water and acid washing which are processing steps commonly used in the seaweed industry for extraction of seaweed bio-polymers. The residues from processing have been pyrolysed in a thermogravimetric analyzer and in by Py-GC-MS and compared with the raw samples. Sample of the brown macro-alga *Macrocystis pyrifera* (commonly known as ‘giant kelp’) was used for this pre-treatment study. This sample was chosen as the study was performed early in the research when fewer samples were available however a similar trend is expected to be found for the other kelp samples.

The stepwise degradation of the sample before and after pre-treatment in water and acid is shown in the TGA and DTG curves in **Figure 6.10a-b**. Their temperature characteristics along with the moisture, volatile matter and char yields are listed in **Table 6.7**. Both pre-treatment methods reduce significantly the char content with a corresponding increase of the available volatile matter. This is due to the extraction of a significant portion of inorganic material by both pre-treatment methods (presented analytically in the next chapter **chapter 7**). However, they follow different decomposition pathways as indicated from the TGA and DTG curves, suggesting that there is a change in their biochemical composition as well as a change in their inorganic content. Fucoïdan and alginates (Ca and Na alginates) decomposition is clear by the broad peak shoulder above 700°C in the DTG curves of giant kelp as received and water washed. This peak shoulder is absent in the DTG curve of acid washed sample suggesting that fucoïdan and cations associated with the alginates were removed by treatment with acid. Treatment in water increases slightly the temperature for initiation of pyrolysis reactions ( $T_i$ ) while treatment in acid reduces this temperature significantly. Acid washing also shifts the first devolatilisation peak ( $T_{p1}$ ) to a lower temperature while the second peak ( $T_{p2}$ ) remains intact. This change in temperature characteristics by the different pre-treatment methods employed is reflected in the initial devolatilisation kinetics as well (**Table 6.8**). Water washing increases the activation energy of the sample as the

pyrolysis reactions start at a higher temperature while acid washing reduces significantly the activation energy as pyrolysis reactions start at lower temperature.



**Figure 6.10** (a) TGA and (b) DTG profiles in nitrogen at 25°C/min of giant kelp (GK) as received, water washed and acid washed.

**Table 6.7** Temperature characteristics, moisture, volatile matter and char yields of different washes of *Macrocystis pyrifera* as determined by thermogravimetric analysis in nitrogen (25 °C/min).

Sample	T <sub>i</sub> (°C)	T <sub>p1</sub> (°C)	T <sub>p2</sub> (°C)	T <sub>c</sub> (°C)	Moisture (Wt. %)	VM (dry) (Wt. %)	Char (Wt. %)
<i>Macrocystis pyrifera</i>							
As received	205	275	340	580	11.2	51.6	37.2
Water washed	230	280	335	565	8.1	65.5	26.4
Acid washed	155	255	340	560	5.8	67.8	26.4

**Table 6.8** Initial devolatilisation kinetics for different treatments of *M. pyrifera* as determined by the Senum and Yang approximation.

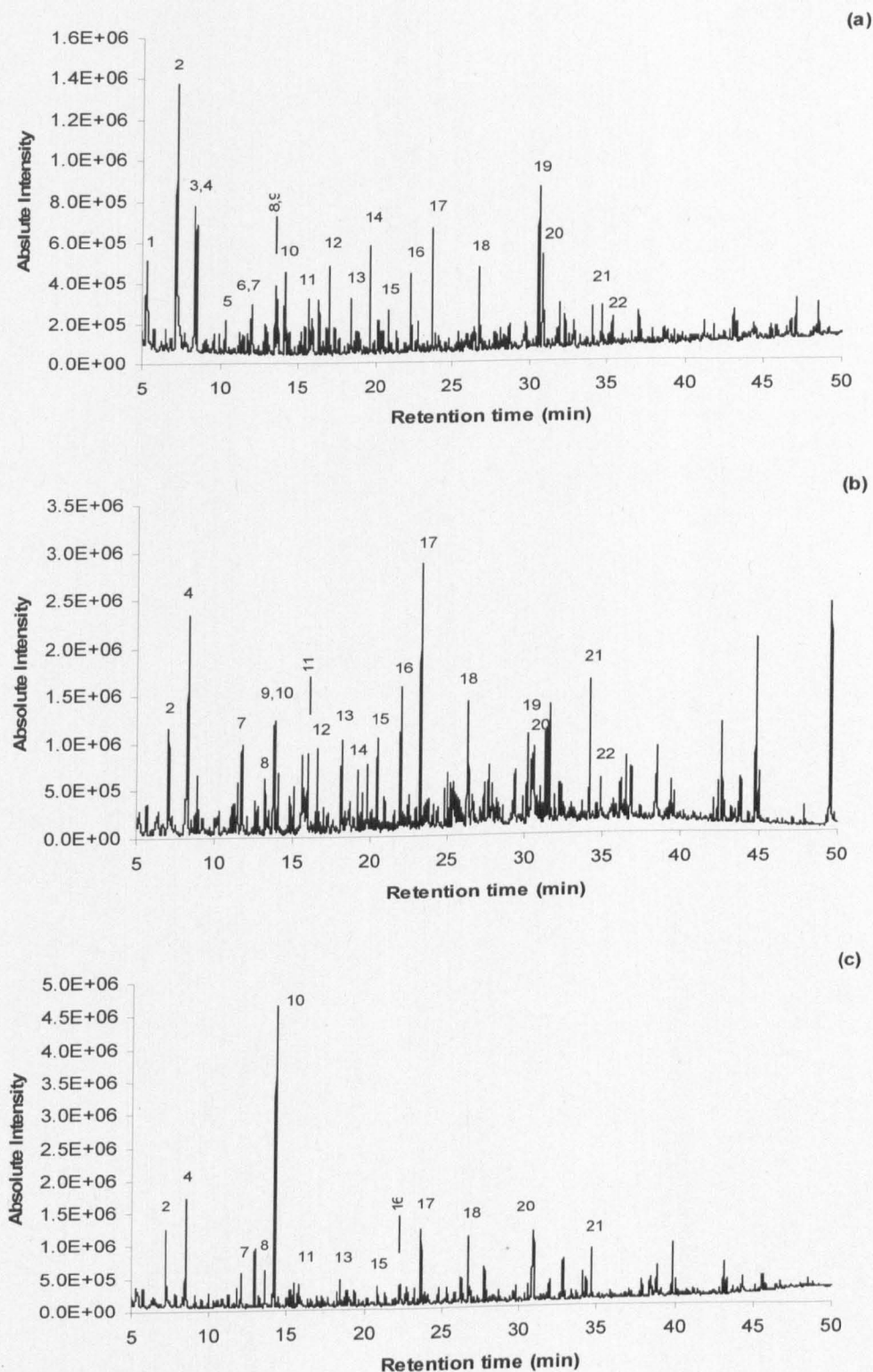
Sample	Temperature range (°C)	Activation Energy, E (kJ/mol)	Pre-exponential factor (lnA)	Variance
<i>Macrocystis pyrifera</i>				
As received	250-290	75	9.9	3 x 10 <sup>-3</sup>
Water washed	255-290	95.7	14.3	2.5 x 10 <sup>-3</sup>
Acid washed	225-270	55.9	6.4	3 x 10 <sup>-3</sup>

In order to better examine the changes in macro-algae biochemical composition upon water and acid treatment, the samples were analysed by Py-GC/MS. The pyrograms of *M. pyrifera* at 500°C before and after pre-treatment are shown in **Figure 6.11** and indicate a significant effect of demineralisation. The main compounds identified in the pyrograms are listed in **Table 6.9**. During water washing the phenolic and the cyclopentenone fractions increase. The effect of acid washing is more significant and indicates a significant change in polymeric structure. In particular, two polymers of brown algae, fucoidan and mannitol seem to have

been removed. Upon pyrolysis of fucoidan, the dominant compound produced is 5-methyl-2-furancarboxaldehyde (peak no. 14), while upon pyrolysis of mannitol, the dominant compounds produced are dianhydromannitol (peak no. 19) and 1-(2-furanyl)-ethanone (peak no.12). As can be seen from **Figure 6.11(c)**, these peaks are absent from the acid treated pyrogram. There is a dominance of furfural and the pyrolysis profile looks similar to that obtained from alginic acid. This suggests that upon treatment in acid, mannitol and fucoidan are extracted from brown macro-algae. Removal of fucoidan agrees with TGA data where there is an absence of the high temperature characteristic fucoidan peak in the acid treated DTG curve.

The removed bio-polymers can be further utilised to subsidise some of the additional cost of acid washing. Mannitol can be used as a feedstock for bio-ethanol through fermentation. Fucoidan is a compound that is undergoing a lot of research because of its anticoagulant, antioxidant, and antiviral properties (**Barahona et al., 2011; Collicec et al., 1991; Ponce et al., 2003**) as well as for its use in cosmetic products (**Fitton et al., 2007**) and could have a significant market value.





**Figure 6.11** Pyrograms at 500°C for (a) *M. pyrifera* as received, (b) *M. pyrifera* pre-treated in water and (c) *M. pyrifera* pre-treated in acid.

**Table 6.9** Main compounds identified in pyrograms from py-GC/MS of different treatments of *M. pyrifera*.

Peak No.	Compound	Peak No.	Compound
1	3-methyl-2-butanone,	12	1-(2-furanyl)-ethanone
2	Acetic acid	13	1,2-Cyclopentanedione
3	1-hydroxy-2-propanone	14	5-methyl-2-furancarboxaldehyde
4	Toluene	15	2(5H)-Furanone
5	Propanoic acid	16	2-hydroxy-3-methyl-2-Cyclopenten-1-one
6	1-hydroxy-2-propanone	17	Phenol
7	Pyrrole	18	4-methyl-phenol
8	Styrene	19	Dianhydromannitol
9	2-Cyclopenten-1-one	20	3-Pyridinol
10	Furfural	21	Indole
11	2-methyl-2-Cyclopenten-1-one	22	Isosorbide

## 6.5 Conclusions

The pyrolysis behaviour of brown macro-algae harvested at different times throughout the year was assessed by using TGA and py-GC/MS. The behaviour of each part of the macro-algal material (e.g. blades or stipes) was also examined. Finally the pyrolysis behaviour of pre-treated seaweed samples in water and acid was assessed.

Devolatilization of blades and stipes from brown macro-algae follow the same degradation pathway. However, more volatile matter is evolved during devolatilization of blades ending in less char content. Initiation of pyrolysis reactions begin at slightly higher temperature for the stipes explaining their higher activation energy. During the main devolatilization stage occurring between 200°C and 350°C, two distinct devolatilization steps are observed due to the different decomposition of their carbohydrates. Maximum conversion rate occurs between 260 and 270°C for the first step and is attributed to the decomposition of alginic acid and fucoidan, while maximum conversion rate for the second step occurs between 310 and 330°C and is attributed to the decomposition of mannitol and laminarin. Different harvest period affects significantly the devolatilization stage with more volatile matter evolving during the first step of main devolatilization for winter harvest and more volatile matter evolving during the second step for summer harvest.

The main volatiles evolved during pyrolysis of brown macro-algae differ significantly with those of terrestrial biomass and are mainly decomposition products of their carbohydrates. The dominant products during pyrolysis appear to be dianhydromannitol, phytol, 1-(2-furanyl)-ethanone, indole, 2-hydroxy-3-methyl-2-cyclopenten-1-one, furfural and toluene among others. These compounds appear in different intensity on the chromatograms depending on the harvest time. The variation of peak areas of some key marker compounds was linked to the variation of certain constituents of brown macro-algae. Seasonal variation in peak concentrations for 1-(2-furanyl)-ethanone, 2-hydroxy-3-methyl-2-cyclopenten-1-one and pyrrole were directly linked with the seasonal variation of mannitol, laminarin and protein content of brown macro-algae.

Demineralization significantly influences pyrolysis behaviour. Pre-treatment in acid was found to change the degradation pathway of the macro-algal sample. By

washing in acid, the pyrolysis reactions start at significantly lower temperatures for the resulting material and its initial activation energy is greatly reduced. Some of the biopolymers of brown macro-algae such as mannitol and fucoidan are removed by this treatment resulting in different pyrolysis products.

## **CHAPTER 7 - Combustion of brown macro-algae**

### **7.1 Introduction**

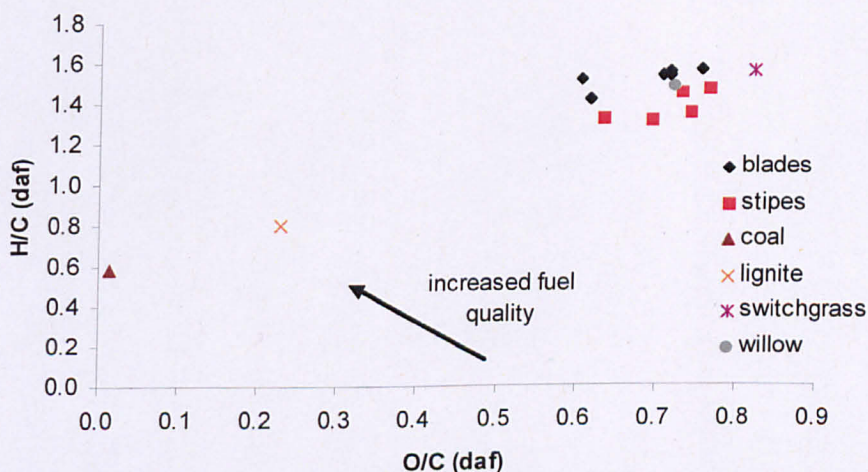
In **chapter 5** it was shown how the different parts of the seaweed (blades or stipes), as well as the time of harvest and location affect the seaweed fuel quality. In the previous chapter (**chapter 6**), it was shown how these variations affect the pyrolysis behaviour of brown macro-algae under slow heating rates by using a thermogravimetric analyser and under high heating rates by using Py-GC-MS. Pyrolysis is the first step of combustion process. This chapter examines the seaweed fuel properties and how these properties might influence their combustion. More specifically, a comparison of the seaweed fuel properties in terms of van Krevelen diagrams is being made. Their high heating values have been determined and the variation throughout their growing cycle is shown. Ash speciation expressed as oxides, and how these oxides might affect the combustion process through the use of empirical indexes for slagging and fouling has also been assessed. Seaweed fuel was also examined during combustion using slow heating rates in a thermogravimetric analyzer under the flow of air in order to explore additive versus non-additive behaviour in an oxidising environment. Finally, the effect of two pre-treatment methods (water and acid washing) on the seaweed fuel quality was assessed.

### **7.2 Classification of seaweed as fuel**

Combustion of fuels involve the devolatilization of the fuel into volatiles and char (pyrolysis) and the subsequent combustion of the released volatiles and char. The moisture content of the fuels used is very important for the devolatilization stage as the moisture has to be removed before volatiles start evolving. Freshly harvested brown macro-algae as described in **chapter 5** can contain up to 90wt% moisture, which adds an important drying step before devolatilization.

Dried seaweeds have high ash content (non combustible material) as was shown in **chapter 5** making them less attractive as fuel for combustion. A common way of comparing fuels is via the van Krevelen diagram, where the molar ratios of

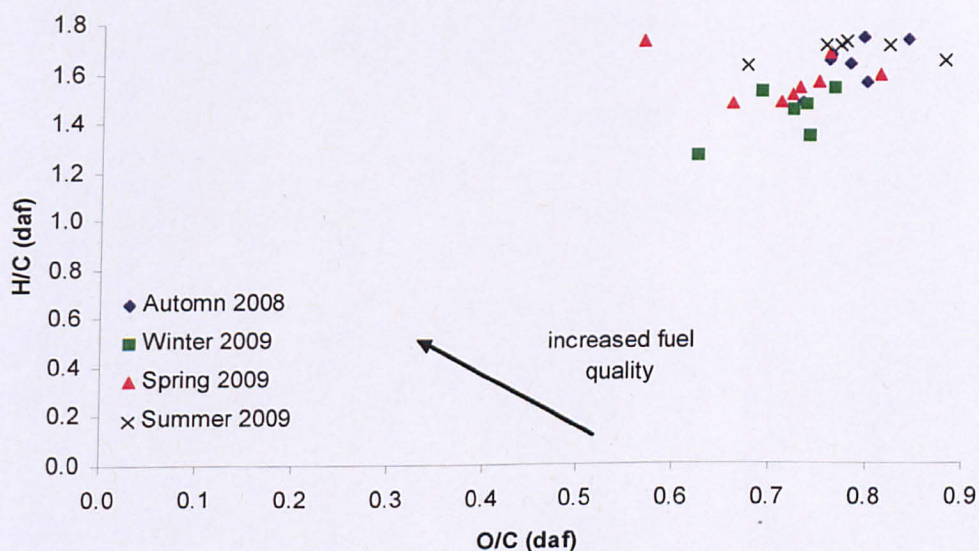
O/C are plotted against H/C on a dry ash free basis. The higher the H/C ratio and the lower the O/C ratio the better the quality of the fuel. **Figure 7.1** shows the van Krevelen diagram for blades and stipes of oven dried winter harvested samples. In the same figure a comparison with other biomass fuels such as switchgrass and willow as well as with coal and lignite is being made. Data for switchgrass and willow were taken from the work of **Fahmi et al., 2007** while data for coal and lignite from the work of **Jenkins et al., 1998**. Both blades and stipes have similar O/C ratios but blades have higher H/C ratios making them a better fuel. The sample with the highest H/C and lowest O/C ratios and thus the better fuel quality was found to be the blades of *L. hyperborea* harvested from Easdale while the stipes of *L. digitata* harvested from Clachan sound showed the worst fuel quality. Also, the stipes have lower HHV than the blades reflecting their higher ash and lower carbon content as can be seen from **Tables B.1 and B.2 in appendix B**. When compared with other biomass fuels macro-algal H/C and O/C ratios are closer to those of willow. They have higher H/C ratio than coal and lignite but their O/C is much higher as well.



**Figure 7.1** Van Krevelen diagram of blades and stipes of oven dried seaweed harvested during winter and comparison with other fuels.

In **chapter 5**, it was demonstrated how the seasonal variation can influence the analytical and chemical properties of seaweed. **Figure 7.2** shows the van Krevelen diagram of freeze dried seaweed samples harvested throughout their growth cycle.

There is a wide variation of their properties reflecting the seasonal variation. In general Winter and Spring harvested samples, when their ash content is at a maximum, have lower O/C ratios than summer and autumn harvested samples, while summer and autumn harvested samples (when minimum ash levels occur) have higher H/C ratio than winter and autumn harvested samples. *L. saccharina* harvested from Barancarry was found to have the highest H/C ratio during winter and autumn while *L. saccharina* harvested from Clachan sound had the highest H/C ratio for spring harvested samples. For summer harvested samples *L. hyperborea* harvested from Easdale had the higher H/C ratio while *A. esculenta* harvested from Easdale had the lowest O/C ratio. *L. hyperborea* harvested from Easdale was found to have the lowest O/C ratio for winter and autumn harvests. Detailed H/C and O/C molar ratios for all samples examined can be found in **appendix B**.



**Figure 7.2** Van Krevelen diagram of freeze dried seaweed harvested throughout the year.

**Table 7.1** shows the maximum and minimum high heating values (HHVs) of freeze dried samples throughout their growth cycle. HHVs for all samples examined can be found in **Appendix B**. *A. esculenta* was found to have the least variation in HHV throughout the year, maintaining relatively high levels (10.88 to 13.89 MJ/kg). This is due to the high levels of carbon throughout the year as was shown in **chapter 5**. The rest of the seaweed have similar variations if we exclude the minimum HHV

content of *L. saccharina* which is unusually low due to the very high ash content of this specific seaweed during winter (58wt%). Samples harvested from Easdale have higher HHVs than samples harvested from Clachan sound due to their lower ash content resulting in more material available for combustion. In general, the seasonal variation in HHV of brown seaweed is between ~9 and ~14 MJ/kg, with maximum values during summer and autumn and minimum values during winter and spring. This makes summer and autumn the most suitable seasons for seaweed harvest for combustion. However, even their maximum HHV (~14 MJ/kg) is relatively low compared to power station biomass fuels such as shea residue (20.37 MJ/kg) and olive residues (16.1-20.25 MJ/kg) (Darvell et al., 2010) and is closer to the HHV of refuse derived fuels (RDF) (15.89 MJ/kg) (Jenkins et al., 1998). This makes seaweed fuel a less attractive fuel for combustion.

**Table 7.1** Variation in high heating value (HHV) of freeze dried seaweed samples harvested from different locations through their annual growth cycle.

Harvest site	HHV (MJ/kg)			
	<i>L. digitata</i>	<i>L. hyperborea</i>	<i>L. saccharina</i>	<i>A. esculenta</i>
Clachan sound	8.76-12.83	9.08-13.41		
Easdale	10.71-13.10	9.63-14.16		
Barancarry			6.16-14	10.88-13.89

### 7.3 Slagging and fouling

In previous chapters (**chapter 5**), it was shown that the high inorganic content of seaweed biomass is composed mainly from alkali (K and Na) and alkaline earth metals (Ca and Mg). They were also shown to contain elements such as S, P, Fe and Si in less concentration. According to **Ross et al., 2008** seaweed biomass also contain significant concentration of Cl. All these elements are involved in reactions leading to ash fouling and slagging, corrosion and erosion of the reactor walls and agglomeration of the bed material (if a fluidised bed is used) leading to increased maintenance and operating costs and reduced plant efficiency and capacity (**Vamvuka and Zografos, 2004**).

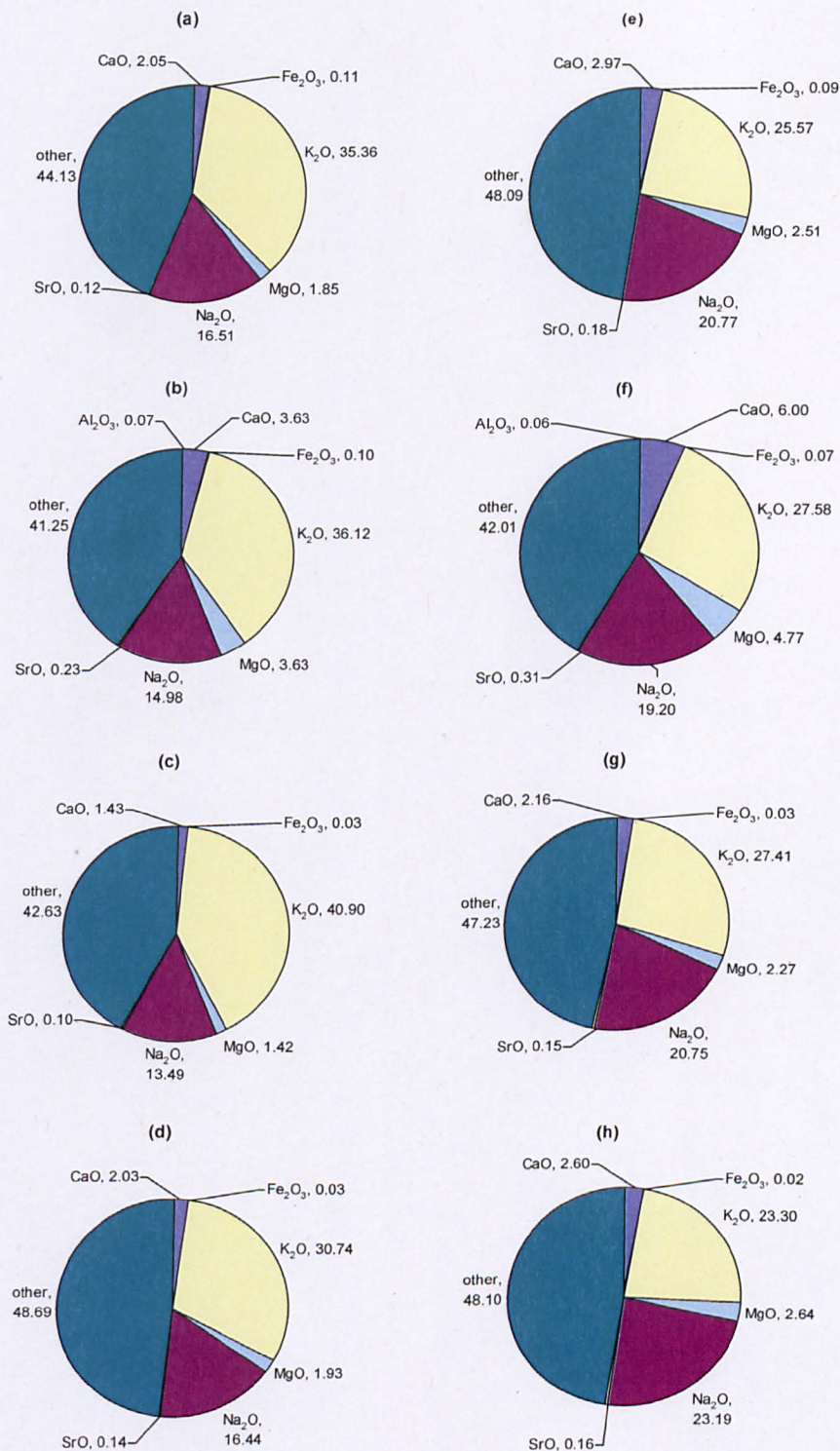


Upon combustion, a fraction of the alkali metals present in the ash of the fuel can volatilise to form alkali oxides (e.g.  $K_2O$ ,  $Na_2O$ ), alkali salts due to the presence of chlorine in the fuel (e.g.  $KCl$ ,  $NaCl$ ) and alkali sulphates due to the presence of sulphur (e.g.  $K_2SO_4$ ,  $Na_2SO_4$ ). Alkali silicates (e.g.  $K_2O_3Si$ ,  $Na_2O_3Si$ ) also form due to the presence of silica. Their concentration in seaweed ash is high enough to lower the ash fusion temperature leading to melting of the ash during combustion. On the other hand, the presence of alkaline earth metals ( $Mg$ ,  $Ca$ ) in seaweed ash can cause an increase in ash fusion temperature inhibiting the effect of the alkalis (Miles et al., 1995). The lower ash fusion temperature of seaweed fuel was shown by Wang et al (2008) who found softening of the ash of the brown alga *Sargassum natans* prepared at  $530^\circ C$ , to occur at  $786^\circ C$ , temperature much lower than woody biomasses softening ( $950-100^\circ C$ ).

The inorganic content of the seaweed ash was expressed as oxides as it is a common method to assess the fouling tendency of the fuel through empirical indexes. It was shown that there is a big seasonal variation in the inorganic content of seaweed. Accordingly there is a seasonal variation in the inorganic composition of ash. Figures 7.3 – 7.6 show this variation for the samples examined. Freeze dried samples were mainly used, however when there was a sample missing from a harvest season, oven dried samples were used as a replacement. It was shown in chapter 5 that freeze dried and oven dried samples followed similar seasonal variation in their properties. The oven dried samples used were samples of *L. saccharina* harvested from Barnacarry during winter, samples of *L. saccharina* harvested during summer from Clachan sound and samples of *A. esculenta* harvested during winter from Easdale.

A large percentage (40-50%) of seaweed ash was unidentified. This is due to the significant concentration of silica, sulphur, phosphorus and chlorine in seaweed material which will combine with a fraction of the alkali and alkaline earth metals to produce silicates, sulphates, phosphates and salts during combustion. All these have higher molecular weight than the alkali and alkaline oxides leading to a larger identified fraction of the ash. However, their inorganic content was expressed as oxides as it is a common way of predicting their fouling, slagging and agglomeration behaviour by using empirical indexes.

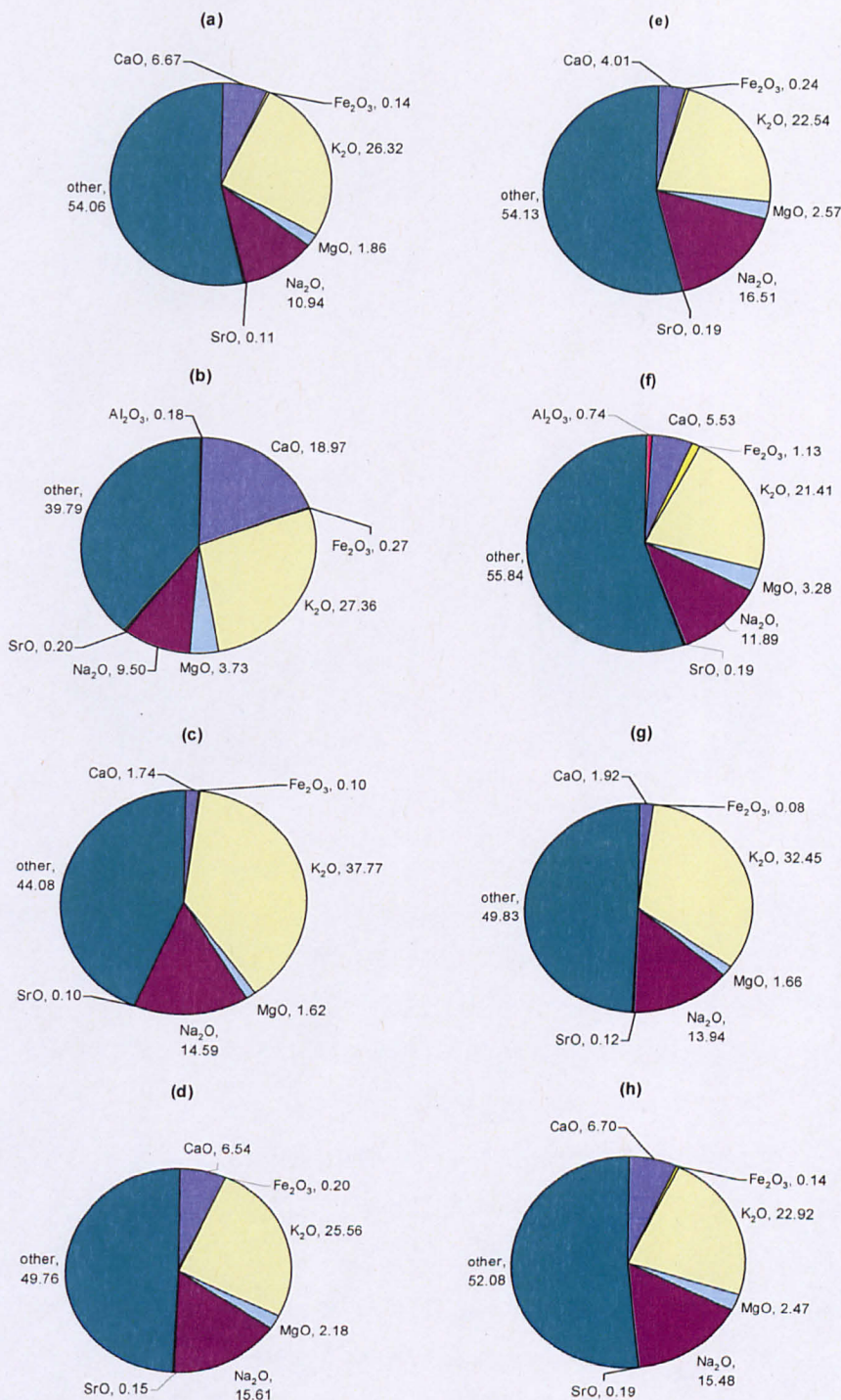
The main oxide of all seaweed ash was found to be  $K_2O$  followed by  $Na_2O$ . These two oxides make up more than 50% of seaweed ash. Other main oxides include  $CaO$  and  $MgO$  which were found in similar concentrations in seaweed ash with  $CaO$  being in slightly higher concentration. The alkali and alkaline oxides follow a large seasonal variation similar to the variation of the inorganic content of seaweed. For all samples examined there is a maximum  $K_2O$  concentration in seaweed ash during winter and spring and a minimum during summer and autumn. Variation of  $Na_2O$  was found to follow the opposite trend with maximum concentration during summer and autumn and minimum during winter and spring in all samples apart of *A. esculenta*. The ash from *A. esculenta* exhibits maximum  $Na_2O$  concentration during spring and minimum during winter. Variation in  $CaO$  and  $MgO$  concentration showed a clear maximum during winter and minimum during spring. Another important observation that was however only noticed for samples of *L. digitata*, is that samples harvested from Clachan sound are consistent with higher  $K_2O$  content and lower  $Na_2O$ ,  $CaO$  and  $MgO$  content in their ash than samples harvested from Easdale.



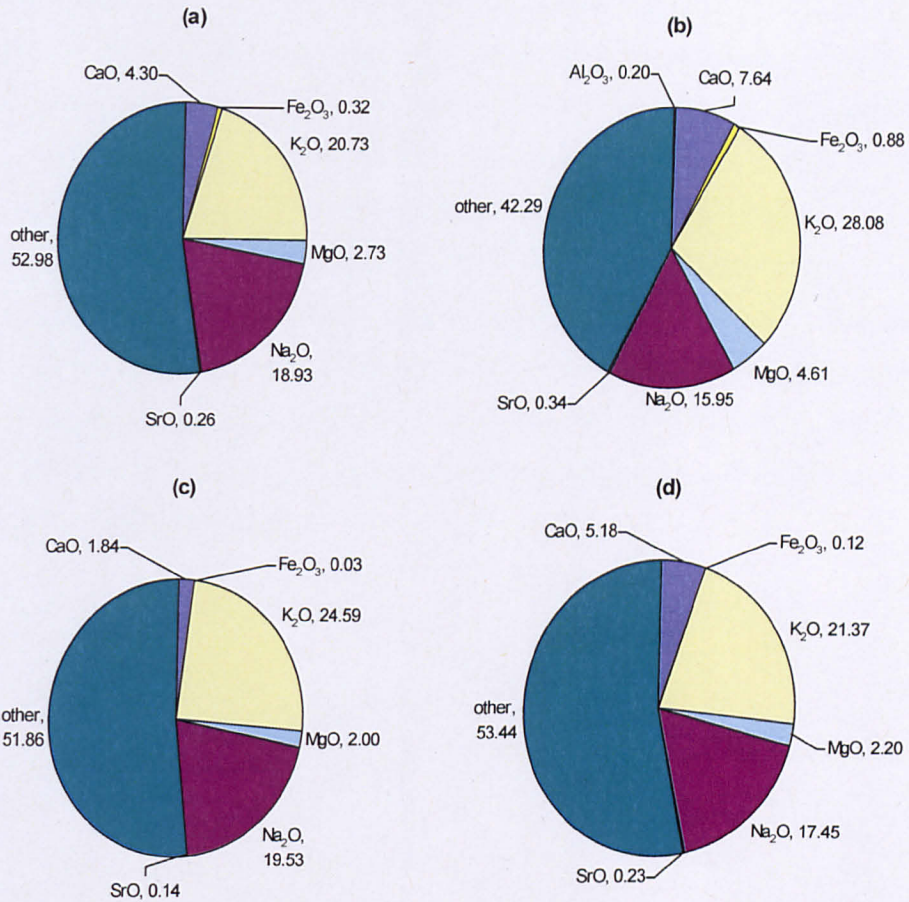
**Figure 7.3** Inorganic composition of ash for samples of *L. digitata* harvested from Clachan sound during (a) autumn, (b) winter, (c) spring, and (d) summer and for samples harvested from Easdale during (e) autumn, (f) winter, (g) spring and (h) summer.



**Figure 7.4** Inorganic composition of ash for samples of *L. hyperborea* harvested from Clachan sound during (a) autumn, (b) winter, (c) spring, and (d) summer and for samples harvested from Easdale during (e) autumn, (f) winter, (g) spring and (h) summer.



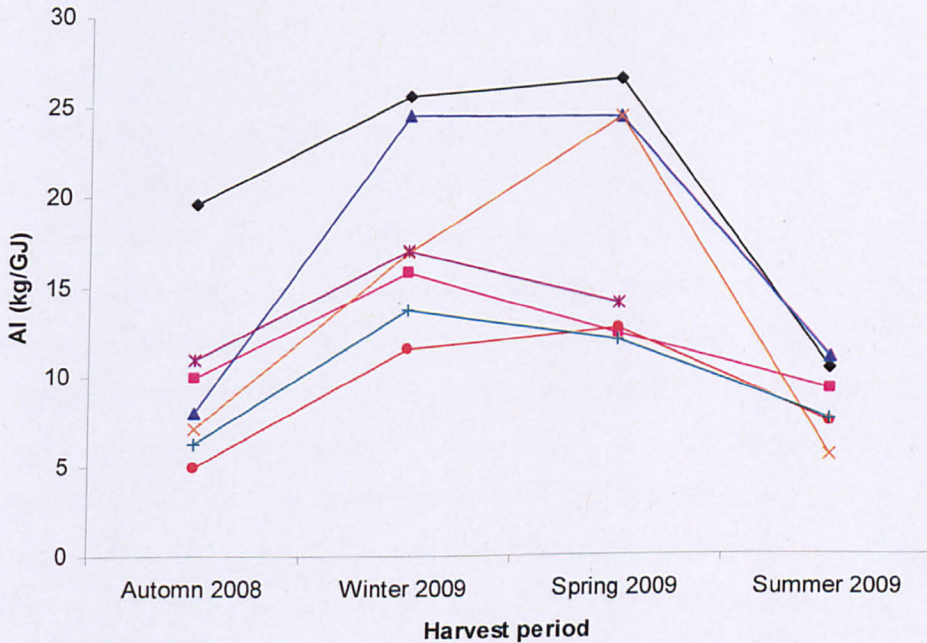
**Figure 7.5** Inorganic composition of ash for samples of *L. saccharina* harvested from Clachan sound during (a) autumn, (b) winter, (c) spring, and (d) summer and for samples harvested from Barnaccary during (e) autumn, (f) winter, (g) spring and (h) summer.



**Figure 7.6** Inorganic composition of ash for samples of *A. esculenta* harvested from Easdale (a) autumn, (b) winter, (c) spring, and (d) summer.

The fouling tendency of seaweed biomass is going to have different severity depending on the harvest season. This fouling behaviour was assessed by using the alkali index (AI) which provides information on the slagging and fouling tendency of a fuel in a combustion boiler by using the concentration of K<sub>2</sub>O and Na<sub>2</sub>O in the fuel's ash. **Figure 7.7** shows this variation in slagging and fouling probability depending on the harvest period through the AI. Fuels with AI greater than 0.34 kg/GJ are certain to slag and foul in a combustion boiler. All seaweed samples during all harvest periods have much higher AI leading to definite slagging and fouling of the chamber upon combustion. However, there is significant fluctuation in these values during the seaweed annual growth cycle and the type of seaweed. All seaweeds have higher AI during winter and spring when the potassium concentration is at its maximum and minimum AI during

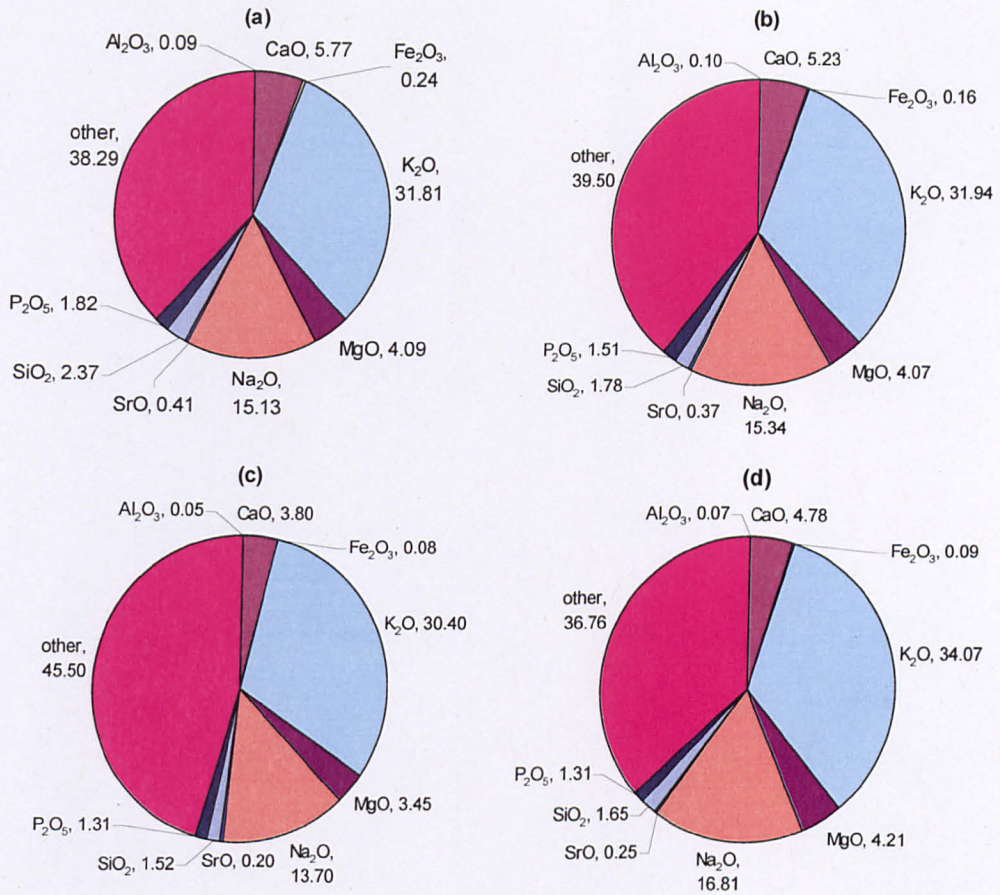
summer and autumn when K concentration is at its minimum. The samples that showed the least variation in AI throughout the year maintaining it at minimum levels were samples of *L. saccharina* harvested from Barancarry and samples of *A. esculenta* harvested from Easdale with minimum AI of 4.84 and 6.2 respectively during autumn. Nonetheless even these lowest values are well above the limit of safe combustion indicating that if seaweed fuels are going to be combusted, a series of measures have to be taken in order to reduce their fouling and slagging behaviour. Such measures can be the reducing of the furnace exit gas temperature, addition of additives to reduce the rate of fouling and/or retrofit of the designs of current plants (e.g. bed combustor integrated with a gasifier for burning the gasification gas).



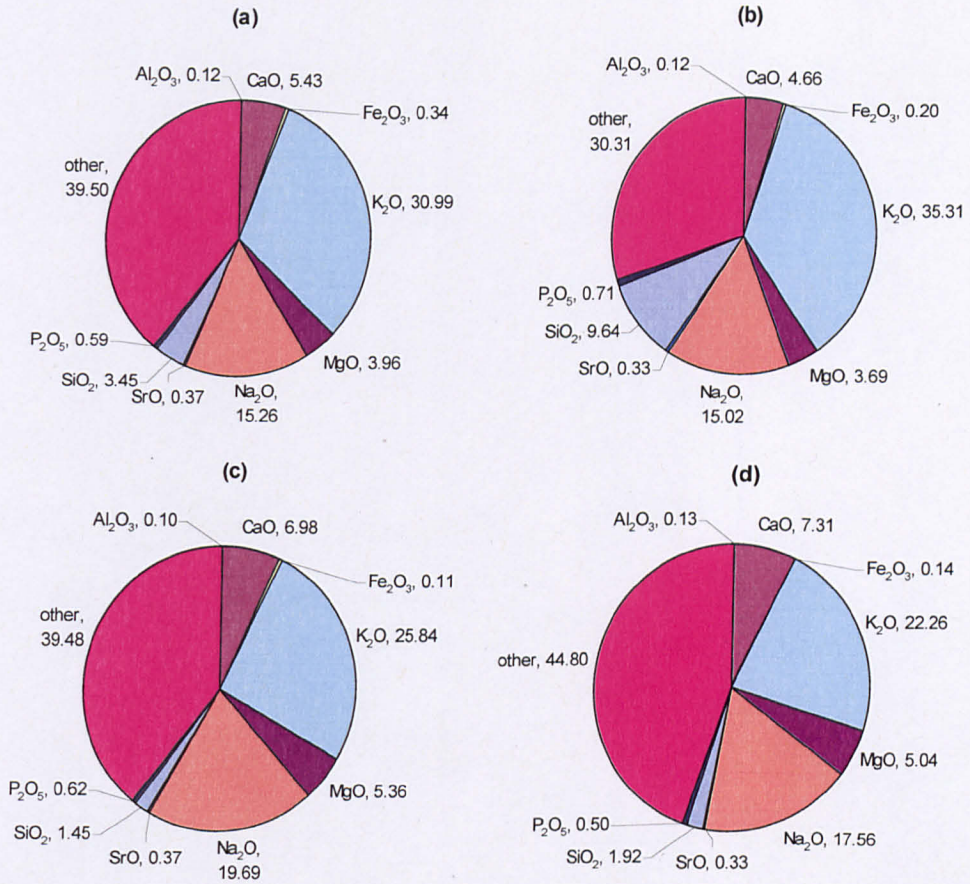
**Figure 7.7** Seasonal variation in alkali index (AI) for samples of (◆) *L. digitata* harvested from Clachan sound, (■) *L. digitata* harvested from Easdale, (▲) *L. hyperborea* harvested from Clachan sound, (×) *L. hyperborea* harvested from Easdale, (\*) *L. saccharina* harvested from Clachan sound, (●) *L. saccharina* harvested from Barancarry and (+) *A. esculenta* harvested from Easdale.

As mentioned previously, a more detailed analysis of seaweed ash was made for air dried samples because of the inclusion of Si and P analysis. Si and P analysis was only performed on air dried samples because of sample availability during the period of analysis. **Figures 7.8 – 7.11** show the seasonal variation in the inorganic composition of ash for air dried samples. Unfortunately the samples were not collected from the same location throughout the season. Only the samples of *L. digitata* that were collected from Clachan sound and the samples of *A. esculenta* that were collected from Easdale were collected from the same location in all harvest periods. Samples of *L. saccharina* were collected from Barancarry apart of the summer harvest that were collected from Clachan sound, while samples of *L. hyperborea* were collected from Clachan sound apart from the summer harvest that were collected from Easdale. The inorganic composition of ash from air dried samples was shown to have similar levels to that of freeze dried samples, but they did not show the same seasonal trend as the one previously stated for the freeze dried samples indicating the apparent changes in their bio-chemical composition during storage and transportation. However, *L. hyperborea* and *A. esculenta* followed the seasonal partitioning of ash with minimum  $K_2O$  and  $Na_2O$  content during summer-autumn and winter-spring respectively. Though the point of expressing these results is to show the  $P_2O_5$  and  $SiO_2$  speciation of ash. These oxides make a significant proportion of the ash. Their levels however are lower than the alkali and alkaline oxides.  $SiO_2$  partitioning in seaweed fuel ash is much lower than that reported for terrestrial biomass fuels (**Darvell et al., 2010; Jenkins et al., 1998**) and typically contributes to about 1.5-6wt% of the ash.  $P_2O_5$  exists in seaweed in similar amounts to terrestrial biomass as reported by **Jenkins and co-workers (1998)** and typically contributes about 0.5-2wt% of the seaweed ash.

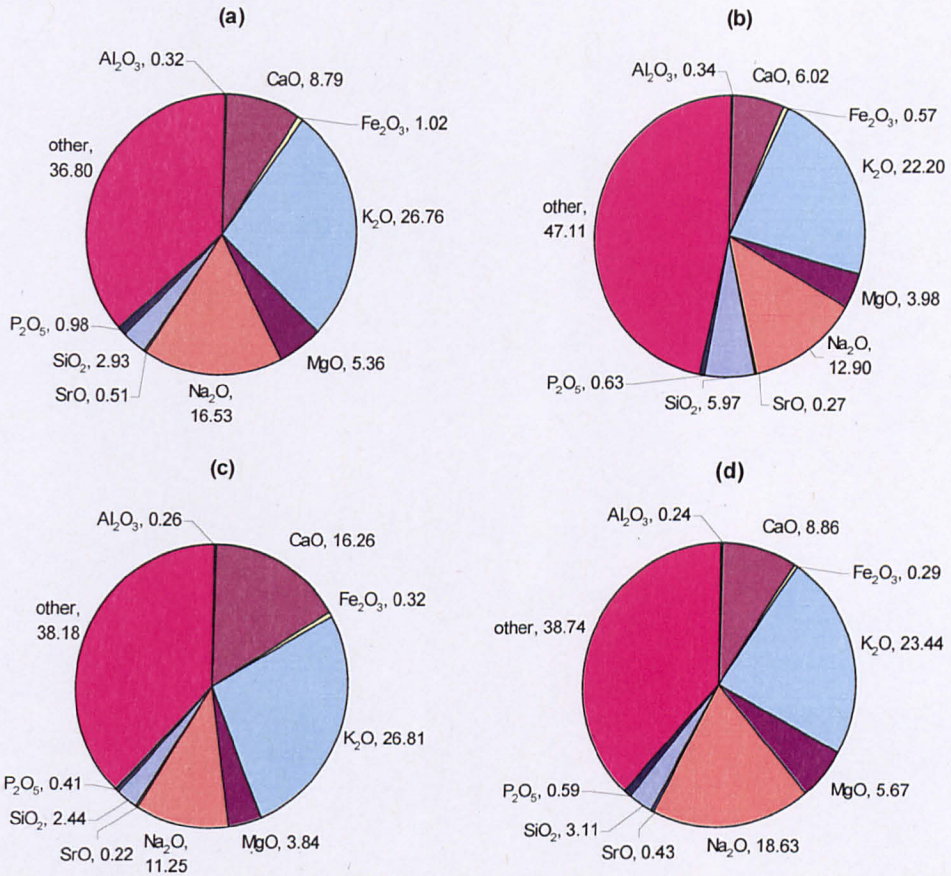




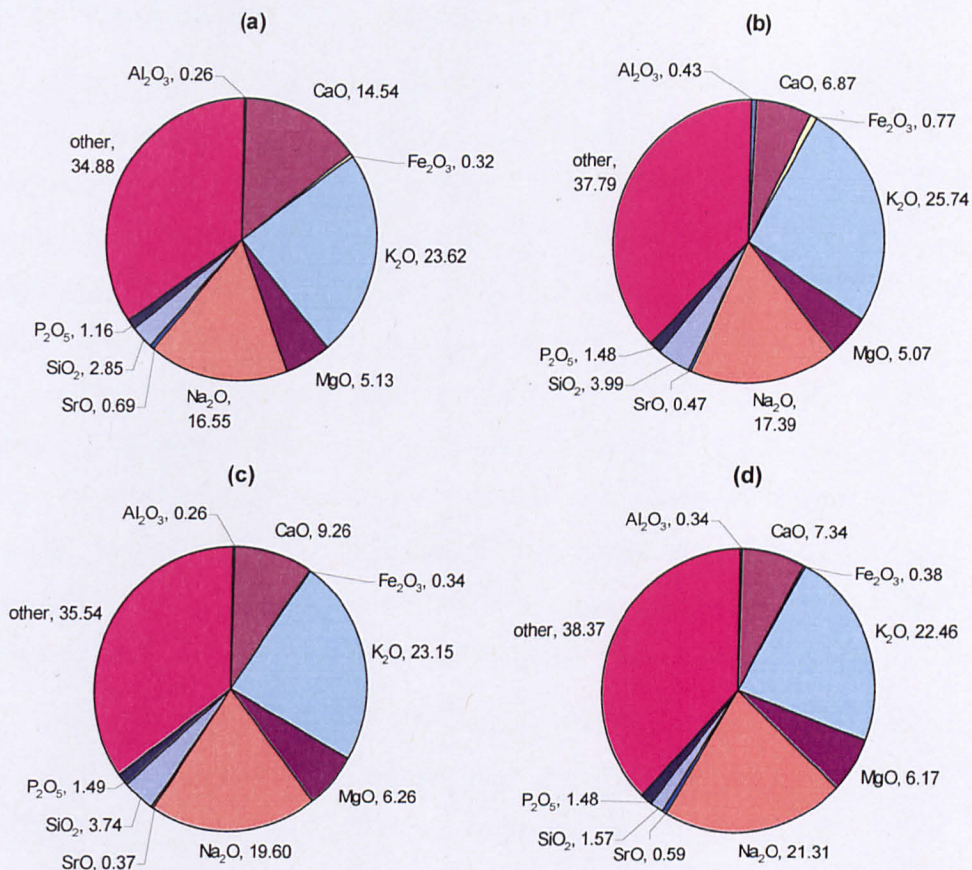
**Figure 7.8** Inorganic composition of ash for air dried samples of *L. digitata* harvested from Easdale (a) winter, (b) spring, (c) summer, and (d) autumn.



**Figure 7.9** Inorganic composition of ash for air dried samples of *L. hyperborea* harvested from Easdale (a) winter, (b) spring, (c) summer, and (d) autumn.



**Figure 7.10** Inorganic composition of ash for air dried samples of *L. saccharina* harvested from Easdale (a) winter, (b) spring, (c) summer, and (d) autumn.



**Figure 7.11** Inorganic composition of ash for air dried samples of *A. esculenta* harvested from Easdale (a) winter, (b) spring, (c) summer, and (d) autumn.

## 7.4 Thermogravimetry of seaweed in air

**Chapter 6** investigated the thermal decomposition of seaweed samples in an inert atmosphere. In this chapter the thermal conversion of the same summer harvested freeze dried seaweed samples is investigated, but in an oxidative atmosphere (combustion). As in **section 6.3**, the samples used were freeze dried samples of *L. digitata* harvested from Clachan sound, *L. hyperborea* harvested from Easdale, *L. saccharina* harvested from Barancarry and *A. esculenta* harvested from Easdale during the summer of 2009. Summer harvested samples were used because of their better properties as fuel (less metal and ash content, higher carbon content) during this period as was shown in **chapter 5**. The samples however, created problems in the TGA crucible as at the end of each run the crucible was found slagged, verifying the serious problems associated with fouling and slagging of seaweed in combustion chambers previously stated.

**Figure 7.12a-b** shows the TGA and DTG profiles obtained during burning of these samples while their combustibility temperature characteristics are listed in **Table 7.2**. **Table 7.3** lists their moisture and ash content as well as their weight loss in the different combustion stages as determined by TGA. The TGA and DTG curves (**Figure 7.12a-b**) revealed 4 different stages common for all seaweed. The first stage is from the initial temperature till the temperature of about 150°C where a small weight loss due to the dehydration of the samples occurs. This weight loss is the moisture content of the samples (**Table 7.3**) and is in a similar range to their moisture content as determined from their proximate analysis (**appendix B**). The second stage is the release and combustion of volatiles where a major weight loss occurs. The ignition of the combustion is noted in **Table 7.2** as VMIT (volatile matter ignition temperature) and was found to typically occur at 210°C for all samples apart of *L. saccharina* that occurred at a slightly lower temperature (205°C). The ease of the release and combustion of volatiles was less than 400°C for all samples. During this stage, the majority of seaweed mass was lost. *L. hyperborea* had the highest mass loss (49.6wt%) followed by *L. saccharina* (43.5wt%) and *L. digitata* (43wt%) while *A. esculenta* showed the least mass loss during this stage (37.1wt%).

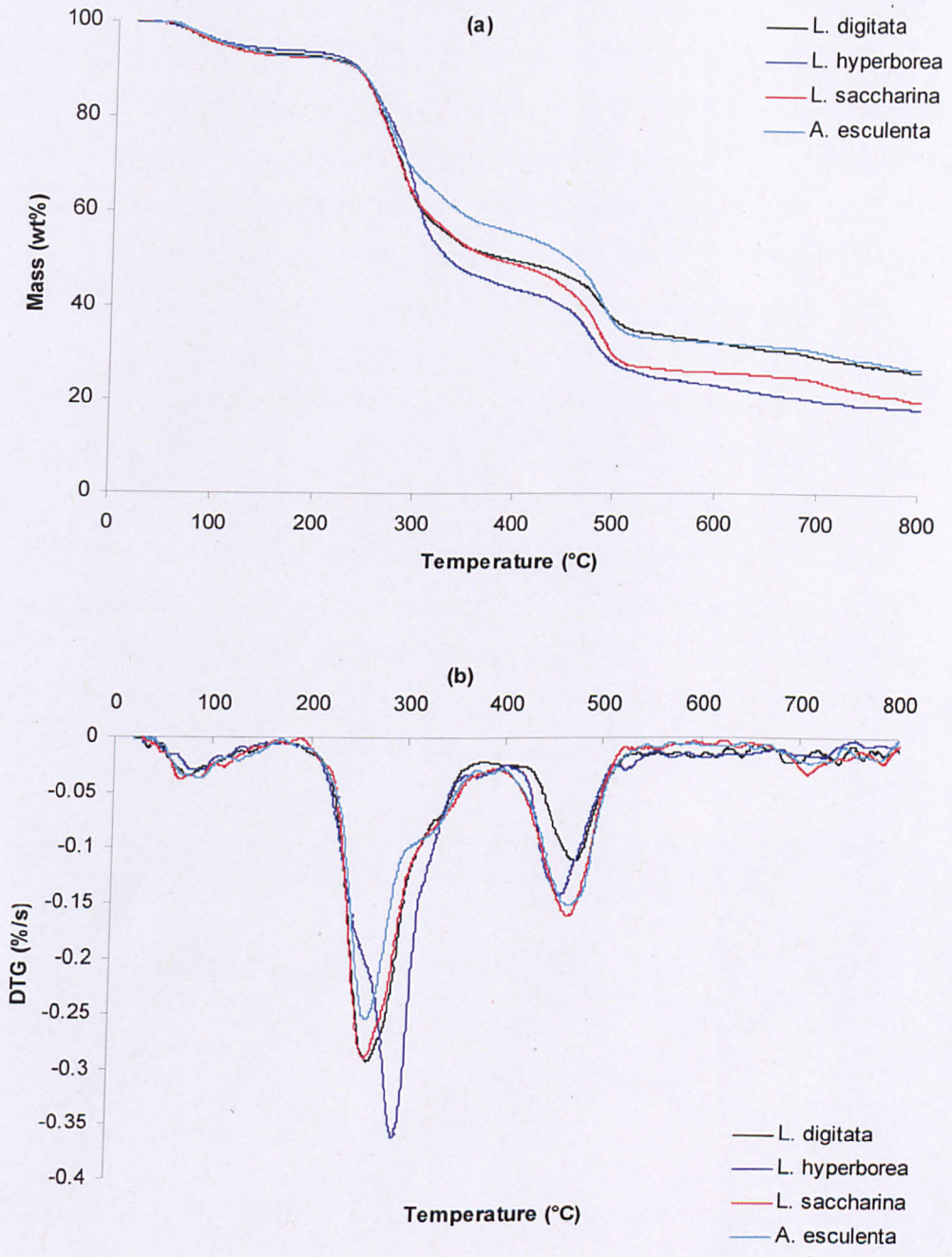


Figure 7.12 (a) TGA and (b) DTG profiles in air at 25°C/min of summer harvested freeze dried samples.

The maximum rate of volatile release (VMPT) was found at 260-265°C for all samples apart from *L. hyperborea* which occurs at a higher temperature (290°C). This might be attributed to a reduced metal content and particularly potassium content of *L. hyperborea* compared with the other samples (**appendix B**). It is known that metals and particularly potassium have a strong catalytic effect in both pyrolysis and combustion (Fahmi et al., 2007; Nowakowski et al., 2007; Jones et al., 2007). After the end of this second stage, and after a small transition stage (between 370 and 400°C), the char begins to ignite revealing the third stage. The onset of ignition of char (or fixed carbon) combustion, noted as FCIT (fixed carbon ignition temperature) in **Table 7.2** starts between 405 and 425°C for the samples examined. *L. digitata*'s char ignites at the higher temperature (425°C) while the other samples had similar FCITs. During this stage, a significant weight loss was observed but was smaller than the one during the 2<sup>nd</sup> stage. *L. saccharina* and *A. esculenta* exhibited the highest weight loss during that stage (21.5 and 21.4wt% respectively) followed by *L. hyperborea* (17.8wt%), while *L. digitata* exhibited a lower weight loss (14.7wt%).

**Table 7.2** Combustibility temperature characteristics of summer harvested freeze dried samples as determined by thermogravimetric analysis in air (25 °C/min).

	VMIT (°C)	VMPT (°C)	FCIT (°C)	FCPT (°C)	BT (°C)
<b>L. digitata</b>	210	265	425	475	520
<b>L. hyperborea</b>	210	290	410	460	520
<b>L. saccharina</b>	205	260	405	470	515
<b>A. esculenta</b>	210	260	405	470	520

**Table 7.3** Weight loss of summer harvested freeze dried samples during the different combustion stages as determined by thermogravimetric analysis in air (25 °C/min).

	Moisture (wt%)	W <sub>loss</sub> 200-400°C	W <sub>loss</sub> 400-520°C	W <sub>loss</sub> 520-800°C	Ash (wt%)
<i>L. digitata</i>	5.9	43.0	14.7	8.7	26.4
<i>L. hyperborea</i>	5.3	49.6	17.8	7.9	18.3
<i>L. saccharina</i>	6.5	43.5	21.5	7.6	19.9
<i>A. esculenta</i>	6.0	37.1	21.4	7.1	26.9

The maximum rate of char conversion (FCPT) was between 460 and 475°C with *L. digitata* having this maximum rate at the highest temperature following the later char ignition temperature of this sample. The burnout temperature (BT), indicating the ease of combustion, was found between 515 and 520°C for all samples. After this temperature, a very slow weight loss is observed up to the final temperature (800°C) was observed revealing the 4<sup>th</sup> stage. During this high temperature, -9wt% of the sample mass was lost due to the complicated decomposition of the alginates (as shown in **chapter 4**) and volatile metal loss and carbonate decomposition. The material left after the end of this final stage represents the ash content of the samples as noted in **Table 3** and is in a similar range to their ash content revealed by the proximate analysis of the samples (**appendix B**).



## 7.5 Demineralization

The high inorganic content present in seaweed ash was shown to cause problems associated with slagging, fouling erosion and corrosion in processing chambers by the use of empirical indices. An attempt to improve seaweed properties as fuels by reducing this fouling tendency was made by trying to remove a significant portion of their inorganic content. Two different pre-treatment methods, hot water washing and acid washing were used in order to reduce their inorganic content. It was shown in the previous chapter (**chapter 6**) that these washings have a significant effect on their bio-chemical composition, with acid washing removing mannitol and fucoidan. In this subsection, the interest is their effect on fuel properties such as ash content, inorganic content, volatile matter content and calorific value. Three seaweed were used, *Laminaria digitata*, *Macrocystis pyrifera* and *Fucus vesticulosus* because of their availability at the time of analysis.

**Table 7.4** shows the proximate and ultimate analysis of the seaweed samples before and after the two pre-treatment methods. Both pre-treatment methods have a positive effect on the fuel quality. Both treatment methods reduce the ash content of the samples as a large fraction of the mineral matter is being removed. At the same time there is an increase in the available volatile matter of the samples, their carbon and hydrogen content resulting in higher calorific values of the treated samples. Acid treated samples exhibit the largest improvement in fuel quality than water treated samples.

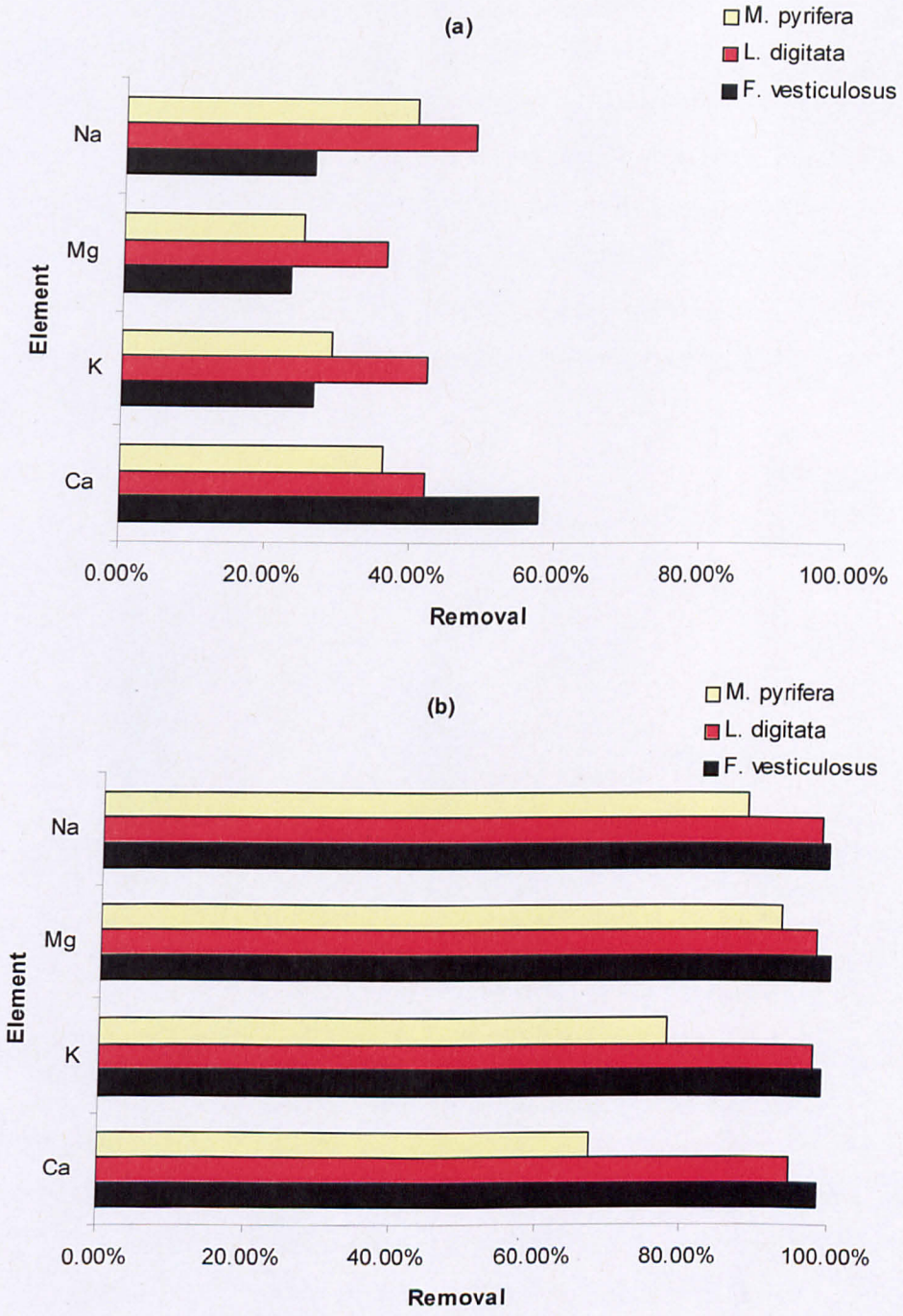
**Table 7.4** Proximate and ultimate analysis of brown macro-algae before and after treatment in water and acid

	Proximate analysis (wt%)			Ultimate analysis (wt%) (dry)				
	Moisture	VM	Ash	C	H	N	O <sup>a</sup>	CV (MJ/kg)
<b>F. vesticulosus</b>								
As received	11.4	46	26.52	37.81	3.97	2.70	29.00	16.67
Water washed	10	49	12.78	40.89	4.19	1.93	40.21	17.28
Acid washed	6	56	2.98	41.91	4.72	3.62	46.77	18.09
<b>L. digitata</b>								
As received	12.40	54	19.75	39.92	4.49	1.28	34.56	17.93
Water washed	9.00	53	11.43	44.29	4.37	2.02	37.89	19.07
Acid washed	6.70	56	1.07	48.39	5.10	2.52	42.92	21.48
<b>M. pyrifera</b>								
As received	8.00	42	27.83	29.67	3.47	2.21	36.82	12.12
Water washed	7.30	41	25.89	31.93	3.60	2.18	36.40	13.23
Acid washed	6.30	59	5.98	40.72	4.91	3.90	44.50	18.18

<sup>a</sup> calculated by difference

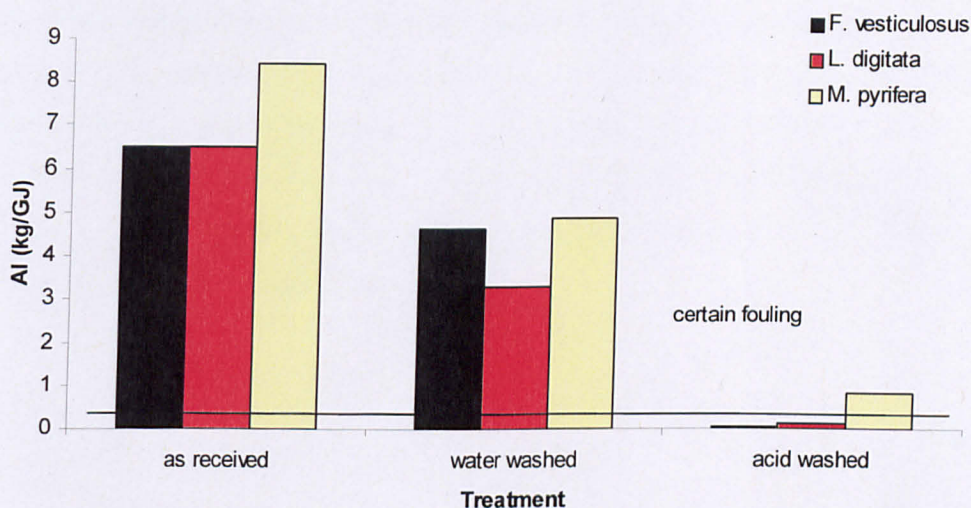
The improvement of seaweed fuel quality is mostly due to the removal of mineral matter. **Figure 7.13a-b** shows the removal of the main elements (K, Na, Ca and Mg) by pre-treatment in water and acid. Washing in water resulted in removing 25-48% of Na, 23-36% of Mg, 26-41% of K and 36-58% of Ca of the original samples, while the trace elements remain unchanged. Acid washing had a greater effect in mineral matter removal. It was found that 88-99% of Na, 92-99% of Mg, 78-99% of K and 67-98% of Ca of the original samples was removed by washing the samples with acid, while a significant portion of the trace elements was also removed.

The removal of large amounts of alkali metals should result in an improvement of seaweed fuel behaviour upon combustion. It was shown before that the large fraction of alkali metals is going to create problems associated with slagging and fouling of the combustion chamber.



**Figure 7.13** Removal of alkali and alkaline earth metals from seaweed samples by pre-treatment in (a) water and (b) acid.

This slagging and fouling probability was assessed for the pre-treated samples through the alkali index (AI) and is shown in **Figure 7.14**. Water washing reduces the AI of the samples but still it is above the range that the fuels are certainly going to foul (greater than 0.34 kg/GJ). However, acid washing resulted in a much lower AI, which indicates safe combustion for two out of three seaweed samples. AI for *F. vesticulosus* was 0.05 kg/GJ while for *L. digitata* was 0.1 kg/GJ indicating the safe combustion for the acid treated samples. *M. pyrifera* had a greater than 0.34 kg/GJ AI suggesting that maybe a stronger acid is needed for better demineralization.



**Figure 7.14** Alkali index of seaweed samples before and after pre-treatment.

Treatment of brown macro-algae in acid improves its fuel quality and removes most of the mineral matter making them safe for combustion. However, a pre-treatment process like this would significantly increase the overall cost of using seaweed as fuel. Though there is the possibility of subsidizing this cost from the extraction of possibly valuable seaweed carbohydrates such as fucoidan and mannitol during the treatment (as was shown in chapter 6).

## 7.6 Conclusions

In this chapter, the combustion behaviour of brown macro-algae was assessed. The blades of the seaweed are more attractive for combustion than the stipes because of their higher calorific value and lower ash content. The time of harvest has a significant effect on their combustion properties. Summer and autumn harvested samples have higher heating values and lower ash content and these periods would be preferred for seaweed harvesting if they are to be used for combustion. However, the high inorganic content of their ash (especially alkali oxides) is going to create problems associated with slagging and fouling of the chamber upon combustion. This fouling tendency although being reduced during summer and autumn is still well above the safe combustion limits. Thus, if seaweeds are going to be combusted, a significant portion of their inorganic material has to be removed. One method of doing this is by pre-treating the seaweeds in acid which results in the removal of the majority of the mineral mater, giving safe combustion predictions.

## **CHAPTER 8 - Hydrothermal liquefaction of brown macro-algae**

### **8.1 Introduction**

Hydrothermal liquefaction was considered as the main thermochemical process for the production of fuels from brown macro-algae due to its ability to handle wet feedstock with high ash content. Initially, in **section 8.2**, the influence of variables such as reactor loading, reaction time, temperature and catalyst loading on the products distribution and quality were investigated. A mass and energy balance has been determined for the different product phases. The bio-crude composition has been analyzed for its elemental content, molecular weight distribution, and chemical composition. The elemental content of the solid residue and composition of the gaseous and aqueous phases are also determined. The fate of metals (particularly the high alkali and alkaline earth metals) and distribution in the different product phases have also been determined. The findings from this section were used in **section 8.3** in order to improve the energy balance of the process and the bio-crude quality. Similar analysis of the resultant products was made. **Section 8.4** includes similar analysis of products obtained from hydrothermal liquefaction of different freeze dried seaweed samples (*L. saccharina*, *L. digitata*, *L. hyperborea* and *A. esculenta*) harvested during the same period (Summer 2009). Finally in **section 8.5** a comparison of hydrothermal liquefaction with other processes of producing fuels from brown macro-algae such as fermentation and anaerobic digestion in terms of energy is attempted.

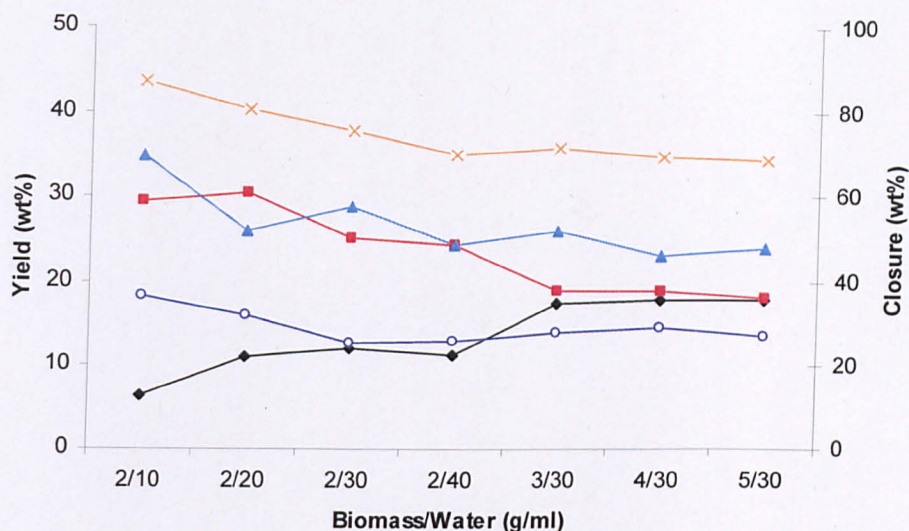
### **8.2 Effect of reaction conditions**

The effect of the reactor loading, residence time, temperature and catalyst (KOH) loading were investigated in order to maximize the bio-crude yield. Bio-crude yield was expressed on dry ash free (daf) basis as it is virtually free of ash while all other product yields and closure were expressed on a dry basis (db). Air dried samples of *L. saccharina* harvested from Barancarry bay during April of

2008 were used for the experiments. The sample used has been analysed for its proximate, ultimate, and metal concentration. It was found to be composed of 9.2 wt% moisture, 26.8 wt% ash (on a dry basis), 31.3 wt% carbon, 3.7 wt% hydrogen (on a dry basis), 2.4 wt% nitrogen, 0.7 wt% sulphur and 26.3 wt% oxygen (on a dry basis). Its high heating value (HHV) was 12 MJ/kg while the main mineral matter present in the ash was potassium (55000 ppm), sodium (34400 ppm), magnesium (12200 ppm) and calcium (5100 ppm).

### 8.2.1 Product yields

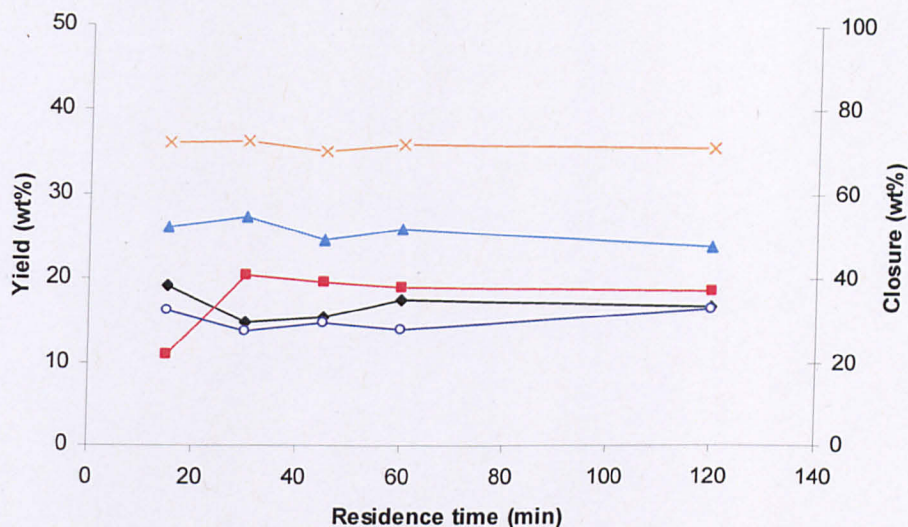
The first experimental parameter studied was the influence of reactor loading on the product yields (**Figure 8.1**). The runs were performed at 350°C and were held at this temperature for 1hr. The amount of water in the system is very important as it acts as both a hydrogen donor and as a solvent for hydrolyzing the high molecular weight carbohydrates present in biomass (**Apell, 1967**). It was found that 30ml of water was needed in order to increase the bio-crude yield when 2g of seaweed were used, representing a biomass: water loading of 1:15. Further increase in water did not influence the yields. With an increased amount of seaweed in the reactor (3g) with 30ml of water, a higher bio-crude yield was accomplished. Similar results were obtained by **Qu et al (2003)** during the liquefaction of woody biomass, where the maximum oil yield at 340°C was obtained with a ratio of 0.10 biomass/ water (g/ml). Further increases in biomass loading did not influence yields. The increase in the bio-crude yield was accompanied by a decrease in the residue yield. The optimum conditions for the bio-crude yield were found to be 3g of seaweed and 30ml of water for the given reactor. At these conditions, the mass balance of the different product fractions included a bio-crude yield of 17.5 wt%, 19 wt% of residue, 25.9 wt% of dissolved aqueous extracts (DAEs) and 14 wt% of gas. Lower reactor loading (2/10 and 2/20 biomass/water ratio) favoured the formation of residue (29.5 wt%) and gas (18.3 wt%).



**Figure 8.1** Effect of reactor loading on yields of liquefaction products, ♦ bio-crude yield, ■ residue yield, ▲ water yield, ○ gas yield, × conversion.

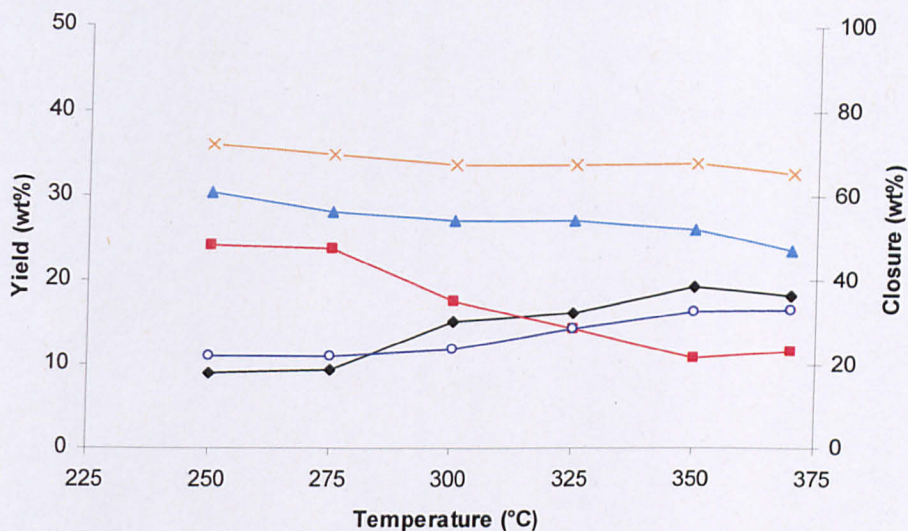
These optimum conditions were chosen for studying the influence of residence time at 350°C (**Figure 8.2**). It was found that a 15-minute holding time at this temperature was sufficient for the seaweed to form oily compounds, giving the highest bio-crude yield (19.3 wt%). Increasing the holding time resulted in a decrease of the bio-crude yield, indicating re-polymerization or re-condensation of the newly formed compounds. Similar results were obtained by **Qu et al (2003)**, where a reaction time of 10 minutes produced the highest oil yield from the liquefaction of woody biomass, and by **Yin et al (2010)** during the hydrothermal liquefaction of cattle manure, while **Zhou et al (2010)** found an increase in the bio-oil yield from the green alga *E. prolifera* by increasing the residence time to 30 min. **Shuping et al (2010)** however found a constant increase in oil yield up to a 1-hour holding time during the hydrothermal liquefaction of microalgae (although microalgae have different biochemical composition). The aqueous phase yields exhibited a gradual decrease with increasing residence time, while the residue showed a similar but opposite trend to that of the bio-crude. The gaseous yield showed a gradual increase with increasing residence time.





**Figure 8.2** Effect of residence time on yields of liquefaction products, ♦ bio-crude yield, ■ residue yield, ▲ water yield, ○ gas yield, × conversion.

A residence time of 15 min was chosen in order to study the influence of temperature on the product streams. The temperature range investigated was between 250 and 370°C, slightly below the critical point of water (374.3 °C). Increasing the temperature resulted in an increase in bio-crude yield and a corresponding decrease in the residue fraction (**Figure 8.3**). Similar results were reported by **Shuping et al (2010)** during the hydrothermal liquefaction of microalgae, while **Qu et al (2003)**, **Zhou et al (2010)** and **Yin et al (2010)** found temperature thresholds after which the bio-crude yield started decreasing during hydrothermal liquefaction of woody biomass (320°C), green macro-algae (300°C) and cattle manure (310°C). In this investigation, the maximum bio-crude yield was 19.3 wt% at 350°C. The aqueous phase yields decreased with increasing temperatures while the gaseous phase yields increased with increasing temperatures. Similarly, the bio-crude yields increased with increasing temperatures, accompanied by a decrease in the solid residue yield. Under conditions producing the highest bio-crude yield, 10.9 wt% of residue, 26 wt% of aqueous phase and 16.4 wt% of gas accompanied the bio-crude.

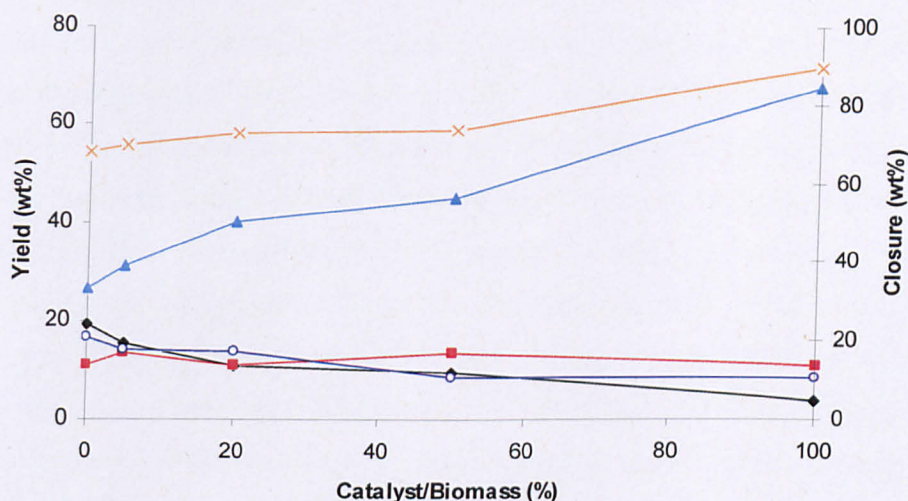


**Figure 8.3** Effect of temperature on yields of liquefaction products, ♦ bio-crude yield, ■ residue yield, ▲ water yield, ○ gas yield, × conversion.

The final parameter investigated was the effect of catalyst dosage on the product yields. Generally hydroxides, carbonates, bicarbonates and formates of the alkali metal are used as catalysts during hydrothermal liquefaction (Apell, 1967). Potassium hydroxide (KOH) was chosen as a typical catalyst to investigate this effect. Increasing the catalyst dosage in the mixture results in a decrease in the bio-crude yield (Figure 8.4). The solid residue yield is slightly increased until a 50 wt% catalyst/biomass loading after which it begins to decrease. The gaseous fraction also decreases with increased catalyst loading, while the aqueous fraction is constantly increasing. It is obvious that KOH reduces the formation of bio-crude and favors the solubility of organics in the aqueous phase.

The largest fraction of the products under all different experimental conditions was distributed in the water phase and, depending upon reaction conditions, ranged from 22.9-67.6 wt %. The yields of the remaining products also varied with experimental conditions. The bio-crude yields ranged from 3.8-19.3 wt% and solid residue yields ranged from 10.7-30.5 wt%, while gas yields ranged from 8.3-18.3 wt%. In general, the higher bio-crude yields correspond to a lower residue fraction and vice versa. The overall conversion or closure after

extraction and workup ranged between 65% and 90%. High conversion (about 90%) is attained when the bio-crude yield is low and the aqueous yields are high (e.g. 2/10 biomass/water and 100 wt% biomass/catalyst), suggesting that the majority of the losses are derived from the bio-crude fraction due to losses during separation (trapped in reactor pipe work) and processing (evaporation of light volatiles during evaporation of DCM).



**Figure 8.4** Effect of catalyst (KOH) loading on yields of liquefaction products, ♦ bio-crude yield, ■ residue yield, ▲ water yield, ○ gas yield, × conversion.

The most important variable in terms of bio-crude yield appears to be temperature and reactor loading. Temperature and reactor loading influences the pressure and whether the water is in the liquid state, the gaseous state, or somewhere in between. At low reactor loading (2/10 and 2/20) and low temperature (250°C and 275°C) char yields were high (23.8-30.5 wt%) and bio-crude yields were low (6.5-11.2 wt%). In general, the lower the temperature and pressure, the higher the char yield. The higher the temperature and pressure, the higher the bio-crude yields. This correlates with low temperature and pressure favoring hydrothermal carbonization, and high temperature and pressure favoring hydrothermal liquefaction.

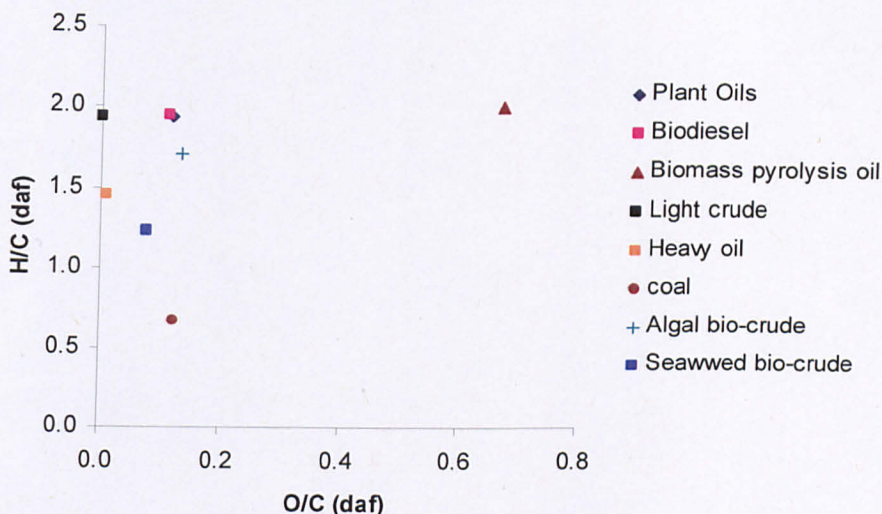
### 8.2.2 Analysis and classification of the bio-crude

The bio-crudes obtained from hydrothermal liquefaction of brown macro-algae were very viscous and virtually solid. Their ultimate analysis is shown in **Table 8.1**. The carbon and hydrogen content of the bio-crudes is greatly increased compared with the starting material while the oxygen content is greatly decreased. This results in high heating values within the range 33.8-38.5 MJ/kg. The average HHV was 36.2 MJ/kg and is comparable with the heating value of petroleum crude (42.7 MJ/kg). The heating values of the bio-crudes produced are significantly higher from those reported by **Zhou et al (2010)** during the hydrothermal liquefaction of the green alga *E. proliferata* (28-30 MJ/kg) and are closer to the bio-crudes produced from the liquefaction of micro-algae (**Biller et al., 2010; Ross et al., 2010**). Their oxygen content was low (average O content of all the bio-crudes produced was 7.85 wt%) and comparable with the oxygen content of the bio-petroleum produced by **Wang et al. (2008)** from deoxy-liquefaction of terrestrial biomass (5.5-8.6 wt%). The different experimental conditions didn't have a major effect on the heating value of the resulting bio-crude. In general by increasing the liquefaction temperature there was an increase in the carbon content of the bio-crudes resulting in an increased HHV, while the use of KOH as catalyst maintained the HHV at almost the same values. Bio-crudes with the lowest heating values were obtained when high quantities of water with small quantity of biomass were fed into the reactor (2g/30ml and 2g/40ml). **Figure 8.5** shows the comparison of seaweed bio-crude to other fuel oils in form of the van Krevelen diagram. The seaweed bio-crude has lower oxygen content than all the other synthetic oils indicating its better quality as a fuel, but has a lower H/C content mainly because of the high carbon concentration in the seaweed bio-crude. It is closer in nature with heavy crude oil. The average H/C ratio of all the bio-crudes produced was 1.23 while the average O/C ratio was 0.08. It has to be noted the significant nitrogen content in the bio-crudes making denitrogenation necessary if the fuel is to be further used.

**Table 8.1** Ultimate analysis and HHV of the bio-crudes from different experimental conditions.

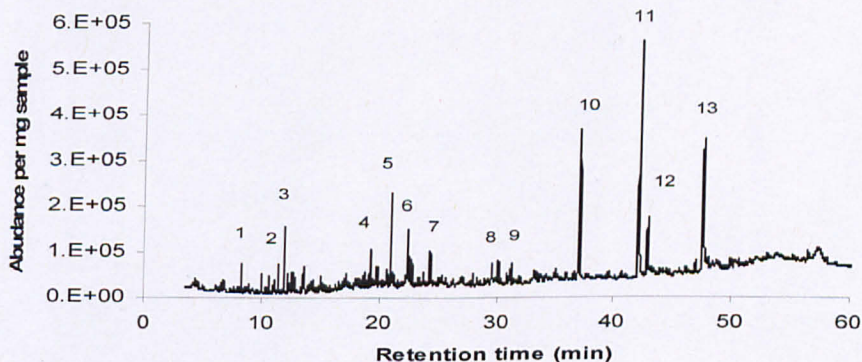
<b>Biomass/Water (g/ml)</b>	<b>C (%)</b>	<b>H (%)</b>	<b>N (%)</b>	<b>O<sup>a</sup> (%)</b>	<b>H/C (daf)</b>	<b>O/C (daf)</b>	<b>HHV (MJ/kg)</b>
2/10	77.6	8.4	6.1	7.9	1.29	0.08	36.0
2/20	79.4	8.0	5.4	7.2	1.20	0.07	36.3
2/30	77.6	8.6	5.0	8.8	1.32	0.09	36.2
2/40	74.4	8.5	4.8	12.4	1.37	0.13	34.6
3/30	80.1	8.3	5.4	6.1	1.24	0.06	37.0
4/30	78.7	10.0	5.4	5.9	1.52	0.06	38.5
5/30	75.7	9.6	5.0	9.6	1.53	0.09	36.7
<b>Holding time (min)</b>							
15	82.0	7.1	4.9	5.4	1.04	0.05	36.5
30	77.0	8.6	5.5	8.9	1.34	0.09	36.0
45	75.1	9.0	5.0	10.9	1.44	0.11	35.6
60	80.1	8.3	5.4	6.1	1.24	0.06	37.0
120	78.9	8.3	5.3	7.5	1.26	0.07	36.4
<b>Temperature (°C)</b>							
250	76.6	7.6	5.2	10.3	1.19	0.10	34.6
275	77.2	7.3	5.9	9.5	1.14	0.09	34.5
300	81.4	7.1	5.3	5.9	1.05	0.05	36.2
325	82.2	7.0	4.8	5.8	1.02	0.05	36.2
350	82.0	7.1	4.9	5.4	1.04	0.05	36.5
370	81.0	7.8	4.4	6.7	1.15	0.06	36.7
<b>Catalyst/Biomass (%)</b>							
0	82.0	7.1	4.9	5.4	1.04	0.05	36.5
5	82.4	7.1	4.7	5.7	1.03	0.05	36.5
20	84.2	7.4	3.6	4.8	1.05	0.04	37.5
50	74.7	7.9	2.5	14.9	1.27	0.15	33.8
100	82.6	8.1	3.0	6.2	1.18	0.06	37.8

<sup>a</sup> calculated by difference



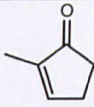
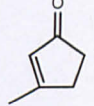
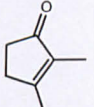
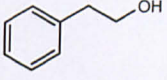
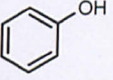
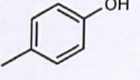
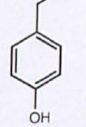
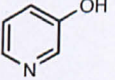
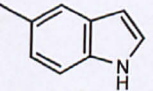
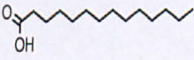
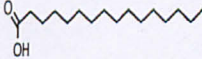
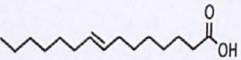
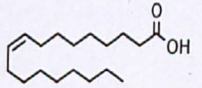
**Figure 8.5** Van Krevelen diagram of seaweed bio-crude compared with different fuel oils.

The bio-crudes obtained contain a complex mixture of hydrocarbons and have been analyzed by GC/MS. The identification of the main compounds has been performed using a NIST mass spectral database. A typical chromatogram (obtained from hydrothermal liquefaction of 3g of biomass in 30ml of water at 350°C with 15min holding time) is shown in **Figure 8.6** and its typical components are presented in **Table 8.2**.

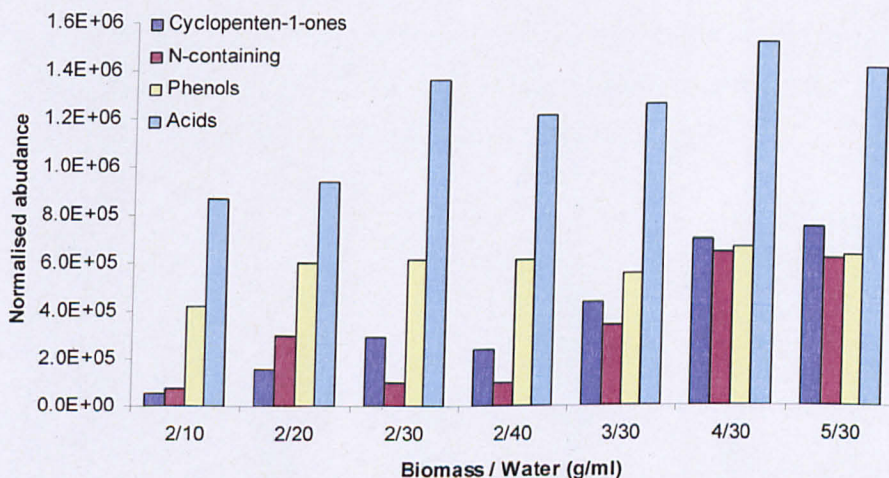


**Figure 8.6** Chromatogram of bio-crude obtained from hydrothermal liquefaction of 3g of seaweed biomass in 30ml of water at 350°C for 15min residence time.

**Table 8.2** Identification of compounds in bio-crude obtained from hydrothermal liquefaction of 3g of seaweed biomass in 30ml of water at 350°C for 15min residence time by GC-MS analysis.

No	RT	Compound Name	Formula	Structure	MW
1	8.314	2-Cyclopenten-1-one, 2-methyl-	C <sub>6</sub> H <sub>8</sub> O		96
2	11.416	2-Cyclopenten-1-one, 3-methyl-	C <sub>6</sub> H <sub>8</sub> O		96
3	11.904	2-Cyclopenten-1-one, 2,3-dimethyl-	C <sub>7</sub> H <sub>10</sub> O		110
4	19.241	Phenylethyl Alcohol	C <sub>8</sub> H <sub>10</sub> O		122
5	20.995	Phenol	C <sub>6</sub> H <sub>6</sub> O		94
6	22.447	Phenol, 4-methyl-	C <sub>7</sub> H <sub>8</sub> O		108
7	24.357	Phenol, 4-ethyl-	C <sub>8</sub> H <sub>10</sub> O		122
8	29.597	3-Pyridinol	C <sub>5</sub> H <sub>5</sub> NO		95
9	31.294	1H-Indole, 6-methyl-	C <sub>9</sub> H <sub>9</sub> N		131
10	37.022	Tetradecanoic acid	C <sub>14</sub> H <sub>28</sub> O <sub>2</sub>		228
11	42.128	n-Hexadecanoic acid	C <sub>16</sub> H <sub>32</sub> O <sub>2</sub>		256
12	42.875	9-Hexadecenoic acid	C <sub>16</sub> H <sub>30</sub> O <sub>2</sub>		254
13	47.561	Oleic Acid	C <sub>18</sub> H <sub>34</sub> O <sub>2</sub>		282

The main compounds identified included ketones such as cyclopentenone, alcohols such as phenylethyl alcohol, phenols, nitrogen heterocycles such as pyridinol and indole derivatives, saturated fatty acids such as tetradecanoic acid and n-hexadecanoic acid and unsaturated fatty acids such as 9-hexadecenoic acid and oleic acid. Similar compounds were identified also by **Zhou et al. (2010)** in the bio-oil obtained from uncatalytic hydrothermal liquefaction of the green alga *E. prolifera* at 300 °C. The ketones and phenols are believed to come from the decomposition of the carbohydrates and cellulose while the nitrogen containing compounds from the decomposition of proteins. Fatty acids were the most abundant group in the bio-crudes although the levels of lipid in seaweeds are known to be low. The reactor loading, holding time and temperature didn't have significant influence in the composition of the resultant bio-crudes. The chromatograms have been normalized based on the amount of bio-crude dissolved in DCM in order to assess differences in product distribution. By increasing the reactor loading there was an increase in ketones, phenolic and acidic fraction which was expected as the yield is increasing (**Figure 8.7**).

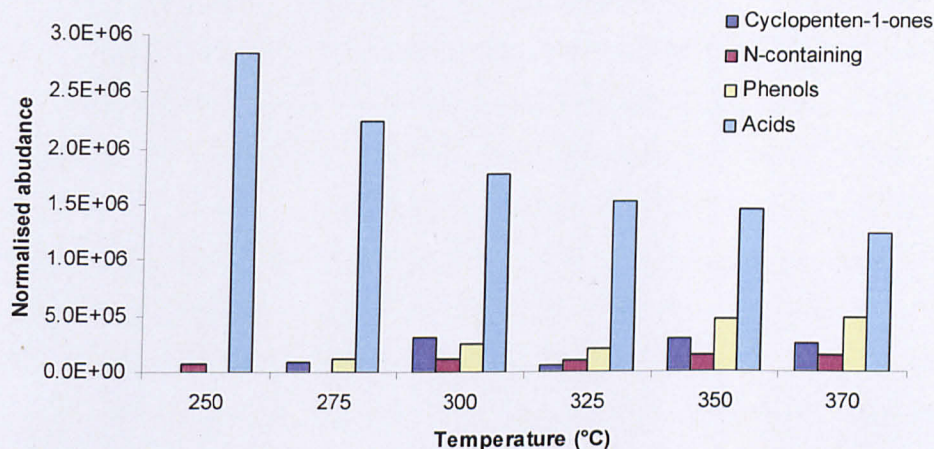


**Figure 8.7** Effect of reactor loading in the main constituents of bio-crude.

At low temperature (250 °C) isophytol was found to be present in the bio-crude, while by increasing the temperature again the ketones and phenolic fraction was increased (**Figure 8.8**). However, by increasing the temperature there was a decrease in the fatty acid fraction. This was unexpected as with

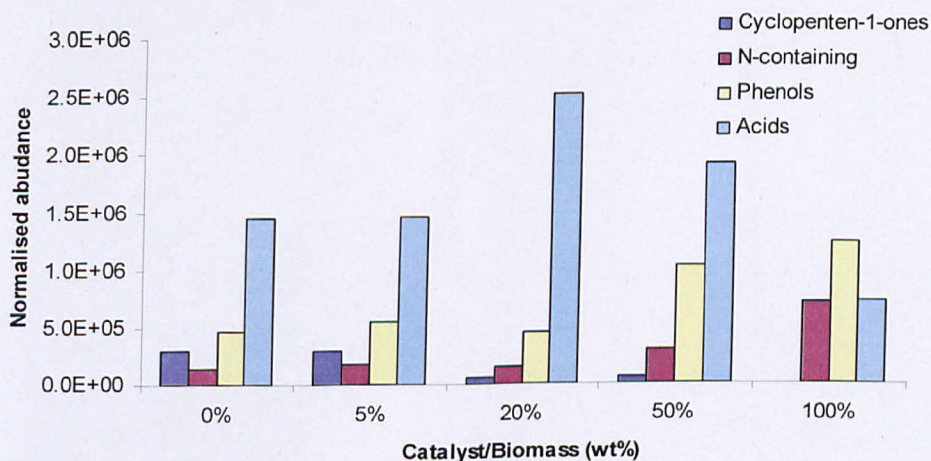


increasing temperature there is an increase in the bio-crude yield. The fatty acids may have been converted to high molecular weight compounds that were not separated by GC/MS.



**Figure 8.8** Effect of temperature in the main constituents of bio-crude.

The addition of catalyst (KOH) resulted in the reduction of the ketone fraction and in the increase of the phenolic fraction (**Figure 8.9**). At 100% catalyst/biomass feed, ketones were absent from the bio-crude. At high catalyst loading (50% and 100%) phytol and isophytol were identified while all the nitrogen contained compounds were indole derivatives.



**Figure 8.9** Effect of catalyst (KOH) loading in the main constituents of bio-crude.

The boiling point distribution of the bio-crudes was assessed by using thermal gravimetric analysis (TGA) in nitrogen as described by **Ross et al. (2010)**. Heating the bio-crude under an inert atmosphere to 900°C typically results in a mass loss of 70-80 wt%. The boiling distribution at 50°C intervals is listed in **Table 8.3** for the main experiments performed. **Table 8.3** indicates that all of the bio-crudes contain significant amounts of high boiling material. Under the conditions resulting in the maximum bio-crude yield (3g of biomass in 30ml of water at 350°C with 15 min holding time), only 23 wt% of the bio-crude had a boiling point <250°C, indicating that only a small fraction of the bio-crude was amenable to GC/MS (oven temperature 250 °C) and much of the bio-crude was of higher molecular weight. As a comparison, about 44.2 wt% of a typical crude oil's fraction has a boiling range <250°C, and about 8 wt % of bitumen's has the same boiling range (**Speight, 2001**). The addition of KOH resulted in a slight increase in the fraction of lower boiling point (<250°C) from 23% (0 wt catalyst) to 28% (100 wt% catalyst). The <250°C material also increased as the water loading increased with constant biomass (20.4 wt% with boiling point <250°C at 2/10 biomass/water and 25.3 wt% at 2/40) and as the biomass loading increased with constant water loading (25.9 wt% at 3/30 biomass/water and 28.4 wt% at 5/30 biomass/water). So it would seem that the increase in the reactor loading rather than the introduction of the catalyst causes an increase in the fraction of bio-crude with a lower molecular weight. The influence of temperature on the boiling point distribution of the oils appears to pass through a maximum where the <250°C gradually increases up to 300°C, but above which it begins to decrease.

Comparing the elemental analysis of a bio-crude produced with that of crude oil and bitumen, we find that the bio-crude is closer in range with bitumen. A typical bio-crude produced contains 82 wt% C, 7.1 wt% H, 4.9 wt% N, 5.4 wt% O and 2.8 wt% ash (at 350°C with 15 min holding time), while conventional crude oil consists of 86 wt% C, 13.5 wt% H, 0.2 wt% N, <0.5 wt% O and is normally free of ash (**Speight, 2001**), and bitumen consists of 83 wt% C, 10.6 wt% H, 0.5 wt% N, 0.9 wt% O and 0.8 wt% ash (**Speight, 2001**). The bio-crude has higher nitrogen and oxygen contents, making further processing such as

deoxygenation and denitrogenation necessary for further use as a fuel. The boiling point distribution and elemental analysis shows that the bio-crude falls between crude oil and bitumen. The bio-crude obtained from hydrothermal liquefaction of brown macro-algae can be classified as closer to bitumen.

**Table 8.3** Boiling point distribution of bio-crudes obtained at different experimental conditions

Distillate Range (°C)	Boiling point of bio-crude														
	Reactor Loading (gbiomass/mlwater)				Residence time (min)				Temperature (°C)					Catalyst	
	2/10	2/40	3/30	5/30	15	30	60	120	250	275	300	325	350	0%	100%
40-200	8.9	11.7	11.7	13.5	9.8	9.0	11.7	9.7	7.4	10.5	11.0	8.9	9.8	9.8	12
200-250	11.5	13.7	14.2	14.9	13.9	13.0	14.2	15.1	14.1	15.2	15.7	13.0	13.9	13.9	15.8
250-300	12.8	14.1	14.6	14.6	15.2	13.8	14.6	14.6	17.3	17.5	15.1	15.5	15.2	15.2	14.4
300-350	11.9	11.8	12.3	12.6	11.9	12.9	12.3	12.8	13.1	10.9	8.7	10.8	11.9	11.9	12.5
350-400	13.4	9.8	7.8	11.6	13.0	9.7	7.8	7.0	8.8	8.4	8.5	12.0	13.0	13.0	11.6
400-450	9.9	5.3	6.7	6.5	7.8	6.0	6.7	9.2	6.7	6.1	9.1	7.3	7.8	7.8	5.4
450-500	5.2	3.8	3.7	3.0	0.9	5.7	3.7	3.1	2.9	3.5	4.1	3.6	0.9	0.9	2.7
500-550	0.1	1.8	1.5	1.5	2.5	0.5	1.5	1.9	1.5	1.7	1.7	2.0	2.5	2.5	1.0
>550	3.7	6.7	2.1	3.3	3.6	3.8	2.1	2.7	5.6	6.0	7.6	2.5	3.6	3.6	4.6

### 8.2.3 Analysis of the residue

The proximate and ultimate analysis of the solid residues produced from hydrothermal liquefaction under all the experimental conditions investigated is given in **Table 8.4**. The different experimental conditions were found to have a large effect on the char composition. The carbon content in the chars ranges from 14.9-52.6 wt%, while hydrogen content ranges from 2.1-5.2 wt%. Consequently, a big variation was observed in the ash content and HHV with ash content ranging from 26.2 wt% to 69.2 wt% and HHV ranging from 4.9 MJ/kg to 22.8 MJ/kg. At low biomass and water feed (2g/10ml), a char with high carbon content, heating value and low ash content is produced. By increasing the volume of water fed in the reactor, the carbon content of the resulting chars is decreased while the ash content is increased resulting in chars with lower heating values. When the biomass loading is increased there is also an increase in carbon content of the chars and a decrease in the ash content resulting in higher heating values of the chars. Reaction time appears to have less influence on the char composition. Increasing the liquefaction temperature, decreases the carbon content and increases the ash content resulting in chars with lower heating values. Addition of catalyst also caused the lowering of char quality. By increasing the catalyst dosage there was a decrease in the carbon content of the char and an increase in the ash content causing the calorific value of the char to decrease to as low as 4.9 MJ/kg. In general, the conditions required for maximizing the bio-crude yields result in the lowest char yields, and the lower heating value (HHV) of the char. However, chars with high heating values and high yields can be obtained at low reactor loading or at low reaction temperatures.

**Table 8.4** Ultimate, proximate analysis and HHV of the solid residues obtained at different experimental conditions

Biomass/Water (g/ml)	C (wt%)	H (wt%)	N (wt%)	O <sup>a</sup> (wt%)	Moisture <sup>b</sup> (wt%)	Ash <sup>b</sup> (wt%)	H/C (daf)	O/C (daf)	HHV (MJ/kg)
2/10	52.6	5.2	3.4	10.0	2.5	26.2	1.2	0.1	22.8
2/20	47.5	4.0	2.6	4.4	2.1	39.3	1.0	0.1	20.0
2/30	36.1	3.0	1.6	11.9	2.6	44.8	1.0	0.2	14.0
2/40	31.7	3.1	1.9	11.1	2.2	48.4	1.2	0.3	12.6
3/30	25.8	4.1	1.8	12.5	1.7	54.0	1.9	0.4	11.4
4/30	32.2	3.7	1.1	11.8	1.8	49.3	1.4	0.3	13.4
5/30	33.3	4.7	1.2	13.1	1.7	45.9	1.7	0.3	14.8
<b>Reaction time (min)</b>									
15	27.5	2.6	2.0	7.6	2.2	56.7	1.2	0.2	10.8
30	27.7	4.3	1.3	6.6	2.2	56.2	1.9	0.2	13.0
45	30.4	4.1	1.1	13.0	3.1	51.0	1.6	0.3	13.2
60	25.8	4.1	1.8	12.5	1.7	54.0	1.9	0.4	11.4
120	28.0	3.2	1.4	9.9	1.5	56.4	1.3	0.2	11.4

Temperature (°C)										
250	39.4	4.2	2.8	20.4	3.2	29.9	1.3	0.4	15.9	
275	37.3	3.9	2.4	13.9	3.3	39.3	1.2	0.3	15.3	
300	35.2	3.2	2.4	12.8	3.7	42.4	1.1	0.3	13.9	
325	34.5	3.2	2.4	8.4	2.7	48.7	1.1	0.2	13.9	
350	27.5	2.6	2.0	7.6	2.2	56.7	1.2	0.2	10.8	
370	27.3	2.7	2.4	7.5	1.5	58.5	1.2	0.2	10.7	
Catalyst/Biomass (%)										
0	27.5	2.6	2.0	7.6	2.2	56.7	1.2	0.2	10.8	
5	26.4	2.7	2.1	12.6	1.6	54.2	1.2	0.4	10.0	
20	24.6	2.8	0.8	9.2	1.9	60.8	1.3	0.3	9.6	
50	14.9	2.1	1.3	11.6	1.0	69.2	1.7	0.6	4.9	
100	17.9	2.4	0.8	15.7	1.5	61.7	1.6	0.7	6.2	

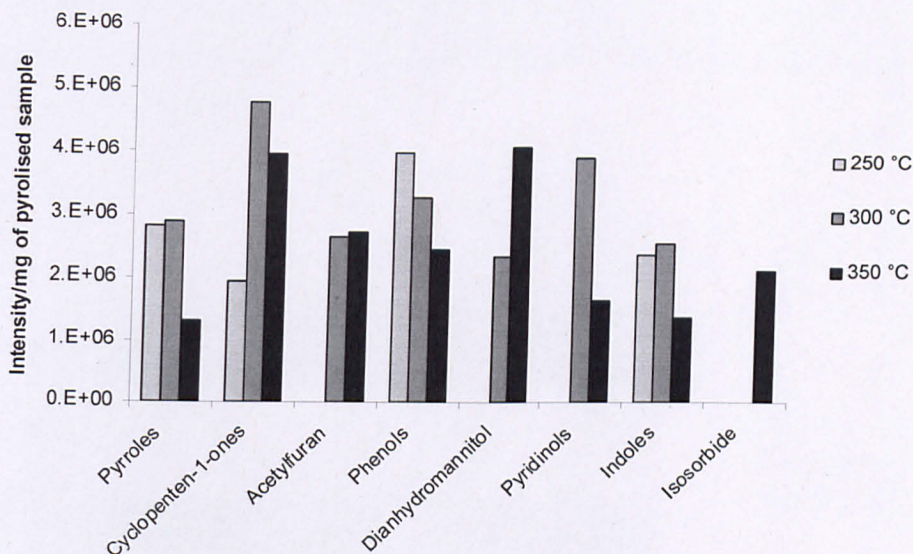
<sup>a</sup> calculated by difference<sup>b</sup> calculated from TGA

#### 8.2.4 Analysis of aqueous phase

The pH values of the aqueous phases were determined immediately after completion of the reaction and were found to range between 7 and 9. Addition of the catalyst increased the pH of the aqueous phase to 9, while in non catalytic runs the pH was close to 8. During hydrothermal liquefaction, a large proportion of the starting biomass distributes in the aqueous phase as dissolved organics. It is necessary to identify the nature of these dissolved organics in order to determine any applications of the liquefaction aqueous phase. In order to do this py-GC/MS of the remaining dissolved organics was performed following evaporation of the water

**Figure 8.10** illustrates the influence of temperature on the main volatiles evolved during py-GC/MS of the dried aqueous extracts (DAE). The graph compares the corrected peak intensities based on uniform mass. At 350 °C with no catalyst present, the main products include dianhydromannitol, 1-(2-furanyl)-ethanone (acetylfuran), isosorbide, indole, 3-amino-phenol and 2-cyclopenten-1-one. Dianhydromannitol and 1-(2-furanyl)-ethanone are the main compounds evolved during pyrolysis of mannitol while isosorbide is a heterocyclic compound derived from glucose which is present in the G-chains of laminarin in brown algae. These characteristic peaks indicating the presence of sugars. This indicates the mannitol and laminarin present in brown seaweed are dissolved in the aqueous phase following liquefaction at 350°C. At lower temperatures (250 °C) sugars are not present in the aqueous phase and start to appear at 300 °C and above. The main nitrogen containing compounds identified include indole, pyrrole derivatives and 3-amino-phenol. The 2-cyclopenten-1-one fraction was also large while monoaromatics such as toluene and styrene were also present in the pyrograms from all the dried aqueous extracts. The addition of catalyst reduced the presence of sugars in the aqueous phase and only isosorbide (found in the pyrogram of the DAE from liquefaction with 50% KOH) indicates the presence of sugars. The pyrogram of the aqueous extract obtained by using 100% catalyst showed the evolution of many new compounds including 1, 3-cyclopentadiene, cyclic alkanes and alkenes. This suggests the alkali catalyst is promoting deoxygenation of the sugars.





**Figure 8.10** Effect of liquefaction temperature on the main volatiles evolved during py-GC/MS of the dried aqueous extracts.

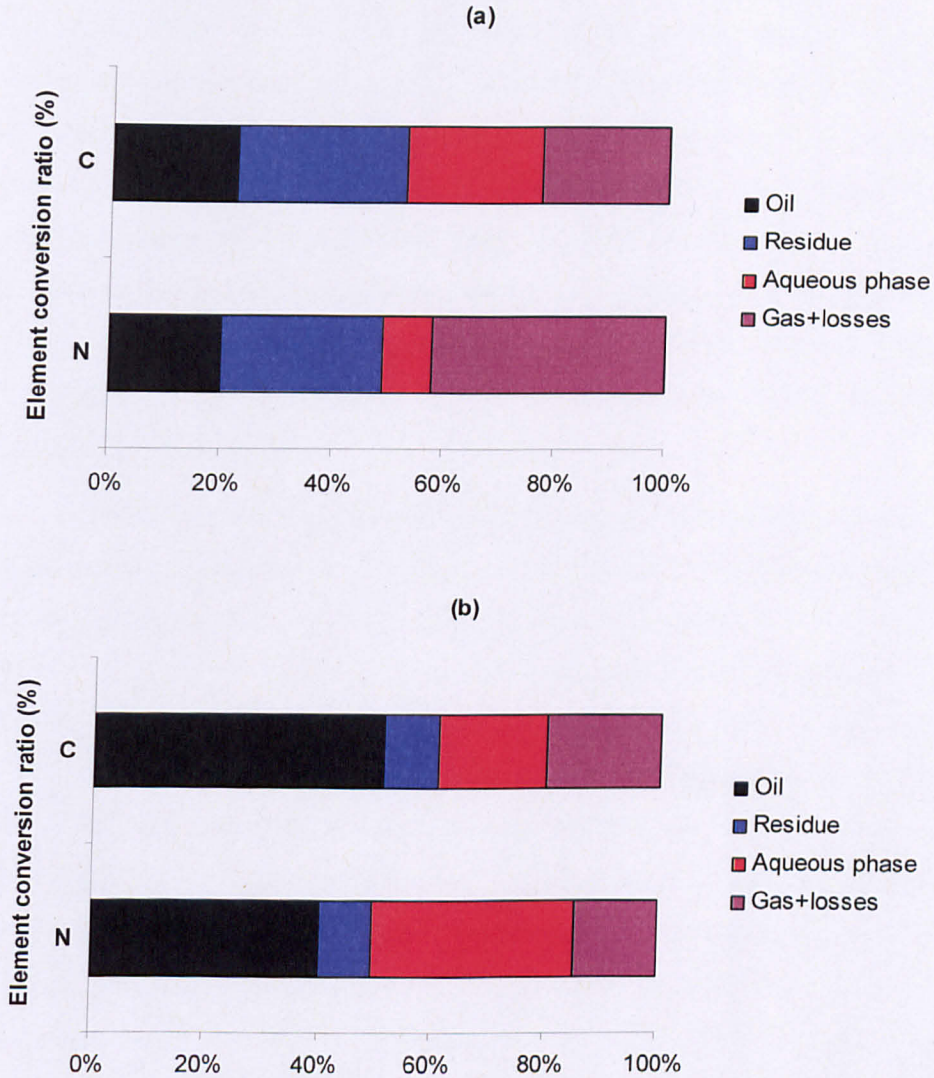
The analysis of the aqueous phase suggests that there are options of further utilizing of the aqueous stream of hydrothermal liquefaction of brown macro-algae. There is evidence of sugars present which may be fermented to produce bio-ethanol as shown by **Horn et al. (2000b)** who produced ethanol from the mannitol and laminarin extracts of *Laminaria Hyperborea*.

### 8.2.5 Elemental balance in product streams

The fate of carbon and nitrogen and its distribution in the product streams is important as it influences the quality of the products. For instance, it is desirable for a fuel to be high in carbon and low in nitrogen in order to minimize  $\text{NO}_x$  formation during combustion. By combining total organic content (TOC) and  $\text{NH}_4$  analysis of the aqueous phase along with CHN content and yields of the bio-crudes and residues, an elemental balance was calculated. The remaining fraction allowed estimation of the carbon and nitrogen content in the gaseous stream and in losses.

An example of an elemental conversion ratio in terms of carbon and nitrogen during hydrothermal liquefaction of brown macro-algae is shown in **Figure 8.11a-b**. Two liquefaction temperatures are given as an example, one

with low bio-crude and high char yield (250°C) and the other with high bio-crude and low char yield (350°C). At 250°C 22wt%, 30.5 wt% and 24.5wt% of the carbon content of the

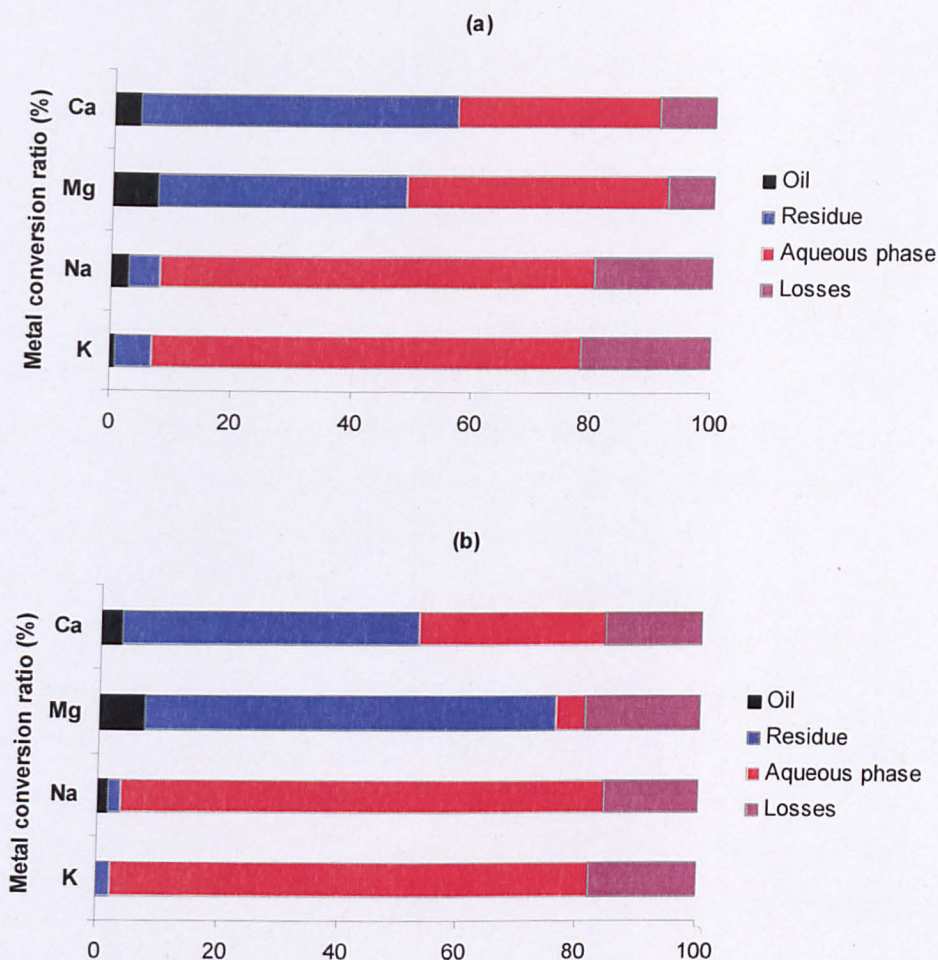


**Figure 8.11** Carbon and nitrogen partitioning in the product streams during hydrothermal liquefaction of 3g seaweed biomass in 30ml of water for 15min residence time at (a) 250°C and (b) 350°C.

original material is passing to the bio-crude, char and aqueous fractions respectively. At 350°C carbon partitioning is increasing in the bio-crude fraction (50wt%) while it is decreasing in the char (10wt%) and aqueous (20wt%) fractions. This is in accordance with higher bio-crude (and higher carbon content

in bio-crude) and lower char (and lower carbon content in the bio-char) and aqueous yields at higher temperature. Nitrogen partitioning follows the same trend with 20wt% of the nitrogen content of the original material passing to the bio-crude fraction, 29wt% in the char fraction and 9wt% passing to the aqueous fraction at 250°C. The low nitrogen content in the aqueous phase is probably attributed to the presence of nitrogen in other forms than  $\text{NH}_4$  at low temperature. At high temperature, the nitrogen partitioning in the bio-crude is increasing (40wt%) while it is decreasing in the char fraction (9wt%). The aqueous phase contains a significant proportion of nitrogen (36wt%) indicating that nitrogen has been converted to  $\text{NH}_4$  at high temperatures. The nitrogen content in the bio-crudes and chars produced was significant when their yields were high making denitrogenation of bio-crude or char a major challenge for hydrothermal liquefaction of macro-algae.

Another important factor is the fate of the mineral matter present in macro-algae during hydrothermal liquefaction. As it was shown in the **characterization chapter (chapter 5)**, macro-algae contain high concentrations of alkali and alkaline earth metals which can cause problems when combusted (**chapter 7**). The fate of these elements was assessed by analyzing the product streams by atomic absorption and a metal balance was calculated (**Figure 8.12a-b**). Again, two liquefaction temperatures are given as an example, one with low bio-crude and high char yield (250°C) and the other with high bio-crude and low char yield (350°C). The distribution of metals at both temperatures shown as in all the different experimental conditions studies was similar. The majority of potassium and sodium is distributed to the aqueous phase while the majority of calcium and magnesium is distributed to the solid residue (char). The low concentration of alkalis in the bio-crude and solid residue fraction makes them combustible without any problems associated with slagging and fouling etc. The significant Ca and Mg content of char is beneficial during combustion as alkaline earth metals have a very high fusion temperature tending to inhibit the eutectic effect of the alkalis (**Miles et al., 1995**).



**Figure 8.12** Alkali and alkaline earth metals partitioning in the product streams during hydrothermal liquefaction of 3g seaweed biomass in 30ml of water for 15min residence time at (a) 250°C and (b) 350°C.

On the other hand, the aqueous phase is rich in K and Na (and nitrogen), which are essential nutrients for plants, and can be recycled back to land as a bio-fertilizer. Calcium and magnesium could also be recycled back either from the aqueous phase or from the solid residue. Ca is a secondary nutrient for the growth of the plants while Mg is very important for photosynthesis. Another application of the aqueous phase could include a recycle solvent for further liquefaction. This concept is the subject of further research. Potassium and sodium carbonates and hydroxides are the most common catalysts used for hydrothermal liquefaction (Demirbas et al., 2000; Karagoz et al., 2006; Minowa et al., 1998; Yang et al., 2004; Zhou et al., 2010 etc.).

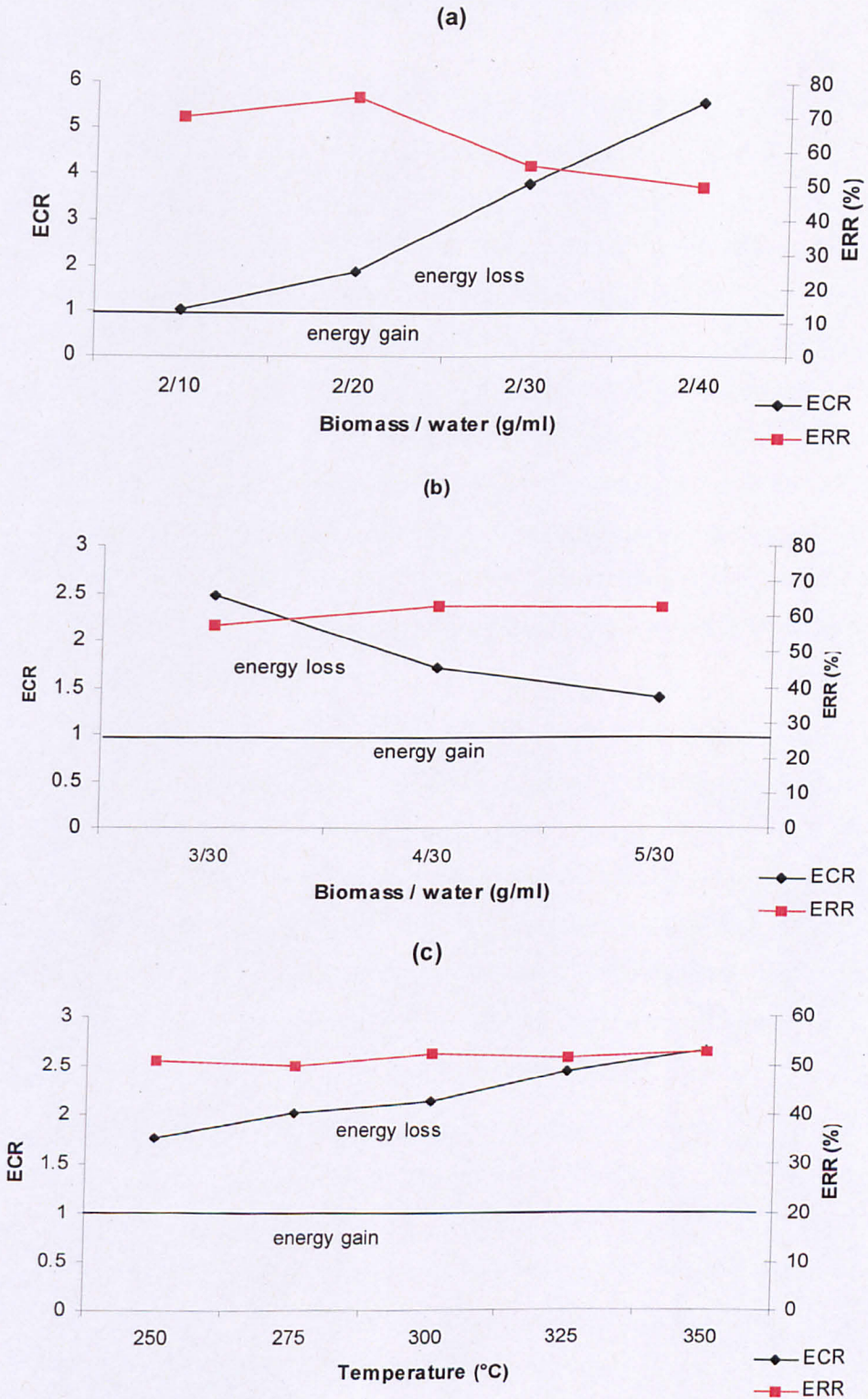
### 8.2.6 Energy balance

During hydrothermal liquefaction of brown macro-algae, the starting material is converted to bio-crude, bio-char, organics in water and gases. It is of interest to evaluate the energy content of the resultant products compared to the energy content of the starting material. In order to do that, the energy recovery ratio (ERR) was used (**eq. 5 in chapter 3**). Only the energy content of the bio-crude and bio-char was considered. This ratio describes the conversion of energy from the starting material to bio-crude and char. In addition, another energy ratio the energy consumption ratio (ECR) (**eq.6 in chapter 3**) was applied in order to study the efficiency of the hydrothermal liquefaction process. Hydrothermal liquefaction is an energy intensive process as it involves heating of water which has very high specific heat capacity. ECR can provide information of energy gain or loss during the hydrothermal liquefaction process. Again only the energy content of the bio-crude and the bio-char was considered. When ECR is lower than 1, then the resultant bio-crude and bio-char have higher energy content than the energy needed for the reaction to occur (heating up the slurry of seaweed and water to the final temperature). When ECR is greater than 1 then there is energy loss, as more energy is spent for the reaction to occur than the energy content of the products.

The two energy ratios were applied for the experimental conditions that were found to have greatest influence on the product yields, i.e biomass loading and temperature (**Figure 8.13a-c**). For low water loading (10 and 20 ml of water) the energy recovery is relatively high at over 70%. Increasing the amount of water in the reactor leads to a gradual reduction in the ERR to 55% in 30 ml of water and 50% in 40 ml of water. This is partially attributed to less closure of the system with increasing water loading as was shown previously (**Figure 8.1**). A similar trend is observed for the ECR. Increasing the amount of water in the reactor increases the ECR. This was anticipated as the increase in the volume of water increases dramatically the required energy for heating, due to its high specific heat capacity. During all the experimental conditions (2/10, 2/20, 2/30, 2/40) ECR was found to be greater than 1 leading to energy loss as more energy is required to heat up the seaweed/water slurry than the available energy of the

resultant bio-crude and bio-char. Only for very low water loading (10ml) was the ECR close to 1, indicating that there is a neutral energy effect. Increasing the biomass loading in 30 ml of water was not found to have a significant influence to the ERR. For 3, 4 and 5 g in 30 ml of water the ERR was close to 60%. This was anticipated as the closure during increasing biomass loading is relatively steady (about 70%). However, increasing biomass loading has a significant effect on ECR. It was found previously that increasing the biomass loading in the same volume of water does not affect the yield of the products. Thus, by increasing the biomass loading there are more available combustible products leading to the decrease of ECR. However, all the experimental conditions studied resulted in an  $ECR > 1$ . The increase in temperature did not have a significant effect on the ERR showing about 50% during all temperatures examined. During the different temperatures studied the closure was relatively steady (about 70%) indicating that the closure of the system is proportional to the energy recovery ratio (ERR). On the other hand, an increase in temperature results in an increase in ECR. The specific heat capacity of water increases significantly with increasing temperature and this is reflected in the results shown in **Figure 8.13c**.

The energy recovery of the system seems to be directly proportional to the closure of the system while high water loading and high temperature have negative effects on the energy balance of the system.



**Figure 8.13** Energy Conversion Ratio (ECR) and Energy Recovery Ratio (ERR) as a function of (a) water loading, (b) biomass loading and (c) temperature.

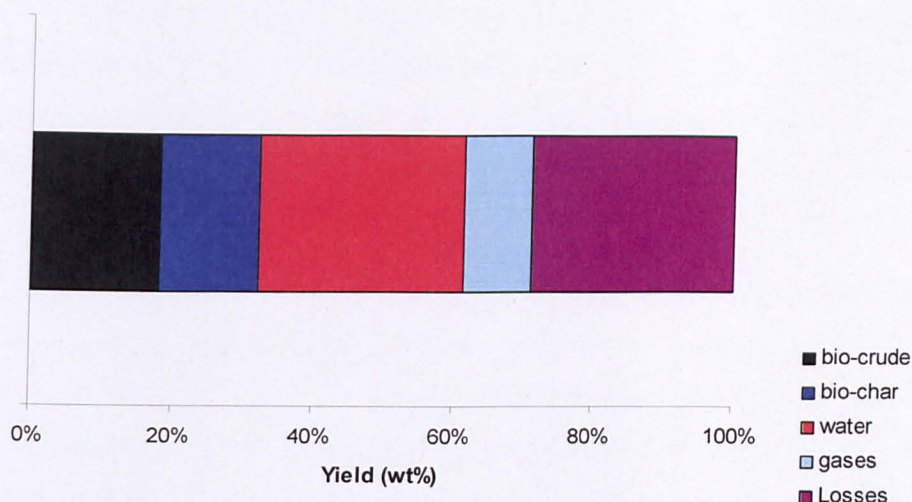
### 8.3 Optimization of reaction conditions for positive energy balance

All the different experimental conditions discussed previously result in a negative energy balance. In this section, an attempt is made to predict the conditions required to obtain a positive energy balance by increasing the biomass loading in the reactor. It was shown before that increasing the biomass loading in the same volume of water results in a lower ECR while the yield of bio-crude remains the same and there is an increase in the low-molecular weight fraction in the bio-crude. These were verified by performing hydrothermal liquefaction of the same sample (*L. saccharina* harvested from Barancarry bay during April of 2008) with increased biomass fed in the reactor and subsequent analysis of the products. 8 g of seaweed biomass and 30 ml of water were fed in the reactor. The reactor was sealed and heated up to 350°C. Reactants were held at this temperature for 15min after which the reactor was cooled down and the resultant products were separated.

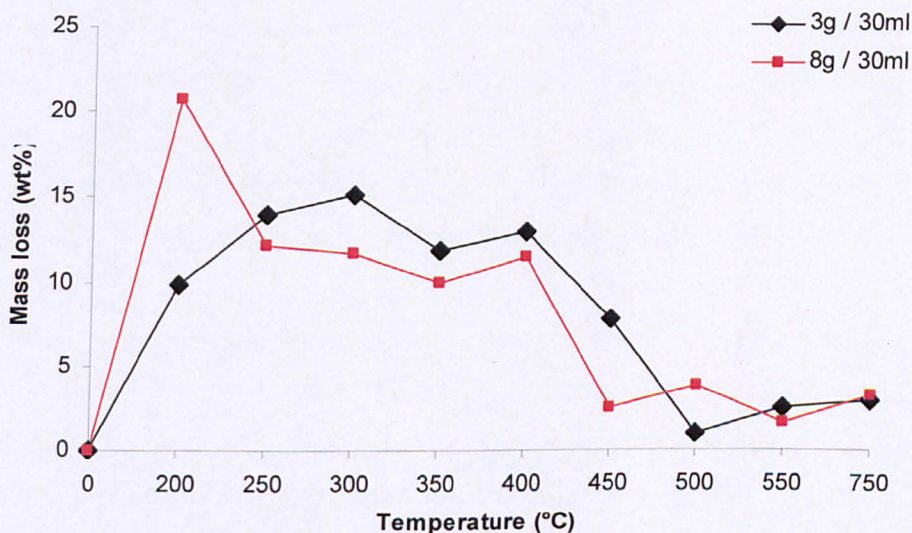
The distribution of the resultant products is shown in **Figure 8.14**. The yields were 19wt%, 15wt%, 31wt% and 10wt% for bio-crude, bio-char, organics in water and gases respectively. Comparing the yields obtained from the hydrothermal liquefaction of 3g of the same sample under the same conditions (19wt%, 11wt%, 26wt% and 16wt% respectively), there is no significant change in product distribution, while the closure of the system was is in both cases about 70%. This verifies the previous statement, that an increase in biomass loading does not have a significant effect on the yields of the resultant products.

The bio-crude obtained (for high biomass loading) had a reduced viscosity from the bio-crudes obtained from previous runs (at low biomass loading) . This was verified by the determination of its boiling point distribution shown in **Figure 8.15**. In this figure, a comparison of the boiling point distribution of bio-crudes obtained from hydrothermal liquefaction of 3g of seaweed and 8g of seaweed under the same conditions is made. A large difference is observed in compounds with <200°C boiling point. The amounts are virtually doubled (20.7wt% compared to 9.9wt%) by increasing the seaweed loading from 3g to 8g.





**Figure 8.14** Products distribution from hydrothermal liquefaction of 8g of *L. saccharina* in 30ml of water at 350°C with 15min RT.



**Figure 8.15** Boiling point distribution of bio-crude obtained from hydrothermal liquefaction of 8g of *L. saccharina* in 30ml of water at 350°C with 15min RT compared to the bio-crude obtained from hydrothermal liquefaction of 3g of *L. saccharina* under the same conditions.

This confirms that increasing the amount of biomass fed to the reactor increases the percentage of compounds with lower MW in the bio-crude. For boiling point temperature ranges greater than 200°C, there was a slight decrease in the mass loss of the bio-crude obtained from liquefaction of 8g of seaweed with the exception of the 450-500°C boiling point range.

However, the bio-crude produced by liquefying 8g of seaweed biomass had a lower heating value than the bio-crude produced by using 3g of seaweed biomass (32.1 compared to 36.5 MJ/kg). **Table 8.5** compares the yields and the ultimate analysis of the bio-crudes and bio-chars obtained by using 3g and 8g of seaweed biomass under the same conditions. The yields for the bio-crudes are expressed on a dry ash free basis (daf) as they are virtually free of ash, while yields for bio-chars are expressed on a dry basis (db). The lower HHV in the bio-crude obtained from 8g of seaweed biomass is mostly due to its lower carbon content and higher oxygen content. The levels of hydrogen and nitrogen remain in the same range between the two bio-crudes. The bio-char showed exactly the opposite trend, with bio-char obtained by liquefying 8g of seaweed biomass having higher yields and HHV, due to its higher carbon content and lower ash content than the bio-char obtained by 3g of biomass. It appears that the carbon content lost from the bio-crude has passed into the bio-char. The energy recovery ratio (ERR) in the bio-crudes and bio-chars obtained by the two different experimental conditions were in similar range (52.8% and 54.7% for 3g and 8g of biomass loading respectively). Although, the big difference between the two experimental conditions is in the energy consumption ratio (ECR). ECR for liquefaction products (bio-crude and bio-char) obtained by 8g of biomass is much lower than that of the products obtained by 3g of biomass (1.01 compared to 2.66 respectively). ECR close to unity means that the products contain as much energy as the energy needed for the reaction, while for values greater than unity, more energy is consumed during the liquefaction process than the energy of the products. This significant reduction in ECR is due to the increase of the biomass loading in the reactor rather than the increase in product yields or product HHVs. With such low bio-crude and bio-char yields, higher amounts of seaweed have to

be fed into the given reactor in order to have an energy gain from the liquefaction process.

**Table 8.5** Yields, proximate, ultimate analysis and energy balance of bio-crudes and bio-chars obtained from hydrothermal liquefaction of 3g and 8g of seaweed biomass in 30 ml of water at 350°C for 15min.

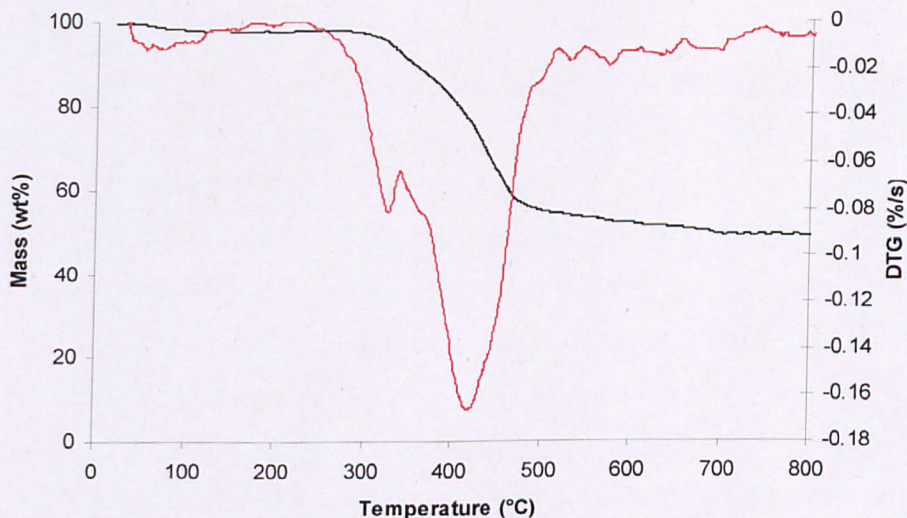
	3g		8g	
	Bio-crude	Bio-char	Bio-crude	Bio-char
<b>Yield (wt%)</b>	19.3	10.9	19	14.8
<b>Moisture<sup>a</sup> (wt%)</b>	-	2.2	-	2.1
<b>Ash<sup>a</sup> (wt%)</b>	2.4	56.7	2.4	49.1
<b>C (wt%)</b>	82	27.5	70.8	35.3
<b>H (wt%)</b>	7.1	2.6	7.7	2.9
<b>N (wt%)</b>	4.9	2.0	4.2	2.1
<b>S (wt%)</b>	n.d.	n.d.	0.7	1.5
<b>O<sup>b</sup> (wt%)</b>	5.4	7.6	14.2	5.1
<b>H/C (daf)</b>	1.04	1.2	1.3	0.97
<b>O/C (daf)</b>	0.05	0.2	0.15	0.11
<b>HHV (MJ/kg)</b>	36.5	10.8	32.1	14.2
<b>ERR (%)</b>	52.8		54.7	
<b>ECR</b>	2.66		1.01	

<sup>a</sup> calculated by TGA

<sup>b</sup> calculated by difference

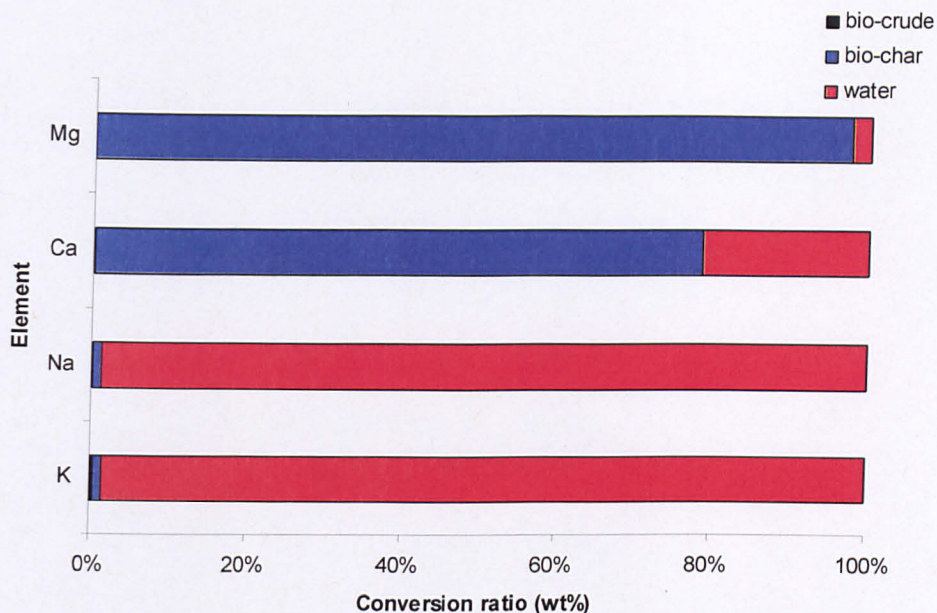
The bio-crude produced from hydrothermal liquefaction is a high heating value fuel virtually ash free that is easy to combust. It was also of interest to see the bio-char behaviour upon combustion. Bio-char from hydrothermal liquefaction of seaweed is a potential secondary (or depending on the conditions main) fuel product as it can be produced in similar or even higher yields than the bio-crude and contains significant heating value.

The bio-char produced from hydrothermal liquefaction of 8g of *L. saccharina* in 30ml of water at 350°C for 15min was analysed by TGA upto a temperature of 800°C under a flow of air at a flow rate of 25°C/min. The TGA and DTG profiles of the char are shown in **Figure 8.16**. The char was found to ignite at 280°C ( $T_i$ ) reaching its maximum reaction rate ( $T_{max}$ ) at 420°C, while burnout of the char was observed at 515°C ( $T_{BT}$ ). These temperature characteristics are important for the design and the development of combustion systems if hydrothermal liquefaction chars are to be used for combustion. The peak temperature ( $T_{max}$ ) is an indicator for the fuel reactivity, with the lower the peak temperature, the higher the fuel reactivity. The temperature characteristics of the combustion of seaweed liquefaction char were found to be similar with those of pyrolysis char of cotton residue as reported by **Kastanaki and Vamvuka (2006)**. At higher temperatures beyond the burnout temperature (insert range) there is a slight weight loss that might be attributed to the decomposition of calcium carbonates. It was shown before that the majority of the calcium present in the seaweed is partitioned in the char, so carbonates are expected to be formed upon combustion.



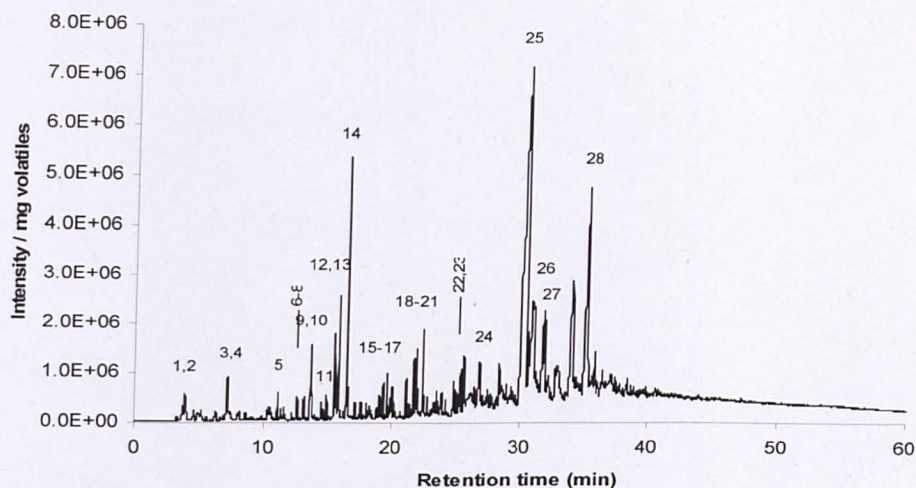
**Figure 8.16** –TGA and –DTG profiles in air (25ml/min) of char produced from hydrothermal liquefaction of 8g of *L. saccharina* in 30ml of water at 350°C for 15min.

It was shown before in **chapter 7** that seaweed biomass is likely to exhibit problems associated with slagging and fouling of the combustion chamber during combustion due to their high alkali metal content. It is therefore of interest to examine the behaviour of the bio-crude and bio-char produced from hydrothermal liquefaction upon combustion. **Figure 8.17** shows the distribution of the main metals present in brown macro-algae (alkali and alkaline earth metals) in the products streams from hydrothermal liquefaction. These results are consistent with previous data that indicated only minimum amounts of the potassium and sodium content of the feedstock are distributed in the bio-crude and in the bio-char. The majority of the K and Na are distributed in the water phase from hydrothermal liquefaction, while the majority of Mg and Ca are distributed in the bio-char. The aqueous phase still contains a significant portion of the calcium content of the starting feedstock. The alkali index (AI) was introduced in order to study the slagging and fouling probability of the bio-crude and bio-char upon combustion. AI for the bio-crude was found equal to  $0.107 \text{ kg}(\text{K}_2\text{O}+\text{Na}_2\text{O})/\text{GJ}$  while AI for the bio-char was found to be  $0.110 \text{ kg}(\text{K}_2\text{O}+\text{Na}_2\text{O})/\text{GJ}$  indicating the safe combustion of the liquefaction products. Fuels with AI lower than  $0.17 \text{ kg}(\text{K}_2\text{O}+\text{Na}_2\text{O})/\text{GJ}$  are safe for combustion. Furthermore, the high concentration in alkaline earth metals (Ca and Mg) in the bio-char could be beneficial upon combustion as they can cause an increase in ash fusion temperature upon combustion inhibiting the opposite effect of the alkalis (**Miles et al., 1995**). Thus, hydrothermal liquefaction of seaweed can be used instead of a pre-treatment process such as alkali washing prior to combustion. It was shown in **chapter 7** that the slagging and fouling probability of seaweed can be reduced by adding a pre-treatment step of acid washing prior to combustion. However, the use of acids in large quantities is both harmful for the environment and expensive. Hydrothermal liquefaction offers an alternative for combustion of liquid (bio-crude) or solid (bio-char) fuels without any use of acids and without any potential danger of the combustion chamber.




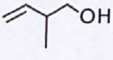
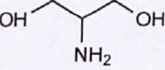
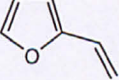
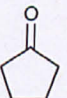
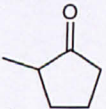
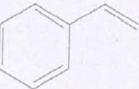
**Figure 8.17** Alkali and alkaline earth metals partitioning in the product streams during hydrothermal liquefaction of 8g seaweed biomass in 30ml of water for 15min residence time 350°C.

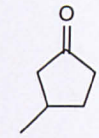
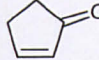
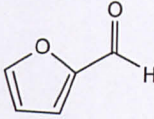
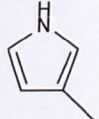
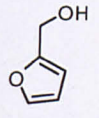
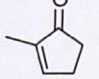
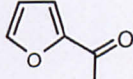
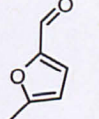
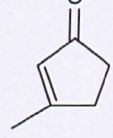
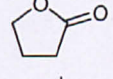
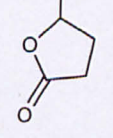
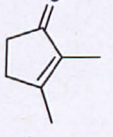
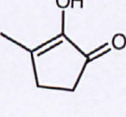
The aqueous phase, apart from containing the largest fraction of metals, also contains a significant fraction of the sugar content of the starting feedstock.. This was confirmed during the 8g loading run by the py-GC/MS of the dried aqueous extract shown in **Figure 8.18**. The highest peaks observed were those of dianhydromannitol, 1-(2-furanyl)-ethanone (acetyl furan) and isosorbide, which are the typical volatiles evolved during the pyrolysis of mannitol and laminarin as was shown in **chapter 4**. Identification of all compounds is presented in **Table 8.6**. The presence of sugars in the aqueous phase can explain the low ERR (energy recovery ratio) in the bio-crude and bio-char (about 55%), as a significant fraction of the seaweed carbohydrates (the sugar fraction) is passing into the aqueous phase. This suggests that the sugars present in brown macro-algae have low (if any) contribution to the formation of the bio-crude and bio-char. Thus, in a wider aspect of seaweed utilization for fuels (bio-refinery), the hydrothermal liquefaction aqueous phase can be utilized for bio-ethanol generation through fermentation. This will increase significantly the energy recovery of the overall process.



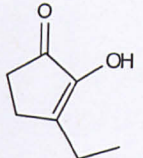
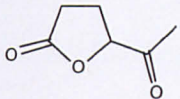
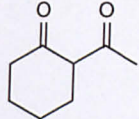
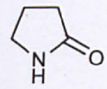
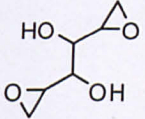
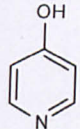
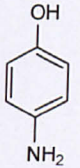
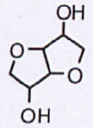
**Figure 8.18** Py-GC/MS chromatogram of dried aqueous extract obtained from hydrothermal liquefaction of 8g of *L. saccharina* in 30ml of water at 350°C for 15 min.

**Table 8.6** Identification of compounds in dried aqueous extract obtained from hydrothermal liquefaction of 8g of *L. saccharina* in 30ml of water at 350°C for 15 min by py-GC/MS.

No	RT	Compound Name	Formula	Structure	MW
1	3.741	Furan	C <sub>4</sub> H <sub>4</sub> O		68
2	3.918	2-methyl-3-Buten-1-ol	C <sub>5</sub> H <sub>10</sub> O		86
3	7.129	2-Amino-1,3-propanediol	C <sub>3</sub> H <sub>9</sub> NO <sub>2</sub>		91
4	7.226	2-Vinylfuran	C <sub>6</sub> H <sub>6</sub> O		94
5	11.127	Cyclopentanone	C <sub>5</sub> H <sub>8</sub> O		84
6	12.651	2-methyl-Cyclopentanone	C <sub>6</sub> H <sub>10</sub> O		98
7	13.082	Styrene	C <sub>8</sub> H <sub>8</sub>		104

8	13.201	3-methyl-Cyclopentanone	$C_6H_{10}O$		98
9	13.667	2-Cyclopenten-1-one	$C_5H_6O$		82
10	13.75	Furfural	$C_5H_4O_2$		96
11	14.971	1H-Pyrrole, 3-methyl-	$C_5H_7N$		81
12	15.564	2-Furanmethanol	$C_5H_6O_2$		98
13	15.848	2-methyl-2-Cyclopenten-1-one	$C_6H_8O$		96
14	16.508	1-(2-furanyl) ethanone	$C_6H_6O_2$		110
15	19.075	5-methyl-2-furancarboxaldehyde	$C_6H_6O_2$		110
16	19.653	3-methyl-2-Cyclopenten-1-one	$C_6H_8O$		96
17	19.98	Butyrolactone	$C_4H_6O_2$		86
18	21.156	2(3H)-Furanone, dihydro-5-methyl-	$C_5H_8O_2$		100
19	21.755	2,3-dimethyl-2-Cyclopenten-1-one	$C_7H_{10}O$		110
20	21.922	2-hydroxy-3-methyl-2-cyclopenten-1-one	$C_6H_8O_2$		112



21	22.449	3-ethyl-2-hydroxy-2-Cyclopenten-1-one	$C_7H_{10}O_2$		126
22	24.827	5-Acetyldihydrofuran-2(3H)-one	$C_6H_8O_3$		128
23	25.405	2-acetyl-Cyclohexanone	$C_8H_{12}O_2$		140
24	26.841	2-Pyrrolidinone	$C_4H_7NO$		85
25	30.538	Dianhydromannitol	$C_6H_{14}O_4$		146
26	30.959	4-Pyridinol	$C_5H_5NO$		95
27	31.838	4-amino-Phenol	$C_6H_7NO$		109
28	35.265	Isosorbide	$C_6H_{10}O_4$		146

## 8.4 Effect of sample composition

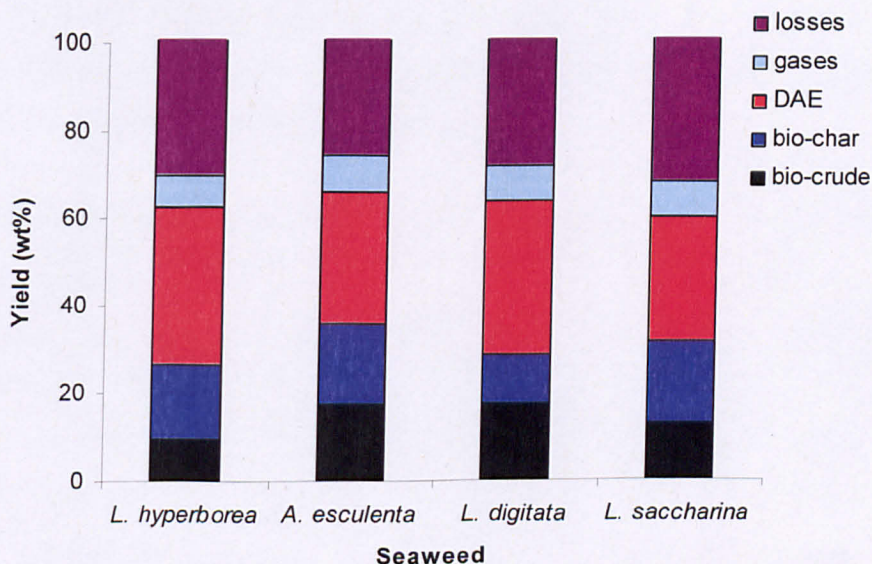
The effect of the sample composition on the liquefaction product yields and properties was investigated in order to understand which of the samples examined performed better in hydrothermal liquefaction. All of the samples used were harvested during summer. It was shown before (**chapters 5, 6 and 7**) that summer and autumn harvested samples have better fuel properties for thermochemical processing and more specifically for pyrolysis and combustion. The samples used were the same as in **sections 6.3 and 7.4** and more specifically

were freeze dried samples of *L. digitata* harvested from Clachan sound, *L. hyperborea* harvested from Easdale, *L. saccharina* harvested from Barancarry and *A. esculenta* harvested from Easdale during the summer of 2009. Their proximate, ultimate and analysis is shown in **Table 8.7**. The conditions used for hydrothermal liquefaction were 8g of seaweed biomass in 30ml of water at 350°C for 15 min holding time.

**Table 8.7** Proximate, ultimate and metal analysis of summer harvested freeze dried samples used for hydrothermal liquefaction experiments

	<i>L. digitata</i>	<i>L. hyperborea</i>	<i>L. saccharina</i>	<i>A. esculenta</i>
<b>Moisture (wt%)</b>	6.6	5.6	6.4	6.8
<b>Ash (wt%)</b>	23.9	16.6	21.8	25.2
<b>C (wt%)</b>	33.1	35.8	32.5	34.6
<b>H (wt%)</b>	4.7	5.1	4.5	4.7
<b>N (wt%)</b>	1.8	1.5	1.1	1.9
<b>S (wt%)</b>	0.8	0.9	0.6	0.6
<b>O (wt%)</b>	33.9	39.1	37.9	31.1
<b>CV (MJ/kg)</b>	13.1	14.2	12.2	13.9
<b>As (ppm)</b>	123	80.3	149	145
<b>B (ppm)</b>	76.5	45.9	68.2	108
<b>Ca (ppm)</b>	4760	2890	11190	10000
<b>Fe (ppm)</b>	35.5	2.9	236	223
<b>K (ppm)</b>	49630	42230	44400	48000
<b>Mg (ppm)</b>	4090	2310	3480	3590
<b>Na (ppm)</b>	44140	20150	26810	35030
<b>Se (ppm)</b>	2.7	2.9	7.3	6.8
<b>Sr (ppm)</b>	344	204	370	534
<b>Zn (ppm)</b>	21.9	5.7	7.3	20.3
<b>Sum (ppm)</b>	103220	67930	86740	97680

**Figure 8.19** shows the yields of the products produced from hydrothermal liquefaction of the different seaweed samples. The bio-crude yields are expressed on a dry ash free (daf) basis while all other yields are on a dry basis. The losses for all samples were found in a similar range close to 30%. *A. esculenta* and *L. digitata* gave the highest bio-crude yields (both 13wt% on dry basis, 17.8wt% and 17.6wt% respectively on daf basis) followed by *L. saccharina* (10wt% on dry basis, 13wt% on daf basis) and *L. hyperborea* (8.1wt% on dry basis, 9.8wt% on daf basis). Samples of *L. hyperborea* shown to have better fuel properties such as lower ash and metal content and higher carbon and hydrogen content resulting in higher calorific value (**Table 8.7**) were found to produce the lowest bio-crude yield. In general the samples with higher metal and ash content (*L. digitata* and *A. esculenta*) gave higher yields than the samples with lower metal and ash content. The bio-crude yields followed the K and Na content of the samples.



**Figure 8.19** Hydrothermal liquefaction product yields of freeze dried summer harvested seaweed samples

K, Na content and the bio-crudes produced from the samples follow the trend *L. digitata* > *A. esculenta* > *L. saccharina* > *L. hyperborea*. Potassium and sodium may be catalysing the reaction as their hydroxides and carbonates are catalysts commonly used during hydrothermal liquefaction of terrestrial biomass. However, seaweed already contain high K and Na content and as was shown in

**section 8.2.1** the increased KOH loading was causing decreased bio-crude yield. This suggests that there is a threshold in potassium or sodium concentration above which they reduce bio-crude formation. Nonetheless this might not be the case for the lower bio-crude yields from the samples of *L. saccharina* and *L. hyperborea*. They might have higher sugar content, which as shown before is passing into the aqueous phase during hydrothermal liquefaction.

**Table 8.8** lists the ultimate analysis and the HHVs of the produced bio-crudes. All the bio-crudes were found to have similar elementary content resulting in similar HHVs (32-34 MJ/kg). However, their oxygen content was higher than the bio-crudes produced at lower biomass loading, resulting in lower HHV than the bio-crudes obtained by using 3g of seaweed biomass (**Table 8.1**). Nonetheless, the material with boiling range <250°C present in the bio-crudes has increased significantly compared to those of lower biomass loading as shown in **Table 8.9**. The bio-crudes fraction with boiling range <250°C ranges between 35wt% and 40wt% for all the samples and is comparable with the typical crude oil's fraction (44.2wt%) (**Speight, 2001**).

**Table 8.8** Ultimate analysis, HHVs and yields of the bio-crudes produced from hydrothermal liquefaction of summer harvested seaweed samples.

	<i>L. digitata</i>	<i>L. hyperborea</i>	<i>L. saccharina</i>	<i>A. esculenta</i>
Yield (wt%) (daf)	17.6	9.8	13	17.8
C (wt%)	70.5	72.8	74.5	73.8
H (wt%)	7.8	7.7	7.9	8
N (wt%)	4.0	3.7	3.0	3.8
S (wt%)	0.7	0.82	0.6	0.8
O* (wt%)	17	14.9	14.0	14.0
HHV (MJ/kg)	32	33	33.9	33.8
H/C	1.32	1.27	1.28	1.3
O/C	0.18	0.15	0.14	0.14

\*calculated by difference

**Table 8.9** Boiling point distribution of bio-crudes obtained from hydrothermal liquefaction of summer harvested seaweed samples.

	<i>L. digitata</i>	<i>L. hyperborea</i>	<i>L. saccharina</i>	<i>A. esculenta</i>
40-200°C	24.64	23.01	19.13	20.78
200-250°C	13.09	16.89	15.78	14.20
250-300°C	13.21	14.96	14.10	14.10
300-350°C	11.29	11.70	11.78	11.83
350-400°C	11.72	9.43	12.78	12.14
400-450°C	5.62	1.62	5.26	5.15
450-500°C	1.03	1.37	0.82	1.35
500-550°C	1.10	3.46	1.17	1.29
>550°C	3.80	4.54	3.86	3.29

The bio-char yields follow the trend *L. saccharina*>*A. esculenta*> *L. hyperborea*> *L. digitata* (18.6wt%, 17.9wt%, 16.7wt% and 10.9wt% respectively). *L. digitata* was found to produce a relatively high bio-crude yield but the bio-char yield was the lowest out of all samples. The rest of the samples had similar bio-char yields with *A. esculenta* having the highest yields of both bio-crude and bio-char. **Table 8.10** lists the proximate and ultimate analysis as well as the HHVs of the bio-chars produced. Unlike the case of bio-crudes, which all have similar fuel properties, the bio-chars were found to significantly differ in their properties. Bio-char produced from *L. hyperborea* has the best fuel properties, with high carbon and low ash contents resulting in very high HHV (26.2 MJ/kg). On the other hand char produced from *L. digitata* has the lowest HHV while chars produced from *L. saccharina* and *A. esculenta* have similar properties and HHV (17.2 and 18.3 MJ/kg respectively).

**Table 8.10** Proximate and ultimate analysis, HHVs and yields of the bio-chars produced from hydrothermal liquefaction of summer harvested seaweed samples.

	<i>L. digitata</i>	<i>L. hyperborea</i>	<i>L. saccharina</i>	<i>A. esculenta</i>
Yield (wt%) (db)	10.9	16.7	18.6	17.9
Moisture <sup>a</sup> (wt%)	3.3	1.9	3.1	3.6
Ash <sup>a</sup> (wt%)	38.6	14.5	33.8	35.1
C (wt%)	39.1	64.2	44.2	45.3
H (wt%)	3.1	4.3	3.1	3.3
N (wt%)	2.2	3.0	1.8	2.3
S (wt%)	2.1	0.6	0.3	0.8
O <sup>b</sup> (wt%)	8.4	9.5	10.7	6.0
HHV (MJ/kg)	15.7	26.2	17.2	18.3
H/C (daf)	0.94	0.80	0.84	0.87
O/C (daf)	0.16	0.11	0.18	0.10

<sup>a</sup> calculated by TGA

<sup>b</sup> calculated by difference

*A. esculenta* was found to produce both bio-crude and bio-char in high yields and with high calorific value, indicating the better performance of this sample under hydrothermal conditions. This is evident by the better energy balance of this specific sample as indicated in **Table 8.11**. This table lists the yields of bio-crudes and bio-chars on a dry basis (db) together with their heating values (HHV) and the calculated energy recovery ratios (ERR) and energy consumption ratios (ECR). *A. esculenta* was found to have the highest ERR (63.84%) indicating that the majority of energy content of the starting feedstock has passed into the bio-crude and bio-char fraction during hydrothermal liquefaction. *L. hyperborea* was the sample with the next higher ERR mostly because of the very high HHV of its bio-char, followed by *L. saccharina* and *L. digitata*. *L. digitata* in spite of having relatively high bio-crude yield, compared to the other samples, had the lowest energy recovery (less than 50%) because of

its very low bio-char yield. The energy consumption ratio (ECR) followed the same trend, being better (lower) for *A. esculenta*, followed by *L. hyperborea*, *L. saccharina* and *L. digitata*. ECR for all samples apart from *L. digitata* was found to be lower than 1 indicating that there is the possibility of net energy production under the given conditions in the given system. ECR for *L. digitata* was found to be greater than 1 indicating that more energy has to be consumed for the heating of the mixture of seaweed with water than the energy content of the resultant bio-crude and bio-char. However, the energy balance was calculated according to the setup of the specific batch reactor. If hydrothermal liquefaction of macro-algae is to be used for mass production of bio-crude and bio-char, a continuous rather than a batch system is going to be used and the energy balance is going to be completely different. Also the heating value of the gases has to be taken into account. As was previously shown, the gases contain hydrogen and methane, two gases with high heating values that can contribute significantly to the overall energy balance. However, this investigation has concentrated on the liquid and solid products from hydrothermal liquefaction rather than the gaseous products. If the gaseous products were taken into account, this would improve the energy balance further.

**Table 8.11** Energy balance for hydrothermal liquefaction products of summer harvested seaweed samples.

	<i>L. digitata</i>	<i>L. hyperborea</i>	<i>L. saccharina</i>	<i>A. esculenta</i>
<b>Bio-crude yield (wt%) (db)</b>	13	8.1	10	13
<b>Bio-crude HHV (MJ/kg)</b>	32	33	33.9	33.8
<b>Bio-char yield (wt%) (db)</b>	10.9	16.7	18.6	17.9
<b>Bio-char HHV (MJ/kg)</b>	15.7	26.2	17.2	18.3
<b>ERR</b>	49.08	58.6	54.77	63.84
<b>ECR</b>	1.098	0.908	0.969	0.844

The organics dissolved in the water follow the trend *L. hyperborea* > *L. digitata* > *A. esculenta* > *L. saccharina* (36.1wt%, 35.4wt%, 30.4wt% and 28.5wt% respectively). A fraction of the aqueous phase was dried and the resultant dried

aqueous extracts were pyrolysed in order to identify the origin of the compounds dissolved in water. The py-GC/MS results (data not shown) revealed the presence of compounds listed on **Table 8.6** for all samples. The highest peaks were again the sugar (mannitol and laminarin) originated volatiles dianhydromannitol, 1-(2-furanyl)-ethanone (acetylfuran) and isosorbide confirming the presence of sugars in the aqueous phase.

Apart from the apparent high fraction of dissolved sugars in the aqueous phase, it also contains the largest fraction of metals present in seaweed. **Figure 8.20a-d** shows the distribution of the main metals present in brown macro-algae in liquefaction product streams. The results are consistent with the majority of potassium and sodium (which are the most abundant metals present in seaweed) present in the aqueous phase and only minimum amounts of them in the bio-char and in the bio-crude. The majority of calcium and magnesium are passing into the bio-char fraction for all the samples apart of *L. hyperborea* (**Figure 8.20b**). For *L. hyperborea* the majority of calcium is passing into the aqueous phase, while magnesium is equally distributed between the bio-char and the aqueous phase.



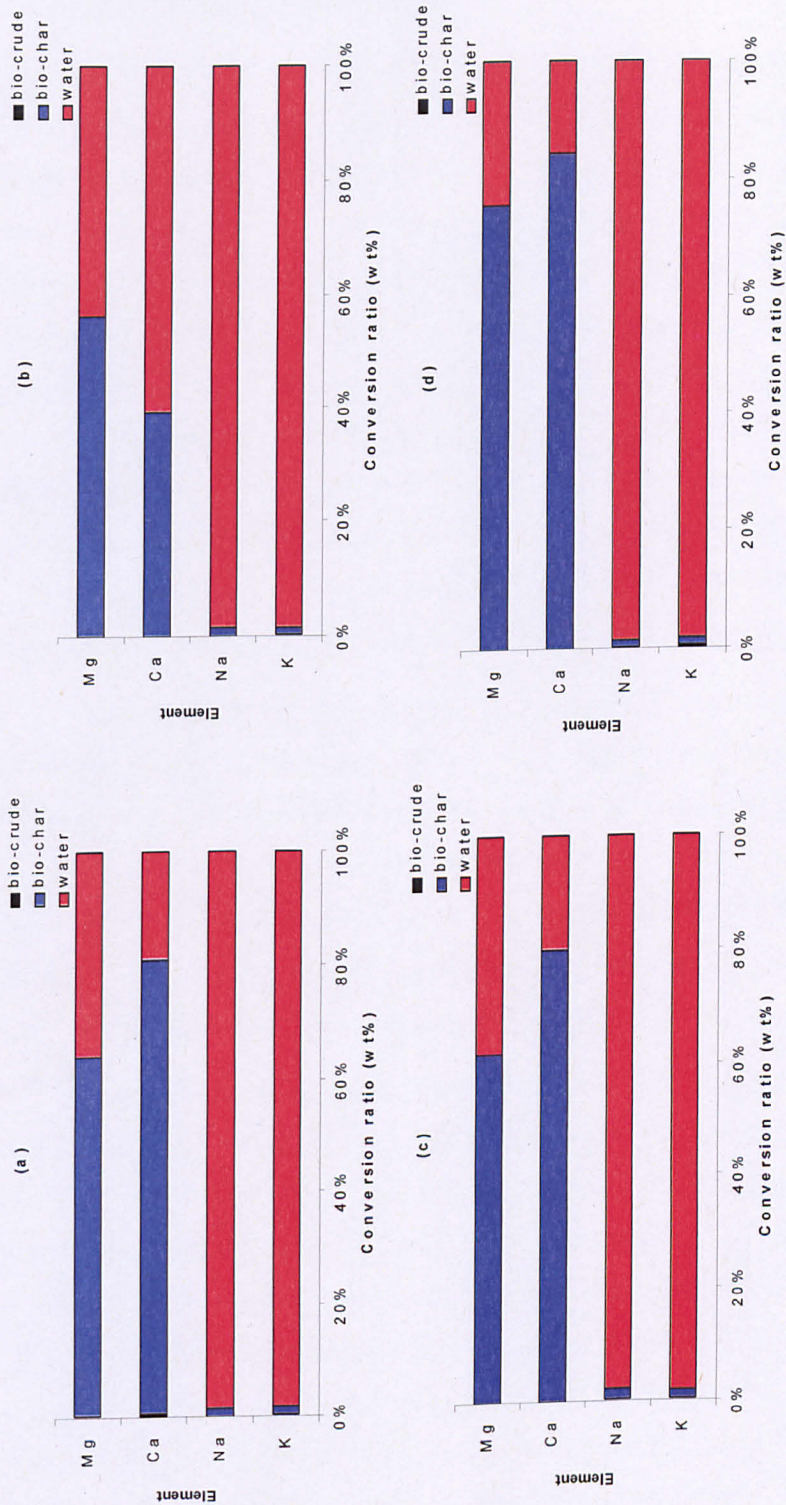


Figure 8.20 Alkali and alkaline earth metals partitioning in the product streams during hydrothermal liquefaction of summer harvested seaweed samples.

## 8.5 Hydrothermal liquefaction of seaweed biomass compared with biological processing

Hydrothermal liquefaction has been successfully demonstrated as a process for producing liquid (bio-crude) or solid (bio-char) fuels from brown macro-algae. Hydrothermal liquefaction was considered as the best thermochemical process for turning macro-algae into energy carriers because of its ability to handle wet feedstock and removing the alkali metals from the combustible products. Combustion of brown macro-algae was shown not to be preferable because of the problems the high alkali content of seaweed is going to create in the combustion chambers. Pyrolysis reactors might experience the same problems due to their high alkaline content. Nonetheless pyrolysis was not considered as a process for fuel production because of the low quality of pyrolysis oil (high water content, high oxygen content, low calorific value, high acidity, etc.) but rather as a process of extracting any valuable chemicals present in the pyrolysis oil.

However, there are other alternative processes for producing energy from seaweed, mainly fermentation and anaerobic digestion. It was of interest to compare how these biological processes compare with hydrothermal liquefaction on energy content of product yields. In order to do that, data from published work by **Horn et al., 2000a; Horn et al., 2000b; Adams et al., 2009** for fermentation of brown macro-algae, as well as data from published work by **Hanssen et al., 1987** for anaerobic digestion of brown macro-algae were used.

**Horn et al., 2000b** used autumn harvested fronds of *L. hyperborea* to extract mannitol and laminarin and subsequently ferment these extracts to produce ethanol. They used 1kg of wet weight of *L. hyperborea* which yielded 20g/l extract (mannitol and laminarin). The best ethanol yield was found to be 0.43g<sub>ethanol</sub>/g<sub>extract</sub> during a batch culture. Assuming a minimum dry weight of 10% of *L. hyperborea* this means that 100g of dry seaweed gave 20g of mannitol and ethanol extract which gave in total  $20 \times 0.43 = 8.6$ g<sub>ethanol</sub>. Thus ethanol yield was 8.6wt%. Ethanol has a HHV of 29.7MJ/kg, so 1kg of seaweed on a dry weight would give 2.554MJ of energy. The authors found that mannitol was the

preferred substrate in batch fermentations while in continuous fermentations laminarin was the preferred one.

In another study by the same author (**Horn et al., 2000a**) they used synthetic mannitol for fermentation to yield a maximum of  $0.38 \text{g}_{\text{ethanol}}/\text{g}_{\text{mannitol}}$ . According to **Black (1950a)** mannitol can reach a maximum content of 30% in seaweed. By assuming this maximum mannitol content, the yield becomes  $0.114 \text{g}_{\text{ethanol}}/\text{g}_{\text{seaweed}}$  (11.4wt%). At this maximum yield and by taking account the HHV of ethanol, 1kg of seaweed on a dry weight would give 3.386MJ of energy if all the mannitol present in the sample could be utilised.

This was the highest ethanol yield produced from fermentation of brown macro-algae found in the literature. **Adams et al., 2009** found lower ethanol yield from fermentation of the brown macro-alga *L. saccharina*. Of course the fermentations in this study were not optimised and the mannitol component was not used. They found maximum ethanol yields of 0.45% v/v. By taking into account the procedure of preparing the substrates and the density of ethanol this translates into  $0.014202 \text{g}_{\text{ethanol}}/\text{g}_{\text{seaweed}}$  (1.42wt%).

In order to make a comparison with hydrothermal liquefaction, the best sample examined (*A. esculenta*) was used. It was shown that bio-crude and bio-char produced by hydrothermal liquefaction of *A. esculenta* had the best energy recovery ratio and energy consumption ratio. The actual weight of the bio-crude produced was  $0.97 \text{g}_{\text{bio-crude}}/8 \text{g}_{\text{seaweed}}$  (12.1wt%) with HHV of 33.81MJ/kg translating into  $121.5 \text{g} \times 33.81 \text{MJ/kg} = 4.1 \text{ MJ}$  of energy from the bio-crude if 1kg of seaweed on a dry weight was to be used. In addition to the bio-crude,  $1.34 \text{g}_{\text{bio-char}}/8 \text{g}_{\text{seaweed}}$  (16.8wt%) with HHV of 18.34MJ/kg translating into  $167.5 \text{g} \times 18.34 \text{ MJ/kg} = 3.07 \text{ MJ}$  of energy from the bio-char if 1kg of seaweed on a dry weight was to be used, was also produced. This makes a total of 7.17MJ of energy in the liquid (bio-crude) and solid (bio-char) products from hydrothermal liquefaction if 1kg (dry weight) of seaweed was used as the starting material. Thus, energy output from hydrothermal liquefaction of brown macro-algae is better than the energy output of fermentation of brown macro-algae. This was expected as fermentation utilises only the sugar fraction present in seaweed. However, the

energy input is higher for hydrothermal liquefaction and this has to be taken into account as well.

The other possibility for energy generation from brown macro-algae is through anaerobic digestion. **Hanssen et al., 1987** investigated the biogas production from three brown macro-algae (*L. hyperborea*, *L. saccharina* and *A. nodosum*) and found maximum methane yield of 0.28 l<sub>CH<sub>4</sub></sub>/g<sub>VS</sub> during semicontinuous cultures of *L. hyperborea*. The yield was expressed in volatile solids (VS), the percentage of which in the sample used was unusually high for brown seaweed (77.5%). By taking into account this volatile solid content, the methane yield becomes 0.217 l<sub>CH<sub>4</sub></sub>/g<sub>seaweed</sub>. By taking into account the density (0.68kg/m<sup>3</sup>) and the HHV of methane (55.5MJ/kg), if 1kg of seaweed was to be used, the energy output of the resultant methane would be 8.189MJ. This energy output is slightly higher than the one for liquefaction previously shown (7.17MJ). However, the energy content of the gases during hydrothermal liquefaction was not taken into account. Also as it was shown previously, a large fraction of the sugars pass in the aqueous phase during hydrothermal liquefaction offering the possibility of further energy generation through the fermentation of the dissolved sugars into ethanol. During anaerobic digestion, the mannitol fraction is used for biogas generation as mannitol and alginates are the most biodegradable carbohydrates during anaerobic digestion (**Gunaseelam, 1997**). It would be of interest to examine the potential of producing bio-crude or bio-char from the digestate of anaerobic digestion in order to combine the two processes for increasing the energy output.

To conclude hydrothermal liquefaction of brown macro-algae gives higher energy output than fermentation and similar but lower energy output than anaerobic digestion. Of course the energy input for hydrothermal liquefaction is higher so the design of the hydrothermal system has to be carefully chosen (e.g. continuous system for better energy balance). However, in a bio-refinery concept where fermentation can utilise the sugars present in the aqueous phase from hydrothermal liquefaction, the energy output of the whole process can potentially be higher than the energy output of anaerobic digestion alone.

## 8.6 Conclusions

Hydrothermal liquefaction of seaweed produces relatively low yields of bio-crude which contain high levels of nitrogen posing a major challenge for utilization for the production of biofuels and bio-energy. Final temperatures of above 300°C are needed in order to obtain maximum yields of bio-crude. The holding time at maximum temperature was found to have a minimal effect on product distribution. The increase in the amount of seaweed fed into the reactor had a large influence on the bio-crude quality, as the fraction of the bio-crude with boiling point <250°C was increased. The HHV of the bio-crude is increased compared to the original seaweed and the oxygen content is significantly lowered. Depending on the conditions used, the bio-crude can contain a fraction of compounds with boiling point <250°C close to that of crude oil, indicating the possibility of getting a variety of different distillate fuels (lighter and heavier). Bio-char can be produced in similar or even higher yields than the bio-crude. The produced bio-char can have a significant heating value. The majority of the alkali metals are distributed in the aqueous phase and therefore the problems associated with slagging and fouling would be significantly reduced if the bio-crude and the bio-char were burnt to produce bio-energy. The energy recovery in the bio-crude and bio-char was relatively low (50-65%) mostly because there is a significant fraction of sugars that is passing in the aqueous phase during hydrothermal liquefaction. Because hydrothermal liquefaction is an energy intensive process and the bio-crude and bio-char yields from liquefaction of seaweed are relatively low, high seaweed biomass loading is needed in order to have a positive energy balance on the given reactor. Bio-crude and bio-char from *A. esculenta* were found to have the highest energy recovery and the lower energy consumption indicating the better performance of this specific type of seaweed under hydrothermal conditions. When compared to biological processes of brown macro-algae (fermentation and anaerobic digestion), hydrothermal liquefaction has higher energy output than fermentation and a slightly lower energy output than anaerobic digestion. However, the aqueous phase from hydrothermal liquefaction can be utilized for ethanol production leading to potentially higher energy output than anaerobic digestion.

## **CHAPTER 9 - Summary of conclusions and future research**

### **9.1 Introduction**

The work in this thesis has investigated the possibility of producing energy or chemicals from brown macro-algae through thermochemical processes. A variety of different kinds of brown kelps harvested quarterly each year from different locations were used in order to assess this possibility through three different thermochemical processes, pyrolysis, combustion and hydrothermal liquefaction. A variety of different laboratory techniques and analysis were used in order to achieve this. This chapter aims to bring together the main findings of this investigation and discuss any additional future research to provide better understanding on how brown macro-algae can contribute to the bio-energy sector.

### **9.2 Conclusions**

#### **9.2.1 Variations in seaweed fuel properties**

Processing and storing of wet harvested seaweed samples is very important as it can affect their bio-chemical composition. During drying, as the water is removed from the aquatic plants it extracts a sugar (mannitol and possibly laminarin) fraction present in brown macro-algae. This extracted material should be collected and utilised among the rest of plant material. The amount of dry weight present varies between 10 and 20wt% of the wet weight.

Different parts of the plant material have significant differences in composition. The stipes of seaweed are perennial while the blades are renewed. This helps in the accumulation of metals in the stipes leading to higher inorganic content and higher ash content compared with the blades of the plants. The main metal present in brown macro-algae (in both blades and stipes) is potassium followed by sodium, calcium and magnesium. Potassium content is directly linked with the ash content of macro-algae with increased potassium intake leading to increases ash content. This higher inorganic content reflects to lower

carbon and hydrogen content in the stipes leading to less volatile matter and less calorific value of the stipes. Thus, stipes of brown macro-algae are less attractive than their blades for energy generation through thermochemical processes.

Of course, if macro-algae are going to be used on a large scale for energy generation, the whole plant material is probably going to be used. The whole plant material exhibits significant variations in composition depending on the inhabit location and on the season. Inhabitants in narrow sea passages such as canals or straits are richer in inorganic material and ash which has negative effect on their fuel properties such as lower carbon and hydrogen content leading to lower calorific value and volatile matter. Such narrow sea paths, help in the accumulation of more metals from natural deposits or land drainage, as refreshing of seawater is occurring at a lower rate than in open sea. Thus, cultivation of macro-algae in the open sea is preferable as it leads to better fuel properties.

Macro-algae bio-chemical composition undergoes significant changes throughout the year affecting their properties as fuel. During winter and spring the ash, inorganic and nitrogen content are at their maximum, while minimum carbon content occurs for the same period. On the other hand, during summer and early autumn the opposite trend is observed. Ash, metal and nitrogen content are at their minimum while carbon reaches its maximum content. Accordingly, during this period calorific value and volatile matter content reach their maximum content. Summer and early autumn harvest of brown-macro-algae is preferred for thermochemical processes.

Summarizing, the main conclusions, harvesting of brown macro-algae for thermochemical processing is preferable during summer and early spring from sites open to the sea. The solid material that is extracted during drying of seaweed should be utilised with the rest of plant material.

### 9.2.2 Pyrolysis of brown macro-algae

Pyrolysis of brown macro-algae is linked with the pyrolysis behaviour of their carbohydrates. The devolatilisation of different parts of the plant material (blades and stipes) follow the same degradation pathway, however, more volatile matter is evolved during pyrolysis of the blades reflecting their proximate and ultimate differences with the stipes. The main devolatilisation stage which occurs between 200°C and 350°C is happening in two distinct steps due to the different temperature region in which each of the seaweed's carbohydrates is decomposing. For the first step, which is attributed to the decomposition of alginic acid and fucoidan, maximum conversion rate occurs between 260°C and 270°C. Maximum conversion rate for the second step occurs between 310°C and 330°C and is attributed to the decomposition of mannitol and laminarin. Winter harvested samples have more volatile matter evolved during the first decomposition step while summer harvested samples during the second decomposition step following the winter peak in alginic acid content and the summer peak in sugar (mannitol and laminarin) content.

The main volatiles evolved during pyrolysis of brown macro-algae originated from their different carbohydrates and protein. The dominant products appear to be dianhydromannitol, phytol, 1-(2-furanyl)-ethanone, indole, 2-hydroxy-3-methyl-2-cyclopenten-1-one, furfural and toluene among others. A variety of these compounds present in the flash pyrolysis oil could have industrial applications as they can be used as solvents, as intermediates for the synthesis of pharmaceuticals and carbohydrates, medicines, dyes, agrochemicals, perfumes etc. Such compounds include dianhydromannitol, isosorbide phytol, furfural and other furan derivatives, acetic acid, toluene, indole and pyrrole derivatives, thiophene among others. The concentration of these compounds in the pyrolysis oil undergoes a seasonal variation similar to that of bio-chemical changes in composition of brown macro-algae. For example dianhydromannitol appears to be in higher concentration during summer when the mannitol content reaches its maximum concentration while indoles and pyrroles appear to be in higher concentration during spring when the protein content of seaweed is at its



maximum. Depending on the target compound, optimization of the harvest period can be made in order to maximize its concentration.

### **9.2.3 Combustion and demineralization of brown macro-algae**

The calorific value of brown macro-algae is the important factor when considering combustion as it is a non selective process where a certain bio-polymer is converted. During combustion all the available volatile matter is turned into gases. The calorific value of brown macro-algae reaches its maximum content during summer early autumn, so harvesting of brown macro-algae during this specific period is preferred if seaweed are to be combusted. However, the inorganic content of seaweed biomass ash is high enough even in the summer and autumn period to create problems associated with slagging and fouling of the combustion chamber upon combustion. This fouling tendency is projected throughout the growing cycle of brown macro-algae, although it is smaller during summer and early autumn. This suggests that brown macro-algae cannot be used for combustion in the current power plants without causing problems in the combustion chamber.

Thus, if brown macro-algae are to be used for combustion, the majority of their inorganic content has to be removed prior to combustion. Washing of seaweed in hot water removes a significant portion of this inorganic material but their predicted behaviour is still associated with slagging and fouling. This is overcome by washing of seaweed with acid prior to combustion. Washing in acid removes the majority of mineral matter present in macro-algae and leads to safe combustion predictions. However, the use of acids on a large scale could have serious environmental implications as well as increasing significantly the cost of the overall process. This cost however can be subsidised by the utilization of certain seaweed bio-polymers that are being removed during the washing process. Washing in acid, apart from removing the majority of mineral matter removes two of brown macro-algae bio-polymers, mannitol and fucoidan. Mannitol can be used as a feedstock for the production of bio-ethanol through fermentation while fucoidan is a chemical used for its anticoagulant, antioxidant, and antiviral properties as well as in cosmetics.

#### 9.2.4 Hydrothermal liquefaction of brown macro-algae

Hydrothermal liquefaction is a process that can produce liquid (bio-crude) and solid (bio-char) fuels from brown macro-algae. Unlike other thermochemical processes it is a wet process so no additional drying step is needed. Also, it is able to handle feedstocks with high inorganic content such as brown macro-algae. The bio-crude produced from hydrothermal liquefaction of brown macro-algae has high heating value and can contain a significant fraction of low molecular weight compounds similar to crude oil. This indicates the possibility of getting a variety of different distillate fuels (lighter and heavier). However, the bio-crude contains significant nitrogen content posing a major challenge for utilising. The bio-char produced can have significant heating value similar to that of coal depending on the experimental conditions. The produced chars have very low alkali metal content indicating their safe combustion in existing power plants. This indicates their possible application as a fuel in power plants possibly through co-firing.

However, yields and consequently energy recovery of both bio-crude and bio-char are relatively low. So in order to get a positive energy balance, higher seaweed biomass loading has to be used. Low biomass loading and low temperature favours the formation of bio-char while high biomass loading and high temperatures favour the formation of bio-crude. The sample with the best performance under hydrothermal conditions, as it has the best energy recovery and energy consumption, is *Alaria Esculenta*.

The aqueous phase produced from hydrothermal liquefaction of brown macro-algae contains the majority of the alkali metals (potassium and sodium) and a significant nitrogen content of the starting material. This suggests its possible use as fertiliser in order to recycle essential nutrients back to the ecosystem. The aqueous fraction was also found to contain significant portion of the sugars (mannitol and possibly laminarin) present in brown macro-algae. This suggests another possible application of the aqueous phase as a feedstock for bio-ethanol through fermentation.

Hydrothermal liquefaction seems the most suitable of the thermochemical processes for utilising brown macro-algae for bio-energy. It has a lower but

similar energy output with anaerobic digestion which is the preferable, on an energy basis, biological process for utilising seaweed for bio-energy.

There are two main pathways with which seaweed can be best utilized in terms of thermo-chemical conversion to power and fuels. The first route is to pre-treat seaweed in order to extract valuable chemicals (e.g. alginates, mannitol, fucoidan, laminarin etc.) and reduce their inorganic content in preparation for combustion for power generation in a bio-refinery concept. The second route is to first process them by hydrothermal liquefaction, and then further utilize the product streams in order to produce fuels and chemicals again in a bio-refinery concept.

### 9.3 Future research

This investigation has provided a basic understanding of the behaviour of brown macro-algae in thermochemical processes. However, it was more a feasibility study as utilisation of seaweed through thermochemical processes is a recently new concept. Further investigation could contribute to the understanding of brown macro-algae behaviour in thermochemical media. Several angles could be brought into investigation.

In chapter 4, an examination of the thermal behaviour of the macro-algae carbohydrates was made. In order to gain a complete representation of the whole macro-alga plant material thermal studies on algal cellulose and protein could be conducted.

In chapter 5, the thermochemical properties of wild macro-algae harvested during different periods and from different locations were analysed. A similar investigation of cultivated macro-algae could be made in order to have a more accurate representation of their variations in their properties. Harvesting of wild macro-algae might not lead in completely accurate conclusions as each harvested sample might be of a different age.

In chapter 6, the analytical pyrolysis experiments revealed the presence of some valuable compounds in the pyrolysis oil. A techno-economic assessment of extracting some of these compounds from the bio-oil could be conducted.

In chapter 7, it was shown that the high alkali metal content of macro-algae ash is going to lead into fouling and slagging of the fuel in a combustion chamber unless being previously demineralised. It would be of interest to conduct ash fusion tests on macro-algae samples before and after demineralization in order to project ash behaviour during combustion.

In chapter 8, it was demonstrated the potential of production of fuels through hydrothermal liquefaction of macro-algae. However, the yields of both bio-crude and bio-char were relatively low and they both contain significant nitrogen content. It would be of interest to examine various catalysts during liquefaction in order to increase bio-crude and/or bio-char yields and decrease their nitrogen content. It would also be of interest to distillate the bio-crude in

order to get different fuel fractions. Also the aqueous phase was shown to contain significant amounts of sugars. It would be of interest to quantify this sugar content and to examine their ability in fermentation in order to get additional fuel. Finally it was shown that hydrothermal liquefaction is an energy intensive process. Various aspects could be examined in order to improve the overall energy balance. One could be the development of a small scale continuous hydrothermal liquefaction reactor. In a continuous system the energy balance is going to differ as the energy requirements and the design of the system are significantly different than batch reactors. Another aspect that could be examined is the possibility of producing bio-char as the main fuel product through hydrothermal carbonization. Hydrothermal carbonization occurs at significantly lower temperature than hydrothermal liquefaction so the energy input for the process would be much less.

## Bibliography

Adams, J.M., Gallagher, J.A., Donnison, I.S., 2009. Fermentation study on *Saccharina latissima* for bioethanol production considering variable pre-treatments. *Journal of Applied Phycology* 21, 569-574.

Adams, J.M.M., Ross, A.B., Anastasakis, K., Hodgson, E.M., Gallagher, J.A., Jones, J.M., Donnison, I.S., 2011. Seasonal variation in the chemical composition of the bioenergy feedstock *Laminaria digitata* for thermochemical conversion. *Bioresource Technology* 102, 226-234.

Ajanovic, A., 2011. Biofuels versus food production: Does biofuels production increase food prices? *Energy* 36, 2070-2076.

Akdeniz, F., Gundogdu, M., 2007. Direct and alkali medium liquefaction of *Laurocerasus officinalis* Roem. *Energy Conversion and Management* 48, 189-192.

Anastasakis, K., Ross, A.B., 2011. Hydrothermal liquefaction of the brown macro-alga *Laminaria Saccharina*: Effect of reaction conditions on product distribution and composition. *Bioresource Technology* 102, 4876-4883

Anastasakis, K., Ross, A.B., Jones, J.M., 2011. Pyrolysis behaviour of the main carbohydrates of brown macro-algae. *Fuel* 90, 598-607.

Anastasakis, K., Saunders, H., Jones, J.M., Ross, A.B., 2010. Predictive fouling behaviour of seaweed ash during combustion. BIOTEN conference.

Andrade, L.R., Salgado, L.T., Farina, M., Pereira, M.S., Mourao, P.A.S., Filho, G.M.A., 2004. Ultrastructure of acidic polysaccharides from the cell walls of brown algae. *Journal of Structural Biology* 145, 216-225.

Apell, H.R., 1967. Fuels from waste, in: Anderson, L., Tilman, D.A., (Eds.). . Academic Press, New York: Academic Press., pp.

## Bibliography

Aresta, M., Dibenedetto, A., Barbeiro G., 2005. Utilization of macro-algae for enhanced CO<sub>2</sub> fixation and biofuels production: Development of a computing software for an LCA study. *Fuel Processing Technology* 86, 1679-1693.

Bae, Y.J., Ryu, C., Jeon, J.K., Park, J., Suh, D.J., Suh, Y.W., Chang, D., Park, Y.K., 2011. The characteristics of bio-oil produced from the pyrolysis of three marine macroalgae. *Bioresource Technology* 102, 3512-3520.

Barahona, T., Chandia, N.P., Encinas, M., Matsuhiro, B., Zuniga, E.A., 2011. Antioxidant capacity of sulfated polysaccharides from seaweeds. A kinetic approach. *Food Hydrocolloids* 25, 529-535.

Beavis, A., Charlier, R.H., 1987. *An economic appraisal for the onshore cultivation of Laminaria spp.* *Hydrobiologia* 151/152, 387-398.

BeMiller, J.N., 2001. Plant Gums. *Encyclopedia of life sciences*. John Wiley & Sons.

Berteau, O, Mulloy B., 2003. Sulfated fucans, fresh perspectives: structures, functions, and biological properties of sulphated fucans and an overview of enzymes active toward this class of polysaccharide. *Glycobiology* 13, 29R-40R.

Bichat, M.P., Raymundo-Pinero, E., Beguin, F., 2010. High voltage supercapacitor built with seaweed carbons in neutral aqueous electrolyte. *Carbon* 48, 4351-4361.

Biller, P., Ross, A.B., 2011. Potential yields and properties of oil from the hydrothermal liquefaction of microalgae with different biochemical content. *Bioresource Technology* 102, 215-225.

Black, W.A.P., 1950a. The seasonal variation in weight and chemical composition of the common British *laminariaceae*. *Journal of the Marine Biological Association UK* 29, 45-72.

Black, W.A.P., 1950b. The seasonal variation in the cellulose content of the common Scottish *laminariaceae* and *fucaceae*. *Journal of the Marine Biological Association UK* 29, 379-387.

## Bibliography

- Black, W.A.P., 1954. Concentration gradients and their significance in *laminaria saccharina (L.) lamour*. Journal of the Marine Biological Association UK 33, 49-60.
- Bold, H.C., Wynne M.J., 1978. Introduction to the Algae, structure and reproduction. Prentice-Hall, Englewood Cliffs, New Jersey.
- Bridgwater, A.V., 2004. Biomass Fast Pyrolysis. Thermal Science 8, 21-49.
- Bridgwater, A.V., Peacocke, G.V.C., 2000. Fast pyrolysis processes for biomass. Renewable and Sustainable Energy Reviews 4, 1-73.
- Brown, T.M., Duan, P., Savage, P.E., 2010. Hydrothermal liquefaction and gasification of *Nannochloropsis* sp. Energy Fuel 24, 3639–3646.
- Bruton, T., Lyons, H., Lerat, Y., Stanley, M., Rasmussen, M.B., 2009. A review of the potential of marine algae as a source of biofuel in Ireland. A report prepared for Sustainable Energy Ireland.
- Buck, B.H., Walter, U., Rosenthal, H., Neudecker, T., 2006. The development of mollusc farming in Germany: past, present and future, World Aquaculture, 37, 6-11, 66-69.
- Carlsson, A.S., van Beilen, J.B., Moller, R., Clayton, D., 2007. Micro- and macro- algae: utility for industrial applications. Outputs from the EPOBIO project, CNAP, University of York.
- CEWEP, 2009, The renewable energy contribution from waste across Europe, Confederation of European Waste-to-Energy Plants, [Online], [Accessed 18 January 2011], from World Wide Web:  
[http://www.cewep.com/storage/med/media/energy/283\\_Renew\\_Energy\\_Europe\\_JM\\_7.pdf](http://www.cewep.com/storage/med/media/energy/283_Renew_Energy_Europe_JM_7.pdf).
- Channiwala, S.A., Parikh, P.P., 2002. A unified correlation for estimating HHV of solid, liquid and gaseous fuels. Fuel 81, 1051-1063.
- Chapman, V.J., 1970. Seaweeds and their uses. The Camelot Press Ltd, London and Southampton, Second edition.



## Bibliography

- Chizhov, A.O., Dell, A., Morris, H.R., Reason, A.J., Haslam, S.M., McDowell, R.A, Chizhov, O.S., Usov, A.I., 1998. Structural analysis of laminarans by MALDI and FAB mass spectrometry. *Carbohydrate Research* 310, 203-210.
- Choi, J.H., Choi, J.W., Suh, Y.W., Song, K.W., Suh, D.J., 2011. Feasibility of *Laminaria japonica* as a feedstock for fast pyrolysis in a bubbling fluidized-bed reactor. *Bioresource Technology*
- Chynoweth, D.P., 2002. Review of biomethane from marine biomass. Department of Agricultural and Biological Engineering, University of Florida.
- Collicec, S., Fischer, A.M., Tapon-Brethaudiere, J., Boisson, C., Durand, P., Jozefonvicz, J., 1991. Anticoagulant properties of a fucoidan fraction. *Thrombosis Research* 64, 143-154.
- Darvell, L.E., Jones, J.M., Gudka, B., Baxter, X.C., Saddawi, A., Williams, A., Malmgren, A., 2010. Combustion properties of some power station biomass fuels. *Fuel* 89, 2881-2890.
- Darwin oceanics, 2008. *Ingredients & Spa Products: Laminaria digitata*.
- Davis, T.A., Volesky, B., Mucci, A., 2003. A review of the biochemistry of heavy metal biosorption by brown algae. *Water Research* 37, 4311-4330.
- Demirbas, A., 2000. Effect of lignin content on aqueous liquid products from biomass. *Energy Conversion and management* 41, 1601-1607.
- Demirbas, A., 2001. Biomass Resource Facilities and biomass conversion processing for fuels and chemicals. *Energy conversion and management* 42, 1357-1378.
- Demirbas, A., 2004. Combustion characteristics of different biomass fuels. *Progress in Energy Combustion Science* 30, 219-230.
- Demirbas, A., 2004. Current Technologies for the thermo-conversion of biomass into fuels and chemicals. *Energy Sources* 26, 715-730.
- Demirbas, A., 2005. Thermochemical conversion of biomass to liquid products in the aqueous medium. *Energy sources* 27, 1235-1243.

## Bibliography

Demirbas, A., Caglar, A., Akdeniz, F., Gullu, D., 2000. Conversion of olive husks to liquid fuel by pyrolysis and catalytic liquefaction. *Energy Sources* 22, 631-639.

Dickinson, C.I., 1963. *British Seaweeds*. Butler and Tanner LTD.

Drew, G.H., 1910. The Reproduction and early Development of *Laminaria digitata* and *Laminaria saccharina*. *Annals of Botany* 14, 177-190.

Drewette, A., Dwyer, S., Farrell, V., Miller, A., 2003. Biofuels for transport. Energy Systems Research Unit (ERSU), University of Strathclyde.

DTI, 2007, Meeting the Energy Challenge, A White Paper on Energy, Department of Trade and Industry, [Online], [Accessed 15 January 2011], from World Wide Web: [http://stats.bis.gov.uk/ewp/ewp\\_full.pdf](http://stats.bis.gov.uk/ewp/ewp_full.pdf).

EEA, 2010, Primary energy consumption by fuel, Assessment publishes Sep 2010, European Environmental Agency, [Online], [Accessed 18 January 2011], from World Wide Web:

<http://www.eea.europa.eu/data-and-maps/figures/final-energy-consumption-by-sector>.

EIA, 2010, Projections: EIA, World Energy Projection System Plus (2010), U.S. Energy Information Administration, [Online], [Accessed 18 January 2011], from World Wide Web: <http://www.eia.doe.gov/oiaf/ieo/world.html>.

Fahmi, R., Bridgwater, A.V., Darvell, L.I., Jones, J.M., Yates, N., Thain, S., Donnison, I.S., 2007. The effect of alkali metals on combustion and pyrolysis of *Lolium* and *Festuca* grasses, switchgrass and willow. *Fuel* 86, 1560-1569.

Feng, W., van der Kooi, H.J., de Swaan, A.J., 2004. Phase equilibria for biomass conversion processes in subcritical and supercritical water. *Chemical Engineering Journal* 98, 105-113.

Fernandez, A.V., Vergas, G., Alarcon, N., Velasco, A., 2008. Evaluation of marine algae as a source of biogas in a two-stage anaerobic reactor system. *Biomass and Bioenergy* 32, 338-344.

## Bibliography

Fitton, J.H., Irhimeh, M., Falk, N., 2007. Macroalgal fucoidan extracts: A new opportunity for marine cosmetics. *Cosmetics & Toiletries* 122, 55-22.

Gevaert, F., Davoult, D., Creach, A., Kling, R., Janquin, M.A., Seuront, L., Lemoine, Y., 2001. Carbon and nitrogen content of laminaria saccharina in the eastern English Channel: biometrics and seasonal variations. *Journal of the Marine Biological Association UK* 81, 727-734.

Goudriaan, F., van de Beld, B., Boerefijn, F.R., Bos, G.M., Naber, J.E., van der Wal, S., Zeevalkink, J.A., 2000. Thermal Efficiency of the HTU Process for Biomass Liquefaction. *Progress in Thermochemical Biomass Conversion conference*: 1312-1325.

Goyal, H.B., Seal, D., Saxena, R.C., 2008. Bio-fuels from thermochemical conversion of renewable resources: A review. *Renewable and Sustainable Energy Reviews* 12, 504-517.

Guiry, M., 2003. Algaebase, [Online], [Accessed 18 January 2011], from World Wide Web:

[http://www.algaebase.org/\\_mediafiles/algaebase/3EE735B1076ca34904JkR2ED8ABC/7FytA48aNKRJ.jpg](http://www.algaebase.org/_mediafiles/algaebase/3EE735B1076ca34904JkR2ED8ABC/7FytA48aNKRJ.jpg).

Guiry, M., 2006. Algaebase, [Online], [Accessed 18 January 2011], from World Wide Web:

[http://www.algaebase.org/search/images/detail/?img\\_id=10182&sk=0](http://www.algaebase.org/search/images/detail/?img_id=10182&sk=0).

Guiry, M., 2007a. Algaebase, [Online], [Accessed 18 January 2011], from World Wide Web:

[http://www.algaebase.org/search/images/detail/?img\\_id=4059&sk=0](http://www.algaebase.org/search/images/detail/?img_id=4059&sk=0).

Guiry, M., 2007b. Algaebase, [Online], [Accessed 18 January 2011], from World Wide Web:

[http://www.algaebase.org/\\_mediafiles/algaebase/3EE735B1076ca33923JGx2E75FE1/CuZb5FVRGJ9p.jpg](http://www.algaebase.org/_mediafiles/algaebase/3EE735B1076ca33923JGx2E75FE1/CuZb5FVRGJ9p.jpg)

## Bibliography

- Guiry, M., 2008. Algaebase, [Online], [Accessed 18 January 2011], from World Wide Web: <http://www.algaebase.org/mediafiles/algaebase/5B7BE95A076ca23506nyp2AC8094/5efq4p9PEYWf.jpg>.
- Gunaseelan, V.N., 1997. Anaerobic digestion of biomass for methane production: a review. *Biomass and Bioenergy* 13, 83-114.
- Hallman, A., 2007. Algal Transgenics and Biotechnology. *Transgenic Plant Journal*.
- Hanssen, J.F., Indergaard, M., Ostgaard, K., Baevre, O.A., Pedersen, T.A., Jensen, A., 1987. Anaerobic digestion of *Laminaria* spp. and *Ascophyllum nodosum* and application of end products. *Biomass* 14, 1-13.
- Hanssen, J.F., Indergaard, M., Ostgaard, K., Baevre, O.A., Pedersen, T.A., Jensen, A., 1987. Anaerobic digestion of *Laminaria* spp. and *Ascophyllum nodosum* and application of end products. *Biomass* 14, 1-13.
- Harun, R., Jason, W.S.Y., Cherrington, T., Danquah, M.K., 2011. Microalgal biomass as a cellulosic fermentation feedstock for, bioethanol production. *Renewable and Sustainable Energy Reviews*, doi:10.1016/j.rser.2010.07.071.
- Hoagland, D.R., 1915. Organic constituents of Pacific coast kelps. *Journal of Agricultural Research* 4, 39-58.
- Horn S.J., 2000. Bioenergy from brown seaweeds. PhD Thesis, Norwegian University of Science and Technology NTNU.
- Horn, S.J., Aasen, I.M., Ostgaard, K., 2000a. Production of ethanol from mannitol by *Zymobacter palmae*. *Journal of Industrial Microbiology and Biotechnology* 24, 51-57.
- Horn, S.J., Aasen, I.M., Ostgaard, K., 2000b. Ethanol production from seaweed extract. *Journal of Industrial Microbiology & Biotechnology* 25, 249-254.

IEA, 2008, World Energy Outlook 2008, International Energy Agency 2008, [Online], [Accessed 18 January 2011], from World Wide Web: <http://www.iea.org/textbase/nppdf/free/2008/weo2008.pdf>

IPCC, 2007, Climate Change 2007: Synthesis Report, Intergovernmental Panel on Climate Change, [Online], [Accessed 18 January 2011], from World Wide Web: [http://www.ipcc.ch/pdf/assessment-report/ar4/syr/ar4\\_syr.pdf](http://www.ipcc.ch/pdf/assessment-report/ar4/syr/ar4_syr.pdf).

Jenkins, B.M., Baxter, L.L., Miles Jr., T.R., Miles, T.R., 1998. Combustion properties of biomass. *Fuel Processing Technology* 54, 17-46.

Jones, J.M., Darvell, L.I., Bridgeman, T.G., Pourkashanian, M., Williams, A., 2007. An investigation of the thermal and catalytic behaviour of potassium in biomass combustion. *Proceedings of the Combustion Institute* 31, 1955-1963.

Jupp, B.P., Drew, E.A., 1974. Studies on the growth of *Laminaria hyperborea* (Gunn.) Fosl. I. Biomass and productivity. *Journal of Experimental Marine Biology and Ecology* 15, 185-196.

Kain, J.M., Dawes, C.P., 1987. Useful European Seaweeds: past hopes and present cultivation. *Hydrobiologia* 151/152, 173-181.

Karagoz, S., Bhaskar, T., Muto, A., Sakata, Y., 2005. Comparative studies of oil compositions produced from sawdust, rice husk, lignin and cellulose by hydrothermal treatment. *Fuel* 84, 875-884.

Karagoz, S., Bhaskar, T., Muto, A., Sakata, Y., 2006. Hydrothermal upgrading of biomass: Effect of  $K_2CO_3$  concentration and biomass/water ratio on products distribution. *Bioresource Technology* 97, 90-98.

Kastanaki, E., Vamvuka, D., 2006. A comparative reactivity and kinetic study on the combustion of coal-biomass char blends. *Fuel* 85, 1186-1193.

Kelly, M.S., Ratcliff, J., Brunner, L., 2008. Workpackage 1: Macroalgal species evaluation and selection. Draft report. Supergen bioenergy plus: marine biomass. Potential of marine biomass to UK energy: fuels and chemicals. Scottish Association for Marine Science (SAMS), Irish Seaweed Centre (ISC).

## Bibliography

- Khotimchenko, Yu.S., Kovalev, V.V., Savchenko, O.V., Ziganshina, O.A., 2001. Physical-Chemical Properties, Physiological Activity, and Usage of Alginates, the Polysaccharides of Brown Algae. *Russian Journal of Marine Biology* 27, S53-S64.
- Kirby, R.H., 1950. Seaweeds in commerce Part I. Colonial Plant and Animal Products 1, 183-216.
- Klass, D.L., 1998. Biomass for renewable energy, fuels, and chemicals. Academic Press.
- Kraan, S., Rueness, J., Guiry, M.D., 2001. Are north Atlantic *Alaria esculenta* and *a. grandifolia* (*alariaceae*, *phaeophyceae*) conspecific? *European Journal of Phycology* 36, 35-42.
- Kruse, A., Dinjus, E., 2007. Hot compressed water as reaction medium and reactant – Properties and synthesis reactions. *The Journal of Supercritical Fluids* 39, 362-380.
- Levring, T., Hoppe, H.A., Schmid, O.J., 1969. Marine Algae. A survey of research and utilization. *Botanica Marina Handbooks*, v. 1. Cram, deGruyter ad Co., Hamburg.
- Lewis, D.H., Smith, D.C., 1967. Sugar alcohols (polyols) in fungi and green plants I. distribution, physiology and metabolism. *New Phytologist* 66, 143-184.
- Li, D., Chen, L., Yi, X., Zhang, X., Ye, N., 2010. Pyrolytic characteristics and kinetics of two brown algae and sodium alginate. *Bioresource Technology* 101, 7131-7136.
- Lim, K.O, Sims, R.E.H., 2004. Liquid and gaseous biomass fuels. In: *Bioenergy options for a cleaner environment in developed countries*, 103-140.
- Lipkin, Y., 1985. Outdoor cultivation of sea vegetables. *Plant and Soil* 89, 159-183.
- Mabeau, S., Kloareg, B., 1987. Isolation and Analysis of the Cell Walls of Brown Algae: *Fucus spiralis*, *F. ceranoides*, *F. vesiculosus*, *F. serratus*,

## Bibliography

*Bifurcaria bifurcate* and *Laminaria digitata*. *Journal of Experimental Botany* 38, 1573-1580.

Marlin, 2011a. The marine life information network, [Online], [Accessed 18 January 2011], from World Wide Web:

<http://www.marlin.ac.uk/species/laminariahyperborea.htm>

Marlin, 2011b, The marine life information network, [Online], [Accessed 18 January 2011], from World Wide Web:

<http://www.marlin.ac.uk/species/Saccorhizapolyschides.htm>

McCormick, E., 2001. Alginate – Lifecasters' Gold. *Art Casting Journal*.

McHugh, D.J., 2003. A guide to the seaweed industry. *FAO Fisheries Technical Paper*, No. 441.

McKendry, P., 2002a. Energy production from biomass (part 1): overview of biomass. *Bioresource Technology* 83, 37-46.

McKendry, P., 2002b. Energy production from biomass (part 2): conversion technologies. *Bioresource Technology* 83, 47-54.

McLean, E., Craig, S., Schwartz, M., 2002. *Macrophyte biotechnology: a brief review of production methods and industrial application of seaweed products*. Virginia Polytechnic Institute and State University.

Miao, X., Wu, Q., 2004. High yield bio-oil production from fast pyrolysis by metabolic controlling of *Chlorella protothecoides*. *Journal of Biotechnology* 110, 85-93.

Miles, T.R., Baxter, L.L., Bryers, R.W., Jenkins, B.M., Oden, L.L., 1995. Alkali deposits found in biomass power plants. A preliminary investigation of their extent and nature. *Summary report for the National Renewable Energy Laboratory*.

Minowa, T., Kondo, T., Sudirjo, S.T., 1998. Thermochemical liquefaction of Indonesian biomass residues. *Biomass and Bioenergy* 14, 517-524.

## Bibliography

- Minowa, T., Zhen, F., Ogi, T., 1998. Cellulose decomposition in hot-compressed water with alkali or nickel catalyst. *The Journal of Supercritical Fluids* 13, 253-259.
- Murakami, M., Yokoyama, S., Ogi, T., Koguchi, K., 1990. Direct liquefaction of activated sludge from aerobic treatment of effluents from the cornstarch industry. *Biomass* 23, 215-228.
- Norton, T.A., 1977. Experiments of the factors influencing the geographical distributions of *saccorhiza polyschides* and *saccorhiza dermatodea*. *New Phytologist* 78, 625-635.
- Norton, T.A., Burrows, E.M., 1969. Studies on marine algae of the british isles. 7. *saccorhiza polyschides (lightf.) batt*. *British Phycological Journal* 4, 19-53.
- Nowakowski, D.J., Jones, J.M., Brydson, R.M.D., Ross, A.B., 2007. Potassium catalysis in the pyrolysis behaviour of short rotation willow coppice. *Fuel* 86, 2389-2402.
- Nowakowski, D.J., Woodbridge, C.R., Jones, J.M., 2008. Phosphorus catalysis in the pyrolysis behaviour of biomass. *Journal of Analytical and Applied Pyrolysis* 83, 197-204.
- Obluchinskaya, E.D., 2008. Comparative chemical composition of the Barents sea brown algae. *Applied Biochemistry and Microbiology* 44, 305-309.
- Ogi, T., Minowa, T., Dote, Y., Yokohama, S.Y., 1994. Characterization of oil produced by the direct liquefaction of Japanese oak in an aqueous 2-propanol solvent system. *Biomass and Bioenergy* 7, 1994.
- Peng, W., Wu Q., Tu P., 2000. Effects of temperature and holding time on production of renewable fuels from pyrolysis of *Chlorella protothecoides*. *Journal of Applied Phycology* 12, 147-152.
- Peng, W., Wu, Q., Tu, P., 2001a. Pyrolytic characteristics of heterotrophic *Chlorella protothecoides* for renewable bio-fuel production. *Journal of Applied Phycology* 13, 5-12.



## Bibliography

Peng, W., Wu, Q., Tu, P., Zhani, N., 2001b. Pyrolytic characteristics of microalgae as renewable energy source determined by thermogravimetric analysis. *Bioresource Technology* 80, 1-7.

Percival, E., 1979. The polysaccharides of green, red and brown seaweeds: Their basic structure, biosynthesis and function. *European Journal of Phycology* 14, 103-117.

Peterson, A.A., Vogel, F., Lachance, R.P., Froling, M., Antal, Jr., M.J., Tester, J.W., 2008. Thermochemical biofuel production in hydrothermal media: A review of sub- and supercritical water technologies. *Energy & Environmental Science* 1, 32-65.

Ponce, N.M.A., Pujol, C.A., Damonte, E.B., Flores, M.L., Stortz, C.A., 2003. Fucoidans from the brown seaweed *Adenocystis utricularis*: extraction methods, antiviral activity and structural studies. *Carbohydrate Research* 338, 153-165.

Qi, Z., Jie, C., Tiejun, W., Ying, X., 2007. Review of biomass pyrolysis oil properties and upgrading research. *Energy Conversion and Management* 48, 87-92.

Qian, Y., Zuo, C., Tan, J., He, J., 2007. Structural analysis of bio-oils from sub- and supercritical water liquefaction of woody biomass. *Energy* 32, 196-202.

Qu, Y., Wei, X., Zhong, C., 2003. Experimental study on the direct liquefaction of *Cunninghamia lanceolata* in water. *Energy* 28, 597-606.

Radmer, R.J., 1996. Algal Diversity and Commercial Algal Products. *Bioscience* 46, 263-270.

Rathmann, R., Szklo, A., Schaeffer, R., 2010. Land use competition for production of food and liquid biofuels: A analysis of the arguments in the current debate. *Renewable Energy* 35, 14-22.

Reijnders, L., 2010. Transport biofuel yields from food and lignocellulosic C<sub>4</sub> crops. *Biomass and Bioenergy* 34, 152-155.

## Bibliography

- Rioux, L.E., Turgeon, S.L., Beaulieu, M., 2007. Characterization of polysaccharides extracted from brown seaweeds. *Carbohydrate Polymers* 69, 530-537.
- Ross, A.B., Anastasakis, K., Kubacki, M., Jones, J.M., 2009. Investigation of the pyrolysis behaviour of brown algae before and after pre-treatment using PY-GC/MS and TGA. *Journal of Analytical and Applied Pyrolysis*, 85, 3-10.
- Ross, A.B., Biller, P., Kubacki, M.L., Li, H., Lea-Langdon, A., Jones, J.M., 2010. Hydrothermal processing of microalgae using alkali and organic acids. *Fuel* 89, 2234-2243.
- Ross, A.B., Hall, C., Anastasakis, K., Westwood, A., Jones, J.M., Crewe, R., 2011. Influence of cation on the pyrolysis and oxidation of alginates. *Journal of Applied and Analytical Pyrolysis*, doi:10.1016/j.jaap.2011.03.012.
- Ross, A.B., Jones, J.M., Kubacki, M.L., Bridgeman, T., 2008. Classification of macroalgae as fuel and its thermochemical behaviour. *Bioresource Technology* 99, 6494-6504.
- Saddawi, A., Jones, J.M., Williams, A., Wojtowicz, M.A., 2010. Kinetics of the thermal decomposition of biomass. *Energy Fuels* 24, 1274-1282.
- Saha, B.C., Racine, F.M., 2011. Biotechnological production of mannitol and its applications. *Applied Microbiology and Biotechnology* 89, 879-891.
- Sharma, O.P., 1986. *Textbook of Algae*. McGraw Hill.
- Shuping, Z., Yulong, W., Mingde, Y., Kaleem, I., Chun, L., Tong, J., 2010. Production and characterization of bio-oil from hydrothermal liquefaction of microalgae *Dunaliella tertiolecta* cake. *Energy* 35, 5406-5411.
- Sims, R.E.H., Bassam, N.E., 2004. In: *Bioenergy options for a cleaner environment in developed countries*, 1-28.
- Sjotun, K., Fredriksen, S., Lein, T.E., Rueness, J., Sivertsen, K., 1993. Population studies of *Laminaria hyperborea* from its northern range of distribution in Norway. *Hydrobiologia* 260/261, 215-221.

## Bibliography

Speight, J.G., 2001. Handbook of petroleum analysis, John Wiley & Sons, Inc.

Stone, K.C., Hunt, P.G., Cantrell, K.B., Ro, K.S., 2010. The potential impacts of biomass feedstock production on water resource availability. *Bioresource Technology* 101, 2014-2025.

Synytsya, A., Kim, W.-J., Kim, S.-M., Pohl, R., Synytsya, A., Kvasnicka, F., Copikova, J., Park, Y.I., 2010. Structure and antitumour activity of fucoidan isolated from sporophyll of Korean brown seaweed *Undaria pinnatifida*. *Carbohydrate Polymers* 81, 41-48.

Tarwadi, S.J., Chauhan, V.D., 1987. Seaweed biomass as a source of energy. *Energy* 12, 375-378.

Tett, P., 2003. *Seaweeds, Lectures for 2002-2003*. [Online], [Accessed 18 January 2007], from World Wide Web:

<http://www.lifesciences.napier.ac.uk/teaching/MB/Index.html>. Last accessed 11/2007.

Tong, B., Liu, R., Meng, C., Yu, F., Ji, S., Tan, Z., 2010. Heat capacities and nonisothermal thermal decomposition reaction kinetics of d-mannitol. *J Chem Eng Data*, 55, pp.119-124.

Troiano, R.A., Wise, D.L., Augenstein, D.C., Kispert, R.G., 1976. *Resource Recovery and Conservation* 2, 171-176.

Vamvuka, D., Zografos, D., 2004. Predicting the behaviour of ash from agricultural wastes during combustion. *Fuel* 83, 2051-2057.

Vincent, J.F.V., Gravell, K., 1986. The mechanical design of kelp, *Laminaria digitata*. *Journal of Materials Science Letters* 5, 353-354.

Wang, C., Du, Z., Pan, J., Li, J., Yang, Z., 2007. Direct conversion of biomass to bio-petroleum at low temperature. *Journal of Analytical and Applied Pyrolysis* 78, 438-444.

## Bibliography

- Wang, C., Pan, J., Li, J., Yang, Z., 2008. Comparative studies of products produced from four different biomass samples via deoxy-liquefaction. *Bioresource Technology* 99, 2778-2786.
- Wang, J., Wang, G., Zhang, M., Chen, M., Li, D., Min, F., Chen, M., Zhang, S., Ren, Z., Yan, Y., 2006. A comparative study of thermolysis characteristics and kinetics of seaweeds and fir wood. *Process Biochemistry* 41, 1883-1886.
- Wang, S., Jiang, X.M., Han, X.X., Liu, J.G., 2009. Combustion characteristics of seaweed biomass. 1. Combustion characteristics of *Enteromorpha clathrata* and *Sargassum natans*. *Energy Fuels* 23, 5173-5178.
- Wang, S., Jiang, X.M., Han, X.X., Wang, H., 2008. Fusion characteristic study on seaweed biomass ash. *Energy & Fuels* 22, 2229-2235.
- Wang, S., Jiang, X.M., Wang, N., Yu, L.J., Li, Z., He, P.M., 2007. Research on pyrolysis characteristics of seaweed. *Energy & Fuels* 21, 3723-3729.
- Weber, R., 2008. Extracting mathematically exact kinetic parameters from experimental data on combustion and pyrolysis of solid fuels. *J Energy Inst*, 81, pp.226-233.
- Williams, A., Pourkashanian, M., Jones, J.M., 2001. Combustion of pulverised coal and biomass. *Progress in Energy Combustion Science* 27, 587-610.
- Yan, Y., Xu, J., Li, T., Ren, Z., 1999. Liquefaction of sawdust for liquid fuel. *Fuel Processing Technology* 60, 135-143.
- Yang, Y.F., Fenf, C.P., Inamori, Y., Maekawa, T., 2004. Analysis of energy conversion characteristics in liquefaction of algae. *Resources, Conservation and Recycling* 43, 21-33.
- Yin, S., Dolan, R., Harris, M., Tan, Z., 2010. Subcritical hydrothermal liquefaction of cattle manure to bio-oil: Effects of conversion parameters on bio-oil yield and characterization of bio-oil. *Bioresource Technology* 101, 3657-3664.

## Bibliography

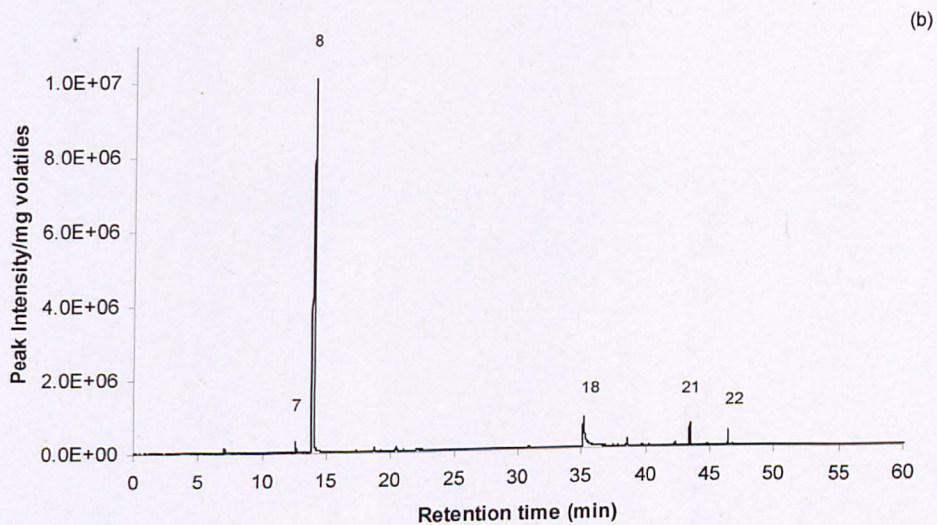
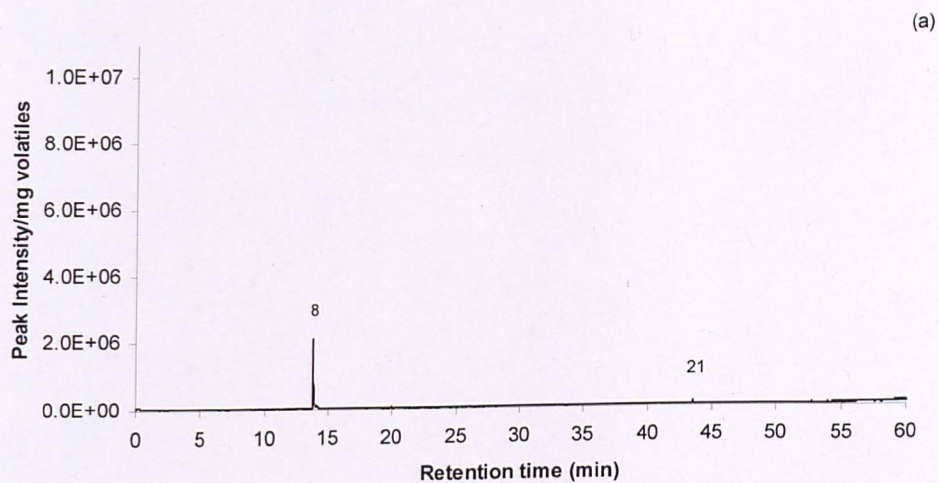
Yokoyama, S., Suzuki, A., Murakami, M., Ogi, T., Koguchi, K., Nakamura, E., 1987. Liquid fuel production from sewage sludge by catalytic conversion using sodium carbonate. *Fuel* 66, 1150-1155.

Yu, L.J., Wang, S., Jiang, X.M., Wang, N., Zhang, C.Q., 2008. Thermal analysis studies on combustion characteristics of seaweed. *Journal of Thermal Analysis and Calorimetry* 93, 611-617.

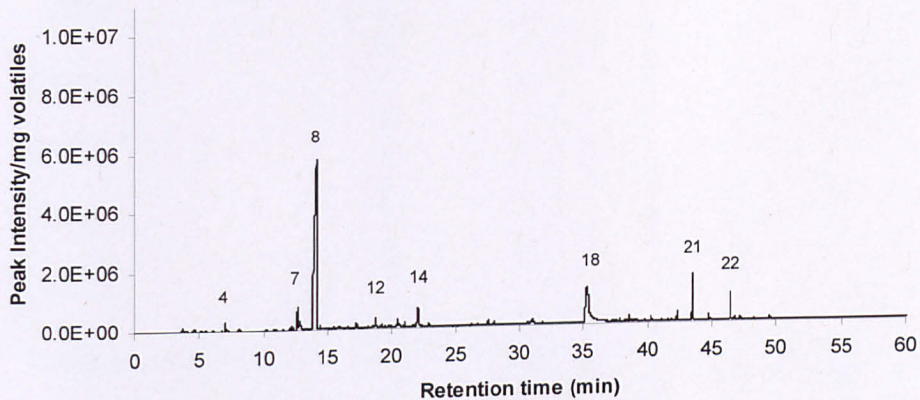
Zhong, C., Wei, X., 2004. A comparative experimental study on the liquefaction of wood. *Energy* 29, 1731-1741.

Zhou, D., Zhang, L., Zhang, S., Fu, H., Chen, J., 2010. Hydrothermal liquefaction of macroalgae *Enteromorpha prolifera* to bio-oil. *Energy and Fuels* 24, 4054-4061.

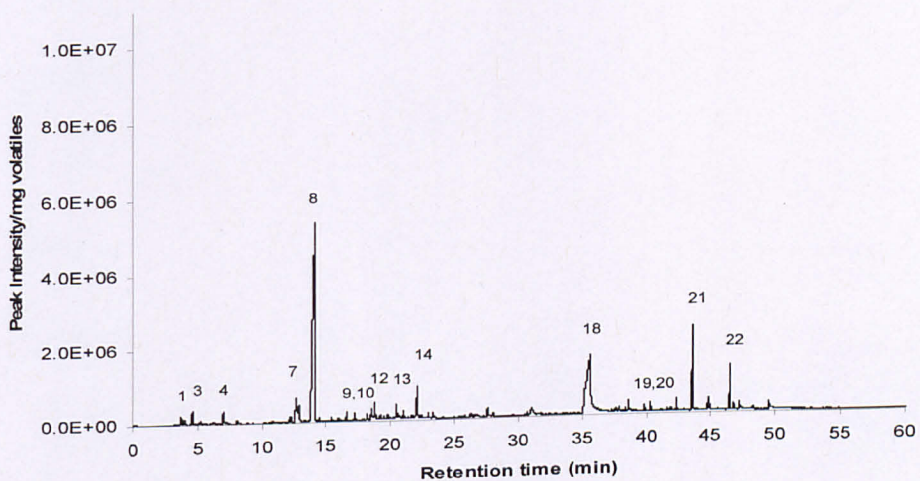
### APPENDIX A - PY-GC/MS chromatograms of model compounds and identified compounds



(c)



(d)



(e)

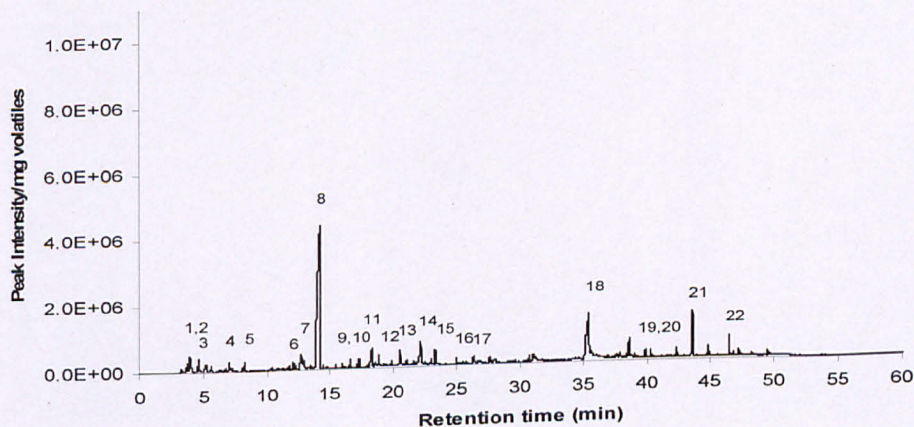
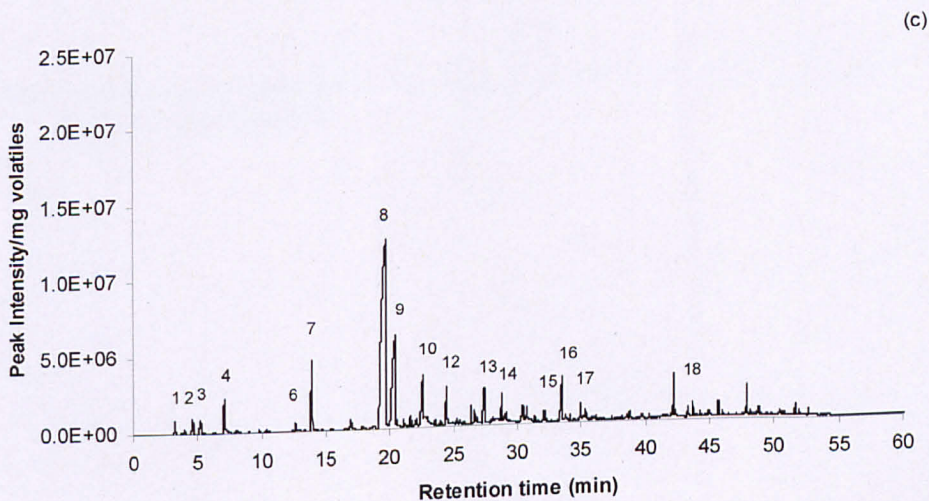
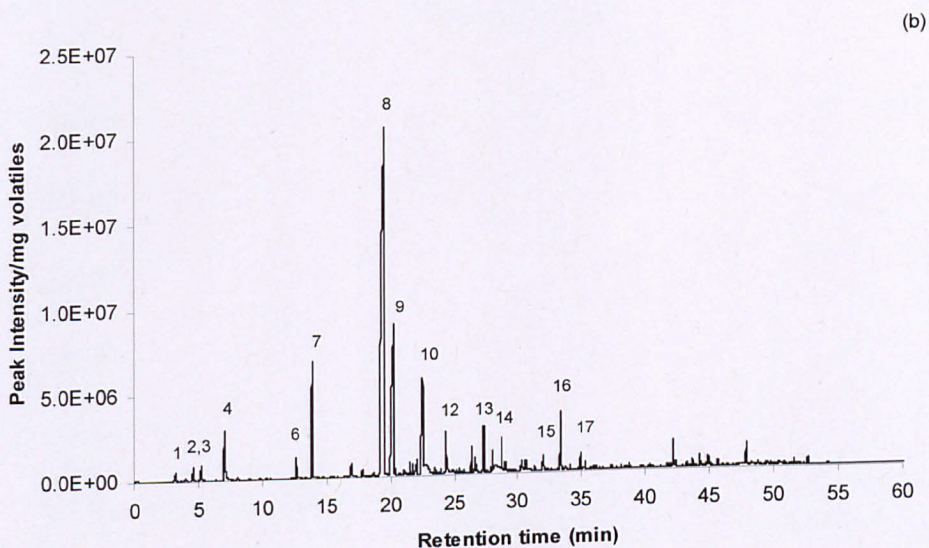
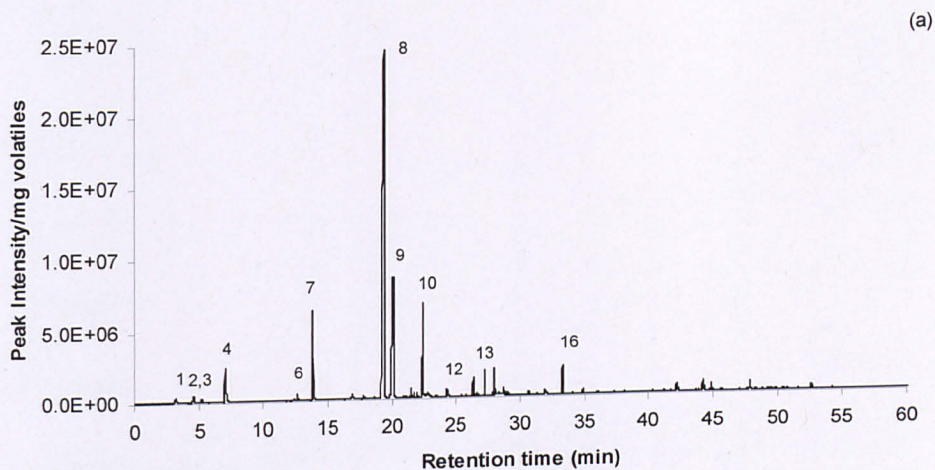
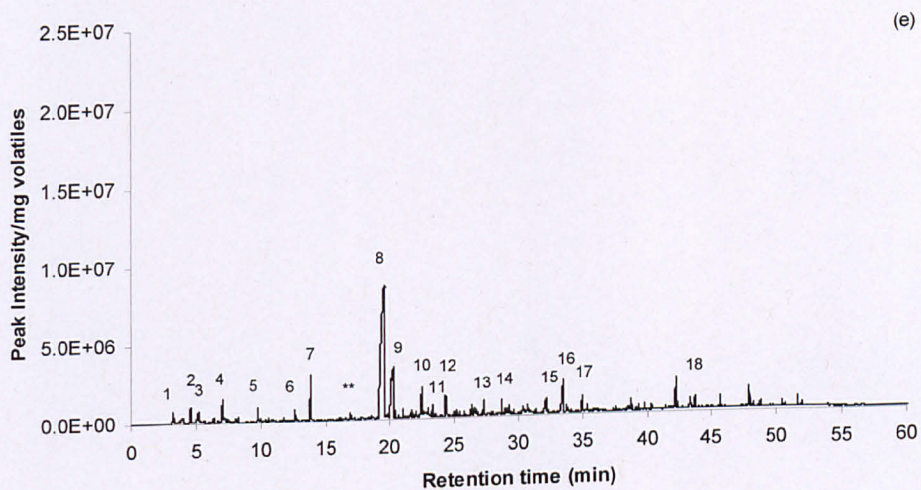
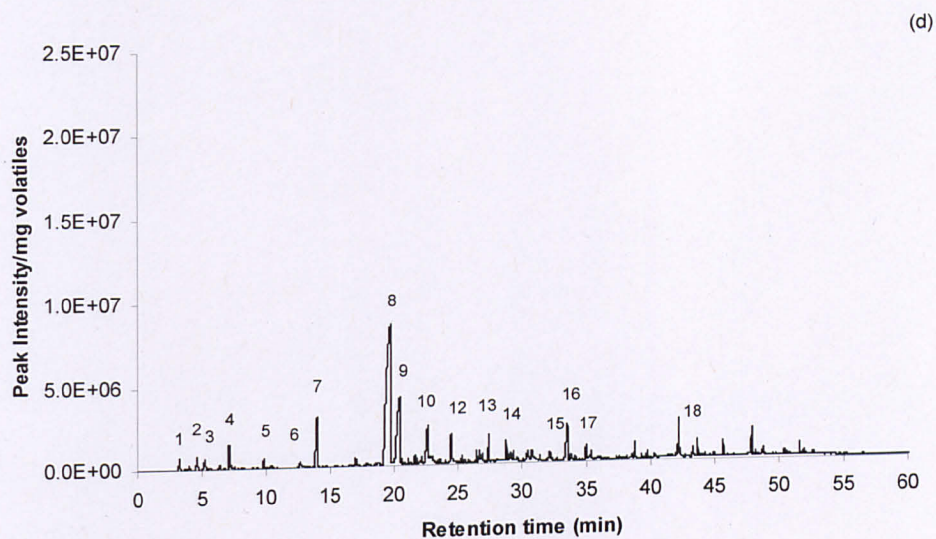


Figure A.1 Py-GC/MS profile for alginic acid at (a) 200°C, (b) 300°C, (c) 400°C, (d) 500°C and (e) 800°C.

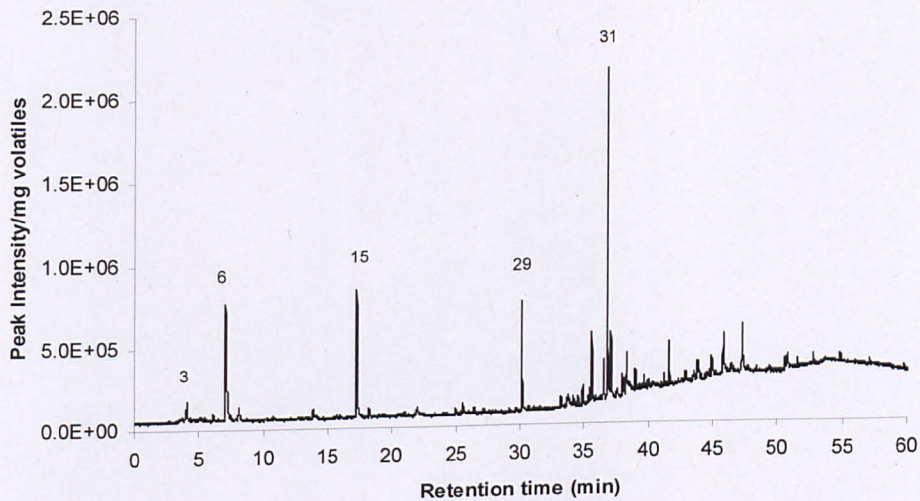




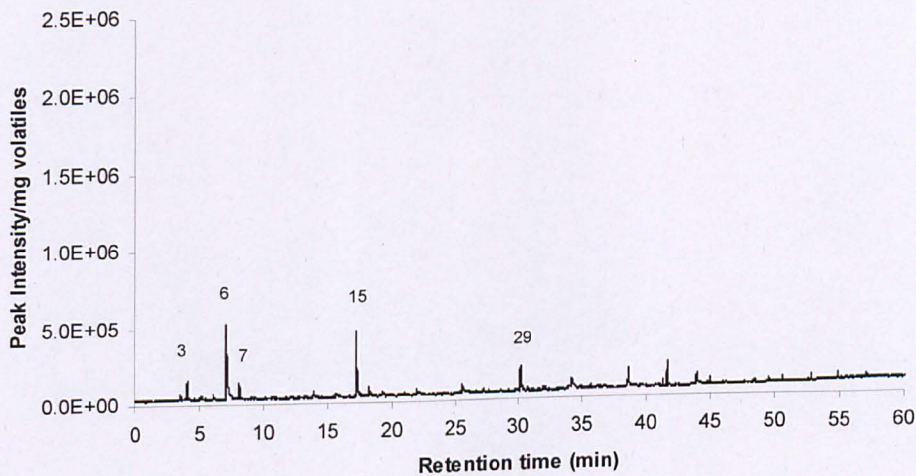


**Figure A.2** Py-GC/MS profile for fucoidan at (a) 200°C, (b) 300°C, (c) 400°C, (d) 500°C and (e) 800°C.

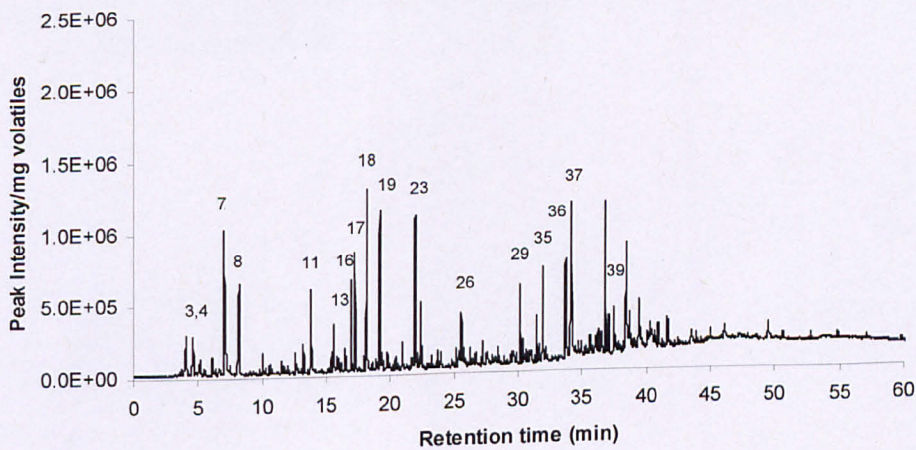
(a)



(b)



(c)



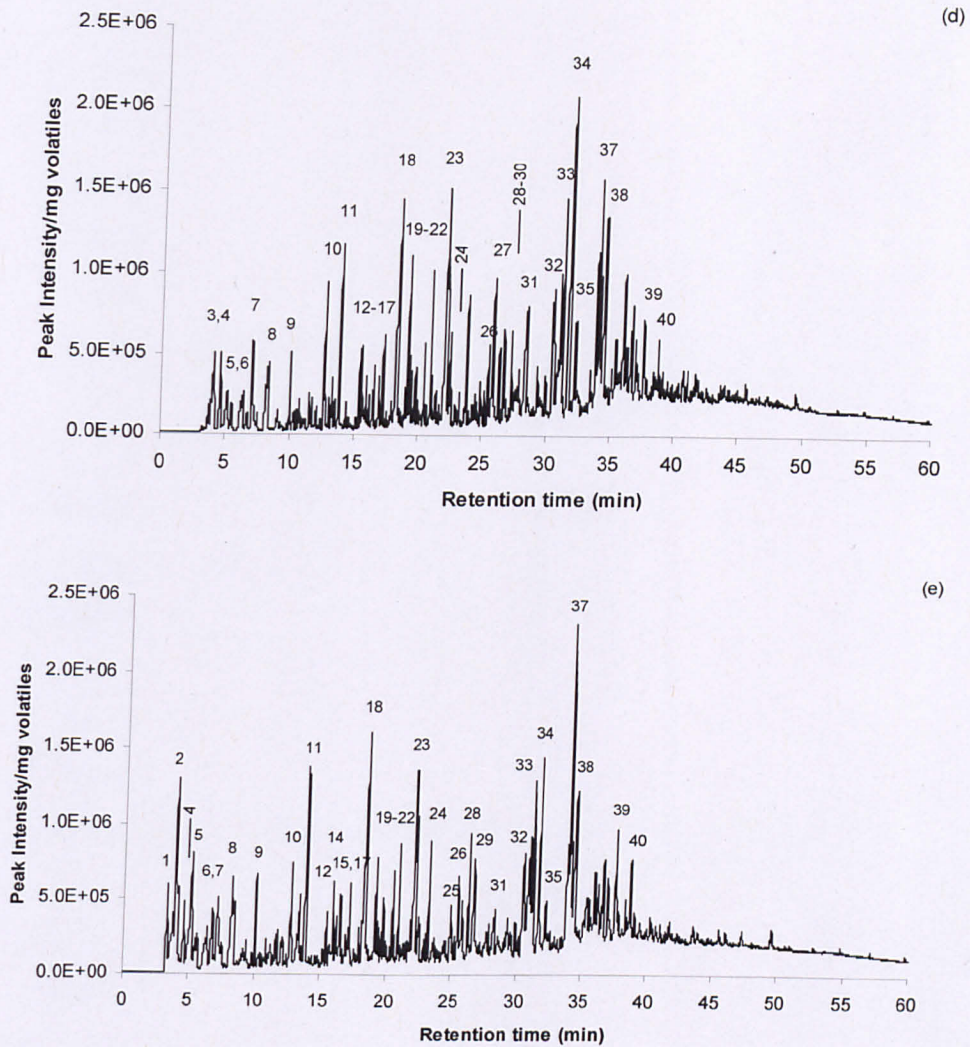
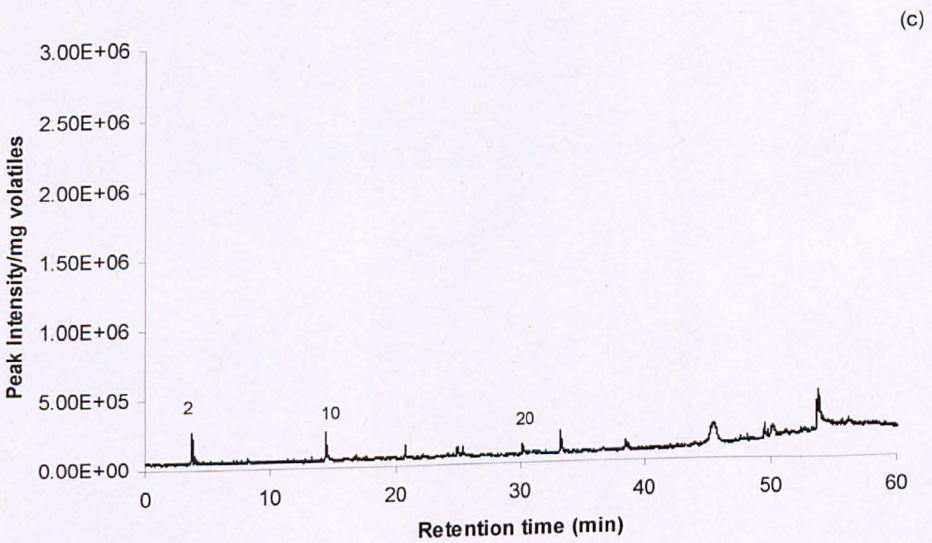
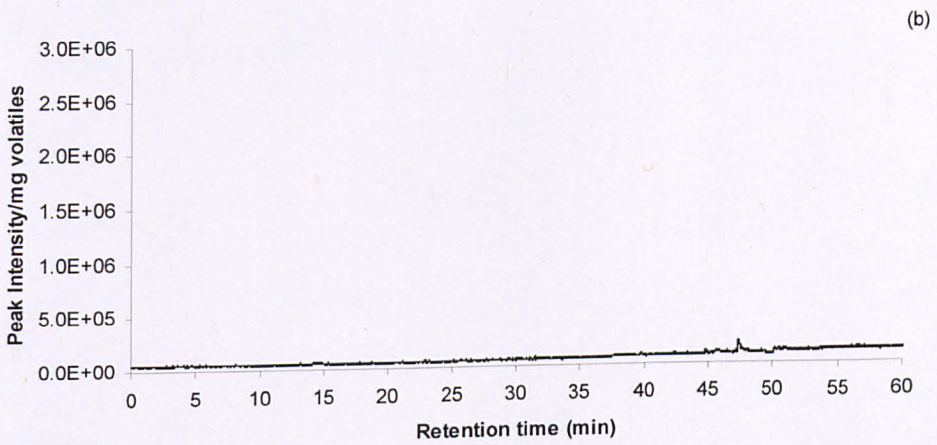
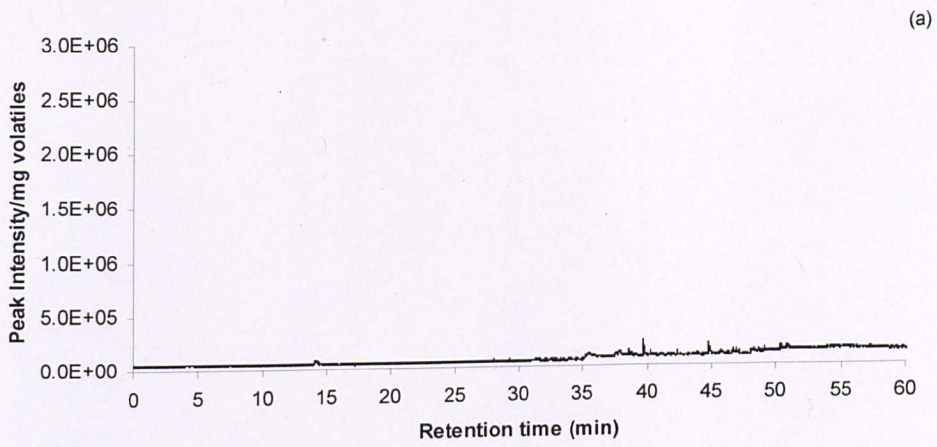
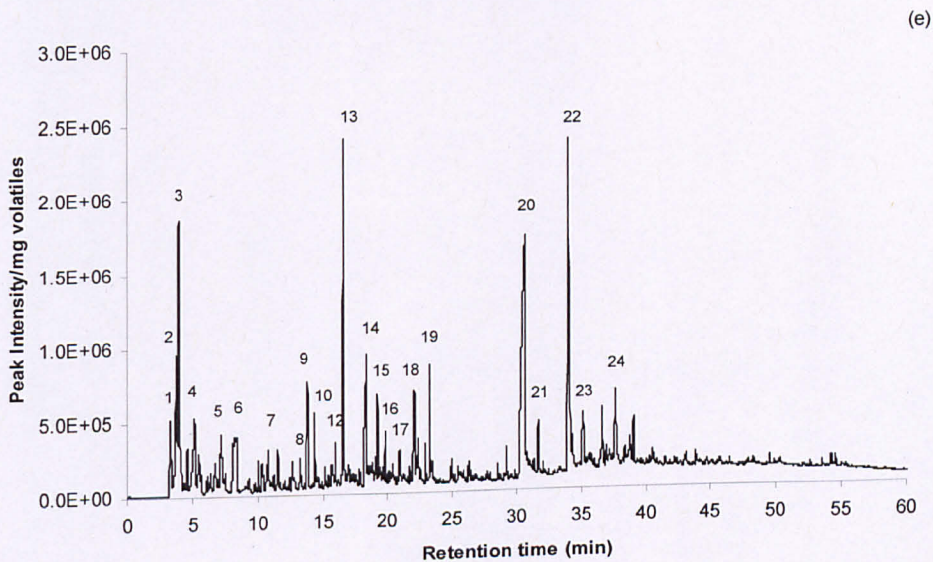
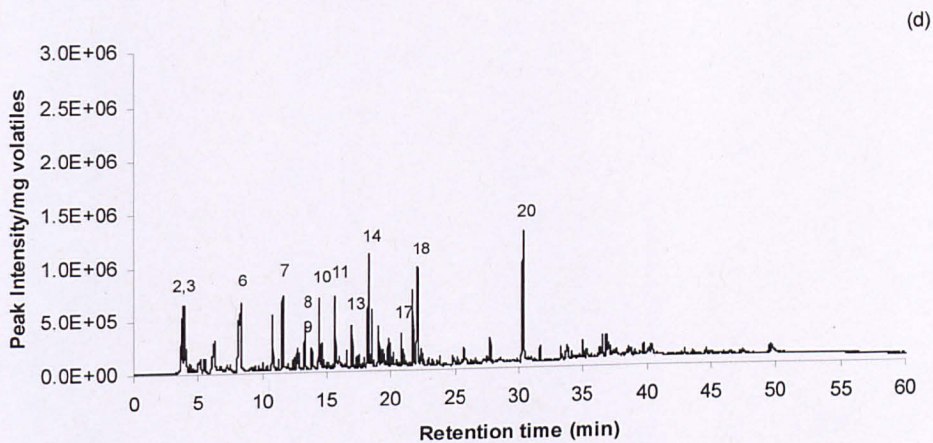


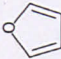
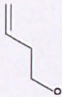
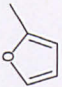
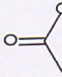
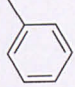

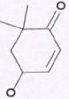
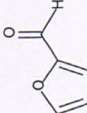
Figure A.3 Py-GC/MS profile for laminarin at (a) 200°C, (b) 300°C, (c) 400°C, (d) 500°C and (e) 800°C.

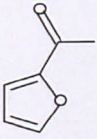
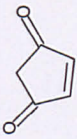
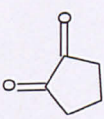
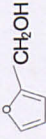
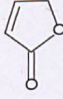
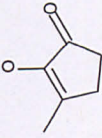
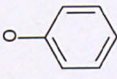


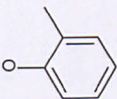
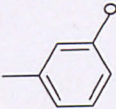
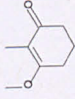
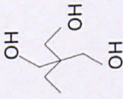
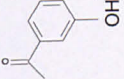
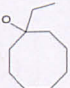


**Figure A.4** Py-GC/MS profile for mannitol at (a) 200°C, (b) 300°C, (c) 400°C, (d) 500°C and (e) 800°C.

**Table A.1** The main peaks identified in pyrograms of alginic acid at different temperatures by mass spectral detection.


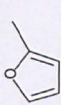

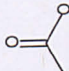
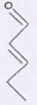
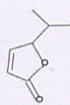
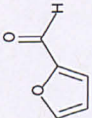
No.	Compound	RT	Formula	MW	Structure	200°C	300°C	400°C	500°C	800°C
1	Furan	3.747	C <sub>4</sub> H <sub>4</sub> O	68					✓	✓
2	3-Buten-1-ol	3.944	C <sub>4</sub> H <sub>8</sub> O	72						✓
3	furan, 2-methyl-	4.632	C <sub>5</sub> H <sub>6</sub> O	82					✓	✓
4	acetic acid	7.038	C <sub>2</sub> H <sub>4</sub> O <sub>2</sub>	60				✓	✓	✓
5	toluene	8.263	C <sub>7</sub> H <sub>8</sub>	92						✓
6	2-Butenal, 2-methyl-	12.102	C <sub>5</sub> H <sub>8</sub> O	84						✓
7	4-Hydroxy-6,6-dimethyl-cyclohex-2-enone	12.722	C <sub>8</sub> H <sub>12</sub> O <sub>2</sub>	140			✓	✓	✓	✓
8	Furfural	14.154	C <sub>5</sub> H <sub>4</sub> O <sub>2</sub>	69		✓	✓	✓	✓	✓

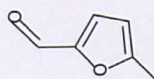
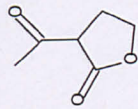
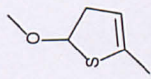
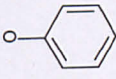
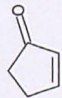
9	Ethanone, 1-(2-furanyl)-	16.59	$C_6H_6O_2$	110		✓	✓
10	4-Cyclopentene-1,3-dione	17.263	$C_5H_4O_2$	96		✓	✓
11	1,2-Cyclopentanedione	18.281	$C_5H_6O_2$	98		✓	
12	2-Furanmethanol, tetrahydro-	18.83	$C_5H_{10}O_2$	102		✓	✓
13	2(5H)-Furanone	20.508	$C_4H_4O_2$	84		✓	✓
14	2-Cyclopenten-1-one, 2-hydroxy-3methyl-	22.128	$C_6H_8O_2$	112		✓	✓
15	Phenol	23.283	$C_6H_6O$	94			✓

16	Phenol, 2-methyl-	25.008	$C_7H_8O$	108		✓
17	Phenol, 3-methyl-	26.37	$C_7H_8O$	108		✓
18	3-Methoxy-2-methyl-cyclohex-2-enone	35.401	$C_8H_{12}O_2$	140		✓
19	1,3-Propanediol, 2-ethyl-2-(hydroxymethyl)-	39.863	$C_6H_{14}O_3$	134		✓
20	Ethanone, 1-(3-hydroxyphenyl)-	40.297	$C_8H_8O_2$	136		✓
21	1-Ethyl-1-cyclooctanol	43.615	$C_{10}H_{16}O$	152		✓

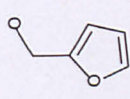

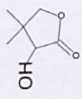
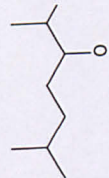
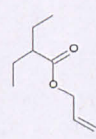
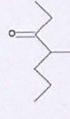


**Table A.2** The main peaks identified in pyrograms of fucoidan at different temperatures by mass spectral detection.


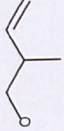
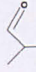
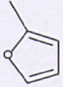
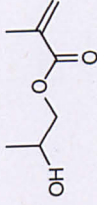

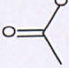
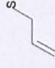
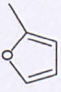
No	Compound	RT	Formula	MW	Structures	200°C	300°C	400°C	500°C	800°C
1	Ethene, 1,1-difluoro-	3.274	C <sub>2</sub> H <sub>2</sub> F <sub>2</sub>			√	√	√	√	√
2	Furan, 2-methyl-	4.627	C <sub>5</sub> H <sub>6</sub> O	82		√	√	√	√	√
3	Butanal	5.239	C <sub>4</sub> H <sub>8</sub> O	72		√	√	√	√	√
4	Acetic acid	7.105	C <sub>2</sub> H <sub>4</sub> O <sub>2</sub>	60		√	√	√	√	√
5	2-Pentenal, (E)-	9.815	C <sub>5</sub> H <sub>8</sub> O	84					√	√
6	2(5H)-Furanone, 5-(1-methyl/ethyl)-	12.627	C <sub>7</sub> H <sub>10</sub> O <sub>2</sub>	126		√	√	√	√	√
7	Furfural	13.917	C <sub>5</sub> H <sub>4</sub> O <sub>2</sub>	69		√	√	√	√	√

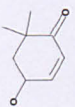
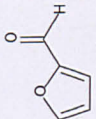
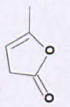
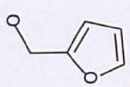
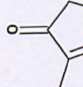
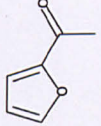
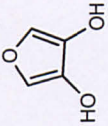
8	2-Furancarboxaldehyde, 5-methyl-	19.578	$C_6H_6O_2$		✓	✓	✓	✓	✓	✓
9	2(3H)-Furanone, 3-acetyl-dihydro-	20.271	$C_6H_8O_3$		✓	✓	✓	✓	✓	✓
10	Thiophene, 2-methoxy-5-methyl-	22.526	$C_6H_8OS$		✓	✓	✓	✓	✓	✓
11	Phenol	23.31	$C_6H_6O$							✓
12	2-Cyclopenten-1-one	24.334	$C_5H_6O$		✓	✓	✓	✓	✓	✓

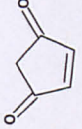
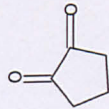
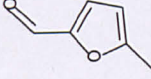
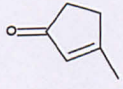
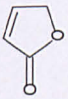
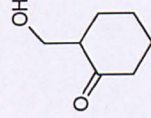
Appendix B

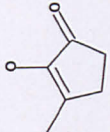
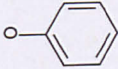
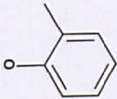
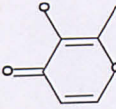
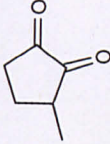
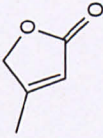
13	2-Furanmethanol	27.315	$C_5H_6O_2$	98		✓	✓	✓	✓	✓
14	3-Octyn-2-one	28.735	$C_8H_{12}O$	124		✓	✓	✓	✓	✓
15	Pantolactone	32.131	$C_6H_{10}O_3$	128		✓	✓	✓	✓	✓
16	3-Heptanol, 2,6-dimethyl-	33.488	$C_9H_{20}O$	144		✓	✓	✓	✓	✓
17	Allyl 2-ethyl butyrate	34.999	$C_9H_{16}O_2$	156		✓	✓	✓	✓	✓
18	3-Heptanone, 4-methyl-	43.342	$C_8H_{16}O$	128		✓	✓	✓	✓	✓

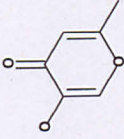
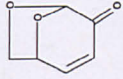
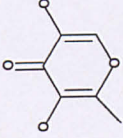
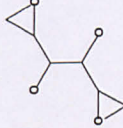
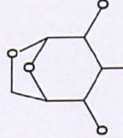
**Table A.3** the main peaks identified in pyrograms of laminarin at different temperatures by mass spectral detection

No	Compound	RT	Formula	M W	Structure	200°C	300°C	400°C	500°C	800°C
						✓	✓	✓	✓	✓
1	1,3-Butadiene	3.306	C <sub>4</sub> H <sub>6</sub>	54						✓
2	3-Buten-1-ol, 2-methyl-	3.942	C <sub>5</sub> H <sub>10</sub> O	86						✓
3	Propanal, 2-methyl-	4.125	C <sub>4</sub> H <sub>8</sub> O	72		✓	✓	✓	✓	
4	Furan, 2-methyl-	4.631	C <sub>5</sub> H <sub>6</sub> O	82		✓	✓	✓	✓	✓
5	2-Propenoic acid, 2-methyl-, 2-hydroxypropyl ester	5.157	C <sub>7</sub> H <sub>12</sub> O <sub>3</sub>	144					✓	✓
6	2-Butenal	6.749	C <sub>4</sub> H <sub>6</sub> O	70		✓	✓	✓	✓	✓
7	Acetic acid	7.148	C <sub>2</sub> H <sub>4</sub> O <sub>2</sub>	60			✓	✓	✓	✓
8	Allyl mercaptan	8.273	C <sub>3</sub> H <sub>6</sub> S	74				✓	✓	✓
9	Furan, 2-methyl-	10.077	C <sub>5</sub> H <sub>6</sub> O	82					✓	✓

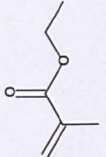
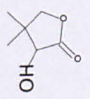
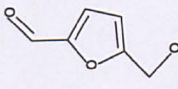
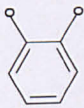
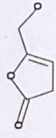
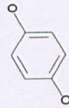
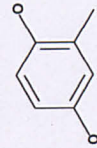
10	4-Hydroxy-6,6-dimethyl-cyclohex-2-enone	12.748	$C_8H_{12}O_2$	140		✓	✓
11	Furfural	13.939	$C_5H_4O_2$	69		✓	✓
12	2(3H)-Furanone, 5-methyl-	15.494	$C_5H_6O_2$	98		✓	✓
13	2-Furanmethanol	15.577	$C_5H_6O_2$	98		✓	✓
14	2-Cyclopenten-1-one, 2-methyl-	16	$C_6H_8O$	96		✓	✓
15	Ethanone, 1-(2-furanyl)-	16.631	$C_6H_6O_2$	110		✓	✓
16	3,4-Furandimethanol	16.939	$C_6H_8O_3$	128		✓	✓

17	4-Cyclopentene-1,3-dione	17.312	$C_5H_4O_2$	96		✓	✓	✓
18	1,2-Cyclopentanedione	18.45	$C_5H_6O_2$	98		✓	✓	✓
19	2-Furancarboxaldehyde, 5-methyl-	19.247	$C_6H_6O_2$	110		✓	✓	✓
20	2-Cyclopenten-1-one, 3-methyl-	19.859	$C_6H_8O$	96		✓	✓	✓
21	2(5H)-Furanone	20.593	$C_4H_4O_2$	84		✓	✓	✓
22	Cyclohexanone, 2-(hydroxymethyl)-	21.018	$C_7H_{12}O$	128		✓	✓	✓


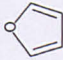
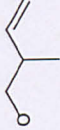
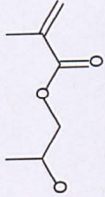
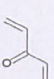
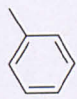
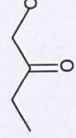
23	2-Cyclopenten-1-one, 2-hydroxy-3-methyl-	22.188	$C_6H_9O_2$	112		✓	✓	✓
24	Phenol	23.315	$C_6H_6O$	94		✓	✓	✓
25	Phenol, 2-methyl-	25.026	$C_7H_8O$	108		✓	✓	✓
26	Maltol	25.576	$C_6H_6O_3$	126		✓	✓	✓
27	1,2-Cyclopentanediol, 3-methyl-	25.898	$C_6H_8O_2$	112		✓	✓	✓
28	4-Methyl-5H-Furan-2-one	26.409	$C_5H_6O_2$	98		✓	✓	✓

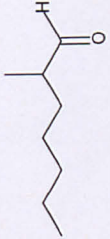
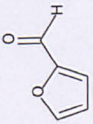
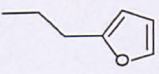
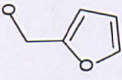
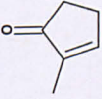
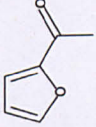
29	4H-Pyran-4-one, 5-hydroxy-2-methyl-	26.784	$C_6H_6O_3$	126		✓	✓	✓	✓
30	Levogluconone	27.313	$C_6H_6O_3$	126		✓			
31	4H-Pyran-4-one, 3,5-dihydroxy-2-methyl-	28.367	$C_6H_6O_4$	142		✓	✓	✓	✓
32	Dianhydromannitol	30.613	$C_6H_{10}O_4$	146		✓			
33	Anhydro-d-mannosan	31.313	$C_6H_{10}O_5$	162		✓	✓	✓	✓

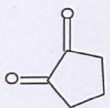
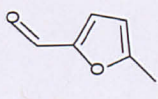
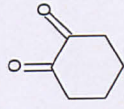
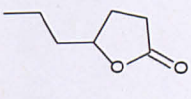
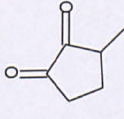


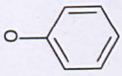
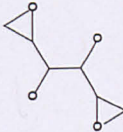
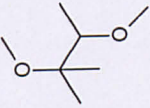
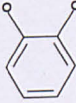
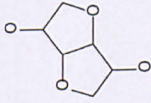
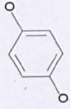
34	2-Propenoic acid, 2-methyl-, ethyl ester	31.827	$C_6H_{10}O_2$	114		✓	✓
35	Pantolactone	32.307	$C_6H_{10}O_3$	128		✓	✓
36	2-Furancarboxaldehyde, 5-(hydroxymethyl)-	33.694	$C_6H_6O_3$	126		✓	
37	1,2-Benzenediol	34.057	$C_6H_6O_2$	110		✓	✓
38	5-Hydroxymethyl-dihydrofuran-2-one	34.526	$C_5H_8O_3$	114		✓	✓
39	Hydroquinone	37.636	$C_6H_6O_2$	110		✓	✓
40	1,4-Benzenediol, 2-methyl-	38.808	$C_7H_8O_2$	124		✓	✓

**Table A.4** The main peaks identified in pyrograms of mannitol at different temperatures by mass spectral detection.

No	Compound	M		RT	Structure	200°C	300°C	400°C	500°C	800°C	
		Formula	W								
1	1,3-Butadiene	C <sub>4</sub> H <sub>6</sub>	54	3.31						✓	
2	Furan	C <sub>4</sub> H <sub>4</sub> O	68	3.75				✓	✓	✓	
3	3-Buten-1-ol, 2-methyl-	C <sub>5</sub> H <sub>10</sub> O	86	3.946					✓	✓	
4	2-Propenoic acid, 2-hydroxypropyl ester	C <sub>6</sub> H <sub>10</sub> O <sub>3</sub>	144	5.165							✓
5	1,4-Pentadien-3-one	C <sub>5</sub> H <sub>6</sub> O	82	7.174							✓
6	Toluene	C <sub>7</sub> H <sub>8</sub>	92	8.289					✓		✓
7	1-Hydroxy-2-butanone	C <sub>4</sub> H <sub>8</sub> O <sub>2</sub>	88	11.567					✓		✓

8	Heptanal, 2-methyl-	13.239	$C_8H_{16}O$	128		✓	✓
9	Furfural	13.798	$C_5H_4O_2$	69		✓	✓
10	Furan, 2-propyl-	14.384	$C_7H_{10}O$	110		✓	✓
11	2-Furanmethanol	15.636	$C_5H_6O_2$	98		✓	✓
12	2-Cyclopenten-1-one, 2-methyl-	15.963	$C_6H_8O$	96		✓	✓
13	Ethanone, 1-(2-furanyl)-	16.66	$C_6H_6O_2$	110		✓	✓

14	1,2-Cyclopentanedione	18.363	$C_3H_6O_2$	98		✓	✓
15	2-Furancarboxaldehyde, 5-methyl-	19.213	$C_6H_6O_2$	110		✓	✓
16	1,2-Cyclohexanedione	19.812	$C_6H_8O_2$	112		✓	✓
17	2(3H)-Furanone, dihydro-5-propyl-	20.808	$C_7H_{12}O_2$	128		✓	✓
18	1,2-Cyclopentanedione, 3-methyl-	22.068	$C_6H_8O_2$	112		✓	✓

19	Phenol	23.279	$C_6H_6O$	94		✓
20	Dianhydromannitol	30.654	$C_6H_{10}O_4$	146		✓
21	Butane, 2,3-dimethoxy-2-methyl-	31.664	$C_7H_{16}O_2$	132		✓
22	1,2-Benzenediol	34.005	$C_6H_6O_2$	110		✓
23	Isosorbide	35.146	$C_8H_{10}O_4$	146		✓
24	Hydroquinone	37.639	$C_6H_6O_2$	110		✓

## APPENDIX B - Proximate and ultimate analysis of freeze dried and air dried seaweed samples.

**Table B.1** Proximate and ultimate analysis of freeze dried samples of *L. digitata* (wt%)

Harvest site	Harvest date	H <sub>2</sub> O	Ash	Dry						CV (MJ/kg)	daf					
				C	H	N	S	O*	C		H	N	S	O	H/C	O/C
Clachan sound	08/09/2008	6.82	38.6	27.84	3.43	2.06	0.96	27.11	10.21	45.34	5.59	3.36	1.56	44.16	1.48	0.73
	06/01/2009	9.36	43.86	25.43	2.85	2.09	0.74	25.04	8.76	45.30	5.07	3.72	1.31	44.60	1.34	0.74
	06/04/2009	6.06	44.23	25.07	3.09	3.07	0.86	23.67	9.05	44.96	5.54	5.50	1.55	42.45	1.48	0.71
Easdale	17/07/2009	5.84	28.15	32.32	4.61	1.75	0.86	32.48	12.83	44.88	6.40	2.43	1.19	45.10	1.71	0.75
	16/10/2008	6.8	38.6	32.52	4.42	1.53	1.00	33.79	12.58	44.39	6.04	2.08	1.36	46.12	1.63	0.78
	13/01/2009	8.49	36.14	29.16	3.50	2.25	0.91	28.03	10.71	45.66	5.49	3.53	1.43	43.89	1.44	0.72
	28/04/2009	7.51	30.21	31.20	4.06	2.63	0.83	31.06	11.87	44.71	5.82	3.77	1.19	44.51	1.56	0.75
	25/07/2009	6.62	25.66	33.09	4.71	1.84	0.79	33.91	13.10	44.51	6.33	2.48	1.07	45.61	1.71	0.77

\* calculated by difference

**Table B.2** Proximate and ultimate analysis of freeze dried samples of *L. hyperborea* (wt%)

Harvest site	Harvest date	Dry										daf				
		H <sub>2</sub> O	Ash	C	H	N	S	O*	CV (MJ/kg)	C	H	N	S	O	H/C	O/C
Clachan sound	08/09/2008	6.49	23.46	33.74	4.88	1.60	0.71	35.60	13.41	44.09	6.38	2.09	0.92	46.51	1.74	0.79
	07/01/2009	7.58	43.41	25.34	3.10	2.39	0.95	24.80	9.08	44.78	5.48	4.22	1.69	43.83	1.47	0.73
	06/04/2009	6.36	42.24	25.61	3.28	3.23	0.83	24.81	9.39	44.34	5.68	5.58	1.44	42.95	1.54	0.73
	16/07/2009	5.66	28.30	31.80	4.57	1.60	0.90	32.83	12.56	44.35	6.37	2.23	1.26	45.79	1.72	0.77
Easdale	16/10/2008	8.52	20.84	35.21	4.57	1.35	0.64	37.39	13.42	44.47	5.78	1.71	0.81	47.23	1.56	0.80
	13/01/2009	8.97	38.53	29.50	3.08	2.06	2.36	24.46	10.79	47.99	5.02	3.35	3.85	39.80	1.25	0.62
	28/04/2009	5.64	44.11	26.03	3.18	2.60	1.24	22.83	9.63	46.58	5.69	4.65	2.22	40.85	1.47	0.66
	25/07/2009	5.63	17.54	35.80	5.10	1.49	0.96	39.11	14.16	43.41	6.18	1.81	1.17	47.43	1.71	0.82

\* calculated by difference

**Table B.3** Proximate and ultimate analysis of freeze dried samples of *L. saccharina* (wt%)

Harvest site	Harvest date	H <sub>2</sub> O	Ash	Dry							daf						
				C	H	N	S	O*	CV (MJ/kg)	C	H	N	S	O	H/C	O/C	
Clachan sound	16/10/2008	4.07	33.59	29.65	4.13	1.64	0.98	30.00	11.48	44.65	6.22	2.47	1.48	45.18	1.67	0.76	
	07/01/2009	5.42	44.04	25.88	3.29	2.17	0.87	23.74	9.58	46.25	5.88	3.88	1.56	42.42	1.52	0.69	
	06/04/2009	5.52	36.29	32.21	4.64	1.75	0.85	24.26	13.49	50.56	7.28	2.74	1.34	38.08	1.73	0.56	
Barnacarry	23/10/2008	3.49	17.37	35.55	5.12	1.68	0.57	39.71	14.00	43.02	6.20	2.03	0.69	48.06	1.73	0.84	
	13/01/2009	4.40	58.06	18.64	2.38	1.44	0.53	18.96	6.16	44.43	5.68	3.43	1.26	45.20	1.53	0.76	
	17/04/2009	4.37	31.84	30.18	4.23	2.54	0.68	30.52	11.73	44.29	6.21	3.72	1.00	44.78	1.68	0.76	
	25/07/2009	6.44	23.35	32.47	4.46	1.14	0.63	37.95	12.22	42.36	5.82	1.49	0.83	49.50	1.65	0.88	

\* calculated by difference



**Table B.4** Proximate and ultimate analysis of freeze dried samples of *A. esculenta* (wt%)

Harvest site	Harvest date	H <sub>2</sub> O	Ash	Dry										O/C		
				C	H	N	S	O*	CV (MJ/kg)	C	H	N	S		O	
Easdale	16/10/2008	4.92	21.72	35.1	4.84	2.08	0.66	35.52	13.89	44.95	6.18	2.66	0.84	45.37	1.65	0.76
				9												
	28/04/2009	5.07	32.44	29.2	3.88	2.16	0.69	31.56	10.88	43.32	5.75	3.19	1.03	46.72	1.59	0.81
				7												
	16/07/2009	6.77	27.05	34.6	4.71	1.90	0.58	31.11	13.89	47.50	6.45	2.60	0.80	42.64	1.63	0.67
				5												
Barancarry	17/04/2009	6.91	30.07	32.0	4.02	2.51	0.69	30.68	12.15	45.80	5.76	3.58	0.99	43.87	1.51	0.72
				3												

\* calculated by difference

**Table B.5** Proximate and ultimate analysis of oven dried samples of *L. digitata* (wt%)

Harvest site	Harvest date	Part of seaweed	Dry											daf			
			H <sub>2</sub> O	Ash	C	H	N	S	O*	CV (MJ/kg)	C	H	N	S	O	H/C	O/C
Clachan sound	06/01/2009	blades	4.65	44.53	24.61	3.20	2.06	0.80	24.81	8.90	44.36	5.77	3.71	1.44	44.72	1.56	0.76
		stipes	5.38	59.37	18.25	2.23	1.11	0.39	18.65	5.84	44.91	5.49	2.73	0.96	45.90	1.47	0.77
	07/04/2009	blades	4.77	40.18	n.d.	n.d.	n.d.	n.d.	n.d.	n.d.	n.d.	n.d.	n.d.	n.d.	n.d.	n.d.	n.d.
Easdale	16/07/2009	stipes	5.81	54.30	n.d.	n.d.	n.d.	n.d.	n.d.	n.d.	n.d.	n.d.	n.d.	n.d.	n.d.	n.d.	n.d.
		whole	4.46	27.64	n.d.	n.d.	n.d.	n.d.	n.d.	n.d.	n.d.	n.d.	n.d.	n.d.	n.d.	n.d.	n.d.
	13/01/2009	blades	4.64	32.83	30.70	3.97	2.15	0.99	29.36	11.73	45.70	5.91	3.21	1.47	43.70	1.55	0.72
26/04/2009	stipes	5.34	53.26	22.77	2.50	1.48	0.74	19.25	7.83	48.71	5.36	3.17	1.57	41.19	1.32	0.63	
	whole	6.58	41.80	32.99	5.05	2.06	0.00	18.10	14.68	56.68	8.68	3.53	n.d.	31.11	1.84	0.41	
26/07/2009	whole	4.27	20.46	32.91	5.41	1.79	0.00	39.43	13.32	41.38	6.80	2.25	n.d.	49.58	1.97	0.90	

\* calculated by difference, n.d. = not determined

Table B.6 Proximate and ultimate analysis of oven dried samples of *L. hyperborea* (wt%)

Harvest site	Harvest date	Part of seaweed	Dry											daf			
			H <sub>2</sub> O	Ash	C	H	N	S	O*	CV (MJ/kg)	C	H	N	S	O	H/C	O/C
Clachan sound	06/01/2009	blades	5.14	38.68	27.94	3.58	2.53	0.91	26.36	10.48	45.56	5.84	4.12	1.48	42.99	1.54	0.71
		stipes	7.43	52.30	22.20	2.42	1.92	0.64	20.52	7.41	46.55	5.07	4.02	1.33	43.02	1.31	0.69
		blades	4.99	42.37	n.d.	n.d.	n.d.	n.d.	n.d.	n.d.	n.d.	n.d.	n.d.	n.d.	n.d.	n.d.	n.d.
		stipes	n.d.	n.d.	n.d.	n.d.	n.d.	n.d.	n.d.	n.d.	n.d.	n.d.	n.d.	n.d.	n.d.	n.d.	n.d.
	18/07/2009	whole	3.52	29.70	n.d.	n.d.	n.d.	n.d.	n.d.	n.d.	n.d.	n.d.	n.d.	n.d.	n.d.	n.d.	n.d.
Easdale	13/01/2009	blades	4.25	29.13	34.37	4.34	2.39	2.05	27.72	13.80	48.50	6.12	3.37	2.89	39.12	1.51	0.60
		stipes	6.80	43.54	25.73	2.88	1.46	0.90	25.50	8.88	45.56	5.10	2.58	1.60	45.16	1.34	0.74
		blades	6.83	33.58	n.d.	n.d.	n.d.	n.d.	n.d.	n.d.	n.d.	n.d.	n.d.	n.d.	n.d.	n.d.	n.d.
	28/04/2009	stipes	7.40	39.94	n.d.	n.d.	n.d.	n.d.	n.d.	n.d.	n.d.	n.d.	n.d.	n.d.	n.d.	n.d.	n.d.
	19/07/2009	whole	3.57	17.97	n.d.	n.d.	n.d.	n.d.	n.d.	n.d.	n.d.	n.d.	n.d.	n.d.	n.d.	n.d.	n.d.

\* calculated by difference, n.d. = not determined

**Table B.7** Proximate and ultimate analysis of oven dried samples of *L. saccharina* (wt%)

Harvest site	Harvest date	Part of seaweed	Dry											daf			
			H <sub>2</sub> O	Ash	C	H	N	S	O*	CV (MJ/kg)	C	H	N	S	O	H/C	O/C
Clachan sound	06/01/2009	blades	3.33	56.27	21.12	2.50	2.04	0.68	17.38	7.38	48.31	5.72	4.67	1.55	39.75	1.42	0.62
		stipes	4.98	62.81	20.50	2.30	1.54	n.d.	12.85	7.19	55.13	6.19	4.13	n.d.	34.55	1.35	0.47
	23/04/2009	blades	4.45	38.25	36.42	4.84	2.76	n.d.	17.72	15.74	58.98	7.84	4.47	n.d.	28.70	1.60	0.36
Barancarry	16/07/2009	whole	2.74	29.94	n.d.	n.d.	n.d.	n.d.	n.d.	n.d.	n.d.	n.d.	n.d.	n.d.	n.d.	n.d.	n.d.
	13/01/2009	blades	5.50	35.93	29.30	3.76	2.05	0.98	27.97	11.08	45.74	5.87	3.20	1.54	43.66	1.54	0.72
		stipes	7.40	30.60	31.83	3.83	1.99	0.72	31.03	11.82	45.86	5.52	2.86	1.04	44.72	1.44	0.73
	17/04/2009	blades	3.83	32.36	31.59	4.27	2.82	0.80	28.16	12.50	46.70	6.31	4.17	1.18	41.64	1.62	0.67
		stipes	7.34	39.01	28.17	3.35	1.82	0.65	27.00	10.20	46.18	5.49	2.99	1.06	44.27	1.43	0.72
	31/07/2009	whole	3.49	34.31	30.06	4.45	1.47	n.d.	29.72	11.92	45.75	6.77	2.24	n.d.	45.24	1.78	0.74

\* calculated by difference, n.d. = not determined

**Table B.8** Proximate and ultimate analysis of oven dried samples of *A. esculenta* (wt%)

Harvest site	Harvest date	Dry										daf				
		H <sub>2</sub> O	Ash	C	H	N	S	O*	CV (MJ/kg)	C	H	N	S	O	H/C	O/C
Easdale	12/01/2009	4.44	35.82	30.07	3.78	2.37	0.95	27.00	11.46	46.85	5.89	3.69	1.4 9	42.08	1.51	0.67
	28/04/2009	5.40	28.15	32.03	4.70	2.25	n.d.	32.87	12.70	44.58	6.55	3.13	n.d.	45.74	1.76	0.77
	20/07/2009	4.43	18.93	26.54	3.84	2.89	n.d.	47.81	8.40	32.73	4.73	3.56	n.d.	58.97	1.74	1.35
Barnacarry	17/04/2009	5.65	25.94	32.85	5.33	1.65	n.d.	34.23	13.64	44.35	7.20	2.23	n.d.	46.22	1.95	0.78

\* calculated by difference, n.d. = not determined

**Table B.9** Proximate and ultimate analysis of air dried samples of *L. digitata* (wt%)

Harvest site	Harvest date	Part of seaweed	Dry										daf				
			H <sub>2</sub> O	Ash	C	H	N	S	O*	CV (MJ/kg)	C	H	N	S	O	H/C	O/C
Clachan sound	05/02/2008	blades	10.16	34.90	33.20	4.09	1.81	n.d.	25.99	12.95	51.01	6.28	2.79	n.d.	39.93	1.48	0.59
		stipes	8.62	41.28	25.95	2.73	1.27	n.d.	28.78	8.41	44.19	4.64	2.16	n.d.	49.01	1.26	0.83
	06/04/2008	whole	8.30	31.21	33.97	4.24	2.18	n.d.	28.40	13.23	49.38	6.16	3.17	n.d.	41.28	1.50	0.63
	15/07/2008	whole	5.83	33.91	30.37	4.81	2.10	n.d.	28.81	12.54	45.95	7.28	3.18	n.d.	43.60	1.90	0.71
	08/10/2008	whole	8.42	35.80	29.20	3.99	1.41	n.d.	29.60	11.06	45.48	6.22	2.19	n.d.	46.11	1.64	0.76

\* calculated by difference, n.d. = not determined

**Table B.10** Proximate and ultimate analysis of air dried samples of *L. hyperborea* (wt%)

Harvest site	Harvest date	Part of seaweed	Dry										daf				
			H <sub>2</sub> O	Ash	C	H	N	S	O*	CV (MJ/kg)	C	H	N	S	O	H/C	O/C
Clachan sound	05/02/2008	blades	8.04	33.34	32.54	4.32	2.06	n.d.	27.75	12.85	48.81	6.49	3.08	n.d.	41.63	1.59	0.64
		stipes	7.45	47.40	25.35	3.15	0.73	n.d.	23.37	9.13	48.19	5.98	1.40	n.d.	44.43	1.49	0.69
Clachan sound	06/04/2008	whole	7.93	35.02	31.53	4.05	1.78	n.d.	27.61	12.16	48.53	6.23	2.74	n.d.	42.50	1.54	0.66
Easdale	15/07/2008	whole	10.36	28.04	34.03	4.76	3.17	n.d.	29.99	13.75	47.30	6.61	4.41	n.d.	41.68	1.68	0.66
Clachan sound	02/10/2008	whole	6.29	22.09	35.74	5.04	1.05	n.d.	36.09	14.20	45.87	6.47	1.34	n.d.	46.32	1.69	0.76

\* calculated by difference, n.d. = not determined

**Table B.11** Proximate and ultimate analysis of air dried samples of *L. saccharina* (wt%)

Harvest site	Harvest date	Part of seaweed	Dry											daf			
			H <sub>2</sub> O	Ash	C	H	N	S	O*	CV (MJ/kg)	C	H	N	S	O	H/C	O/C
Barnacarry	05/02/2008	blades	10.73	29.01	35.23	4.24	1.30	n.d.	30.21	13.54	49.63	5.98	1.83	n.d.	42.56	1.45	0.64
		stipes	11.20	28.08	35.23	4.04	0.95	n.d.	31.71	13.17	48.98	5.61	1.32	n.d.	44.09	1.38	0.68
Barnacarry	06/04/2008	whole	9.18	26.62	34.31	4.11	2.61	0.73	31.62	12.95	46.76	5.60	3.56	n.d.	43.10	1.44	0.69
Clachan sound	15/07/2008	whole	5.93	36.22	29.10	4.24	2.18	n.d.	28.25	11.44	45.62	6.65	3.42	n.d.	44.30	1.75	0.73
Barnacarry	02/10/2008	whole	8.24	22.65	35.87	4.72	1.14	n.d.	35.61	13.91	46.38	6.11	1.48	n.d.	46.04	1.58	0.74

\* calculated by difference, n.d. = not determined



**Table B.12** Proximate and ultimate analysis of air dried samples of *A. Esculenta*(wt%)

Harvest site	Harvest date	Part of seaweed	Dry										daf				
			H <sub>2</sub> O	Ash	C	H	N	S	O*	CV (MJ/kg)	C	H	N	S	O	H/C	O/C
Easdale	09/01/2008	whole	9.64	29.75	36.68	4.52	1.18	n.d.	27.87	14.61	52.21	6.44	1.69	n.d.	39.67	1.48	0.57
	06/04/2008	whole	9.47	28.40	36.44	4.53	1.81	n.d.	28.82	14.45	50.90	6.32	2.53	n.d.	40.25	1.49	0.59
	22/07/2008	whole	8.39	19.65	36.26	5.37	2.78	n.d.	35.95	14.81	45.12	6.68	3.46	n.d.	44.74	1.78	0.74
	16/10/2008	whole	7.95	24.76	34.90	4.52	2.50	n.d.	33.32	13.50	46.39	6.00	3.32	n.d.	44.28	1.55	0.72

\* calculated by difference, n.d. = not determined

**APPENDIX C - Metal analysis of freeze dried, oven dried and air dried seaweed samples.**

**Table C.1** Metal analysis of freeze dried samples of *L. digitata* (wt%)

	Clachan sound							Easdale			
	15/07/2008	08/09/2008	06/01/2009	06/04/2009	17/07/2009	22/07/2008	16/10/2008	13/01/2009	28/04/2009	25/07/2009	
<b>Al</b>	172	n.d.	157	n.d.	n.d.	113	n.d.	122	n.d.	n.d.	
stdev	1.93	n.d.	5.05	n.d.	n.d.	7.05	n.d.	14.09	n.d.	n.d.	
<b>As</b>	122	178.96	159	119	123	101	141	150	111	123	
Stdev	2.86	3.04	1.11	3.50	n.d.	1.05	0.35	6.09	0.92	n.d.	
<b>B</b>	182	63	158	64	73	138	59	128	55	76	
Stdev	2.59	0.76	1.14	2.25	n.d.	1.70	2.42	6.10	1.24	n.d.	
<b>Ba</b>	6.91	n.d.	9.34	n.d.	n.d.	6.48	n.d.	10.40	n.d.	n.d.	
Stdev	0.33	n.d.	0.27	n.d.	n.d.	0.09	n.d.	0.51	n.d.	n.d.	
<b>Ca</b>	9421	5659	11369	4512	4089	8938	5679	15494	4663	4762	
Stdev	160	102	78	47	n.d.	176	4	177	36	n.d.	

<b>Cd</b>	2.47	n.d.	3.16	n.d.	n.d.	2.08	n.d.	3.02	n.d.	n.d.
Stdev	0.01	n.d.	0.10	n.d.	n.d.	0.14	n.d.	0.42	n.d.	n.d.
<b>Cr</b>	6.41	n.d.	6.58	n.d.	n.d.	5.25	n.d.	7.01	n.d.	n.d.
Stdev	0.01	n.d.	0.52	n.d.	n.d.	0.38	n.d.	0.50	n.d.	n.d.
<b>Cu</b>	3.58	n.d.	9.87	n.d.	n.d.	5.13	n.d.	6.41	n.d.	n.d.
Stdev	0.16	n.d.	0.78	n.d.	n.d.	0.11	n.d.	0.43	n.d.	n.d.
<b>Fe</b>	283	300	292	99	50	165	161	166	54	36
Stdev	6.07	0.35	6.50	1.46	n.d.	11.04	7.10	9.56	6.26	n.d.
<b>K</b>	111711	113289	131514	150183	71825	34848	56784	82743	68762	49629
Stdev	1926	1410	2583	3783	n.d.	633	279	3874	841	n.d.
<b>Li</b>	1.23	n.d.	1.37	n.d.	n.d.	0.85	n.d.	1.33	n.d.	n.d.
Stdev	0.01	n.d.	0.06	n.d.	n.d.	0.16	n.d.	0.37	n.d.	n.d.
<b>Mg</b>	7975	4304	9603	3785	3280	7707	4055	10400	4141	4087
Stdev	144	38	100	48	n.d.	116	3	272	14	n.d.
<b>Mn</b>	10.24	n.d.	5.63	n.d.	n.d.	4.52	n.d.	4.95	n.d.	n.d.
Stdev	0.17	n.d.	0.05	n.d.	n.d.	0.10	n.d.	0.51	n.d.	n.d.

<b>Na</b>	41212	47266	48723	44253	34318	35458	41208	51469	46511	44143
Stdev	651	374	957	695	n.d.	716	175	2015	411	n.d.
<b>Ni</b>	1.73	n.d.	1.78	n.d.	n.d.	1.22	n.d.	1.57	n.d.	n.d.
Stdev	0.32	n.d.	0.13	n.d.	n.d.	0.09	n.d.	0.37	n.d.	n.d.
<b>Sr</b>	622	407	864	390	328	570	411	948	376	344
Stdev	9.12	0.67	17.36	5.44	n.d.	11.67	4.02	34.38	3.31	n.d.
<b>Zn</b>	47	26	49	20	26	41	17	83	31	22
Stdev	1.57	1.41	3.33	0.94	n.d.	1.52	0.25	3.74	0.58	n.d.
<b>Total</b>	171780	171496	202925	203428	114115	88106	108519	161740	124707	103224
stdev	2044	1463	2758	3847	n.d.	978	329	4379	937	n.d.

n.d. = not determined

Table C.2 Metal analysis of freeze dried samples of *L. hyperborea* (wt%)

	Clachan sound										Easdale		
	15/07/2008	08/09/2008	07/01/2009	06/04/2009	16/07/2009	22/07/2008	16/10/2008	13/01/2009	28/04/2009	25/07/2009			
<b>Al</b>	132	n.d.	245	n.d.	n.d.	117	n.d.	124	n.d.	n.d.			
stdev	2.95	n.d.	5.94	n.d.	n.d.	6.35	n.d.	22.14	n.d.	n.d.			
<b>As</b>	136	129	220	122	146	104	121	144	105	80			
Stdev	1.48	0.48	2.99	7.75		0.54	4.33	2.39	4.18	n.d.			
<b>B</b>	190	53	128	63	67	123	51	112	53	46			
Stdev	2.64	2.42	0.15	1.17	n.d.	0.95	1.65	3.70	0.84	n.d.			
<b>Ba</b>	8.97	n.d.	10.12	n.d.	n.d.	9.09	n.d.	6.57	n.d.	n.d.			
Stdev	0.10	n.d.	0.14	n.d.	n.d.	0.17	n.d.	0.15	n.d.	n.d.			
<b>Ca</b>	10099	4347	12936	4201	4708	12877	5110	9248	3533	2899			
Stdev	382	43	247	58	n.d.	88	91	251	37	n.d.			
<b>Cd</b>	2.68	n.d.	4.40	n.d.	n.d.	2.14	n.d.	3.16	n.d.	n.d.			
Stdev	0.11	n.d.	0.10	n.d.	n.d.	0.17	n.d.	0.09	n.d.	n.d.			
<b>Cr</b>	8.29	n.d.	26.50	n.d.	n.d.	7.89	n.d.	14.68	n.d.	n.d.			

Stdev	0.23	n.d.	0.62	n.d.	n.d.	0.27	n.d.	0.72	n.d.	n.d.
<b>Cu</b>	5.22	n.d.	5.86	n.d.	n.d.	4.81	n.d.	3.69	n.d.	n.d.
Stdev	0.08	n.d.	0.15	n.d.	n.d.	0.02	n.d.	0.75	n.d.	n.d.
<b>Fe</b>	292	199	629	76	70	184	88	326	22	3
Stdev	1.23	8.16	7.40	11.94	n.d.	2.88	1.19	10.08	6.97	n.d.
<b>K</b>	119638	53016	126152	139987	75074	53549	39793	113239	157002	42230
Stdev	702	643	1523	3113	n.d.	456	80	2175	3394	n.d.
<b>Li</b>	1.07	n.d.	1.46	n.d.	n.d.	1.07	n.d.	1.01	n.d.	n.d.
Stdev	0.10	n.d.	0.16	n.d.	n.d.	0.17	n.d.	0.10	n.d.	n.d.
<b>Mg</b>	8578	3110	9998	3718	3398	8173	3542	8113	3072	2308
Stdev	59.02	37.64	105.85	66.23	n.d.	6.92	23.46	152.90	60.78	n.d.
<b>Mn</b>	8.43	n.d.	11.85	n.d.	n.d.	5.35	n.d.	4.56	n.d.	n.d.
Stdev	0.10	n.d.	0.26	n.d.	n.d.	0.17	n.d.	0.33	n.d.	n.d.
<b>Na</b>	44385	31154	52547	44547	35450	37602	34557	34358	34224	20150
Stdev	226	308	593	1081		312	120	740	814	n.d.
<b>Ni</b>	1.47	n.d.	2.52	n.d.	n.d.	2.01	n.d.	2.80	n.d.	n.d.

Appendix C

Stdev	0.22	n.d.	0.47	n.d.	n.d.	0.25	n.d.	0.53	n.d.	n.d.
<b>Sr</b>	714	306	871	365	340	784	348	638	350	204
Stdev	0.32	1.27	7.09	4.57	n.d.	13.71	7.69	13.78	2.61	n.d.
<b>Zn</b>	52	20	94	18	19	58	13	27	27	6
Stdev	0.72	2.24	0.64	0.40	n.d.	0.18	0.41	0.48	0.47	n.d.
<b>Total</b>	184252	92340	203882	193101	119275	113604	83626	166368	198390	67929
stdev	833	715	1656	3296	n.d.	559	172	2316	3491	n.d.

n.d. = not determined

Table C.3 Metal analysis of freeze dried samples of *L. saccharina* (wt%)

	Clachan sound					Barancarry				
	16/10/2008	07/01/2009	06/04/2009	12/07/2008	23/10/2008	13/01/2009	17/04/2009	30/07/2009		
<b>Al</b>	n.d.	431	n.d.	1025	n.d.	n.d.	n.d.	n.d.		
stdev	n.d.	9.53	n.d.	15.65	n.d.	n.d.	n.d.	n.d.		
<b>As</b>	180	104	101	101	108	124	100	149		
Stdev	11.95	0.43	5.30	0.51	1.68	1.61	1.92	n.d.		
<b>B</b>	67	127	68	210	35	81	80	68		
Stdev	4.23	0.97	1.22	2.25	1.91	0.84	0.56	n.d.		
<b>Ba</b>	n.d.	6.43	n.d.	10.07	n.d.	n.d.	n.d.	n.d.		
Stdev	n.d.	0.12	n.d.	0.26	n.d.	n.d.	n.d.	n.d.		
<b>Ca</b>	16024	59695	4519	21938	4971	6355	4359	11185		
Stdev	261	6031	8	437	209	75	174	n.d.		
<b>Cd</b>	n.d.	2.19	n.d.	2.31	n.d.	n.d.	n.d.	n.d.		
Stdev	n.d.	0.13	n.d.	0.28	n.d.	n.d.	n.d.	n.d.		
<b>Cr</b>	n.d.	10.18	n.d.	13.35	n.d.	16.83	n.d.	n.d.		



Stdev	n.d.	0.66	n.d.	0.82	n.d.	0.42	n.d.	n.d.
<b>Cu</b>	n.d.	2.60	n.d.	4.22	n.d.	n.d.	n.d.	n.d.
Stdev	n.d.	0.82	n.d.	0.05	n.d.	n.d.	n.d.	n.d.
<b>Fe</b>	329	834	242	1390	296	720	189	236
Stdev	16.10	18.98	8.72	5.78	16.41	6.51	16.63	n.d.
<b>K</b>	73413	100032	113781	106949	32497	85147	85781	44427
Stdev	1438	593	468	603	1240	936	3614	n.d.
<b>Li</b>	n.d.	2.44	n.d.	2.99	n.d.	n.d.	n.d.	n.d.
Stdev	n.d.	0.12	n.d.	0.27	n.d.	n.d.	n.d.	n.d.
<b>Mg</b>	3772	9907	3548	9708	2686	3566	3188	3482
Stdev	46	362	15	119	81	27	145	n.d.
<b>Mn</b>	n.d.	21.75	n.d.	43.82	n.d.	n.d.	n.d.	n.d.
Stdev	n.d.	0.19	n.d.	0.70	n.d.	n.d.	n.d.	n.d.
<b>Na</b>	27253	31034	39291	51299	21270	38288	32933	26812
Stdev	622	232	70	377	777	392	1507	n.d.
<b>Ni</b>	n.d.	2.71	n.d.	2.99	n.d.	n.d.	n.d.	n.d.

Appendix C

Stdev	n.d.	0.32	n.d.	0.27	n.d.	n.d.	n.d.	n.d.
<b>Sr</b>	308	746	309	729	273	354	319	370
Stdev	4.39	49.18	0.57	5.13	11.15	5.04	11.82	n.d.
<b>Zn</b>	7.04	29.23	12.50	28.40	6.24	14.43	11.57	7.30
Stdev	1.66	0.86	0.48	1.83	0.88	0.37	1.17	n.d.
<b>Total</b>	121362	202988	161876	193457	62148	134666	126966	86743
stdev	1589	6076	474	844	1481	1018	3923	n.d.

n.d. = not determined

Table C.4 Metal analysis of freeze dried samples of *A. esculenta* (wt%)

	Easdale			Barancarry		
	22/07/2008	16/10/2008	28/04/2009	25/07/2009	22/07/2008	17/04/2009
<b>Al</b>	225	n.d.	n.d.	n.d.	175	n.d.
stdev	3.98	n.d.	n.d.	n.d.	13.81	n.d.
<b>As</b>	67	129	86	145	50	94
Stdev	0.75	2.63	14.93	n.d.	1.09	4.21
<b>B</b>	160	61	59	108	187	94
Stdev	1.58	2.21	10.50	n.d.	3.47	0.77
<b>Ba</b>	7.50	n.d.	n.d.	n.d.	9.93	n.d.
Stdev	0.38	n.d.	n.d.	n.d.	0.26	n.d.
<b>Ca</b>	10046	6679	4266	10017	11858	4801
Stdev	17	25	607	n.d.	352	23
<b>Cd</b>	2.63	n.d.	n.d.	n.d.	1.65	n.d.
Stdev	0.34	n.d.	n.d.	n.d.	0.20	n.d.
<b>Cr</b>	7.11	n.d.	n.d.	n.d.	4.98	n.d.

Stdev	0.34	n.d.	n.d.	n.d.	0.46	n.d.
<b>Cu</b>	4.61	n.d.	n.d.	n.d.	5.25	n.d.
Stdev	0.51	n.d.	n.d.	n.d.	3.01	n.d.
<b>Fe</b>	274	487	73	223	320	284
Stdev	4.41	37.70	6.22	n.d.	11.08	6.29
<b>K</b>	73896	37375	66219	48003	51505	70807
Stdev	232	33	9494	n.d.	1872	775
<b>Li</b>	1.05	n.d.	n.d.	n.d.	1.27	n.d.
Stdev	0.34	n.d.	n.d.	n.d.	0.20	n.d.
<b>Mg</b>	7846	3575	3914	3592	10024	4074
Stdev	31	5	548	n.d.	264	27
<b>Min</b>	8.03	n.d.	n.d.	n.d.	19.49	n.d.
Stdev	0.38	n.d.	n.d.	n.d.	0.54	n.d.
<b>Na</b>	48145	30497	46992	35032	58436	44980
Stdev	186	41	6492	n.d.	1275	483
<b>Ni</b>	2.11	n.d.	n.d.	n.d.	2.03	n.d.

Appendix C

Stdev	0.34	n.d.	n.d.	n.d.	0.29	n.d.
<b>Sr</b>	791	484	397	534	937	410
Stdev	8.95	2.45	54.11	n.d.	20.39	6.23
<b>Zn</b>	30	22	9	20	31	10
Stdev	0.44	0.21	1.89	n.d.	0.21	0.48
<b>Total</b>	141514	79315	122019	97682	133566	125558
stdev	299	70	11531	n.d.	2308	914

n.d. = not determined

**Table C.5** Metal analysis of oven dried samples of *L. digitata* (wt%)

	Clachan sound						Easdale	
	06/01/2009		07/04/2009		16/07/2009	13/01/2009	26/04/2009	26/07/2009
	blades	stipes	blades	stipes	whole	blades	whole	whole
<b>Al</b>	229	134	n.d.	n.d.	n.d.	301	n.d.	n.d.
stdev	8.46	3.74	n.d.	n.d.	n.d.	10.06	n.d.	n.d.
<b>As</b>	156	58	144	104	113	143	111	104
Stdev	0.79	0.55	5.14	2.37	n.d.	3.43	0.95	n.d.
<b>B</b>	138	156	119	74	70	124	63	48
Stdev	8.90	3.25	24.27	27.14	n.d.	2.02	1.41	n.d.
<b>Ba</b>	5.61	4.73	n.d.	n.d.	n.d.	51.78	n.d.	n.d.
Stdev	1.47	0.45	n.d.	n.d.	n.d.	53.55	n.d.	n.d.
<b>Ca</b>	11105	8708	5626	5095	4709	17574	3918	4671
Stdev	116	95	106	44	n.d.	614	25	n.d.
<b>Cd</b>	3.26	1.28	n.d.	n.d.	n.d.	2.90	n.d.	n.d.
Stdev	0.34	0.02	n.d.	n.d.	n.d.	0.06	n.d.	n.d.

<b>Cr</b>	3.31	9.85	5.37	0.00	21.36	2.33	9.84	26.55
Stdev	0.79	0.03	0.35	0.03	n.d.	0.14	0.61	n.d.
<b>Cu</b>	14.57	14.54	n.d.	n.d.	n.d.	18.46	n.d.	n.d.
Stdev	0.63	4.24	n.d.	n.d.	n.d.	0.18	n.d.	n.d.
<b>Fe</b>	9444	474	611	622	332	949	686	340
Stdev	95	0.26	8.89	3.52	n.d.	4.70	7.12	n.d.
<b>K</b>	130291	217110	117805	203663	69895	69865	145538	36589
Stdev	2364	808	645	2854	n.d.	1401	835	n.d.
<b>Li</b>	2.05	1.79	n.d.	n.d.	n.d.	1.63	n.d.	n.d.
Stdev	0.45	0.03	n.d.	n.d.	n.d.	0.10	n.d.	n.d.
<b>Mg</b>	8243	6412	3969	3063	3350	9423	3099	3213
Stdev	107	9.23	47	42	n.d.	102	20	n.d.
<b>Mn</b>	34.42	4.47	n.d.	n.d.	n.d.	13.81	n.d.	n.d.
Stdev	0.46	0.11	n.d.	n.d.	n.d.	0.09	n.d.	n.d.
<b>Na</b>	44996	45052	47346	45769	36479	44976	37829	31918
Stdev	655	128	452	775	n.d.	620	116	n.d.

<b>Ni</b>	4.37	2.05	n.d.	n.d.	n.d.	4.30	n.d.	n.d.
<b>Stdev</b>	0.35	0.03	n.d.	n.d.	n.d.	0.09	n.d.	n.d.
<b>Sr</b>	786	580	502	337	398	984	328	319
<b>Stdev</b>	20	0.91	10.44	3.30	n.d.	11	1.99	n.d.
<b>Zn</b>	91	29	21	8.14	23	100	22	19
<b>Stdev</b>	3.20	0.24	0.46	0.69	n.d.	2.05	0.34	n.d.
<b>Total</b>	205546	278752	176159	256741	115392	144533	191607	77248
<b>stdev</b>	2460	824	797	2958	n.d.	1655	843	n.d.

n.d. = not determined



Table C.6 Metal analysis of oven dried samples of *L. hyperborea* (wt%)

	Clachan sound						Easdale				
	06/01/2009		07/04/2009		18/07/2009		13/01/2009		28/04/2009		19/07/2009
	blades	stipes	blades	stipes	whole	blades	stipes	blades	stipes	whole	
<b>Al</b>	295	458	n.d.	n.d.	n.d.	117	204	n.d.	n.d.	n.d.	
stdev	27.40	11.60	n.d.	n.d.	n.d.	8.35	13.92	n.d.	n.d.	n.d.	
<b>As</b>	132	63	153	167	167	109	66	128	125	85	
Stdev	3.16	0.73	2.56	n.d.	n.d.	2.14	0.63	3.46	5.70	n.d.	
<b>B</b>	116	198	77	81	81	100	156	63	60	46	
Stdev	2.52	3.45	8.55	n.d.	n.d.	2.57	1.09	2.33	4.06	n.d.	
<b>Ba</b>	9.80	6.73	n.d.	n.d.	n.d.	5.69	6.02	n.d.	n.d.	n.d.	
Stdev	0.63	0.15	n.d.	n.d.	n.d.	0.36	0.35	n.d.	n.d.	n.d.	
<b>Ca</b>	16466	11213	5667	6753	6753	9738	13352	5651	8693	3194	
Stdev	306	21	30	n.d.	n.d.	173	283	115	3.82	n.d.	

<b>Cd</b>	2.65	1.60	n.d.	n.d.	2.38	1.50	n.d.	n.d.	n.d.
Stdev	0.09	0.12	n.d.	n.d.	0.33	0.13	n.d.	n.d.	n.d.
<b>Cr</b>	1.46	14.17	8.06	13.56	1.19	7.77	11.28	84.33	7.72
Stdev	0.23	0.37	0.51	n.d.	0.38	0.13	1.33	1.89	n.d.
<b>Cu</b>	6.88	6.40	n.d.	n.d.	24.07	3.26	n.d.	n.d.	n.d.
Stdev	0.17	0.21	n.d.	n.d.	0.39	0.35	n.d.	n.d.	n.d.
<b>Fe</b>	1913	1562	1032	334	1057	235	392	759	129
Stdev	55	19.46	23	n.d.	19.59	0.53	7.14	14.09	n.d.
<b>K</b>	111033	190432	133995	78931	77116	145288	81611	129183	37248
Stdev	955	364	3098	n.d.	664	687	1554	272	n.d.
<b>Li</b>	1.59	2.97	n.d.	n.d.	1.06	1.50	n.d.	n.d.	n.d.
Stdev	0.07	0.12	n.d.	n.d.	0.33	0.13	n.d.	n.d.	n.d.
<b>Mg</b>	7956	6441	3668	3763	6865	6297	4258	3125	2307
Stdev	142	69	50	n.d.	81	4	80	32	n.d.
<b>Mn</b>	19.06	94.14	n.d.	n.d.	7.80	18.80	n.d.	n.d.	n.d.
Stdev	0.54	1.26	n.d.	n.d.	0.35	0.13	n.d.	n.d.	n.d.

Na	39572	36370	47207	39848	29156	33668	51495	29520	20892
Stdev	556	131	979	n.d.	234	615	965	240	n.d.
Ni	2.65	3.30	n.d.	n.d.	3.44	2.38	n.d.	n.d.	n.d.
Stdev	0.09	0.12	n.d.	n.d.	0.33	0.21	n.d.	n.d.	n.d.
Sr	956	716	469	402	536	1111	484	798	231
Stdev	15.01	1.09	5.58	n.d.	4.01	3.61	12.06	4.98	n.d.
Zn	59	33	27	27	38	24	28	9.98	7.72
Stdev	1.30	0.50	1.43	n.d.	0.66	0.22	0.50	0.30	n.d.
Total	178542	247614	192311	130325	124878	200442	144129	172366	64154
stdev	1157	394	3250	n.d.	730	965	1835	364	n.d.

n.d. = not determined

**Table C.7** Metal analysis of oven dried samples of *L. saccharina* (wt%)

	<b>Barnacarry</b>						<b>Clachan sound</b>		
	<b>13/01/2009</b>		<b>17/04/2009</b>		<b>31/07/2009</b>		<b>23/04/2009</b>		<b>15/07/2009</b>
	blades	stipes	blades	stipes	whole	stipes	blades	whole	blades
<b>Al</b>	1402	183	n.d.	n.d.	n.d.	n.d.	n.d.	n.d.	n.d.
stdev	363	22	n.d.	n.d.	n.d.	n.d.	n.d.	n.d.	n.d.
<b>As</b>	86	61	124	124	192	124	130	164	164
Stdev	29	2.24	1.61	0.65	n.d.	0.65	2.20	n.d.	n.d.
<b>B</b>	101	205	81	82	64	82	74	77	77
Stdev	30	9.79	0.84	10.27	n.d.	10.27	2.21	n.d.	n.d.
<b>Ba</b>	16.34	10.57	n.d.	n.d.	n.d.	n.d.	n.d.	n.d.	n.d.
Stdev	3.97	0.68	n.d.	n.d.	n.d.	n.d.	n.d.	n.d.	n.d.
<b>Ca</b>	14189	16532	6355	7098	28610	7098	6905	14000	14000
Stdev	1521	174	75	9	n.d.	9	39	n.d.	n.d.

<b>Cd</b>	2.01	1.58	n.d.	n.d.	n.d.	n.d.	n.d.	n.d.	n.d.
Stdev	0.63	0.40	n.d.	n.d.	n.d.	n.d.	n.d.	n.d.	n.d.
<b>Cr</b>	0.00	13.56	16.83	21.15	6.20	12.29	9.65	n.d.	n.d.
Stdev	0.10	0.45	0.42	0.64	n.d.	1.16	n.d.	n.d.	n.d.
<b>Cu</b>	17.08	2.70	n.d.	n.d.	n.d.	n.d.	n.d.	n.d.	n.d.
Stdev	4.96	0.58	n.d.	n.d.	n.d.	n.d.	n.d.	n.d.	n.d.
<b>Fe</b>	2833	264	720	524	779	866	417	n.d.	n.d.
Stdev	453	6.91	6.51	32	n.d.	14	n.d.	n.d.	n.d.
<b>K</b>	63872	81624	85147	114555	52053	110132	63524	n.d.	n.d.
Stdev	2512	1026	936	960	n.d.	1875	n.d.	n.d.	n.d.
<b>Li</b>	5.18	1.09	n.d.	n.d.	n.d.	n.d.	n.d.	n.d.	n.d.
Stdev	0.98	0.39	n.d.	n.d.	n.d.	n.d.	n.d.	n.d.	n.d.
<b>Mg</b>	7110	8069	3566	3636	4379	3652	3933	n.d.	n.d.
Stdev	2232	297	27	48	n.d.	58	n.d.	n.d.	n.d.
<b>Mn</b>	47.07	18.54	n.d.	n.d.	n.d.	n.d.	n.d.	n.d.	n.d.
Stdev	15.15	0.67	n.d.	n.d.	n.d.	n.d.	n.d.	n.d.	n.d.

Appendix C

Na	31701	33253	38288	37744	25773	40127	34675
Stdev	1257	929	392	151	n.d.	727	n.d.
Ni	0.00	3.76	n.d.	n.d.	n.d.	n.d.	n.d.
Stdev	0.10	0.41	n.d.	n.d.	n.d.	n.d.	n.d.
Sr	563	930	354	431	448	349	386
Stdev	187	29	5.04	1.24	n.d.	4.31	n.d.
Zn	34	33	14.43	9.50	14.46	12.29	12.06
Stdev	11	1.66	0.37	0.17	n.d.	1.16	n.d.
<b>Total</b>	121979	141206	134671	164231	112325	162266	117206
stdev	3945	1427	1018	974	n.d.	2012	n.d.

n.d. = not determined

**Table C.8** Metal analysis of oven dried samples of *A. esculenta* (wt%)

	<b>Easdale</b>		<b>Barancarry</b>	
	<b>12/01/2009</b>	<b>28/04/2009</b>	<b>20/07/2009</b>	<b>17/04/2009</b>
<b>Al</b>	373	n.d.	n.d.	n.d.
stdev	3.74	n.d.	n.d.	n.d.
<b>As</b>	90	114	124	109
Stdev	1.27	4.56	n.d.	1.15
<b>B</b>	116	74	81	68
Stdev	0.17	5.44	n.d.	0.65
<b>Ba</b>	9.77	n.d.	n.d.	n.d.
Stdev	0.48	n.d.	n.d.	n.d.
<b>Ca</b>	19564	5928	7773	5866
Stdev	457	114	n.d.	80
<b>Cd</b>	3.86	n.d.	n.d.	n.d.
Stdev	0.09	n.d.	n.d.	n.d.
<b>Cr</b>	2.57	17.01	12.44	7.84

Stdev	0.06	1.16	n.d.	0.86
<b>Cu</b>	9.39	n.d.	n.d.	n.d.
Stdev	0.05	n.d.	n.d.	n.d.
<b>Fe</b>	2213	415	383	823
Stdev	46	21	n.d.	26
<b>K</b>	83502	51120	30272	44878
Stdev	1417	627	n.d.	200
<b>Li</b>	1.80	n.d.	n.d.	n.d.
Stdev	0.05	n.d.	n.d.	n.d.
<b>Mg</b>	9960	4629	3188	3902
Stdev	142	53	n.d.	53
<b>Min</b>	24.19	n.d.	n.d.	n.d.
Stdev	0.50	n.d.	n.d.	n.d.
<b>Na</b>	42396	49394	26875	40185
Stdev	590	531	n.d.	481
<b>Ni</b>	5.14	n.d.	n.d.	n.d.



Appendix C

Stdev	0.58	n.d.	n.d.	n.d.
<b>Sr</b>	1044	498	423	344
Stdev	13.62	11.92	n.d.	7.80
<b>Zn</b>	56	15.51	25	12.57
Stdev	1.35	0.38	n.d.	0.75
<b>Total</b>	159371	112212	69162	96202
stdev	1608	832	n.d.	531

n.d. = not determined

**Table C.9** Metal analysis of air dried samples of *L. digitata* (wt%)

	Clachan sound				
	05/02/2008	06/04/2008	15/07/2008	08/10/2008	
	blades	stipes	whole	whole	
<b>Al</b>	175	523	159	96	141
stdev	13	354	18.47	4.35	15
<b>As</b>	125	67	76	101	160
Stdev	1.81	5.33	3.46	0.15	4.40
<b>B</b>	114	158	99	161	156
Stdev	3.05	42.13	2.28	3.27	2.72
<b>Ba</b>	14.95	7.95	13.08	5.77	9.35
Stdev	0.45	0.92	2.35	0.17	0.30
<b>Ca</b>	14381	16355	11659	9198	12242
Stdev	402	1504	560	122	308
<b>Cd</b>	2.43	1.18	1.49	2.13	3.24
Stdev	0.12	0.10	0.43	0.12	0.25

## Appendix C

<b>Cr</b>	20.20	12.94	8.80	1.76	1.01
Stdev	0.50	0.60	0.60	0.07	0.45
<b>Cu</b>	8.06	49.51	5.01	7.76	3.74
Stdev	0.36	3.73	0.50	1.44	0.24
<b>Fe</b>	583	388	345	186	218
Stdev	9.58	58	18	0.65	9.45
<b>K</b>	92162	141607	82766	85581	101260
Stdev	583	1362	5055	9	4301
<b>Li</b>	1.02	1.07	0.94	1.26	1.12
Stdev	0.06	0.42	0.44	0.38	0.25
<b>Mg</b>	8605	8393	7652	7052	9084
Stdev	51	460	318	23	177
<b>Mn</b>	8.95	8.68	6.49	5.15	7.73
Stdev	0.12	0.40	0.56	0.06	0.27
<b>Na</b>	39169	37170	35529	34457	44659
Stdev	485	635	1619	50	1361

Appendix C

Ni	128	81	47.41	2.51	1.63
Stdev	5.09	16	1.14	0.09	0.35
Sr	1198	887	985	568	762
Stdev	16	48	41	1.24	20
Zn	56	32	71	45	54
Stdev	1.55	9.13	2.83	0.34	1.16
<b>Total</b>	<b>156753</b>	<b>205742</b>	<b>139426</b>	<b>137471</b>	<b>168764</b>
stdev	860	2206	5347	135	4525

n.d. = not determined

**Table C.10** Metal analysis of air dried samples of *L. hyperborea* (wt%)

	Clachan sound				Easdale			
	05/02/2008		06/04/2008		02/10/2008		27/07/2008	
	blades	stipes	whole	whole	whole	whole	whole	whole
<b>Al</b>	210	217	228	149	141			
stdev	10.46	39	21	33	6.13			
<b>As</b>	133	66	87	97	94			
Stdev	4.06	0.82	2.49	12	1.06			
<b>B</b>	102	174	119	110	145			
Stdev	1.75	21	3.80	14.74	1.54			
<b>Ba</b>	17.84	9.66	11.33	7.92	9.37			
Stdev	0.55	0.10	0.52	1.06	0.10			
<b>Ca</b>	12947	15029	11662	11537	13988			
Stdev	72	404	644	1159	69			

## Appendix C

<b>Cd</b>	2.71	1.31	1.89	1.98	2.01
Stdev	0.11	0.13	0.37	0.29	0.16
<b>Cr</b>	9.58	4.41	10.92	1.87	13.52
Stdev	0.97	2.53	0.39	0.43	0.64
<b>Cu</b>	12.03	46.80	4.05	2.12	16.71
Stdev	0.54	4.98	0.44	0.46	2.39
<b>Fe</b>	785	435	498	218	223
Stdev	123	36	12.34	35	0.12
<b>K</b>	85757	159359	102662	40819	60154
Stdev	1078	4169	3511	5353	601
<b>Li</b>	0.90	1.17	0.94	0.74	0.80
Stdev	0.15	0.13	0.37	0.15	0.05
<b>Mg</b>	7955	7885	7802	6715	9071
Stdev	85	85	252	869	35
<b>Mn</b>	9.83	22.89	7.82	12.29	6.15
Stdev	0.64	1.07	0.38	2.13	0.08

Appendix C

<b>Na</b>	37742	36547	39013	28773	40964
Stdev	214	214	2016	3631	326
<b>Ni</b>	72	42	59	1.87	4.82
Stdev	3.21	1.86	0.91	0.43	0.73
<b>Sr</b>	1039	1059	989	623	886
Stdev	8.09	13.24	37	81	9.63
<b>Zn</b>	61	34	63	33	62
Stdev	2.38	0.13	1.97	4.51	0.11
<b>Total</b>	146855	220934	163220	89103	125781
stdev	1112	4195	4108	6629	688

---

n.d. = not determined

**Table C.11** Metal analysis of air dried samples of *L. saccharina* (wt%)

	<b>Barancarry</b>				<b>Clachan sound</b>			
	<b>28/02/2008</b>		<b>06/04/2008</b>		<b>13/10/2008</b>		<b>15/07/2008</b>	
	blades	stipes	whole	stipes	whole	whole	whole	
<b>Al</b>	498	248	486	497	497	149		
stdev	24	77	62	6.25	6.25	33		
<b>As</b>	57	66	40	95	95	97		
Stdev	2.98	8.49	1.43	4.28	4.28	11.75		
<b>B</b>	120	128	109	188	188	110		
Stdev	10.18	20	4.10	9.84	9.84	15		
<b>Ba</b>	18.57	13.75	10.04	6.36	6.36	7.92		
Stdev	0.74	1.46	0.53	0.19	0.19	1.06		
<b>Ca</b>	18226	17191	11445	42105	42105	11537		
Stdev	1198	306	437	1746	1746	1159		
<b>Cd</b>	1.42	1.32	0.97	2.08	2.08	1.98		
Stdev	0.14	0.04	0.16	0.12	0.12	0.29		



<b>Cr</b>	110	70	21.75	10.25	1.87
Stdev	18	10.10	1.40	0.32	0.43
<b>Cu</b>	6.25	4.63	3.07	3.38	2.12
Stdev	0.68	0.43	0.06	0.19	0.46
<b>Fe</b>	2066	808	1070	817	218
Stdev	128	27	48	2.90	35
<b>K</b>	64460	68382	49073	80630	40819
Stdev	2167	3927	2349	1645	5353
<b>Li</b>	1.42	1.06	1.53	1.95	0.74
Stdev	0.14	0.32	0.15	0.09	0.15
<b>Mg</b>	9379	8659	6388	8393	6715
Stdev	375	712	235	207	869
<b>Mn</b>	17.46	10.19	17.15	42.33	12.29
Stdev	1.40	0.35	0.94	0.19	2.13
<b>Na</b>	35575	34033	25471	30225	28773
Stdev	1212	1193	1052	445	3631

<b>Ni</b>	736.10	466.86	121.76	3.37	1.87
Stdev	54.94	55.11	4.05	0.17	0.43
<b>Sr</b>	1242	1026	599	668	623
Stdev	42	42	24	4.28	81
<b>Zn</b>	50	31	27	27	33
Stdev	3.06	3.19	1.12	0.49	4.51
<b>Total</b>	132564	131142	94884	163714	89103
stdev	2786	4179	2622	2448	6629

---

n.d. = not determined

**Table C.12** Metal analysis of air dried samples of *A. esculenta* (wt%)

	Easdale			
	09/01/2008	06/04/2008	22/07/2008	16/10/2008
<b>Al</b>	417	652	265	439
stdev	303	193	5.31	3.86
<b>As</b>	70	39	80	85
Stdev	0.34	3.16	9.74	0.89
<b>B</b>	108	95	145	176
Stdev	10.32	2.52	6.90	3.34
<b>Ba</b>	20.97	18.19	6.58	14.94
Stdev	0.18	5.03	0.25	0.37
<b>Ca</b>	30904	13947	13002	12984
Stdev	1618	542	215	197
<b>Cd</b>	2.90	1.69	3.03	3.40
Stdev	0.14	0.22	0.13	0.36
<b>Cr</b>	7.25	32.84	7.11	2.17

## Appendix C

Stdev	0.50	7.16	0.11	0.45
<b>Cu</b>	6.33	11.71	3.69	3.95
Stdev	0.35	4.89	0.07	0.49
<b>Fe</b>	668	1523	468	653
Stdev	32	50	14	81
<b>K</b>	58315	60684	37759	46162
Stdev	2251	2254	1458	736
<b>Li</b>	1.19	1.43	1.18	1.36
Stdev	0.22	0.22	0.16	0.36
<b>Mg</b>	9200	8683	7421	9212
Stdev	8.37	430	546	129
<b>Mn</b>	15.96	25.90	10.40	16.84
Stdev	0.81	0.89	0.05	0.52
<b>Na</b>	36526	36648	28565	39152
Stdev	119	1311	859	701
<b>Ni</b>	4.75	134.63	4.60	3.93

Stdev	0.35	21.43	0.79	0.52
<b>Sr</b>	1744	1135	614	1232
Stdev	19.66	42	7.66	22
<b>Zn</b>	141	44	39	65
Stdev	1.07	0.93	3.70	0.96
<b>Total</b>	138152	123676	88394	110208
stdev	2791	2706	1791	1047

---

n.d. = not determined